

Important Notice

This copy may be used only for the purposes of research and private study, and any use of the copy for a purpose other than research or private study may require the authorization of the copyright owner of the work in question. Responsibility regarding questions of copyright that may arise in the use of this copy is assumed by the recipient.

THE UNIVERSITY OF CALGARY

**On Elastic-wave Propagation in Anisotropic Media:
Reflection/Refraction Laws, Raytracing, and
Traveltime Inversion**

by

Michael A. Slawinski

A DISSERTATION
SUBMITTED TO THE FACULTY OF GRADUATE STUDIES
IN PARTIAL FULFILMENT OF THE REQUIREMENT FOR THE
DEGREE OF DOCTOR OF PHILOSOPHY

DEPARTMENT OF GEOLOGY AND GEOPHYSICS

CALGARY, ALBERTA

MARCH, 1996

©Michael A. Slawinski 1996

THE UNIVERSITY OF CALGARY
FACULTY OF GRADUATE STUDIES

The undersigned certify that they have read, and recommend to the Faculty of Graduate studies for acceptance, a dissertation entitled “On elastic-wave propagation in anisotropic media: reflection/refraction laws, raytracing, and travelttime inversion” submitted by Michael A. Slawinski in partial fulfilment of the requirement for the degree of Doctor of Philosophy.

Supervisor, Dr. R.J. Brown,
Department of Geology and Geophysics

Dr. E.S. Krebs,
Department of Geology and Geophysics

Dr. D.C. Lawton,
Department of Geology and Geophysics

Dr. M. Epstein,
Department of Mechanical Engineering

External Examiner, Dr. D.R. Schmitt,
Department of Physics, University of

Alberta

Date

ABSTRACT

An analytic method relating incidence, reflection and transmission angles at an interface between anisotropic media is presented. The method relies on the continuity conditions relating tangential components of phase slowness across the interface, and on the fact that the ray is perpendicular to the phase-slowness surface. The rather familiar concepts of vector calculus are used in a template for calculating phase and group angles. The angles involved in wave propagation through layered anisotropic media are, at times, significantly different than their isotropic counterparts. Thus the trajectories derived in raytracing by the isotropic versus the anisotropic approach differ significantly.

This template is used to derive analytic expressions for phase and group angles, and to elaborate a raytracing scheme for qP, qSV and qSH waves using expressions for phase velocities under the assumption of weak anisotropy. The raytracing method can be used to calculate traveltimes for layered weakly anisotropic media composed of TI materials.

The results of a physical laboratory experiment, which involved propagation in the symmetry plane of an orthorhombic material with known characteristics, have been compared with theoretical calculations. The comparison indicates that the anisotropic approach predicts reasonably well the experimental results and yields a significantly better prediction than an isotropic one. It also suggests that weak-anisotropy assumptions can be useful in practical applications as long as one remains within the intended limits of approximation.

The analytical approach is further extended to provide a traveltimes inversion scheme for the anisotropic parameter characterizing qSH waves. The inversion method can be used in multi-layer media and accounts for raybending at interfaces. It is, however, very sensitive to errors in input parameters.

The results of both theoretical and laboratory investigations indicate that ignoring anisotropic effects can, in certain cases, lead to significant errors. This dissertation offers

an approach which might prove helpful in such circumstances. Also, I believe, the usefulness of the present work to lie in clearly relating mathematical analytical formulations to physical consequences, thus contributing to a more intuitive understanding of phenomena exhibited by wave propagation in anisotropic media.

R É S U M É

Une méthode analytique liant les angles d'incidence, de réflexion et de réfraction à l'interface de deux milieux anisotropes est proposée. Cette méthode s'appuie sur les conditions de continuité liant les composantes tangentielles de la *lenteur* (inverse de la vitesse) de phase à l'interface d'une part et d'autre part, sur le fait que le rai est perpendiculaire à la surface de la lenteur de phase. Les concepts relativement familiers du calcul vectoriel sont appliqués dans un modèle de calcul des angles de phase et de groupe. Les angles impliqués dans la propagation des ondes au travers de milieux stratifiés anisotropes sont parfois très différents de leur homologues isotropes. Ainsi les trajectoires déduites du traçage de rais suivant les approches isotrope et anisotrope peuvent différer de manière significative.

Le modèle permet d'obtenir les expressions analytiques des angles de phase et de groupe et d'élaborer un schéma de traçage de rai pour les ondes qP (quasi longitudinale), qSV (quasi transversale verticale) et qSH (quasi transversale horizontale) en utilisant pour les vitesses de phase, des expressions assumant une faible anisotropie. La méthode de traçage de rai peut s'appliquer lors du calcul des temps de propagation lorsque le milieu stratifié faiblement anisotrope est composé de matériaux IT (Isotrope Transverse).

Les résultats d'une expérience physique en laboratoire, impliquant la propagation dans le plan de symétrie d'un matériau orthorhombique aux caractéristiques connues, ont été comparés avec les solutions du calcul théorique. La comparaison indique que l'approche anisotrope prédit de manière raisonnable les résultats expérimentaux et autorise une prédiction plus juste que l'approche isotrope. Il est également suggéré que la condition de faible anisotropie assumée lors du calcul se révèle être fort utile dans le cas

d'applications pratiques tant que l'on demeure dans les limites de validité de l'approximation.

Enfin cette démarche analytique est étendue afin de proposer un moyen d'inversion du temps de propagation pour les paramètres anisotropes qui caractérisent les ondes qSH. La méthode d'inversion peut ainsi être appliquée dans un milieu multicouche et prendre en compte la courbure du rai aux interfaces. Ce type de calcul est toutefois extrêmement sensible aux erreurs dans les paramètres d'entrée.

En conclusion, les résultats des investigations théoriques et expérimentales montrent qu'en certains cas, ignorer les effets de l'anisotropie peut conduire à des erreurs significatives. Cette dissertation propose une approche applicable en pareilles circonstances. Je crois également que l'utilité de ce travail réside en ce qu'il lie clairement les formules mathématiques analytiques aux conséquences physiques. Ceci contribue à une compréhension plus intuitive des phénomènes induits lors de la propagation d'ondes au sein de milieux anisotropes.

Traduction: Marc Villéger

ACKNOWLEDGMENTS

The author would like to thank Dr. R.J. Brown for supervising the study. His thorough revisions of the manuscript have significantly enhanced the quality of the present dissertation.

The present work would not have been possible without physical insights and mathematical prowess of Raphaël A. Slawinski. Also, the unrivaled skill of Eric Gallant in designing and operating the laboratory apparatus allowed for valuable comparisons between theoretical and experimental results.

In addition, the author would like to acknowledge financial support provided by The University of Calgary in the form of teaching assistantships, and by the CREWES Project and NSERC grant (through Dr. R.J. Brown) in the form of research assistantships.

TABLE OF CONTENTS

Approval page	ii
Abstract	iii
Acknowledgements	v
Table of Contents	vi
List of Tables	x
List of Figures	xi
CHAPTER I : DEFINITION OF THE PROBLEM	1
1.0. INTRODUCTION	1
1.1. RUDIMENTARY CONCEPTS	2
1.2. TRANSVERSE ISOTROPY	6
1.3. THE OBJECTIVE OF THE WORK	8
CHAPTER II : REFLECTION AND TRANSMISSION ANGLES IN ANISOTROPIC MEDIA	13
2.0. INTRODUCTION	13
2.1. IMPORTANT CONCEPTS	15
2.1.1. Phase and group velocities	15
2.1.2. Snell's law	16
2.1.3. Slowness surfaces	16
2.2. GEOMETRICAL FORMULATION	17
2.3. MATHEMATICAL FORMULATION	19
2.4. EXAMPLES	24
2.4.1. General case of elliptical anisotropy	24
2.4.2. A particular case of isotropic/anisotropic interface	27
2.5. DISCUSSION	27
CHAPTER III : SNELL'S LAW FOR WEAKLY ANISOTROPIC MEDIA	30
3.0. INTRODUCTION	30
3.1. QUASI-COMPRESSIONAL WAVES	34
3.1.1. Phase velocity	34
3.1.2. Transmission angle	36
3.2. QUASI-SHEAR WAVES (SV)	42
3.2.1. Phase velocity	43
3.2.2. Transmission angle	43
3.3. SHEAR WAVES (SH)	47
3.3.1. Phase velocity	48
3.3.2. Transmission angle	49
3.4. A COMMENT TO USERS AND PROGRAMMERS	54
CHAPTER IV : RAYTRACING THROUGH A TWO-LAYER ISOTROPIC/ANISOTROPIC MEDIUM	56

4.0. INTRODUCTION	56
4.1. MATHEMATICAL METHODS	57
4.1.1. General remarks	57
4.1.2. SH-wave raytracing based on Snell's law formalism	58
4.1.3. Fermat's-Principle Approach	59
4.2. RAYTRACING THROUGH SEVERAL LAYERS	63
4.2.1. Raytracing based on minimization of traveltime	63
4.2.3. Raytracing based on Snell's law	64
4.2.4. Raytracing through multiple layers	64
CHAPTER V : TRAVELTIMES IN WEAKLY ANISOTROPIC MEDIA	68
5.0. INTRODUCTION	68
5.1. MAGNITUDE OF GROUP VELOCITY	69
5.1.1. Magnitude using linearized method	69
5.1.2. Magnitude using approximate method	71
5.2. TRAVELTIME CALCULATIONS	75
CHAPTER VI : ANISOTROPIC/ANISOTROPIC INTERFACE	78
6.0. INTRODUCTION	78
6.1. THE APPROACH	80
6.2. SPECIFIC CASES	81
6.2.1. SH-SH case	82
6.2.1.1. Numerical example	85
6.2.2. P-P case	88
6.2.2.1. Numerical example	90
6.2.3. P-SV case	92
6.2.3.1. Numerical example	95
6.3. PHYSICAL IMPLICATIONS	97
6.3.1. Points of verification	97
6.3.2. Refraction angle and Fermat's principle	98
6.4. REMARKS ON THE METHOD	106
CHAPTER VII : PHYSICAL MODELLING	110
7.0. INTRODUCTION	110
7.1. MATERIALS	111
7.2. EXPERIMENTAL SET-UP	115
7.3. DATA ANALYSIS	116
7.3.1. P-P case	117
7.3.2. SH-SH case	120
7.4. EXPERIMENTAL ERRORS	125
7.4.1. Measurement errors	125
7.4.2. Computational errors	125
7.4.3. Interpretation errors	126

CHAPTER VIII : INVERSION FOR ANISOTROPIC PARAMETER IN LAYERED MEDIA	127
8.0. INTRODUCTION	127
8.1. FORMULATION OF THE PROBLEM	128
8.2. GENERAL MATHEMATICAL FORMULATION	129
8.3. FORMULATION IN TERMS OF FERMAT'S PRINCIPLE	130
8.4. VISUALIZATION OF SOLUTION SPACES	132
8.5. EXAMPLES OF INVERSION APPLICATIONS	139
8.5.1. Numerical modelling	139
8.5.2. Physical modelling	139
8.5.3. Discussion of inversions applications	140
8.6. ANISOTROPIC/ANISOTROPIC CASE	141
8.7. MULTI-LAYER CASE	143
CHAPTER IX : CONCLUSIONS	154
9.1. GENERAL REMARKS	154
9.2. SOME PRACTICAL APPLICATIONS	156
9.2.1. Modelling	156
9.2.2. Near-surface static corrections	156
9.2.3. Vertical seismic profiling (VSP)	157
9.2.4. Intuitive understanding	158
REFERENCES	159
APPENDIX 1 : THE CHARACTERISTIC BIQUADRATIC	162
A1.1. PHASE VELOCITY, SLOWNESS AND RAY PARAMETER	162
A1.2. QUARTIC EQUATION AND BIQUADRATIC	163
A1.3. THE CRITICAL ANGLE	165
A1.4. REDUCTION TO THE PURELY ISOTROPIC CASE	166
A1.5. CONCLUSIONS	167
APPENDIX 2 : IMPLICATIONS OF WEAK-ANISOTROPY APPROXIMATION ON PHASE-SLOWNESS CURVES	168
APPENDIX 3 : CONCERNS OF NUMERICAL PRECISION	180
A3.1. INTRODUCTION	180
A3.2. OBSERVATION	180
A3.3. FURTHER INVESTIGATION	181
A3.3.1. Calculation using ray parameter	182
A3.3.2. Calculation using the traveltime function	182
A3.4. CONCLUSIONS	183
A3.5. FINAL REMARKS	184
APPENDIX 4 : PROOF THAT $d\gamma/dr = 0$ FOR THE ACTUAL γ	185

APPENDIX 5 : AN APPROXIMATE METHOD FOR CALCULATING ANISOTROPIC PARAMETERS FROM P-WAVE TRAVELTIMES	188
A5.1. INTRODUCTION	188
A5.2. OBSERVATION ON THE FORWARD MODEL	189
A5.3. STRATEGY FOR AN INVERSE CALCULATION	190
A5.4. ALGEBRAIC FORMULATION	191
APPENDIX 6 : DEGREES OF APPROXIMATION	193
A6.1. INTRODUCTION	193
A6.2. EXACT METHOD	194
A6.3. ANISOTROPIC PARAMETER AS γ AND $\gamma\sim$	195
A6.4. APPROXIMATE METHOD (WEAK ANISOTROPY)	197
A6.5. LINEARIZED METHOD (FURTHER SIMPLIFICATIONS)	198
A6.6. NUMERICAL EXAMPLE	199
A6.7. GEOMETRICAL EXPLANATION	202
A6.8. ANGLE OF PROPAGATION AND OTHER CONCEPTS	204
APPENDIX 7 : THE APPROACH INVOLVING EXACT FORMULÆ	207

LIST OF TABLES

6.1. Computational results for an SH-SH case.	87
6.2. Computational results for a P-P case.	91
6.3. Computational results for a P-SV case.	95
6.4. Computational results for an isotropic/anisotropic model.	99
6.5. Group and phase angles and velocities of an SV wave.	101
6.6. Computational results for two source-receiver offsets.	103
6.7. Computational results using linearized scheme	108
7.1. The principal dimensions and characteristics of the physical model.	111
7.2. Vertical speeds in the physical model.	112
7.3. Anisotropic parameters of the physical model.	112
7.4. Comparison of measured and calculated traveltimes for P waves.	119
7.5. Traveltimes for P waves calculated based on isotropic approach	119
7.6. Comparison of measured and calculated traveltimes for SH waves.	123
7.7. Traveltimes for SH waves calculated based on isotropic approach.	124
8.1. The results of forward numerical modelling and inversion.	140
8.2. Inverted anisotropic parameter, γ for SH waves in 31-plane.	141
8.3. Model parameters used in numerical calculation of a multilayer case.	149
A2.1. Anisotropic parameters corresponding to Figure A2.1.	170
A6.1. Traveltimes for $\gamma = 0.1$ using several methods.	199
A6.2. Traveltimes for $\gamma = 0.2$ using several methods.	200
A6.3. Traveltimes for $\gamma = 0.3$ using several methods.	201
A6.4. Group and phase angles and speeds at 3000 m offset.	204
A6.5. Group angle, phase and group velocities as function of phase angle	205

LIST OF FIGURES

2.1. The geometrical construction yielding reflection and transmission angles of slowness vectors in an isotropic medium using the phase-slowness surface.	18
2.2. Illustration of ray angles for incident, reflected and transmitted rays in anisotropic media separated by a horizontal, planar interface using phase-slowness surface.	20
2.3. Illustration of the mathematical solution giving three reflected ray vectors. The one pointing towards the interface is not physically realizable.	22
3.1. Plots in the slowness space; Picture (a) illustrates the function $f(r, \xi)$. In picture (b) the function $f(r, \xi)$ is intersected by a plane illustrating the speed value of α_0 . The line of intersection corresponds to the slowness curve. Map view of the slowness curve is shown in picture (c)	37
4.1. The illustration of a ray travelling through a two-layer between a source and a receiver separated by a horizontal distance X .	62
6.1. Slowness curves in slowness space, i.e., cross-sections of corresponding to slowness surfaces in a vertical plane, for media of incidence and transmission.	86
6.2. A ray diagram of an SH wave at a horizontal interface between two anisotropic layers.	87
6.3. Compressional (P) wave slowness curves, i.e., cross-sections of corresponding slowness surfaces in a vertical plane.	91
6.4. A ray diagram of a P wave at a horizontal interface between two anisotropic layers.	92
6.5. P- and SV-slowness curves.	96
6.6. A ray diagram of a P wave incident at a horizontal interface between two anisotropic layers and generating a transmitted SV wave.	97
6.7. Phase and group velocities as functions of phase angle for an SV wave.	100
6.8. Phase and group angles as functions of the incidence angle for an SV wave.	102
6.9. Phase and group velocities as a function of the incidence angle for an SV wave.	103
6.10. Group angle as a function of phase angle for an SV wave.	104

6.11. Illustration of consequences of Fermat's principle of stationary time.	105
6.12. Group angle, θ , as a function of phase angle, ϑ , based on the linear approximation.	107
7.1. Phase slowness curves for Phenolic CE laminate in 31- and 32-planes.	113
7.2. Phase velocity plots for Phenolic CE laminate in 31- and 32-planes.	113
7.3. A schematic diagram of the experimental set-up.	115
7.4. A seismic record obtained in the 31-plane using vertically polarized transducers as both sources and receivers.	117
7.5. A seismic record obtained in the 32-plane using vertically polarized transducers as both sources and receivers.	118
7.6. A graphical comparison of results for compressional (P-P) waves in the 31-plane.	120
7.7. A seismic record obtained in the 31-plane using transversally polarized transducers as both sources and receivers.	121
7.8. A seismic record obtained in the 32-plane using transversally polarized transducers as both sources and receivers.	122
7.9 A graphical comparison of results for shear (SH-SH) waves in 31-plane.	124
8.1 The illustration of a ray travelling through the model between a source and receiver separated by a horizontal distance X .	131
8.2. The surface representing the travelttime as a 3-D visualization and as a contour plot.	133
8.3. Two, almost opposite, views of the surface representing the travelttime cut by a plane corresponding to the given travelttime value.	134
8.4. The inclined surface corresponding to the derivative $dt(\gamma,r)/dr$ and the horizontal plane representing the $d[t(\gamma,r)]/dr = 0$.	136
8.5. The projections of the curves $\mathcal{C}_2 = dt/dr = 0$ and $\mathcal{C}_1 = \gamma(r,T)$ on the $r\gamma$ -plane.	137
8.6. The multilayer model used to explain the inversion algorithm.	147

8.7. The travelttime function for a three-layer case.	148
8.8. The travelttime surface cut by an actual travelttime value calculated by forward modelling. The illustration is limited to the neighbourhood of the absolute minimum of the travelttime function.	149
8.9.a & b. The graph of γ as a function of r for a given value of the travelttime. Picture a) illustrates the behaviour of the function for the entire range of r . Picture b) illustrates the behaviour of the function in the neighbourhood of the Fermatian solution.	151
A1.1. A graph of a characteristic biquadratic.	164
A1.2. A graph of a characteristic biquadratic curve and the straight line plotted versus $x \equiv \sin \vartheta$.	165
A1.3. Degenerate biquadratic, the graph of a fourth-order polynomial for isotropic media.	167
A2.1. Slowness curves of P and SV waves using exact and approximate equations.	170-176
A2.2. Slowness curves of SH waves using exact and approximate equations.	177
A5.1. Travelttime surfaces for P waves.	190
A5.2. The illustration of the intersection point between the curves corresponding to the intersection of surfaces.	191
A6.1. The travelttime of SH waves between the source and receivers calculated using four different approaches: exact, approximate, linearized and isotropic.	201
A6.2. The normalized difference in travelttime in an anisotropic medium calculated using four different approaches: exact, approximate, linearized and isotropic.	202
A6.3. Illustration of ray and phase vectors in an anisotropic medium.	203
A6.4. Phase and group angles as functions of phase angle.	205
A6.5. Magnitudes of phase and group velocities as functions of phase angle.	206

CHAPTER I

*“Settle thy studies Faustus, and begin
To sound the depth of that thou wilt profess.
Having commenc’d, be a divine in show,
Yet level at the end of every art,
And live and die in Aristotle’s works.
Sweet Analytics, ‘tis thou hast ravish’d me:
Bene disserere est finis logices.
Is to dispute well logic’s chieffest end?
Afford this art no greater miracle?
Then read no more, thou hast attain’d the end.
A greater subject fitteth Faustus’ wit:*

Christopher Marlow
“Doctor Faustus”

DEFINITION OF THE PROBLEM

1.0. INTRODUCTION

The Oxford English Dictionary on Historical Principles states that the term isotropic derives from the Greek ισοσ (equal) and τροπος (turn). It began to be used in the modern vocabulary in 1864. The opposite of the isotropic is anisotropic or æolotropic. The former term is, at present, widely used, while the latter term was in favour with earlier researchers, e.g., Love (1927). Winterstein (1990) restates the definition of anisotropy as variation of one or more properties of a material with direction. Within the scope of this dissertation, the anisotropic effects exhibited by velocity are considered. This means that the speed of the ray propagating through a medium depends on the direction of propagation and entails concepts of phase and group

velocities. Other interesting effect, e.g., amplitude, wavelet shape, etc., are not considered.

A very brief introduction to several rudimentary concepts is given below. Certain notions and definitions are stated, when necessary, throughout the dissertation. In general, however, a reasonable familiarity of the reader with description of anisotropic phenomena is assumed. Several textbooks provide an extensive and rigorous introduction, e.g., Love, 1927, Chapter 13; Auld, 1973, Volume I, Chapter 7, and Volume II, Chapter 9; Helbig, 1994.

1.1. RUDIMENTARY CONCEPTS

In an anisotropic medium Hooke's law can be written as:

$$\sigma_{ij} = c_{ijkl} \varepsilon_{kl}, \quad (1.1)$$

where σ , and ε are the second-order stress and strain tensors, while c is the fourth-rank tensor of elastic constants (stiffnesses) of the medium. The tensor can be "visualized" as a $3 \times 3 \times 3 \times 3$ matrix in a 4-D space. In general, c , has eighty-one (3^4) components. However, both stress and strain tensors are symmetric, resulting in:

$$c_{ijkl} = c_{jikl} = c_{ijlk}, \quad (1.2)$$

and giving only thirty-six independent constants. Furthermore, due to strain energy considerations::

$$c_{ijkl} = c_{klij}, \quad (1.3)$$

and the number of elastic constants is further reduced to twenty-one. This is the largest number of elastic constants that one might need to uniquely describe an anisotropic material. A material requiring all twenty-one elastic constants for a complete description

belongs to the triclinic symmetry class. Notably, the smallest number of elastic constants necessary to describe a material is two. Materials requiring only two elastic constants for a complete description are called isotropic, and the two elastic constants can be expressed as the well known Lamé parameters, λ , and μ .

For infinitesimal strains, appropriate in the geophysical context, the strain tensor may be approximated by the Cauchy strain tensor:

$$\varepsilon_{ij} = \frac{1}{2} \left(\frac{\partial u_i}{\partial x_j} + \frac{\partial u_j}{\partial x_i} \right) \quad (1.4)$$

where \mathbf{u} denotes displacement, and \mathbf{x} denotes position. Ignoring any body forces, e.g., gravity, the equation of linear momentum can be written as:

$$\frac{\partial \sigma_{ij}}{\partial x_j} = \rho \frac{\partial^2 u_i}{\partial t^2}, \quad (1.5)$$

where t is time, and ρ is the density of the medium. Combining the equations (1.1), (1.4) and (1.5), one arrives at the wave equation (e.g., Daley and Hron, 1977):

$$\rho \frac{\partial^2 u_i}{\partial t^2} - \frac{\partial}{\partial x_j} \left(c_{ijkl} \frac{\partial u_k}{\partial x_l} \right) = 0. \quad (1.6)$$

Consider the displacement, \mathbf{u} , of the form

$$u_k = A p_k \exp[i\omega(m_r x_r - t)], \quad (1.7)$$

(e.g., Cheadle et al., 1991), where A is the amplitude factor, \mathbf{p} corresponds to the particle displacement or polarization, ω is the angular frequency, and \mathbf{m} denotes the phase-

slowness vector defined in terms of the unit normal parallel to the wave direction, \mathbf{n} , and the phase velocity, v . That is,

$$\mathbf{m} = \frac{\mathbf{n}}{v}. \quad (1.8)$$

Combining equations (1.6), (1.7) and (1.8) yields:

$$\left(c_{ijkl} n_j n_l - \rho v^2 \delta_{ik} \right) p_k = 0. \quad (1.9)$$

Expression (1.9) constitutes a system of linear homogeneous equations. The system has a non-trivial solution if and only if the determinant of the coefficient matrix is identically zero, i.e.:

$$\left| c_{ijkl} n_j n_l - \rho v^2 \delta_{ik} \right| = 0. \quad (1.10)$$

Introducing the Christoffel symbol, $\Gamma_{ik} \equiv c_{ijkl} n_j n_l$, the determinantal equation (1.10) can be written in a matrix form as a typical eigenvalue problem:

$$\begin{vmatrix} \Gamma_{11} - \rho v^2 & \Gamma_{12} & \Gamma_{13} \\ \Gamma_{21} & \Gamma_{22} - \rho v^2 & \Gamma_{23} \\ \Gamma_{31} & \Gamma_{32} & \Gamma_{33} - \rho v^2 \end{vmatrix} = 0. \quad (1.11)$$

The expression ρv^2 takes on values equal to the eigenvalues of the matrix $\mathbf{\Gamma}$. The matrix, $\mathbf{\Gamma}$, is symmetric and real because of the properties of c_{ijkl} . Therefore, in general, there are three distinct and real phase velocities, v . One of them corresponds to the compressional-wave speed and the remaining two, to the shear-wave speeds. In general, the expressions for phase velocities for an arbitrary symmetry system and in an arbitrary direction are very complicated. Much meaningful information, however, can be obtained

by limiting the solution to a particular symmetry system, and by confining the propagation to specific symmetry planes or symmetry axes (e.g., Cheadle et al., 1991).

One must remember, however, that in confining oneself to considering anisotropic propagation within particular symmetry planes one does not embrace the entire complexity of the problem. The trade-off between complexity and generality of approach or complexity and accuracy of description is constantly present in mathematical physics. This dissertation is no exception to this rule. The author attempts, as much as possible, to make the reader aware of limitations and approximations.

In a qualitative sense one could distinguish two methods of dealing with inherent complexities while describing Nature. Firstly, one can use a simplified view of the physical phenomenon in question, e.g., considering the motion along the inclined plane ignoring effects of friction. Secondly, one could choose to use an approximate mathematical description, e.g., truncation of higher-order terms in a series. Although in most cases in this dissertation both simplifications are used, it is important, from the philosophical stand-point, to distinguish between the two.

In some cases it might be more convenient to express the possible twenty-one independent components of the tensor, \mathbf{c} , as a 6x6 symmetric matrix (e.g., Love 1927):

$$\mathbf{C} = \begin{bmatrix} C_{11} & C_{12} & C_{13} & C_{14} & C_{15} & C_{16} \\ \cdot & C_{22} & C_{23} & C_{24} & C_{25} & C_{26} \\ \cdot & \cdot & C_{33} & C_{34} & C_{35} & C_{36} \\ \cdot & \cdot & \cdot & C_{44} & C_{45} & C_{46} \\ S & Y & M & \cdot & C_{55} & C_{56} \\ \cdot & \cdot & \cdot & \cdot & \cdot & C_{66} \end{bmatrix}. \quad (1.12)$$

There exists a simple method of index translation between the tensor notation, c_{ijkl} and the matrix notation C_{mn} (e.g., Winterstein, 1990):

Tensor	ij or kl	11	22	33	32 = 23	31 = 13	21 = 12
Matrix	m or n	1	2	3	4	5	6

1.2. TRANSVERSE ISOTROPY

As an illustration of possible simplification, used extensively in Chapter III, and subsequent chapters, one can consider a *hexagonal symmetry system*. In the geophysical context one can often limit the hexagonal symmetry system to the so called *transverse isotropy with an infinite-fold vertical symmetry axis*: TIV. The TIV system implies, in terms of velocity anisotropy, equal velocity in the azimuthal sense. The velocity is varying, however, with the angle of propagation, in the vertical plane. The angular velocity dependence is the same in all vertical planes, i.e., a single vertical plane at any azimuth is representative of the entire medium. One could also say that any vertical plane is a symmetry plane.

This system is particularly applicable in the case of horizontally stratified media, or in media with predominantly vertical stress direction, which in a geophysical study can be associated with the weight of the overburden. A TIV medium is uniquely described in terms of five independent elastic constants (e.g., Thomsen, 1986) and in matrix notation one can write:

$$\mathbf{C} = \begin{bmatrix} C_{11} & C_{11} - 2C_{66} & C_{13} & 0 & 0 & 0 \\ \cdot & C_{11} & C_{13} & 0 & 0 & 0 \\ \cdot & \cdot & C_{33} & 0 & 0 & 0 \\ \cdot & \cdot & \cdot & C_{44} & 0 & 0 \\ S & Y & M & \cdot & C_{44} & 0 \\ \cdot & \cdot & \cdot & \cdot & \cdot & C_{66} \end{bmatrix}. \quad (1.13)$$

The phase velocities for three waves with mutually orthogonal polarization directions can be expressed in terms of the elastic constants (e.g., Thomsen, 1986). The phase velocity of a compressional wave is expressed by:

$$v_p(\xi) = \frac{\sqrt{C_{33} + C_{44} + (C_{11} + C_{33}) \cos^2 \xi + D(\xi)}}{2\rho}. \quad (1.14)$$

The phase velocity of a shear wave with the vertical polarization direction is expressed by:

$$v_{SV}(\xi) = \frac{\sqrt{C_{33} + C_{44} + (C_{11} + C_{33}) \cos^2 \xi - D(\xi)}}{2\rho}. \quad (1.15)$$

The symbol $D(\xi)$, used in expressions for phase velocities of P and SV waves, denotes:

$$D(\xi) \equiv \sqrt{(C_{33} - C_{44})^2 + 2[2(C_{13} + C_{44})^2 - (C_{33} - C_{44})E] \cos^2 \xi + [E^2 - 4(C_{13} + C_{44})^2] \cos^4 \xi} \quad (1.16)$$

Another useful symbol is:

$$E \equiv (C_{11} + C_{33} - 2C_{44}). \quad (1.16a)$$

The phase velocity of a shear wave polarized in the horizontal direction is expressed by:

$$v_{SH}(\xi) = \frac{\sqrt{C_{66} \cos^2 \xi + C_{44} \sin^2 \xi}}{\rho}. \quad (1.17)$$

The angle ξ is the phase angle, measured with respect to the horizontal, i.e., the phase-latitude angle. The convention, contrary to most geophysical descriptions where the phase angle is measured with respect to the vertical, i.e., colatitude, was chosen in order to facilitate the use of standard expressions of vector calculus in polar coordinates in subsequent chapters of the dissertation. When, in this dissertation, the phase colatitude is used it is clearly stated and denoted by a symbol ϑ .

1.3. THE OBJECTIVE OF THE WORK

The objective of the work is to investigate several aspects of elastic-wave propagation in anisotropic media. Since layered sedimentary rocks are of special interest to a petroleum geophysicist, the investigation of phenomena at a planar horizontal interface between two media is given particular attention. The primary goal of this dissertation is to provide an approach offering a better understanding of physics of anisotropic media as observed through elastic waves. For this reason a special effort is made to express physical quantities in terms of analytical formulæ. To remain within the realm of analytical expression one must, at times, resort to some simplification. This dissertation provides a thorough investigation of a very convenient *weak-anisotropy approximation* (Thomsen, 1986).

The investigation of the Earth's interior through seismic studies is primarily based on the measurement of traveltimes of a wave travelling between a source and receiver. Travelpath, traveltimes and velocity of the ray are interrelated, in general, by an underdetermined system of equations. One of the key problems for a geophysicist performing the measurements on, or near, the surface of the Earth is to use the traveltimes information to deduce both the raypath and the velocities of the propagating ray in various layers of the medium. This is an inverse problem for which, in general, no unique solution exists, i.e., the observed data can be satisfied by numerous different models. The problem is complicated further if the speed of the ray travelling through a medium varies with direction, i.e., if the medium is anisotropic. In a series of anisotropic layers separated by interfaces, the traveltimes depends directly on the ray (group) velocity of the medium. The travelpath is governed by Snell's law depending directly on phase velocities.

The incorporation of anisotropic phenomena into geophysical investigation provides two major benefits. Firstly, anisotropic characteristics of a material are indicative of its composition and its state. For instance, a material composed of fine laminae, much smaller in thickness than the wavelength of a propagating signal, exhibits a particular anisotropic behaviour. Also, fracturing of a material with the particular

orientation of cracks due to stresses results in anisotropic effects. Secondly, since, in general, anisotropy affects the traveltimes, the accurate reconstruction of the subsurface based on the traveltimes observations requires the knowledge of anisotropic parameters. Thus, in the geophysical context, the study of anisotropy is important for both lithology information, and imaging of the subsurface.

Ray theory, derived originally from geometrical optics, is an elegant and powerful method for investigating wave propagation. In this dissertation, prior to approaching an inverse problem, a new forward method is considered. Given a medium composed of anisotropic layers with known properties, a method of raytracing between a given source and receiver is proposed. The result of this method is the computed traveltimes and the raypath. Once a reliable method of forward modelling has been elaborated and tested both numerically and experimentally (Chapters II - VII), an inverse solution is derived (Chapter VIII). The result of this method is the computation of anisotropic parameters of a stratified medium based on the measured traveltimes. A more detailed synopsis of the dissertation is given below.

Firstly, a new formalism of Snell's law for anisotropic media in terms of vector calculus is derived (Chapter II). The formalism is described, for the ease of vector calculus operations, in terms of Cartesian coordinates. Based on this formalism several key attributes of an elastic wave can be given in both incidence and transmission media. The description includes phase and group angles, as well as magnitudes of phase and group velocities. The relationship between various quantities constitutes an important aspect of comprehending elements of anisotropic wave propagation.

This general formalism is adapted for use in raytracing based on approximate (weak anisotropy) expressions for slowness surfaces in anisotropic media. Initially the method is developed under the assumption that the incident ray propagates through an isotropic layer (Chapter III). This assumption, which implies the equivalence of phase and group velocities in the medium of incidence, allows an initialization of the process by relating the direction of propagation of the group-velocity vector to the continuity conditions expressed with respect to the phase-velocity vector. Also, in Chapter III the formalism developed in the previous chapter in terms of Cartesian coordinates is

translated to polar coordinates. This allows for ease in expressing various quantities with respect to the angle of propagation.

A raytracing scheme for a stack of horizontal anisotropic layers is developed in Chapter IV, leading to the traveltimes calculations (Chapter V). The relationship of modelling results between the approach using the anisotropic formalism of Snell's law and the direct approach using Fermat's principle of stationary time is discussed. Snell's law, of course, can be viewed as a consequence of Fermat's principle. In raytracing through anisotropic media, the relative equivalence of two approaches forms an important verification of the methods since the Snell approach relies directly on the concept of phase velocity, while the Fermat approach relies on the concept of group velocity.

Chapter VI introduces the formalism of Snell's law with the angle of transmission given in terms of the angle of incidence for a boundary between two anisotropic media. This means that one does not benefit from the facility provided by the coincidence of phase and group velocities in the medium of incidence. The results of this chapter, which can be viewed as an extension of the treatment presented in Chapter III, provide further insight into the concept of Snell's law and Fermat's principle of stationary time, as well as into consequences of approximations and linearizations.

Chapter VII deals with the physical measurement performed in the laboratory with a medium composed of an isotropic and an anisotropic layer separated by a planar interface. The results of physical modelling provide a comparison of numerical forward modelling and actual experimental measurements. The results of physical modelling are also used in the inversion process (Chapter VIII).

Chapter VIII introduces an innovative way of inverting traveltimes information from a seismic experiment to yield the anisotropic parameters of a stack of horizontal layers through which the ray propagates. The method is explicitly derived for shear waves with transverse direction of polarization, and for any other waves exhibiting an elliptical velocity dependence.

In this dissertation, which aims at understanding certain aspects of anisotropic wave propagation, many peripheral or esoteric concepts and investigations,

delegated to appendices, constitute an important part of the whole work. Thus, the reader, is asked not to ignore them.

Appendix 1 investigates a concept of a quartic equation relating, for compressional (P) waves, ray parameter and phase angle under the weak-anisotropy assumption. It is observed that the concept can be illustrated as an intersection of a curve and a straight line. The curve remains constant for a given medium and hence is termed *the characteristic biquadratic*. The straight line always passes through the origin while its slope depends on the angle of incidence.

Phase-slowness surfaces or curves form a kernel of anisotropic Snell's law and therefore influence all subsequent calculations. The only major mathematical simplification used in this dissertation consists of employing simplified expressions of phase slowness curves under the assumption of weak anisotropy (Thomsen, 1986). In Appendix 2 a comparison of slowness curves generated using exact and approximate equations is illustrated.

Although the spirit of this dissertation is to remain within the realm of analytical expressions, some exceptions could not be avoided. Calculation of roots of a polynomial expression or of a take-off angle in raytracing between a source and receiver in a multilayer medium are examples of such instances. Appendix 3 investigates the numerical precision of such computation using the mathematical software Mathematica®.

Appendix 4 contains a mathematical proof based on the implicit function theorem. The proof relates to the method of inversion described in Chapter VIII. It demonstrates the necessity of existence of a physical solution at a unique point of a mathematical solution space which forms the crux of the aforementioned inversion method.

The inversion method derived in Chapter VIII applies only to SH waves or other waves with elliptical velocity dependence. Appendix 5 contains some attempts at approximate estimation of anisotropic parameters for P and SV waves.

Equations derived under the concept of weak anisotropy can be simplified further by full linearization (Thomsen, 1986). Appendix 6 illustrates that, although by using the initial simplification, i.e., truncation of higher-order terms in expressions for phase velocities (or slownesses), one does not lose fundamental physical attributes of

anisotropic wave propagation, those attributes can be lost in subsequent steps by employing linearized expressions. It is further demonstrated that the initial use of the weak-anisotropy approximation, which greatly facilitates the application of the formalism of anisotropic Snell's law, followed in subsequent steps by exact (or at least not fully linearized) expressions for group velocity and group angles, constitutes a preferable approach. It is not insinuated here that the initial loss of accuracy, however small, can be recovered, but that no loss of physical attributes results.

Appendix 7 provides a starting point for developing an anisotropic form of Snell's law using the exact equations of Daley and Hron (1977). The exact equations for slowness curves, analogous in meaning and equivalent in form to those used in the dissertation, are also shown.

CHAPTER **II**

REFLECTION AND TRANSMISSION ANGLES IN ANISOTROPIC MEDIA¹

2.0. INTRODUCTION

The mathematical description of phenomena related to wave propagation in anisotropic media is considerably more complicated than that for isotropic media. This complexity stems from the many physical properties distinguishing the anisotropic from the isotropic medium. This chapter presents a method of calculating the angles of reflection and transmission for a ray impinging on a boundary between two anisotropic media. The innovation of the method introduced in this chapter consists in providing a rather general analytical formalism for calculating the ray (group) angles at discontinuities between anisotropic media. This formalism is then used, in Chapter III, for a weakly anisotropic medium yielding several useful equations, and leading, through the raytracing method, to an inversion scheme presented in Chapter VIII.

For an interface between two isotropic media the relationship among all the angles is elegantly and concisely described by the classical form of Snell's law, i.e.,

$$\frac{\sin \vartheta_i}{v_1} = \frac{\sin \vartheta_r}{v_1} = \frac{\sin \vartheta_t}{v_2}, \quad (2.1)$$

¹ This chapter is based on work published by Slawinski M.A., and Slawinski R.A. in CREWES Research Report (1994).

where θ 's with, respectively, subscripts i , r and t , correspond to incident, reflected and transmitted waves and v_1 and v_2 are the velocities in the two media, 1 and 2, which are separated by a planar interface.

In general, the inclusion of anisotropy renders the mathematical formulation quite complicated. Snell's law is not an exception and the calculation of reflection and transmission angles is not a trivial task². A graphical approach to calculating reflection and transmission angles for anisotropic media is presented by Auld (1973) and Rokhlin et al. (1986). Rokhlin et al. (1986) also outline a numerical scheme using tensor equations. Daley and Hron (1977, 1979) derive Snell's law in the particular cases of transversely isotropic and ellipsoidally anisotropic media. This chapter seeks to express the concept of incidence, reflection and transmission angles using the intuitively clear mathematical apparatus of vector calculus in a rather general case.

Although it lies beyond the scope of this chapter to provide a thorough overview of numerous physical phenomena in anisotropic media, it can be stated that two aspects of physical properties inherent in wave propagation in anisotropic media are responsible for the more complicated formulation than in the isotropic case. Firstly, the velocity of the ray depends on direction and thus, for instance, the velocity of the incident ray is, in general, unequal to the velocity of the unconverted reflected ray, although both rays propagate in the same medium. This means that, in general, the angle of incidence is not equal to the angle of reflection, even when the wave type is unchanged. This consequence is analogous to the phenomena observed in studying converted waves exhibiting different velocities for incident and reflected rays. Secondly, both group and phase velocities, \mathbf{w} and \mathbf{v} , have to be considered in studying wave propagation in anisotropic media. The two are related (e.g., Rokhlin et al., 1986) by the formula:

$$\mathbf{w} \cdot \mathbf{k} = |\mathbf{v}| = v, \quad (2.2)$$

² Note that the “standard” form of Snell’s law still holds in anisotropic media for phase velocities and phase angles.

where \mathbf{k} is the wave normal, i.e., the unit vector perpendicular to lines of constant phase, or in other words, pointing in the direction of the phase velocity, \mathbf{v} . From the definition of the dot product it follows immediately that:

$$|\mathbf{w}|\cos(\theta - \vartheta) = |\mathbf{v}| \equiv v, \quad (2.3)$$

where $(\theta - \vartheta)$ represents the difference between phase and group angles. i.e., the angle between \mathbf{w} and \mathbf{v} .

2.1. IMPORTANT CONCEPTS

In formulating the method for calculating reflected and transmitted angles at an interface between isotropic and anisotropic media, it is helpful to restate certain basic concepts. The intention is not to present those concepts in a rigorous and complete way but to invoke those aspects which are most useful for the task at hand. The concepts in question include: phase and group velocities, refraction/reflection laws and phase-slowness surfaces.

2.1.1. Phase and group velocities

Phase velocity is defined as the velocity with which plane-wave crests and troughs travel through a medium and is expressed as the ratio of the frequency of vibration and the wave number (i.e., the number of wavelengths per unit distance normal to the wavefronts). Group velocity, also known as energy or ray velocity, is defined as a velocity with which the energy of a wave propagates³. Direct measurements of traveltime usually yield the group velocity.

In dispersive media, e.g., an anelastic medium exhibiting frequency dispersion or an anisotropic medium exhibiting angular dispersion, phase and group velocities are different; both in magnitude and direction. For an anisotropic medium, at the same point

on the wavefront, the group velocity is higher than the phase velocity. The direction of the group velocity is perpendicular to the phase-slowness surface, i.e., to the surface representing the inverse of the phase-velocity surface (Rokhlin et al, 1986). Also, the phase velocity is perpendicular to the wave surface (Helbig, 1994). As a matter of fact, both above-mentioned statements are equivalent.

2.1.2. Snell's law

Snell's law is a direct consequence of Fermat's principle of stationary time. In horizontally layered media, it can be conveniently restated as a requirement for the horizontal component of the wave number, k_x , to be continuous across the boundary. As a matter of fact, the horizontal component of the wave number remains constant for all layers and is analogous to the ray parameter. This property must be preserved for both isotropic and anisotropic media regardless of the type of the wave generated at the boundary, e.g., longitudinal or transverse, and serves as a kernel for the strategy of calculating reflected and transmitted angles. A description of physical principles involved in Snell's law with emphasis on anisotropic media is given by Helbig (1994) on pages 32 to 38.

2.1.3. Slowness surfaces

Phase-slowness is defined (e.g., Winterstein, 1990) as the reciprocal of the scalar phase velocity, and therefore can be expressed as the ratio of wave number, k , and angular frequency, ω . In an isotropic medium the phase-slowness surface is a sphere with radius equal to the inverse of the phase velocity (which does not vary with direction). In such a case, phase and group velocities are collinear since the normal to the surface of a sphere is collinear with its radius vector. For an anisotropic medium the shape of the phase-slowness surface can form a much more complicated figure including concave and convex shapes. The number of symmetry planes decreases as the number of elastic constants necessary to describe the material increases. An infinite number of symmetry

³ In dissipative, anisotropic media, i.e., media which are not perfectly elastic, the notions of group and energy velocity do not coincide (Carcione, 1992). Other physical restrictions might also apply (e.g., Krebes and Le, 1994)

planes exist for an isotropic medium described by two elastic constants, e.g., Lamé parameters; no symmetry planes exist for a triclinic medium which requires twenty-one elastic constants to be uniquely characterized (see e.g., Crampin and Kirkwood, 1981).

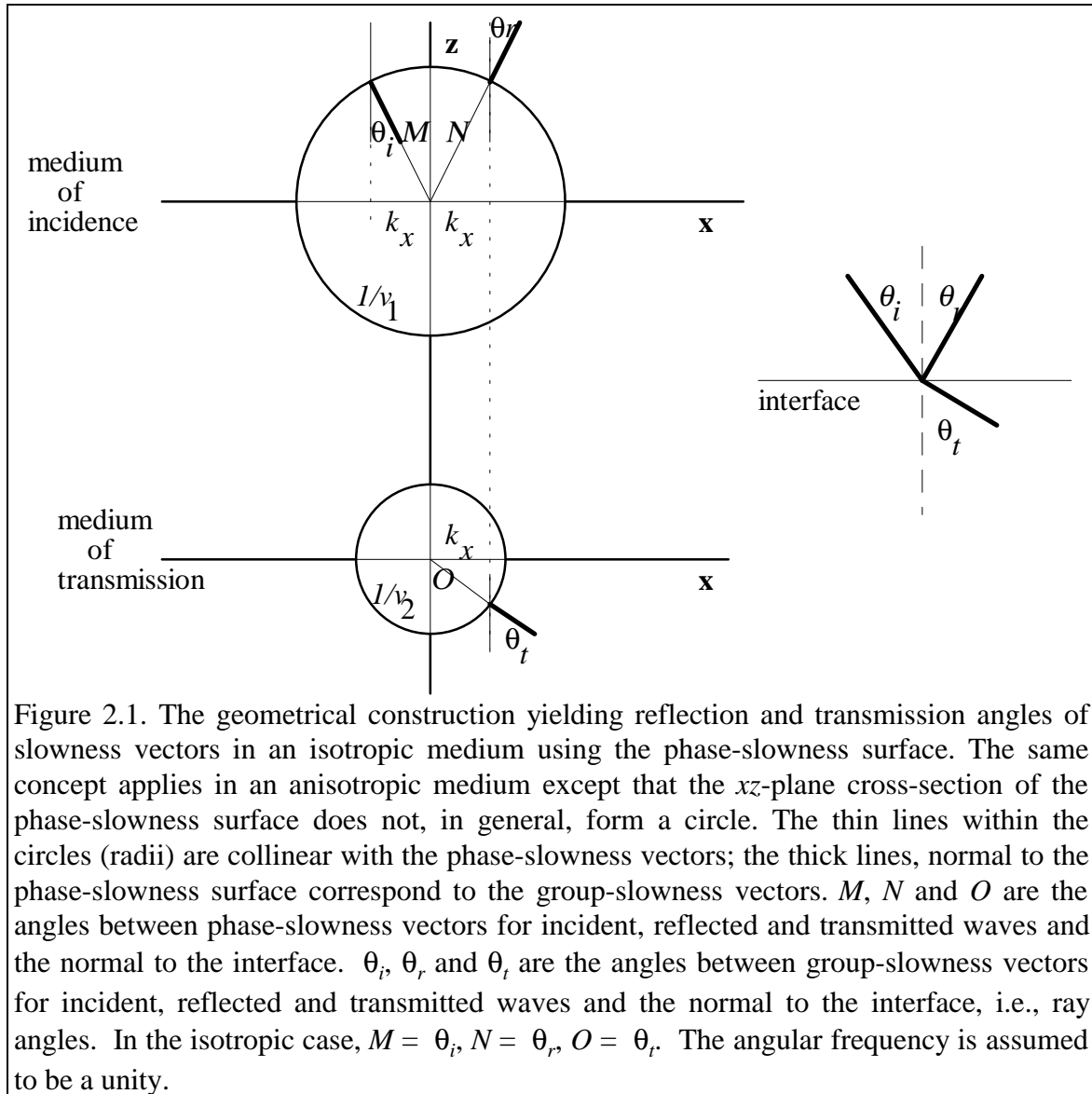
There are, in general, three slowness surfaces, each corresponding to a given wave type: one for quasi-compressional and two for quasi-shear waves. The quasi-shear-wave slowness surfaces can touch or intersect, thus forming singularities, i.e., points corresponding to orientations along which qS phase velocities become equal for two wave types. Interesting phenomena relating to polarization occur in the neighbourhood of those points (Crampin and Yedlin, 1981).

2.2. GEOMETRICAL FORMULATION

Snell's law can be illustrated using phase-slowness surfaces for both incident and transmitted media (Auld, 1973). The geometrical construction is facilitated by the fact that the phase-slowness vectors of the incident, reflected and refracted waves are coplanar. Their being coplanar is guaranteed by the necessity to satisfy boundary conditions at all times and at every point of the interface. Therefore, it is convenient to choose a Cartesian coordinate system such that all the phase-slowness vectors lie in the xz -plane. To familiarize the reader with the method, the familiar case of isotropic media is considered below.

Invoking the continuity of the horizontal component of the wave number, k_x , across a boundary, and by applying simple trigonometry to Figure 2.1, it is easy to obtain the usual form of Snell's law for an isotropic medium, i.e., equation (2.1). Other concepts, such as total internal reflection, also have their geometrical interpretation. For a sufficiently large incidence angle one has $k_x \geq \omega/v_2$, in which case no transmitted ray is possible. The equality $k_x = \omega/v_2$ yields the angle at which this first occurs, i.e., the critical angle. Note that if the radius of the phase-slowness sphere in the transmitted medium is larger than in the incident medium, there is always a transmitted ray and total internal reflection cannot occur. For anisotropic media, each phase-slowness surface is, in general, described by a different function and the phase- and group-velocity angles do not coincide. To deal with a more complex situation, a more complicated mathematical

scheme has to be employed. Figure 2.1, without loss of generality, illustrates a generic case, i.e., the wave type is not specified. Consideration of mode conversion would yield, in an isotropic case, two concentric circles in both media, representing phase-slowness surfaces for compressional and shear waves. In an anisotropic case three geometrical figures would appear in each medium due to the birefringence of quasi-shear waves, i.e., due to different velocities of two types of quasi-shear waves.



2.3. MATHEMATICAL FORMULATION

The geometrical approach described above for the isotropic case (i.e., spherical slowness surfaces) is easily extended to include more general scenarios, where the slowness surface is an arbitrary surface in slowness space. Although there exist more efficient computational schemes, e.g., Keith and Crampin (1976), Rokhlin et al. (1986), the following analytical description provides an intuitive insight which is lost in various numerical methods.

Consider two anisotropic media separated by a planar, horizontal interface. Let the phase-slowness surface in the upper medium be given by the *level surface*⁴ of a function $f(x, y, z)$, in a slowness space spanned by Cartesian coordinates x , y , and z :

$$f(x, y, z) = a. \quad (2.4)$$

Similarly, let the phase-slowness surface in the lower medium be given by the level surface of a function $g(x, y, z)$,

$$g(x, y, z) = b. \quad (2.5)$$

A ray is incident on the boundary from above. Since all phase-slowness vectors (for incident, reflected and transmitted waves) must be coplanar, without loss of generality we take them to lie in the xz -plane (see Figure 2.2). Denoting the phase-slowness vector as \mathbf{m} , the continuity conditions require that:

$$\mathbf{m}_i \cdot \bar{\mathbf{x}} = \mathbf{m}_r \cdot \bar{\mathbf{x}} = \mathbf{m}_t \cdot \bar{\mathbf{x}}, \quad (2.6)$$

where $\bar{\mathbf{x}}$ is a unit vector in the x -direction and subscripts i , r , and t refer to incident, reflected and transmitted waves respectively. Recall that the group(ray)-slowness vector, \mathbf{w} , is normal to the phase-slowness surface at the corresponding phase-slowness point. A

detailed description of geometrical relationships and their physical basis is given by Helbig (1994) on pages 21 to 29.

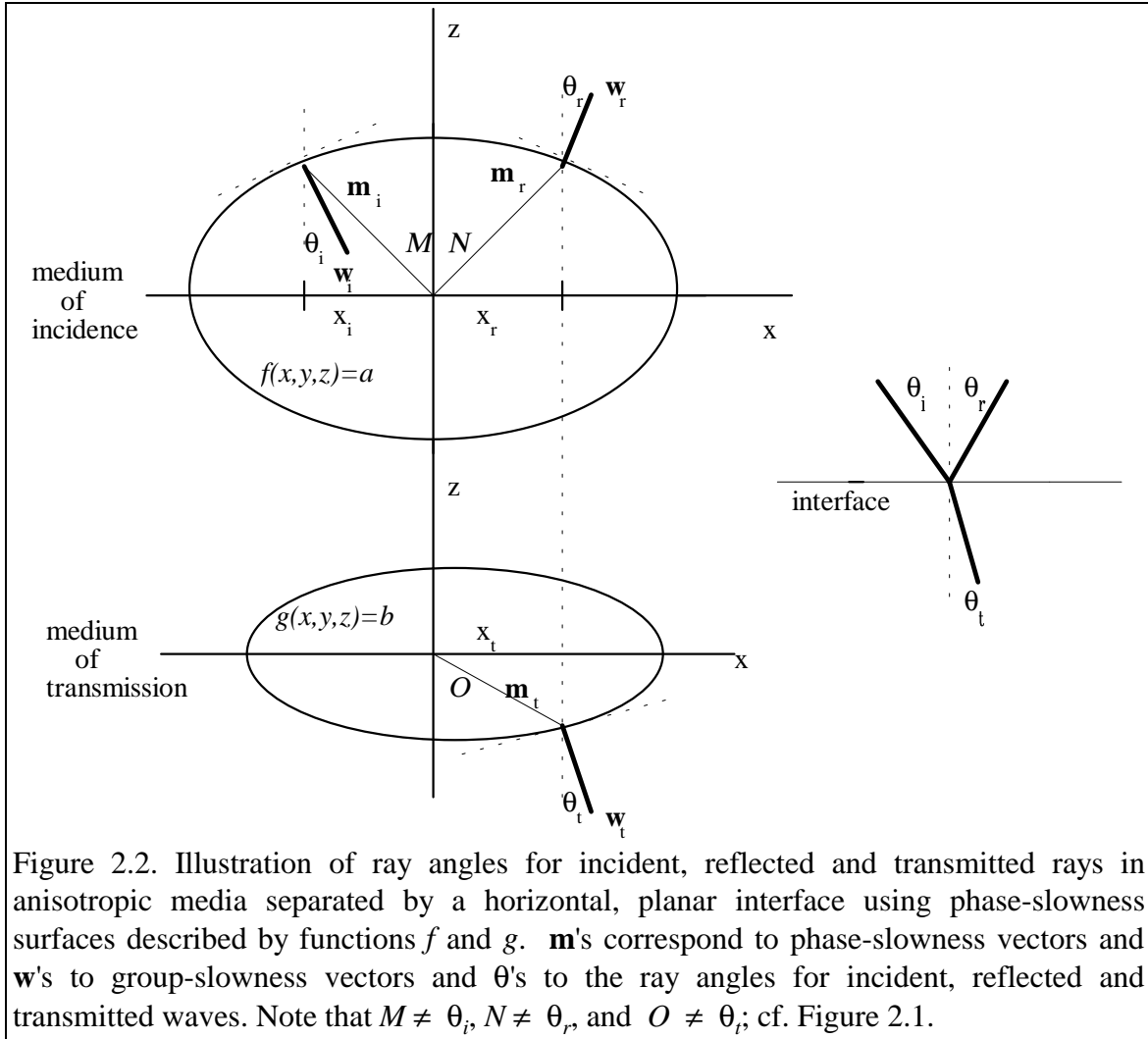


Figure 2.2. Illustration of ray angles for incident, reflected and transmitted rays in anisotropic media separated by a horizontal, planar interface using phase-slowness surfaces described by functions f and g . \mathbf{m} 's correspond to phase-slowness vectors and \mathbf{w} 's to group-slowness vectors and θ 's to the ray angles for incident, reflected and transmitted waves. Note that $M \neq \theta_i$, $N \neq \theta_r$, and $O \neq \theta_t$; cf. Figure 2.1.

Using properties of the gradient, i.e., its pointing in the direction along which f is increasing the fastest and its being normal to the surface on which f is constant, gives:

$$\mathbf{w}_i \parallel \nabla f(x, y, z)|_{(x_i, y_i, z_i)}. \quad (2.7)$$

⁴ The *level set of value a* is defined to be those points at which $f(x, y, z) = a$. For the case of three variables, one speaks of *level surface* or *equipotential surface*. For the case of two variables, one speaks of *level curve* (e.g., Marsden and Tromba, 1981).

i.e., the ray vector, \mathbf{w} , is parallel to the gradient. Normalizing, and choosing the function f to have a minimum at the origin $O(0,0,0)$ and to be monotonically increasing outwards, yields:

$$\bar{\mathbf{w}}_i = -\frac{\nabla f(x, y, z)|_{(x_i, y_i, z_i)}}{\|\nabla f(x, y, z)|_{(x_i, y_i, z_i)}\|}, \quad (2.8)$$

where the negative sign ensures that the incident unit ray, $\bar{\mathbf{w}}_i$, vector points towards the boundary. The angle of incidence, i.e., the angle between the ray vector and the normal to the interface is given by:

$$\cos \theta_i = \bar{\mathbf{w}}_i \cdot (-\bar{\mathbf{z}}) = \frac{\bar{\mathbf{z}} \cdot \nabla f(x, y, z)|_{(x_i, y_i, z_i)}}{\|\nabla f(x, y, z)|_{(x_i, y_i, z_i)}\|} = \frac{\frac{\partial f}{\partial z}|_{(x_i, y_i, z_i)}}{\|\nabla f(x, y, z)|_{(x_i, y_i, z_i)}\|} \quad (2.9)$$

where $\bar{\mathbf{z}}$ is the unit vector parallel to the z-axis.

Now by choice of the coordinate system, $y_i = 0$; given x_i , z_i is determined by equation (2.4). Thus equation (2.4) provides an expression for θ_i as a function of x_i . Typically θ_i is taken as an independent parameter; however, it may not always be possible to invert equation (2.4) to obtain a closed-form expression for x_i as a function of θ_i . Thus, in the general case, as already emphasized the present approach is presented chiefly for the intuitive understanding it provides, rather than for its computational convenience. In specific cases, illustrated in subsequent chapters, it is always possible to express reflected and transmitted angles as functions of the incidence angle.

Similarly, the normalized reflected ray vector can be expressed as:

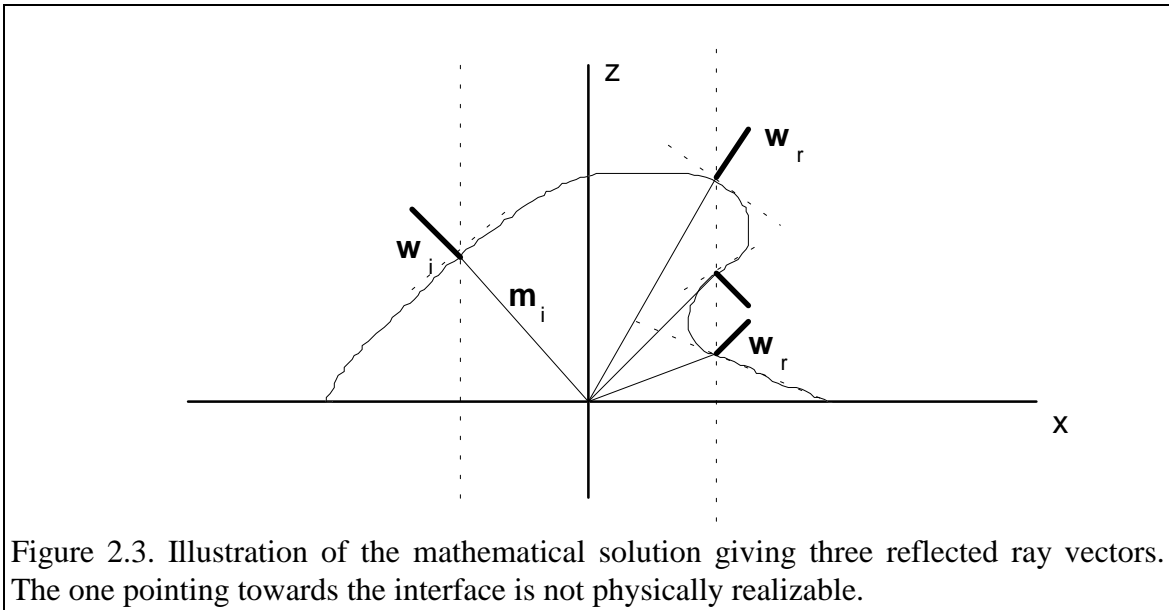
$$\bar{\mathbf{w}}_r = \frac{\nabla f(x, y, z)|_{(x_r, y_r, z_r)}}{\|\nabla f(x, y, z)|_{(x_r, y_r, z_r)}\|}, \quad (2.10)$$

and the angle of reflection, i.e., the angle between the ray vector and the normal is given by:

$$\cos \theta_r = \frac{\bar{\mathbf{w}}_r \cdot \bar{\mathbf{z}}}{|\bar{\mathbf{w}}_r| |\bar{\mathbf{z}}|} = \frac{\bar{\mathbf{z}} \cdot \nabla f(x, y, z)|_{(x_r, y_r, z_r)}}{|\nabla f(x, y, z)|_{(x_r, y_r, z_r)}} = \frac{\frac{\partial f}{\partial z}|_{(x_r, y_r, z_r)}}{|\nabla f(x, y, z)|_{(x_r, y_r, z_r)}}. \quad (2.11)$$

In evaluating the above expression one uses the fact that by continuity $x_r = -x_i$; y_r is zero by the choice of the coordinate system, and z_r can be found by substituting into equation (2.4). Recall that x , y and z are components of slowness while subscripts i and r refer to incidence and reflection.

Physically, we require that the reflected ray be directed back into the incident medium; thus the physical solutions must have $\bar{\mathbf{w}}_r \cdot \bar{\mathbf{z}} \geq 0$. Note that the reflected ray need not be unique: given the slowness surface in Figure 2.3, for instance, we have two physical reflected solutions and one non-physical solution.



The normalized transmitted ray vector is given by:

$$\bar{\mathbf{w}}_t = \frac{\nabla g(x, y, z)|_{(x_t, y_t, z_t)}}{|\nabla g(x, y, z)|_{(x_t, y_t, z_t)}}, \quad (2.12)$$

and thus the angle of the transmitted ray measured between the transmitted ray vector and the normal is given by:

$$\cos \theta_t = (-\bar{\mathbf{z}}) \cdot \bar{\mathbf{w}}_t = -\frac{\bar{\mathbf{z}} \cdot \nabla g(x, y, z)|_{(x_t, y_t, z_t)}}{|\nabla g(x, y, z)|_{(x_t, y_t, z_t)}} = \frac{\frac{\partial g}{\partial z}|_{(x_t, y_t, z_t)}}{|\nabla g(x, y, z)|_{(x_t, y_t, z_t)}}. \quad (2.13)$$

Again, as in equation (2.11), in evaluating the above expression one uses the fact that $x_t = -x_i$; y_t is zero by the choice of the coordinate system and z_t can be found by substituting into equation (2.5). Similar comments to the ones discussed in the case of reflected waves apply to physical realizability and uniqueness of transmitted rays; the only difference in the latter case is that one requires the rays to be directed into the transmitted medium, i.e., physical solutions must have $\bar{\mathbf{w}}_t \cdot (-\bar{\mathbf{z}}) \geq 0$.

It must be emphasized that, although the phase-slowness vectors, \mathbf{m} , are coplanar for the incident, reflected and transmitted waves, the ray vectors, \mathbf{w} , need not lie in the same plane. Their directions are determined by that of the normal to the plane tangent to the phase-slowness surface. They will, however, remain in the same plane if the phase-slowness surfaces are, for instance, rotationally symmetric about the x -axis. In all cases the magnitude of the ray velocity is obtained from equation (2.2).

If the phase-slowness surface does not possess rotational symmetry, the incident, reflected and transmitted group vectors need not be coplanar. In such a case the angle of deviation, χ , from the sagittal plane assumed to coincide with the xz -plane, containing all phase vectors, \mathbf{m} , can be found by considering the projection, \mathbf{w}_{xz} , of the ray vector, \mathbf{w} , on this plane:

$$\mathbf{w}_{xz} = [\mathbf{w} \cdot \mathbf{x}, 0, \mathbf{w} \cdot \mathbf{z}], \quad (2.14)$$

and thus from the definition of scalar (dot) product, it follows that:

$$\cos \chi = \frac{\mathbf{w} \cdot \mathbf{w}_{xz}}{|\mathbf{w}| |\mathbf{w}_{xz}|}. \quad (2.15)$$

The above formulation can be easily adapted to be used specifically for incident, reflected, or transmitted rays. Other concepts, such as total internal reflection, also emerge naturally from the present formulation. Although for complicated slowness surfaces it may be impossible to characterize total internal reflection by a single critical angle as in the isotropic case, the general approach remains as described above.

2.4. EXAMPLES

The approach described above can be illustrated by several examples. Some cases allow simple analytical solutions leading to valuable physical insight.

2.4.1. General case of elliptical anisotropy

Consider the ellipsoidal case where the velocities are different in the x , y and z directions and where xz -, xy -, and yz -planes constitute symmetry planes. Considering the xz -plane, the two phase-slowness surfaces can be written as:

$$f(x, z) = (v_x x)^2 + (v_z z)^2 = 1, \quad (2.16)$$

and

$$g(x, z) = (v'_x x)^2 + (v'_z z)^2 = 1, \quad (2.17)$$

for the media of incidence and transmission respectively. Again, without loss of generality, one can treat a generic case, i.e., not specifying the type of conversion at the interface.

Using equation (2.8) one can write:

$$\bar{\mathbf{w}}_i = -\frac{[v_x^2 x_i, v_z^2 z_i]}{\sqrt{(v_x^2 x_i)^2 + (v_z^2 z_i)^2}}, \quad (2.18)$$

and by equation (2.9):

$$\cos \theta_i = \frac{v_z^2 z_i}{\sqrt{(v_x^2 x_i)^2 + (v_z^2 z_i)^2}}. \quad (2.19)$$

Solving for z in equation (2.16) yields:

$$z_i = \frac{\sqrt{1 - (v_x x_i)^2}}{v_z}, \quad (2.20)$$

in the case of the incident ray. Substituting equation (2.20) into equation (2.19) gives:

$$\cos \theta_i = \frac{v_z \sqrt{1 - (v_x x_i)^2}}{\sqrt{v_x^4 x_i^2 + v_z^2 [1 - (v_x x_i)^2]}}, \quad (2.21)$$

which can be explicitly solved for x_i^2 :

$$x_i^2 = \frac{v_z^2 (1 - \cos^2 \theta_i)}{v_x^4 \cos^2 \theta_i + v_x^2 v_z^2 (1 - \cos^2 \theta_i)}. \quad (2.22)$$

Analogous expressions can be derived for reflected and transmitted rays. Furthermore, since $x_i^2 = x_r^2 = x_t^2$, the three expressions can be equated, thus giving Snell's

law for ellipsoidally anisotropic media. Upon some algebraic manipulation this can be expressed as:

$$v_x'^2 \left[\frac{v_x'^2}{v_z'^2} \cot^2 \theta_i + 1 \right] = v_x'^2 \left[\frac{v_x'^2}{v_z'^2} \cot^2 \theta_r + 1 \right] = v_x'^2 \left[\frac{v_x'^2}{v_z'^2} \cot^2 \theta_t + 1 \right], \quad (2.23)$$

where primed quantities refer to the medium of transmission. Equivalent expressions for Snell's law with elliptical velocity dependence were obtained by Dunoyer de Segonzac and Laherrere (1959) directly from elliptical geometry, and successfully used in studying anisotropy in well-bore seismic in the Sahara desert. For further discussion on geophysical applications of elliptical anisotropy see Chapter IV. Examining equation (2.23) we see that $\theta_r = \theta_t$. Also, the critical angle can be obtained by setting $\theta_t = \pi/2$. After some algebraic manipulation one gets:

$$\cot \theta_c = \frac{v_z}{v_x} \sqrt{\frac{v_x'^2}{v_x^2} - 1}. \quad (2.24)$$

For isotropic media one can write:

$$v_x = v_z = v_1, \quad (2.25)$$

and:

$$v_x' = v_z' = v_2. \quad (2.26)$$

Equation (2.23) then reduces to equation (2.1), i.e., the standard form of Snell's law in isotropic media and equation (2.24) to the standard expression for the critical angle in the isotropic medium.

2.4.2. A particular case of isotropic/anisotropic interface

Let us consider a planar boundary between the isotropic and elliptically anisotropic media. Let the velocities be so chosen that:

$$v_x = v_z \equiv v = v'_x, \quad (2.27)$$

i.e., the horizontal velocity in the anisotropic medium equals the velocity in the isotropic medium. Using Equation (2.23) gives:

$$\tan \theta_t = \frac{v}{v'_z} \tan \theta_i. \quad (2.28)$$

An interesting phenomenon can be observed by examining equation (2.28). To observe the phenomenon more clearly we can write:

$$\frac{\tan \theta_t}{\tan \theta_i} = \frac{v}{v'_z}. \quad (2.29)$$

Thus if $v'_z > v$, $\theta_i > \theta_t$ and the transmitted ray is bent towards the normal, which is the opposite of what happens in the isotropic case. This phenomenon is related to the complicated form Fermat's principle takes in the anisotropic case, as discussed below, and more extensively in Chapter VI.

2.5. DISCUSSION

Numerous physical consequences can be described using the approach presented above. First of all, however, mathematical solutions stemming from this formulation must be examined in the light of physical realizability. The ray vector for an incident ray must be pointing towards the boundary, while for reflected and transmitted rays must point

away from it. This physically intuitive requirement is not satisfied naturally by the mathematical formalism. Employing either the numerical approach stemming from tensor analysis (Rokhlin et al., 1986) or the analytical approach described above, one must select correct ray vectors and reject the ones which fail to satisfy the obvious physical requirements.

As already mentioned above, an interesting phenomenon related to Fermat's principle of stationary time can be particularly easily observed by applying the small-angle approximation to equation (2.23):

$$\theta_t \approx \frac{v_x'^2}{v_x^2} \frac{v_z}{v_z'} \theta_i. \quad (2.30)$$

This phenomenon is not restricted to small-angle cases and the approximation was used only for clarity of notation.

In the isotropic case if, say, the velocity in the medium of transmission is greater than in the medium of incidence, we obtain the familiar result that the transmitted ray is bent away from the normal. However in the particular case of an isotropic/anisotropic interface considered in equation (2.29), we obtain the opposite result. Equation (2.30) gives the behaviour in the case of general ellipsoidal anisotropy.

The behaviour in the isotropic case may be intuitively understood as being the consequence of Fermat's principle of stationary time; the behaviour in the particular anisotropic case, considered in equation (2.29), appears counterintuitive when viewed from this point of view. However, the form of Fermat's principle in the general anisotropic case can be formulated as (Helbig, 1994):

$$\delta \int \mathbf{m} \cdot d\mathbf{w} = \delta \int \mathbf{m}_w \cdot d\mathbf{w} = 0 \quad (2.31)$$

where \mathbf{m} is the phase-slowness vector, \mathbf{m}_w is the ray-slowness vector and $d\mathbf{w}$ is a length element along the ray. Thus in deriving Snell's law we are minimizing the traveltime along the ray with respect to the group (ray) velocity, rather than the phase velocity. As a consequence, the group- (ray-) slowness surface as well as the phase-slowness surface

must be considered in order to understand the behaviour of the ray at the interface. Therefore, in the general anisotropic case, ray bending does not lend itself to such an intuitive understanding as in the isotropic case. In the latter case, the phase and group velocities are collinear, and the ray bending away from the normal when it passes from a slower to a faster medium is easily understood as a consequence of Fermat's principle which favours shortening the distance travelled by the ray in the slower medium.

An elegant and rigorous proof of Fermat's principle in elastodynamics has been established by Epstein and Sniatycki (1992). The authors elaborate the proof based on Hamiltonian constraints and homogeneous Lagrangians. This proof, however, applies only to convex slowness surfaces, since Fermat's principle can only be formulated for such cases. For slowness surfaces with concave sections, the singularities of the inflection point create insurmountable difficulties (A. Hanyga, pers. comm., 1996).

The usefulness of the above approach is extended in the next chapter where the Snell's law formalism is expressed in polar coordinates and thus can be conveniently related to slowness surfaces of various materials.

CHAPTER III

SNELL'S LAW⁵ FOR WEAKLY ANISOTROPIC MEDIA⁶

3.0. INTRODUCTION

In Chapter II a Snell's law formalism for anisotropic media is presented. All expressions are exact and can be applied in many circumstances. The fact that the phase slowness surface is smooth and never has cusps (Winterstein, 1990) ensures the applicability of vector calculus methods required by the formalism. The direct use of the formalism presented in Chapter II requires that the slowness surfaces be expressible in slowness space as analytic functions of three Cartesian coordinates x , y , and z . Slowness surfaces are three-dimensional closed surfaces of various degrees of symmetry, reducing in the isotropic case to the shape of a sphere. The choice of spherical coordinates for description of slowness surface, or polar coordinates for description of slowness curve, is natural. Thus, instead of directing one's efforts towards developing a method of expressing slowness surfaces or curves in Cartesian coordinates, or as parametric plots, another method is adopted. The formalism developed in Chapter II serves as a template for linking, through the relation between Cartesian and polar coordinates, the analytical method for calculating angle of transmission across an interface, with actual measures of

⁵ The term "Snell's Law" is used, in this dissertation, to denote formulæ dealing with incident, reflected and transmitted angles in anisotropic media. Thus the scope of this notion goes beyond the initial formulation of Snellius.

⁶ Parts of this chapter have been published by Slawinski, M.A., Slawinski, R..A., and Brown, R.J., in CREWES Research Report (1995).

anisotropy defining the materials. Most commonly they are expressed as elastic constants, C_{ij} , the entries of a 6×6 stiffness matrix relating stress and strain vectors, i.e., the anisotropic form of Hooke's law. Thomsen (1986) suggests particular combinations of elastic constants as convenient measures of anisotropy. They are referred to, in this dissertation, as *anisotropic parameters*, and are denoted by δ , ε and γ . The velocities of both compressional and shear waves can be expressed in terms of those parameters.

The formulæ for phase velocities can be developed in a Taylor series and, if the anisotropy is not very pronounced, higher-order terms ignored without significant loss of accuracy (Thomsen, 1986); see Appendix 2. In the geophysical context, this process can be justified by the fact that, although on a small scale many crystals are highly anisotropic, the rocks they form exhibit, in general, only moderate anisotropy as perceived by a wavelet of a relatively low frequency typical in seismic studies. The phase-velocity formulæ for three wave types in a weakly anisotropic medium provide the expressions used in deriving the mathematically tractable, as well as easily coded, Snell's law, i.e., a set of equations for calculating incident, reflected and transmitted angles.

In principle, it is possible to use the exact formulæ derived by Daley and Hron (1977) and expressed in terms of anisotropic parameters by Thomsen (1986). The significant loss of clarity of development caused by employing such complicated equations has been avoided here by using, in their stead, the equations governing weak anisotropy. Appendix 7, however, provides the initial steps necessary in developing exact equations applicable to cases of strong anisotropy. Thomsen suggests further simplifications aiding greatly in the intuitive understanding of the concept. In this development, however, the minimal amount of approximation was introduced (see Appendix 6), i.e., allowing one to obtain the slowness surface in a form clearly manageable by the Snell's law formalism. As described in Chapter II, slowness surfaces form the kernel of Snell's law. Since the formulæ for phase slowness can be elegantly described in polar coordinates it is necessary to translate the formalism described in the previous chapter to this system.

The formulæ below refer explicitly to the propagation within a transversely isotropic system with a vertical symmetry axis (TIV), or within a symmetry plane of a

given medium (e.g., an orthorhombic medium was used in laboratory measurements described in Chapter VII). Distinctive elastic properties of the transversely isotropic symmetry system are an infinite-fold rotational axis of symmetry, and an infinite set of two-fold axes perpendicular to it (Winterstein, 1990). It is described by five independent elastic constants. Transverse isotropy with a vertical symmetry axis describes well the intrinsic anisotropy found in a horizontally reposing sedimentary layer, e.g., a shale unit. Also, a series of isotropic layers, each of thickness considerably smaller than the wavelength, exhibits, as a whole, transverse isotropy with a vertical symmetry axis, e.g., Postma (1955), Levin (1979), Schoenberg (1994).

Weak anisotropy implies that for the compressional-wave solution, the divergence of displacements is much larger than its rotation, while for the other two solutions i.e., shear waves, the rotation is much larger than the divergence (Helbig, 1994). Thus the solutions are only weakly coupled and the particle displacement is almost parallel, in the case of quasi-compressional waves, or almost orthogonal, in the case of quasi-shear waves, to the direction of propagation. It can be shown that the wave equation for transverse isotropy yields three independent solutions corresponding to mutually orthogonal polarization directions. The solutions refer to one quasi-longitudinal wave (qP), one quasi-transverse wave (qSV) and one exactly-transverse wave (SH) (e.g., Keith and Crampin, 1977). Along the symmetry axis all polarizations become pure and all expressions reduce to the isotropic form. An important consequence of weak anisotropy in transversely isotropic media is that it is reasonable to consider two separate cases, i.e., the first case involving P and SV waves and the second case involving SH waves.

The simplification of expressions for phase velocities is achieved by developing the original expressions in Taylor series and neglecting higher-order terms under the assumption that the anisotropic parameters are much smaller than unity. The simplification of expressions is very considerable (see Thomsen, 1986, or Appendix 2), and, when remaining within the bounds of assumptions imposed by weak anisotropy, the accuracy is high.

Thanks to the weak-anisotropy assumption and the entailing simplifications, the entire mathematical treatment developed and used in this dissertation is tractable, and, in

almost all cases, leads to analytical expressions. This is not to say, however, that various problems, particularly while considering the inversion process in multilayer media, do not arise. Here again, however, the tractability allows for investigation and comprehension of results of raytracing and inversion. It often permits one to visualize a solution geometrically, a method favoured by Dr. Helbig, the author of an important text-book dealing with anisotropy from an exploration seismologist's point of view.

Thomsen (1986), the developer of the weak-anisotropy expressions, himself states in his paper that, with today's computers, there is little excuse for using the linearized equations for computational purposes⁷, but that the linearized equations are useful because their simplicity of form aids in the understanding of the physics. In this dissertation the approximate, but not fully linearized, expressions for phase velocities were used. Other quantities, although given in a linear approximation by Thomsen (1986), were developed in this dissertation, based on exact relations, e.g., the relation between the phase and group angles (see Appendix 6).

Furthermore, if any computational algorithm is to work for strong anisotropy it must also work for weak anisotropy, as the concept of anisotropy (spanned by two end members, namely, strong anisotropy and isotropy) forms a continuum (Helbig, 1994). Thus, a mathematically tractable approach provides a potential verification for a machine-intensive programme which would use the full form of equations for velocity anisotropy (see Appendix 7). The innovative aspect of the approach presented in this chapter consists of a clear analytical method for calculating propagation angles across an interface in anisotropic media, with all quantities related to a measurable set of parameters proposed by Thomsen (1986) and widely used by numerous researchers (e.g., Stewart, 1988; Cheadle et al., 1991; Brown et al., 1991). Except for using the weak-anisotropy form of expression for phase velocity, the presented method makes no simplifications or approximations in deriving the expressions of the generalized Snell's law in weakly anisotropic media. Another approach of developing the relationship between incident and refracted rays was proposed by Byun (1982, 1984). Byun's method is based on the assumption of elliptical velocity dependence or its perturbation.

3.1. QUASI-COMPRESSIONAL WAVES

3.1.1. Phase velocity

Dealing with weakly anisotropic media one often refers to a *quasi-compressional* wave (qP) as a *compressional* wave (P). Such simplification of terminology is due to the fact that the particle displacement is almost aligned with the direction of propagation. Similarly, *quasi-shear* waves (qS) can be, for simplicity, referred to as *shear* waves due to the fact that in weakly anisotropic media the particle displacements are almost perpendicular to the direction of propagation. Strictly, however, the distinction can be omitted only for SH waves in transversely isotropic media, in which case the particle displacement is exactly perpendicular to direction of propagation (Thomsen, 1986). In this dissertation the prefix *quasi-* is sometimes omitted when no possible confusion with isotropic propagation arises.

The phase velocity of a quasi-compressional, qP, wave in a weakly anisotropic medium is given by Thomsen (1986):

$$v_{qP}(\xi) = \alpha_0(1 + \delta \sin^2 \xi \cos^2 \xi + \epsilon \cos^4 \xi). \quad (3.1)$$

In this dissertation the phase angle, ξ , is the phase latitude, and a complement of the angle, ϑ , in Thomsen's paper, which is equivalent to the phase colatitude, i.e.,

$$\xi = \pi / 2 - \vartheta, \quad (3.2)$$

thus changing in some equations, the cosine function to the sine function. In this form, one can take advantage of standard vector calculus expressions in polar coordinates, where the argument is measured with respect to the horizontal axis. Thus the gradient can be expressed as follows:

⁷ Interestingly, in spite of powerful computers employed in seismic data processing, the moveout velocity is not commonly computed beyond its first term of the binomial expansion.

$$\nabla f(r, \xi) = \mathbf{r} \frac{\partial f}{\partial r} + \Xi \frac{1}{r} \frac{\partial f}{\partial \xi}, \quad (3.3)$$

where the angle is measured with respect to the x -axis. The symbol \mathbf{r} refers to the unit vector parallel to the radius, and Ξ is the azimuthal unit vector, i.e., the unit vector perpendicular to the radius.

The anisotropic parameters used in the expression for phase velocity, are defined in terms either of elastic constants, C_{ij} , or measured velocities. The latter definition proves very helpful in experimental studies, e.g., Cheadle et al. (1991). From the experimental point of view it is easier to use group (ray) velocities since, to obtain mathematically more convenient, phase velocities, one requires a plane-wave source. In either case, it is important to be aware of how one can determine phase and group velocities, separately, from laboratory measurements (Vestrum, 1994). Thus one can write:

$$\delta \equiv \frac{(C_{13} + C_{44})^2 - (C_{33} - C_{44})^2}{2C_{33}(C_{33} - C_{44})} \approx 4 \left[\frac{V_P(\pi/4)}{V_P(0)} - 1 \right] - \left[\frac{V_P(\pi/2)}{V_P(0)} - 1 \right], \quad (3.4)$$

and

$$\varepsilon \equiv \frac{C_{11} - C_{33}}{2C_{33}} \approx \frac{V_P(\pi/2) - V_P(0)}{V_P(0)}, \quad (3.5)$$

where C_{ij} are entries in the stiffness matrix relating six components of stress to six components of strain, i.e., Hooke's law and V_P is associated with measured, i.e., group velocities. For deriving anisotropic parameters from actual measurements, however, it is advisable to use exact equations instead of their approximate counterparts. Particularly δ is prone to the propagation of experimental errors in its approximate form (e.g., Brown et al., 1991).

The symbol α_0 , denotes the speed of a ray propagating vertically, along the symmetry axis of the medium. It can be expressed in terms of the elastic constant or,

similarly to the isotropic case, in terms of the Lamé parameters, λ and μ , and the density of the medium, ρ , that is:

$$\alpha_0 = \sqrt{\frac{C_{33}}{\rho}} = \sqrt{\frac{\lambda + 2\mu}{\rho}}. \quad (3.6)$$

Notice that, for a ray propagating vertically or horizontally, the phase and group velocities coincide, both in exact and approximate expressions. This is not the case in any other direction of propagation and it is of considerable importance to distinguish between the two concepts.

3.1.2. Transmission angle

The subsequent description follows the formalism developed by Slawinski and Slawinski (1994) and described in Chapter II. Firstly, one must formulate an expression for a slowness surface. The phase slowness is the reciprocal of the phase velocity, obtained by taking reciprocals at all points on the phase-velocity surface (e.g., Winterstein, 1990). Let $f(r, \xi)$ be a function in slowness space defined by:

$$f(r, \xi) = \frac{1}{r} - \alpha_0 (\delta \sin^2 \xi \cos^2 \xi + \varepsilon \cos^4 \xi), \quad (3.7)$$

where r is the radius of the slowness surface, i.e., the magnitude of the slowness. For a particular TI medium, slowness as a function of ξ is $r(\xi)$ which is given by equation (3.16). This set of points $[r(\xi), \xi]$ is also given by the intersection of $f(r, \xi)$ with the plane $f = \alpha_0$, i.e., by the set of points (r, ξ) for which:

$$f(r, \xi) = \alpha_0. \quad (3.8)$$

This set of points forms a slowness curve or, mathematically, a level curve. The above description can be illustrated by Figure 3.1:

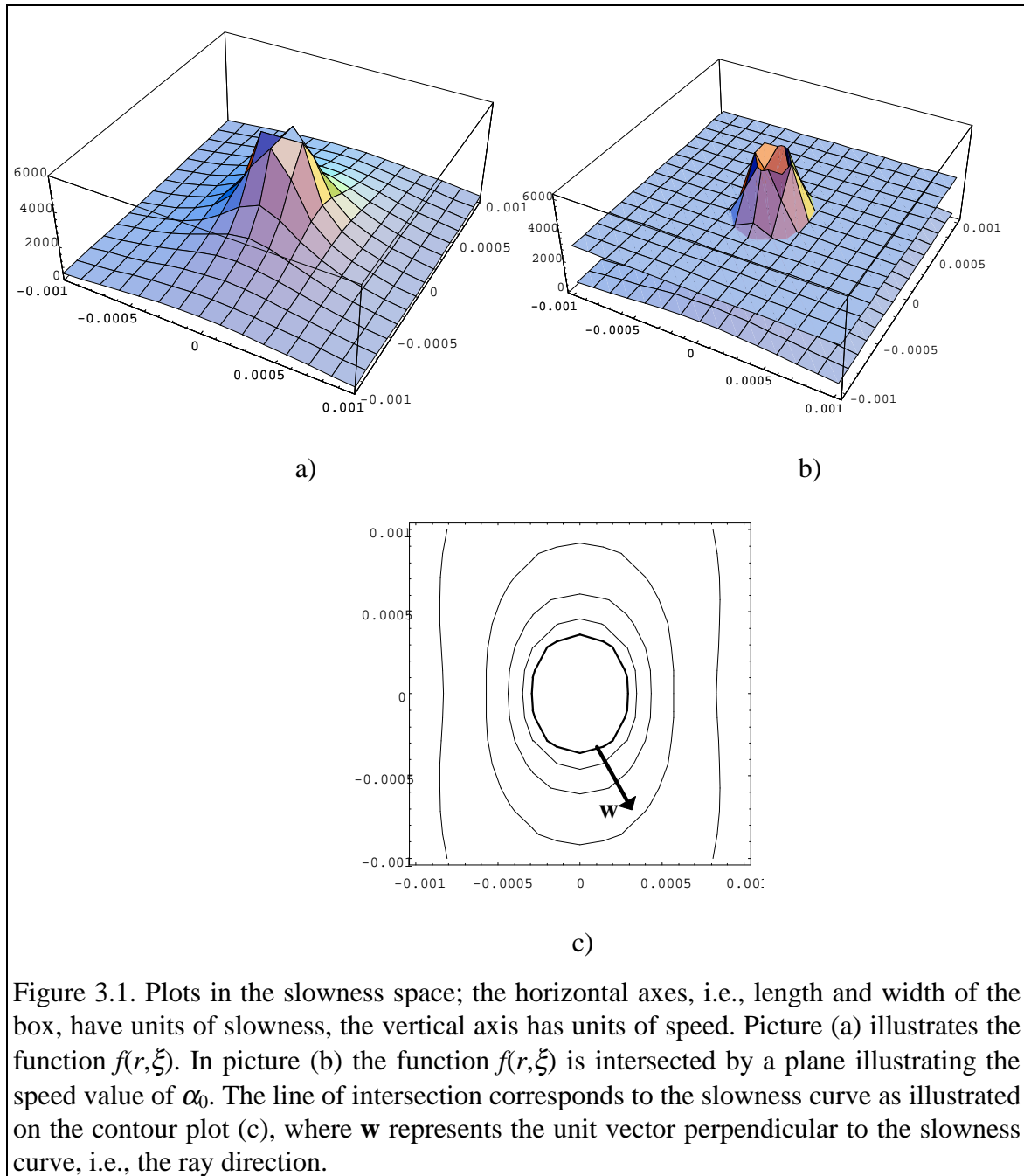


Figure 3.1. Plots in the slowness space; the horizontal axes, i.e., length and width of the box, have units of slowness, the vertical axis has units of speed. Picture (a) illustrates the function $f(r, \xi)$. In picture (b) the function $f(r, \xi)$ is intersected by a plane illustrating the speed value of α_0 . The line of intersection corresponds to the slowness curve as illustrated on the contour plot (c), where \mathbf{w} represents the unit vector perpendicular to the slowness curve, i.e., the ray direction.

The propagation (ray, group) vector is always perpendicular to the slowness surface, i.e., its direction is parallel to the gradient of the surface. Using calculus and various trigonometric identities, the gradient can be written as follows:

$$\nabla f(r, \xi) = \mathbf{r} \frac{\partial f}{\partial r} + \Xi \frac{1}{r} \frac{\partial f}{\partial \xi} = \mathbf{r} \left(-\frac{1}{r^2} \right) + \Xi \left(\frac{\alpha_0 \sin(2\xi) [\delta \cos(2\xi) - 2\varepsilon \cos^2 \xi]}{r} \right), \quad (3.9)$$

whose length is:

$$|\nabla f| = \sqrt{\left(\frac{\partial f}{\partial r} \right)^2 + \left(\frac{1}{r} \frac{\partial f}{\partial \xi} \right)^2} = \frac{1}{r} \sqrt{\frac{1}{r^2} + \left(\alpha_0 \sin(2\xi) [\delta \cos(2\xi) - 2\varepsilon \cos^2 \xi] \right)^2}. \quad (3.10)$$

The unit ray vector, \mathbf{w} , in the direction of the ray can then be determined from equation (2.8):

$$\mathbf{w} = \frac{\nabla f}{|\nabla f|}. \quad (3.11)$$

The angle between the unit ray vector, \mathbf{w} , and the normal can be found using the definition of the dot product. Using the vertical unit vector, \mathbf{z} , one may write:

$$\cos \theta = \mathbf{z} \cdot \mathbf{w} \quad (3.12)$$

In polar coordinates, the Cartesian unit vector, \mathbf{z} , can be expressed through its relation to the angle ξ , i.e., the argument. In the present context the argument corresponds to the phase angle, i.e.,

$$\mathbf{z} = \mathbf{r} \sin \xi + \Xi \cos \xi. \quad (3.13)$$

This form is used in the desired dot product. The group angle, θ , that the group slowness vector makes with the normal to the interface, can be expressed in terms of the phase angle, ξ , measured from the horizontal:

$$\cos\theta = \mathbf{z} \cdot \mathbf{w} = \frac{\alpha_0 \cos\xi \sin(2\xi)(\delta \cos(2\xi) - 2\varepsilon \cos^2 \xi) - \frac{\sin\xi}{r(\xi)}}{\sqrt{\frac{1}{[r(\xi)]^2} + [\alpha_0 \sin(2\xi)(\delta \cos(2\xi) - 2\varepsilon \cos^2 \xi)]^2}} . \quad (3.14)$$

In relating the incidence group angle to the transmission group angle at a horizontal interface, one uses the fact that the horizontal component of slowness, x_0 , i.e., the ray parameter, must be constant. If the medium of incidence is isotropic⁸ then phase and group angles (and velocities) coincide. The horizontal component of slowness can be calculated, given the angle of incidence, i.e.,

$$x_i = \frac{\sin\theta_i}{v} \equiv x_0, \quad (3.15)$$

where the angle of incidence, θ_i , is measured from the vertical, and v is the speed in the isotropic medium. The symbol x_0 denotes the ray parameter. The radius of the cross-section of the qP-slowness surface in the xz -plane of the anisotropic medium of transmission is given by the inverse of the phase velocity:

$$r(\xi) = \frac{1}{\alpha_0(1 + \delta \sin^2 \xi \cos^2 \xi + \varepsilon \cos^4 \xi)} . \quad (3.16)$$

Using standard relationships between the Cartesian and polar coordinates, one can relate a given point on a slowness surface to its horizontal component through the phase angle, ξ :

$$x(\xi) = r(\xi) \cos \xi . \quad (3.17)$$

⁸ The formalism can be extended to the case of an anisotropic/anisotropic interface (see Chapter VI) . The clarity of presentation is enhanced by assuming the medium of incidence to be isotropic. Also the experimental set-up (see Chapter VII) involves isotropic/anisotropic interface.

Inserting the equation (3.15) into the equation (3.16) gives a relationship between the horizontal component of slowness and the slowness surface for compressional waves:

$$x(\xi) = \frac{\cos \xi}{\alpha_0 (1 + \delta \sin^2 \xi \cos^2 \xi + \varepsilon \cos^4 \xi)}. \quad (3.18)$$

Equation (3.17) can be rewritten as a quartic in $\cos \xi$ and solved explicitly for the phase angle, ξ_0 , corresponding to a given ray parameter, x_0 . Thus, given the incidence angle, θ_i , and thus the ray parameter, x_0 , one obtains:

$$\alpha_0 x_0 (\varepsilon - \delta) \cos^4 \xi_0 + \alpha_0 x_0 \delta \cos^2 \xi_0 - \cos \xi_0 + \alpha_0 x_0 = 0. \quad (3.19)$$

The appropriate value of ξ_0 can be inserted in the equation (3.19) and the angle of transmission calculated. An insightful look into the solution of the quartic equation is given in Appendix 1. Note that in the case of elliptical anisotropy, i.e., $\varepsilon = \delta$, the quartic is reduced to a quadratic of the form analogous to the equation for SH waves (equation (3.39)). Also note that, in all expressions, θ is the group (ray) angle measured with respect to the normal to the interface, and ξ is the phase angle measured with respect to the horizontal.

Method of Computation⁹: Snell's Law for Isotropic/Anisotropic Interface: Angle of Transmission of a qP wave.

Given a P or SV wave with speed v in an anisotropic medium, incident at an angle θ_i upon a planar, horizontal interface separating it from an anisotropic medium with vertical

⁹ The inserts providing step-by-step calculations of various values appear throughout the dissertation and are clearly distinguished from the main body of the text by including them in a shaded box. They can be skipped without disturbing the continuity of presentation. Their purpose is to provide a convenient method of calculation. To further enhance such usefulness, a brief code for a widely available mathematical software, Mathematica®, is also provided.

speed α_0 and anisotropic parameters δ and ε , the angle of transmission, θ_t , of qP can be calculated by following the steps below.

Step 1

Calculate the ray parameter, x_0 , given the angle of incidence, θ_i :

$$x_0 = \frac{\sin \theta_i}{v}$$

Step 2

Calculate the phase angle, ξ , in the anisotropic medium by solving the quartic equation.

$$\alpha_0 x_0 (\varepsilon - \delta) \cos^4 \xi + \alpha_0 x_0 \delta \cos^2 \xi - \cos \xi + \alpha_0 x_0 = 0.$$

Choose the root which yields real value for ξ . Note that although this equation can be solved algebraically it is a very laborious process. An alternative approach is to use a widely available software, e.g., Mathematica® (Wolfram, 1991) to solve the equation. A code is given below.

v = speed of P wave or SV wave in the isotropic medium, v .

A = vertical speed velocity in the anisotropic medium, α_0 .

e = anisotropic parameter, ε .

d = anisotropic parameter, δ .

m = incident angle (in degrees)

$x = \text{Sin}[(m*180/\text{Pi})]/v$

`FindRoot[A*x*(e-d)*C^4+A*x*d*C^2-C+A*x==0,{C,0.5,0,1}]`

Note that using the command “FindRoot” between 0 and 1 guarantees the programme returning the desired real root, i.e., yielding the angle ξ between 0 and 90°. If all four roots of the quartic are of interest then use the code below.

`NSolve[A*x*(e-d)*C^4+A*x*d*C^2-C+A*x==0,C]`

Also note that C stands for $\cos \xi$ and thus the argument must be found using the inverse trigonometric function.

Step 3

Calculate the length of the radius of the phase-slowness surface in the anisotropic medium corresponding to the calculated ray parameter, x_0 .

$$r(\xi) = \frac{1}{\alpha_0 (1 + \delta \sin^2 \xi \cos^2 \xi + \varepsilon \cos^4 \xi)}.$$

Go to Variant A or to Variant B.

Variant A**Step 4**

Calculate the angle of transmission¹⁰, θ_t , of a qP wave in the anisotropic medium.

$$\theta_t = \text{Arc cos} \left\{ \frac{\alpha_0 \cos \xi \sin(2\xi) (\delta \cos(2\xi) - 2\varepsilon \cos^2 \xi) - \frac{\sin \xi}{r(\xi)}}{\sqrt{[r(\xi)]^2 + [\alpha_0 \sin(2\xi) (\delta \cos(2\xi) - 2\varepsilon \cos^2 \xi)]^2}} \right\} .$$

Variant B**Step 4**

Evaluate the derivative of phase-slowness radius using the phase angle, ξ , from Step 2.

$$\frac{dr(\xi)}{d\xi} = - \frac{\sin(2\xi) [\delta \cos(2\xi) - 2\varepsilon \cos^2 \xi]}{\alpha_0 (1 + \delta \sin^2 \xi \cos^2 \xi + \varepsilon \cos^4 \xi)^2} .$$

Step 5

Calculate the angle of transmission, θ_t , of a qSV-wave in the anisotropic medium.

$$\theta_t = \text{Arc cot} \left\{ \frac{\frac{dr(\xi)}{d\xi} - r(\xi) \tan \xi}{\frac{dr(\xi)}{d\xi} \tan \xi + r(\xi)} \right\} .$$

N.B. Convenient Mathematica® code for equations above is given as parts of programmes to calculate the traveltime of a ray in Chapter V which can be easily used just for the purpose of calculated the angle of transmission.

3.2. QUASI-SHEAR WAVES (SV)

This section follows the development presented above for quasi-compressional waves. Some details, therefore, are omitted.

¹⁰ Throughout the dissertation, inverse trigonometric functions are denoted by a prefix *Arc*. This is to indicate the principle value, i.e., a value corresponding to an acute angle.

3.2.1. Phase velocity

The phase velocity of a quasi-shear, qS, wave in a weakly anisotropic medium is given by Thomsen (1986):

$$v_{qSV}(\xi) = \beta_0 \left[1 + \frac{\alpha_0^2}{\beta_0^2} (\varepsilon - \delta) \sin^2 \xi \cos^2 \xi \right]. \quad (3.20)$$

Note that angle, ξ , is a complement of the angle, ϑ , in Thomsen's paper. The anisotropic parameters, ε and δ , are defined in section 3.1.1. The speed of a wave propagating vertically through the medium is:

$$\beta_0 = \sqrt{\frac{C_{44}}{\rho}}, \quad (3.21)$$

where ρ is the density of the medium.

3.2.2. Transmission angle

The slowness surface is associated with the function:

$$g(r, \xi) = \frac{1}{r} - \frac{\alpha_0^2}{\beta_0} (\varepsilon - \delta) \sin^2 \xi \cos^2 \xi = \beta_0. \quad (3.22)$$

Therefore the gradient is given by:

$$\nabla g(r, \xi) = \mathbf{r} \left(-\frac{1}{r^2} \right) + \Xi \left(\frac{-\frac{\alpha_0^2}{\beta_0} (\varepsilon - \delta) \sin(2\xi) \cos(2\xi)}{r} \right), \quad (3.23)$$

whose length is:

$$|\nabla g| = \frac{1}{r} \sqrt{\frac{1}{r^2} + \left[\frac{\alpha_0^2}{\beta_0} (\varepsilon - \delta) \sin(2\xi) \cos(2\xi) \right]^2}. \quad (3.24)$$

The angle, θ_i , that the unit group-velocity vector, $\bar{\mathbf{w}}$, of a transmitted ray makes with the unit normal to the interface, $\bar{\mathbf{z}}$, is found following the generalized Snell's law formalism:

$$\cos \theta_i = \bar{\mathbf{z}} \cdot \bar{\mathbf{w}} = - \frac{\frac{\sin \xi}{r(\xi)} + \frac{\alpha_0^2}{\beta_0} \cos \xi (\varepsilon - \delta) \sin(2\xi) \cos(2\xi)}{\sqrt{\frac{1}{[r(\xi)]^2} + \left[\frac{\alpha_0^2}{\beta_0} (\varepsilon - \delta) \sin(2\xi) \cos(2\xi) \right]^2}}. \quad (3.25)$$

The above expression must be evaluated at a point on the slowness surface corresponding to the horizontal component of slowness, x_0 , i.e., the ray parameter. It can be calculated from a given angle of incidence. Assuming the medium of incidence to be isotropic yields:

$$x_i = \frac{\sin \theta_i}{v} \equiv x_0, \quad (3.26)$$

where the angle of incidence, θ_i , is measured from the vertical, and v is the speed in the isotropic medium. The radius of the cross-section of the qSV-slowness surface in the xz -plane is the inverse of the phase velocity, which can be written as:

$$r(\xi) = \frac{1}{\beta_0 \left(1 + \frac{\alpha_0^2}{\beta_0^2} (\varepsilon - \delta) \sin^2 \xi \cos^2 \xi \right)}. \quad (3.27)$$

Using the standard relationships between Cartesian and polar coordinates, one can relate the horizontal component to the slowness surface, namely:

$$x(\xi) = r(\xi) \cos \xi = \frac{\cos \xi}{\beta_0 \left(1 + \frac{\alpha_0^2}{\beta_0^2} (\varepsilon - \delta) \sin^2 \xi \cos^2 \xi \right)}. \quad (3.28)$$

For a given angle of incidence, θ_i , the corresponding value of $x(\xi)$ can be denoted by x_0 . The above expression can be rewritten as a quartic equation in $\cos \xi$ to give:

$$\frac{\alpha_0^2 x_0 (\varepsilon - \delta)}{\beta_0} \cos^4 \xi - \frac{\alpha_0^2 x_0 (\varepsilon - \delta)}{\beta_0} \cos^2 \xi + \cos \xi - x_0 \beta_0 = 0. \quad (3.29)$$

Equation (3.29) has four roots. The required solution, i.e., the angle of transmission, θ_t , must be real. In general, only one root is real and less than unity (in absolute value), i.e., whose inverse cosine yields a real angle.

Method of Computation: Snell's Law for Isotropic/Anisotropic Interface: Angle of Transmission of an SV wave.

Given a P or SV wave with speed v in an anisotropic medium, incident at an angle θ_i upon a planar, horizontal interface separating it from an anisotropic medium with vertical speed β_0 and anisotropic parameters δ and ε , the angle of transmission, θ_t , of qSV can be calculated by following the steps below.

Step 1

Calculate the ray parameter, x_0 , given the angle of incidence, θ_i :

$$x_0 = \frac{\sin \theta_i}{v}$$

Step 2

Calculate the phase angle, ξ , in the anisotropic medium by solving the quartic equation.

$$\frac{\alpha_0^2 x_0 (\varepsilon - \delta)}{\beta_0} \cos^4 \xi - \frac{\alpha_0^2 x_0 (\varepsilon - \delta)}{\beta_0} \cos^2 \xi + \cos \xi - x_0 \beta_0 = 0$$

Choose the root which yields real value for ξ . Note that although this equation can be solved algebraically it is a very laborious process. An alternative approach is to use a widely available software, e.g., Mathematica®.

v = speed of P wave or SV wave in the isotropic medium, v .

A = vertical speed of a compressional wave in the anisotropic medium, α_0 .

B = vertical speed of a shear wave in the anisotropic medium, β_0 .

e = anisotropic parameter, ε .

d = anisotropic parameter, δ .

m = incident angle (in degrees)

$x = \text{Sin}[(m * \text{Pi}/180)]/v$

`FindRoot[(A^2*x*(e-d)/B)*C^4-(A^2*x*(e-d)/B)*C^2+C-x*B==0,{C,0.5,0,1}]`

Note that using the command “FindRoot” between 0 and 1 guarantees the programme returning the desired real root, i.e., yielding the angle ξ between 0 and 90°. If all four roots of the quartic are of interest then use the code below.

`NSolve[(A^2*x*(e-d)/B)*C^4-(A^2*x*(e-d)/B)*C^2+C-x*B==0,C]`

Also note that C stands for $\cos \xi$ and thus the argument must be found using the inverse trigonometric function.

Step 3

Calculate the length of the radius of the phase-slowness surface in the anisotropic medium corresponding to the calculated ray parameter, x_0 .

$$r(\xi) = \frac{1}{\beta_0 \left(1 + \frac{\alpha_0^2}{\beta_0^2} (\varepsilon - \delta) \sin^2 \xi \cos^2 \xi \right)}$$

Go to Variant A or to Variant B.

Variant A

Step 4

Calculate the angle of transmission, θ_t , of a qSV wave in the anisotropic medium.

$$\theta_t = \text{Arc cos} \left\{ \frac{\frac{\sin \xi}{r(\xi)} + \frac{\alpha_0^2}{\beta_0} \cos \xi (\varepsilon - \delta) \sin(2\xi) \cos(2\xi)}{\sqrt{\frac{1}{[r(\xi)]^2} + \left[\frac{\alpha_0^2}{\beta_0} (\varepsilon - \delta) \sin(2\xi) \cos(2\xi) \right]^2}} \right\}.$$

Variant B

Step 4

Evaluate the derivative of phase-slowness radius and evaluate using the phase angle from Step 2.

$$\frac{dr(\xi)}{d\xi} = - \frac{\frac{\alpha_0^2}{\beta} (\varepsilon - \delta) \sin(2\xi) \cos(2\xi)}{\left[\beta_0 \left(1 + \frac{\alpha_0^2}{\beta_0^2} (\varepsilon - \delta) \sin^2 \xi \cos^2 \xi \right) \right]^2}.$$

Step 5

Calculate the angle of transmission, θ_t , of a qSV wave in the anisotropic medium.

$$\theta_t = \text{Arc cot} \left\{ \frac{\left[\frac{dr(\xi)}{d\xi} - r(\xi) \tan \xi \right]}{\left[\frac{dr(\xi)}{d\xi} \tan \xi + r(\xi) \right]} \right\}.$$

N.B. Convenient Mathematica® code for the equations above are given as parts of programmes to calculate the traveltime of a ray in Chapters 5. They can be easily used just for the purpose of calculated the angle of transmission.

3.3. SHEAR WAVES (SH)

Investigation of transverse shear waves provides the clearest illustration of the method. Firstly, the expression for the phase velocity is simpler than for either compressional or radial shear waves. Secondly, considering the propagation within the symmetry planes, they are not subject to mode conversion. Furthermore, since even the

exact expression for phase velocity is quite simple (Appendix 2), one can easily compare the results of approximate and exact approaches (Appendix 6).

3.3.1. Phase velocity

The angular dependence of the phase velocity of a quasi-shear wave, SH, in a weakly anisotropic medium can be expressed in terms of the speed of the wave travelling vertically, β_0 , the anisotropic parameter, γ , and the phase angle, ξ , as described by Thomsen (1986):

$$v_{SH}(\xi) = \beta_0(1 + \gamma \cos^2 \xi). \quad (3.30)$$

Again, as in qP and qSV cases, the angle, ξ , is the phase latitude. The anisotropic parameter is defined in terms of elastic constants, C_{ij} , and can be measured experimentally in terms of group velocities, V . For vertical and horizontal propagation phase and group velocities, v and V , coincide. Thus one can write:

$$\gamma \equiv \frac{C_{66} - C_{44}}{2C_{44}} \approx \frac{V_{SH}(\pi/2) - V(0)}{V(0)}, \quad (3.31)$$

where angles $\pi/2$ and 0 correspond to horizontal and vertical propagation, respectively. The speed of a wave propagating vertically, along a symmetry axis, through the medium can be expressed in terms of the elastic constant or, as in the isotropic case, the Lamé parameter μ , i.e., the shear modulus, and the density of the medium, ρ :

$$\beta_0 = \sqrt{\frac{C_{44}}{\rho}} = \sqrt{\frac{\mu}{\rho}}. \quad (3.32)$$

3.3.2. Transmission angle

The slowness surface is associated with the function:

$$h(r, \xi) = \frac{1}{r} - \beta_0 \gamma \cos^2 \xi = \beta_0. \quad (3.33)$$

The gradient of the slowness surface, $h(r, \xi)$, is equivalent to the direction of the unit ray vector, \mathbf{w} , i.e., to the direction of energy propagation. It can be calculated using a standard formula of vector calculus in polar coordinates:

$$\nabla h(r, \xi) = \mathbf{r} \left(-\frac{1}{r^2} \right) + \Xi \left(\frac{\beta_0 \gamma \sin(2\xi)}{r} \right). \quad (3.34)$$

The magnitude of the gradient is calculated in order to normalize it.

$$|\nabla h| = \frac{1}{r} \sqrt{\frac{1}{r^2} + [\beta_0 \gamma \sin(2\xi)]^2}. \quad (3.35)$$

The angle between the unit group slowness vector, $\overline{\mathbf{w}}$, and the unit normal to the interface, $\overline{\mathbf{z}}$, results directly from the definition of the dot product:

$$\cos \theta_i = \overline{\mathbf{z}} \cdot \overline{\mathbf{w}} = \frac{\sin \xi \left(2\beta_0 \gamma \cos^2 \xi - \frac{1}{r(\xi)} \right)}{\sqrt{\frac{1}{[r(\xi)]^2} + [(\beta_0 \gamma \sin(2\xi))]^2}}. \quad (3.36)$$

Equation (3.36) must be evaluated at the point on the slowness surface corresponding to the horizontal component of slowness, i.e., ray parameter, x_0 , which is constant across the interface, i.e., the same for both incident and reflected waves. The

radius of the cross-section of the qSH-slowness surface in the xz -plane can be expressed as the inverse of the phase velocity:

$$r(\xi) = \frac{1}{\beta_0(1 + \gamma \cos^2 \xi)}. \quad (3.37)$$

The slowness surface and the ray parameter, for a horizontal interface, can be related by a formula for coordinate transformation between the Cartesian and polar systems:

$$x(\xi) = r(\xi) \cos(\xi) = \frac{\cos \xi}{\beta_0(1 + \gamma \cos^2 \xi)}. \quad (3.38)$$

The above expression can also be expressed as a quadratic equation in $\cos \xi$: For a given the incidence angle, θ_i , and thus a fixed ray parameter, x_0 , one can calculate a corresponding transmitted phase angle, ξ_0 :

$$x_0 \beta_0 \gamma \cos^2 \xi_0 - \cos \xi_0 + x_0 \beta_0 = 0. \quad (3.39)$$

The “zero” subscript in ξ is used to indicate a specific value corresponding to the ray parameter, x_0 . It will be dropped in further development but any given value of ξ is functionally related to the ray parameter. The discriminant of the quadratic equation (3.39) illustrates the limitation imposed on the physical solutions requiring it to be positive:

$$\Delta = 1 - (2x_0 \beta_0)^2 \gamma > 0. \quad (3.40)$$

Since x_0 is, in general, smaller than $1/\beta_0$, and $\gamma \ll 1$ for weak anisotropy, the discriminant is, normally, positive and the solutions, in terms of the cosine function, real. There are two algebraic solutions to the quadratic, that is:

$$\cos \xi_{1,2} = \frac{1 \pm \sqrt{1 - (2x_0\beta_0)^2 \gamma}}{2x_0\beta_0\gamma}. \quad (3.41)$$

It is obvious from Figure 2.2.1, and can be determined from equation (3.37), that for noncritical incidence one must require that:

$$x_0 < r(\xi = 0) = \frac{1}{\beta_0(1 + \gamma)}, \quad (3.42)$$

i.e., the horizontal components of slowness must be contained within the slowness curve of the transmission medium. This insures that the angle ξ is real, i.e., the value of the cosine is smaller than unity. For a standard solution one should choose the second root, i.e., the subtraction in equation (3.41)¹¹. The first root, i.e., the addition, gives the value greater than unity and results in a complex angle. As a confirmation of this choice, one can consider the limiting case $\gamma \rightarrow 0$, and use the de l'Hôpital's rule:

$$\cos \xi_2 = \lim_{\gamma \rightarrow 0} \frac{1 - \sqrt{1 - (2x_0\beta_0)^2 \gamma}}{2x_0\beta_0\gamma} = x_0\beta_0, \quad (3.43)$$

which, solved for x_0 , leads to the standard form of Snell's law for isotropic media¹².

¹¹ Considering vertical incidence, i.e., $x_0 = 0$, one has $\cos \xi_1 = 2/0$ and $\cos \xi_2 = 0/0$. The first result is physically meaningless, whereas the second case becomes, using limits and de l'Hôpital's rule $\cos \xi_2 = 0$, i.e., vertical incidence causes vertical transmission, as expected.

¹² The limiting, i.e., isotropic case results in an expression for Snell's law:

$$\frac{\sin \theta_i}{v_1} = x_0 = \frac{\cos \xi}{\beta_0}.$$

Method of Calculation: Snell's Law for Isotropic/Anisotropic Interface: Angle of Transmission of an SH wave.

Given an SH wave with speed v in an isotropic medium incident at an angle θ_i on the planar, horizontal interface separating it from an anisotropic medium with vertical speed β_0 and anisotropic parameter γ , the angle of transmission, θ_t , of qSH can be calculated by following the steps below.

Method I

Step 1

Calculate the ray parameter, x_0 , given the angle of incidence, θ_i :

$$x_0 = \frac{\sin \theta_i}{v},$$

Note that for the noncritical incidence one must choose

$$\theta_i < \text{Arc cot} \sqrt{\left[\frac{\beta_0}{v} (\gamma + 1) \right]^2 - 1}$$

Step 2

Calculate the phase angle, ξ , in the anisotropic medium .

$$\xi = \text{Arc cos} \left\{ \frac{1 - \sqrt{1 - (2x_0\beta_0)^2 \gamma}}{2x_0\beta_0\gamma} \right\}.$$

Step 3

Calculate the length of the radius of the phase-slowness surface in the anisotropic medium corresponding to the calculated ray parameter, x_0 .

$$r(\xi) = \frac{1}{\beta_0 (1 + \gamma \cos^2 \xi)}.$$

Go to Variant A or to Variant B.

Variant A

Step 4

Calculate the angle of transmission of a qSH wave in the anisotropic medium.

$$\theta_t = \text{Arc cos} \left\{ \frac{\sin \xi \left(2\beta_0 \gamma \cos^2 \xi - \frac{1}{r(\xi)} \right)}{\sqrt{\left[\frac{1}{r(\xi)} \right]^2 + [\beta_0 \gamma \sin(2\xi)]^2}} \right\}.$$

Mathematica® code for Variant A is given below.

v = velocity of a shear-wave in the isotropic layer, v .
 B = vertical shear-wave velocity in the anisotropic layer, β_0 .
 g = anisotropic parameter, γ .
 m = angle of incidence in degrees, θ_i
 $x = \text{Sin}[(m*\text{Pi}/180)]/v$
 $z = \text{ArcCos}[(1-\text{Sqrt}[1-g*(2*x*B)^2])/(2*x*B*g)]$
 $dz = 2*z$
 $r = 1/(B*(1+g*\text{Cos}[z]^2))$
 $n = \text{Sin}[z]*(2*B*g*\text{Cos}[z]^2-1/r)$
 $d = \text{Sqrt}[1/r^2+(B*g*\text{Sin}[dz])^2]$
 $\text{N}[\text{ArcCos}[\text{Abs}[n/d]]]$

where the angle of transmission, θ_t , is given in radians.

Variant B

Step 4

Evaluate the derivative of phase-slowness radius and evaluate using the phase angle from Step 2.

$$\frac{dr}{d\xi} = \frac{\gamma \sin(2\xi)}{\beta_0 (1 + \gamma \cos^2 \xi)^2}.$$

Step 5

Calculate the angle of transmission, θ_t , of a qSH wave in the anisotropic medium.

$$\theta_t = \text{Arc cot} \left\{ \frac{\frac{dr(\xi)}{d\xi} - r(\xi) \tan \xi}{\frac{dr(\xi)}{d\xi} \tan \xi + r(\xi)} \right\}.$$

Mathematica® Code for Variant B is given below.

v = velocity of a shear-wave in the isotropic layer, v .
 B = vertical shear-wave velocity in the anisotropic layer, β_0 .
 g = anisotropic parameter, γ .
 m = angle of incidence in degrees, θ_i .
 $x = \text{Sin}[m \cdot \text{Pi}/180]/v$
 $z = \text{ArcCos}[(1 - \text{Sqrt}[1 - (2 \cdot x \cdot B)^2 \cdot g]) / (2 \cdot x \cdot B \cdot g)]$
 $dz = 2 \cdot z$
 $r = 1 / (B \cdot (1 + g \cdot \text{Cos}[z]^2))$
 $dr = g \cdot \text{Sin}[dz] / (B \cdot (1 + g \cdot \text{Cos}[z]^2)^2)$
 $N[\text{ArcCot}[(dr - r \cdot \text{Tan}[z]) / (dr \cdot \text{Tan}[z] + r)]]$

where the angle of transmission, θ_t , is given in radians.

Method II

Since the expression for SH wave slowness surface is equivalent to an ellipse one may use, recalling the definition of γ , equation (2.23).

$$\theta_t = \text{Arc cot} \left\{ \frac{1}{\gamma + 1} \sqrt{\left(\frac{v}{\beta_0 (\gamma + 1)} \csc \theta_i \right)^2 - 1} \right\}.$$

3.4. A COMMENT TO USERS AND PROGRAMMERS

The results of some formulæ appearing in this development depart from intuitive expectations based upon wave propagation in isotropic media. Several interesting phenomena of this nature are illustrated in this dissertation, e.g., Chapter VI. Consequently, the correctness of results is difficult to ascertain by inspection. A helpful method to gain some insight is provided by various limiting cases and interrelations between equations.

Firstly, setting the anisotropic parameters to zero leads to well known isotropic equations. The form of the latter is very familiar, and, if desired, numerical examples can easily be verified.

Secondly, the expressions for the three types of waves are related among themselves. Setting $\varepsilon = \delta$ results in elliptical velocity dependence for compressional waves. Transverse shear (SH) waves always, even in the case of strong anisotropy, exhibit elliptical dependence. Thus equating the two anisotropic parameters reduces the

equations of compressional waves to the form displayed by those for transverse shear waves. Therefore, both compressional and transverse-shear-waves results can be tested against each other as well as against the elliptical form of Snell's law described in details in Chapter II. Also, the setting of $\varepsilon = \delta$ results in no angular velocity dependence for radial shear (SV) waves under the weak-anisotropy approximation. Hence, all formulæ for radial shear waves should reduce to the isotropic form. Physical validity of setting the anisotropic parameters to be equal is limited (e.g., Daley and Hron, 1977, Thomsen, 1986) but provides a method for testing derived expressions.

Thirdly, for vertical and horizontal directions of propagation, phase and group velocities coincide. Therefore all equations are reduced to isotropic forms.

In many cases, because of the form of the anisotropic equations the process of reducing one form of equation to another might require some mathematical manipulation and not just a straightforward substitution. For instance, the concept of limits, and various methods related to it (e.g., de l'Hôpital's rule) might have to be used.

The interrelations stated above, although necessary for correctness of the derived anisotropic equations, are not sufficient to prove it. It is quite possible that, in the reduction process, a canceling of a term due to the peculiar combination of values annihilates the error existing in the general form. To increase the confidence in correctness of equations one can perform several calculations with increasing values of anisotropic parameters. The results should depart smoothly and monotonically from the easily calculated isotropic case.

Another point should not escape one's consideration. As the anisotropy of the medium increases, i.e., parameters δ , ε , and γ become larger, the adequacy of formulations based on the weak-anisotropy assumption decreases. Appendix 2 illustrates the discrepancy between slowness surfaces obtained using exact and approximate approaches, while Appendix 7 provides a starting point for development of exact expressions of Snell's law applying also to strongly anisotropic media. The latter method should be used if strong anisotropy is to be considered and/or an extremely high accuracy is required.

CHAPTER **IV**

RAYTRACING THROUGH A TWO-LAYER, ISOTROPIC/ANISOTROPIC MEDIUM

4.0. INTRODUCTION

An important element of studying wave propagation consists of the ability of predicting theoretically the results which one would obtain by measuring, at a given receiver, various aspects (e.g., amplitude, phase, travelttime) of a signal emitted by a distant source. A powerful and rather intuitive technique, for this purpose, is provided by ray theory. It is an approximation to the full wave theory and it derives from the approach used in geometrical optics. With the aid of Snell's law, using a raytracing theory, and knowing all relevant parameters of the medium, one can calculate the trajectory of a ray between the source and receiver, as well as the travelttime required. This is a, so called, forward problem or forward modelling: one calculates the results knowing all parameters. The, in principle, more difficult, inverse problem, in which one infers parameters of the medium from the results is treated in Chapter VIII.

The crucial point of raytracing between a given source and receiver consists of finding the incidence (take-off) angle which, in combination with transmission angles, obeying Snell's law at all interfaces, yields the raypath corresponding to a given source-receiver distance. This is, as a matter of fact, a little inverse problem, here used in a larger context of forward modelling. The required equation, for a two-layer case, can be written as follows:

$$X_1 + X_2 = X , \quad (4.1)$$

i.e., the sum of horizontal distances travelled in the first, X_1 , and the second, X_2 , layer, must equal the total horizontal distance between the source and receiver, X . In terms of layer thickness, h_1 and h_2 , as well as angles of incidence, θ_i , and transmission, θ_t , it can be written as:

$$h_1 \tan \theta_i + h_2 \tan \theta_t = X , \quad (4.2)$$

or in terms of angle of incidence:

$$h_1 \tan \theta_i + h_2 \tan[\theta_t(\theta_i)] = X , \quad (4.3)$$

where the expression in square brackets denotes that the angle of transmission is a function of the angle of incidence, i.e., Snell's law.

4.1. MATHEMATICAL METHODS

4.1.1. General remarks

Even in isotropic layers, i.e., with no angular dependence of velocity, the above equation has to be solved by iteration since one cannot express θ_t explicitly in terms of all other variables and parameters. The problem becomes still more computationally intensive in anisotropic media. However, using the appropriate form of Snell's law derived in previous chapters, one can iterate the above equation for different values of the incident angle, θ_i , until the solution is found.

In parameterizing the problem by considering a traveltime between two given points, one can also use a more straightforward and computationally efficient approach of Fermat's principle of stationary time, described in section 4.1.3. Note, however, that Fermat's formulation requires a simplification of some expressions, namely the formulæ for phase and group velocities need to assume the same form. It entails a loss of some

physical attributes, and thus it has to be used with caution. The problems arising from the direct Fermat formulation are treated more fully in Chapter 6.

4.1.2. SH-wave raytracing based on the Snell's law formalism

The computational method below is given for SH waves as an example of raytracing using the Snell's law formalism. It is superior, for any given source-receiver configuration, to the proposed computational method using the Fermat's-principle approach, as it reflects more accurately the relationship between phase and group speeds (see Chapter VI and Appendix 6.).

Method of Computation: RayTracing for a Two-layer, Isotropic/Anisotropic Medium Using Snell's Law Formalism

Given a medium composed of an isotropic layer of thickness h_1 , and anisotropic layer of thickness h_2 separated by a planar horizontal interface, with a source situated at the surface of the isotropic layer and the receiver on the bottom of the anisotropic layer, separated by a horizontal distance D , the incidence angle, θ_i , corresponding to a given source-receiver separation can be calculated by following the steps below.

Incident SH \Rightarrow Transmitted SH

X = horizontal distance between source and receiver, d .

ht = thickness of the isotropic layer, h_1 .

hb = thickness of the anisotropic layer, h_2 .

v = velocity of a shear-wave in the isotropic layer, v .

B = vertical shear-wave velocity in the anisotropic layer, β_o .

g = anisotropic parameter, γ .

$x = \sin[m]/v$

$z = \text{ArcCos}[(1 - \text{Sqrt}[1 - (2*x*B)^2*g]) / (2*x*B*g)]$

$dz = 2*z$

$r = 1 / (B*(1 + g*\text{Cos}[z]^2))$

$t = \text{Sin}[z]*(2*B*g*\text{Cos}[z]^2 - 1/r)$

$b = \text{Sqrt}[1/r^2 + (B*g*\text{Sin}[dz])^2]$

$s = \text{ArcCos}[Abs[t/b]]$

$\text{FindRoot}[ht*\text{Tan}[m] + hb*\text{Tan}[s] == X, \{m, \{0.1, 0.3\}\}]$

Note that the resulting incidence (take-off) angle is given in radians

4.1.3. Fermat's-principle Approach

The operation of calculating the travelpath and traveltime between a given source and receiver can be facilitated significantly by using Fermat's principle of stationary time, provided one is willing to limit the approach to the fully linearized approach and thus to decrease somewhat the accuracy (see Appendix 6). At this point some clarification is required.

Fermat's principle of stationary time is, perhaps, the most fundamental concept of raytracing theory. Therefore, the above statement, implying some loss of accuracy by using the Fermat's-principle approach, calls for some explanation, since, in principle, the most accurate of solutions must obey Fermat's principle of stationary time. The above-mentioned loss of accuracy is a result of the method through which Fermat's principle is treated, not the essence of the principle itself. The difficulty of the method lies in the fact that Fermat's principle relates to traveltime, which in turn, is intimately linked to the concept of group angle and group velocity. In order to calculate the group angle and the magnitude of group velocity properly, one needs the expression for phase velocity and a given value of phase angle (see equation (6.3)). The given value of phase angle is provided by the formalism of Snell's law. If one chooses to calculate group angles directly by finding a stationary point of the traveltime, one must provide a function describing group velocity with respect to a group angle. Applying Thomsen's (1986) linearization of weak-anisotropy equations implies the equivalence of expressions for phase, v , and group, V , velocities with corresponding phase, ϑ ¹³, and group, θ , angles, that is:

$$V(\theta) \cong v(\vartheta). \quad (4.4)$$

Although the above expression does not imply a general equivalence of phase and group velocities, it constitutes a departure from the exact expression of equation (6.3). Consequently, both ray path and traveltime calculated using the Fermat's principle

¹³ Recall that the angle ϑ is the phase angle measured with respect to the vertical, i.e., phase colatitude; it is the complement of the angle ξ .

approach suffer from (in the case of weak anisotropy) slight inaccuracy.

In considering various mathematical difficulties one must remember that, physically speaking, Snell's law is a direct consequence of Fermat's principle and, ideally, results obtained through either method must be identical. Fermat's principle states that the path of the ray between two points is such that the first-order variation with respect to all neighbouring paths is zero. In other words, it is the path of least or greatest time. To gain a more intuitive understanding of this concept one can visualize rays travelling through a multitude of paths. However, in the neighbourhood of a stationary path the rays travel in phase and arrive at the receiver at the same time, while the rays travelling along other paths arrive at the receiver with various delays. The former scenario leads to constructive interference while the latter scenario results in destructive interference. For a primary ray travelling in a stack of horizontal layers the path is a minimum and the principle is often referred to as a principle of least time. For a P-P wave in global geophysics (source and receiver at the surface, reflection at the surface in the midpoint), for example, the path is one of maximum time with respect to lateral variation of the position of the halfway reflection point.

As mentioned earlier, the approach based on Fermat's principle used in this dissertation, relies solely on the concept of group velocity. The magnitude of the group velocity, however, is a function of the phase velocity. Thus, without an explicit formula for phase velocity one needs to assume the same form of equations between for both phase and group velocities as proposed by Thomsen (1986). In the case of weak anisotropy the accuracy of results is still very high, in spite of the simplifying assumption. One has to be aware, however, of the assumptions made and their consequences. Appendix 6 is devoted to an investigation of this matter, where from the point of view of degree of approximation, the Fermat's principle approach is equivalent to the linearized approach.

In the context of raytracing between a given source and receiver, Fermat's principle allows one to obtain results, which under assumptions of full linearization, are equivalent to those reached via Snell's law while being simpler from the calculational viewpoint. The approach using the calculation of Snell's law, as described in Chapter II

and Chapter III is necessary if one considers incidence, refraction and reflection of a ray at an interface, without specifying two points between which the ray travels. Also, the case of non-horizontal layers calls for the Snell's law formulation. It must be emphasized that, the Snell's law formalism, involving both phase and group velocities, is more general in all cases, even when the two points, most commonly source and receiver, are specified, but Fermat's principle provides, algorithmically, a more straightforward approach. In other words, one may say that by adding some constraints to the problem, i.e., the locations of the two end-points of the trajectory of the ray, one can omit the explicit use of the Snell's law formalism and obtain a result directly from Fermat's principle. Also, since, as shown in Appendix 6, it yields results very close to those obtained through a more exact method, it provides an independent verification of algorithms and coding. Furthermore, it forms the core of the inversion scheme developed in Chapter VIII. Thus, taking advantage of the convenience of Fermat's approach, the case of two anisotropic layers separated by an interface is considered. The problem consists in determining the path of a ray shown in Figure 4.1.

For a given horizontal source-receiver separation, X , layer thicknesses H_1 , H_2 , vertical wave speeds V_1 , V_2 , and anisotropic parameters δ_1 , δ_2 , ϵ_1 , ϵ_2 , or γ_1 , γ_2 , the problem reduces to that of finding the path of stationary traveltime. One can conveniently parameterize the problem, denoting the distance between the refraction point and the receiver as r , see Figure 4.1. Both the distances travelled by a ray in a given medium and the angles of propagation can be expressed in terms of r . This results in a general form of a system of equations (4.5) to be solved:

$$\left\{ \begin{array}{l} \frac{\sqrt{(X-r)^2 + H_1^2}}{V_1(r)} + \frac{\sqrt{r^2 + H_2^2}}{V_2(r)} = t(r) \\ \frac{dt(r)}{dr} = 0 \end{array} \right. \quad (4.5)$$

Appropriate expressions for group velocities $V_1(r)$ and $V_2(r)$ can be inserted depending on the types of waves considered. Namely, P-P, SV-SV, P-SV, SV-P, or SH cases.

Method of Computation: Raytracing for a Two-layer, Anisotropic/Anisotropic Medium Using Fermat's Principle

Incident SH \Rightarrow Transmitted SH

X	=	<i>horizontal distance between source and receiver</i>
HJ	=	<i>thickness of the upper layer</i>
HD	=	<i>thickness of the lower layer</i>
VJ	=	<i>vertical wave speed in the upper layer</i>
VD	=	<i>vertical wave speed in the lower layer</i>
GJ	=	<i>anisotropic parameter in the upper medium, γ_1</i>
GD	=	<i>anisotropic parameter in the lower medium, γ_2</i>

```
FindMinimum[
Sqrt[r^2-2*X*r+X^2+HJ^2]/
(VJ*(1+GJ*((X-r)^2/((X-r)^2+HJ^2)))+
Sqrt[r^2+HD^2]/
(VD*(1+GD*r^2/(r^2+HD^2))),{r,{0,X}}]
```

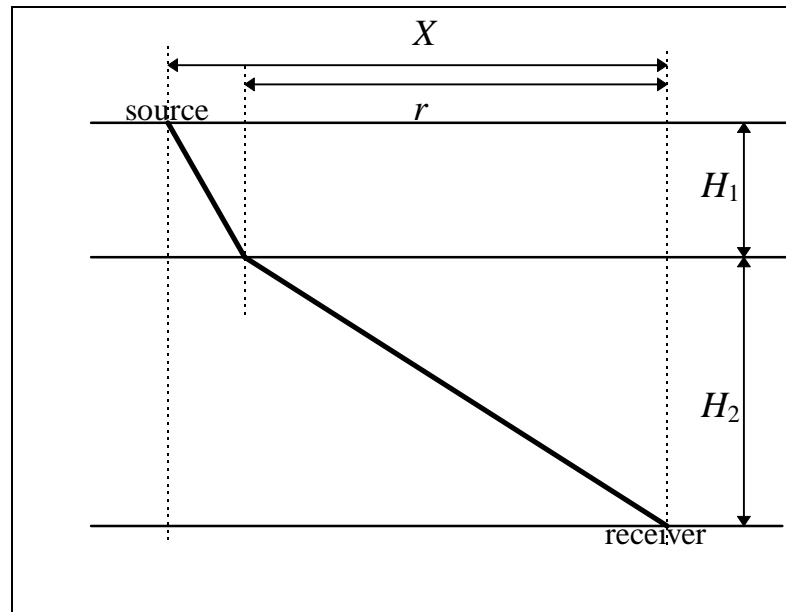


Figure 4.1. The illustration of a ray travelling through a two-layer between a source and receiver separated by a horizontal distance X . The value of r corresponds to the horizontal distance between the refraction point and the receiver.

4.2. RAYTRACING THROUGH A STACK OF SEVERAL HORIZONTAL LAYERS

4.2.1. Raytracing method based on the global minimization of travelttime

The parameterization of the travelttime function based on the horizontal distance between the refraction point and the receiver, r , can be used most conveniently for a two-layer case, i.e., comprising only one interface at which refraction occurs. In the case of a model comprising several layers, the same approach leads immediately to a rather complicated system, for there are as many different values of r , as there are interfaces. One can, of course, minimize the travelttime function with respect to several variables r_j , where j corresponds to an interface number. Because of an extremely simple and convenient way of programming such an approach in Mathematica®, the code is given below. There are, however, some reservations concerning fine precision using this method (see Appendix 3).

Computational Method: Raytracing through multiple anisotropic layers using Fermat's principle of stationary time formulation

Mathematica® code for a three layer case. Note that the code can be very easily extended for any desired number of layers. It suffices to add analogous modules in the FindMinimum statement, and provide additional input information concerning those layers.

X = horizontal source/receiver distance
 HJ = thickness of the first layer
 HD = thickness of the second layer
 HT = thickness of the third layer
 GJ = anisotropic parameter in the first layer
 GD = anisotropic parameter in the second layer
 GT = anisotropic parameter in the third layer
 VJ = vertical speed in the first layer
 VD = vertical speed in the second layer
 VT = vertical speed in the third layer

FindMinimum[
travelttime in the first layer

$HJ * \text{Sec}[\text{ArcTan}[(X-r_j)/HJ]] /$
 $(VJ * (1 + GJ * \text{Sin}[\text{ArcTan}[(X-r_j)/HJ]^2]) +$

$$\begin{aligned}
 & \text{traveltime in the second layer} \\
 & \text{HD*Sec[ArcTan[(rj-rd)/HD]]/} \\
 & (\text{VD}*(1+\text{GD}*\text{Sin}[\text{ArcTan}[(\text{rj-rd})/\text{HD}]^2]))+ \\
 & \text{traveltime in the third layer} \\
 & \text{HT*Sec[ArcTan[(rd/HT)]]/} \\
 & (\text{VT}*(1+\text{GT}*\text{Sin}[\text{ArcTan}[(\text{rd}/\text{HT})]^2])), \\
 & \{\text{rj},0,\text{X}\},\{\text{rd},0,\text{X}\}
 \end{aligned}$$

4.2.2. Raytracing method based on Snell's law

One can also parameterize the raypath without direct use of the traveltime. Using Snell's law, the entire model can be parameterized with a single value of r . For instance, r can correspond to the horizontal distance between the refraction point and the receiver for the first interface. Thus one defines the take-off angle in terms of r , and follows through other interfaces, obeying Snell's law for anisotropic media. In general the offset equation can be written as a series of horizontal distances traveled in each layer (equation (4.6)). The use of r , as opposed to a take-off angle itself, θ_1 or θ_i , is introduced by design, as it proves to be convenient in inverse calculations (Chapter VIII). Thus:

$$(X - r) + H_2 \tan \theta_2 + \dots + H_n \tan \theta_n = X. \quad (4.6)$$

The value of θ_1 is given immediately as a function of r , and all subsequent values of θ are related to the previous one by Snell's law. Therefore, the entire raypath is parameterized in terms of r , the horizontal distance between the refraction point and the receiver, r , for the first interface.

4.2.3. Raytracing through multiple layers (SH waves or any waves with elliptical phase-velocity dependence).

Elliptical velocity dependence allows for many a valuable mathematical demonstration. It is, from the mathematical point of view, the most convenient formulation of anisotropy. Isotropy is a special case of this formulation, as a circle is a particular ellipse, one for which the foci coincide. The elliptical velocity dependence can

be defined with two parameters, e.g., horizontal and vertical speeds as used in section 2.4.1, or vertical speed and the anisotropic parameter γ as in the case of weak-anisotropy approximation for SH waves as illustrated by equation (3.30). Note that the phase velocity of P and SV waves, requires three parameters as illustrated by equations (3.1) and (3.20) respectively.

There exists, however, a conflict between physical applicability and mathematical elegance. Helbig (1994) states that elliptic anisotropy although it exists is so rare an occurrence that it seems hardly worth an extended discussion. However, according to Helbig, it is important for several reasons. In particular, *elliptical* slowness curves, i.e., two dimensional cross-sections of slowness surfaces, are not as rare, by far, as *ellipsoidal* slowness surfaces. In other words, although a velocity surface might not be ellipsoidal, various selected cross-sections might be elliptical. For transversely isotropic media, SH waves exhibit elliptical slowness curves for all planes that contain the axis of symmetry¹⁴. The concepts of elliptical anisotropy, with all that it entails are perfectly applicable to the propagation of SH waves in TI media, as the wavefronts of SH waves are always ellipsoids. In general, the wavefronts of P and SV waves are not ellipsoids, thus for those waves, the concept of elliptical anisotropy can be, at best, an approximation. Certain pieces of the wavefront may be represented with sufficient accuracy by ellipsoids (Helbig, 1983). Illustrations of various slowness curves are shown in Appendix 2; it is clear that although some of them could be very well approximated by ellipses, others exhibit peculiarities of shapes which do not lend themselves to such an approximation.

A strict adherence to the mathematical formulation of elliptical velocity dependence for compressional waves, in the context of transversely isotropic media, implies that $\delta = \varepsilon$ in the equations for phase velocities (Thomsen, 1986). This implies, (see equation (3.20)) an isotropic SV wave, i.e., no angular dependence (e.g., Daley and Hron, 1977). This according to Thomsen (1986) constitutes a nonphysical situation. In a general case, it can, however, according to Helbig (1994), be a natural consequence of a particular symmetry if the combination of elastic constants is such that:

¹⁴ Note that following the definition of transverse isotropy, in the plane perpendicular to the symmetry axis, slowness curves for all waves are circular.

$$(C_{11} - C_{55})(C_{33} - C_{55}) - (C_{13} + C_{55})^2 = 0, \quad (4.7)$$

in which case the qP wave possesses an elliptical slowness curve, while the qSV wave has a circular one. Early field studies, e.g., of Dunoyer de Segonzac and Laherrere (1959), who used elliptical velocity dependence to reconcile theory and observation from vertical seismic profiles (VSP), indicate that the usefulness of elliptical formulation, goes beyond an elegant expression of mathematically tractable equation. Dellinger (1991) states appropriately in the conclusions of his doctoral dissertation “even elliptical anisotropy is better than nothing”.

Firstly, in many cases, the velocity dependence resembles an elliptical shape, and can, within the experimental context, e.g., in exploration geophysics, be approximated by an ellipse. As Dellinger and Muir (1988) point out, geophysicists, for reasonable offsets, find the hyperbolic move-out a good approximation, although it is not strictly true. They conclude by remarking that the hyperbolic moveout assumption is equivalent to an elliptical wavefront assumption, thus the elliptical model applies in any case where the hyperbolic moveout approximation is appropriate.

Secondly, for an SH wave the elliptical velocity dependence holds true even in the case of strong anisotropy. Thus, the formulation based on elliptical velocity dependence provides an excellent basis for shear-wave exploration, and might be used as a reasonably approximation for compressional waves in some circumstances.

Dellinger (1991) shows by visualizing an ellipse as a stretched circle that, in general, only SH waves can undergo the stretching without losing the orthogonality of polarization (particle motion) with respect to other wave types. The simple coordinate stretching transforming a circle into an ellipse for either P- or SV- wavefronts entails the loss of the orthogonality of particle motion which is intrinsically embedded in the standard elastic-wave equation.

There also exists, introduced by Muir (see Michelena, Muir, and Harris, 1993), a double elliptical approximation, which fits a wider range of P and SV wavefronts. Particularly, it fits well some SV wavefronts which can be described as resulting from the

superposition of two ellipses, with major axes perpendicular to each other, e.g., Figure A2.1.(j). The double elliptical approximation is not, however, used in this dissertation.

Computational Method: Raytracing through multiple layers using Snell's law formulation for SH waves

A Mathematica® code for calculating the raypath travelling across three layers. The surface layer is assumed to be isotropic while deeper layers are anisotropic. Note that the code can be very easily extended for any desired number of layers. It suffices to add analogous modules, and provide additional input information concerning those layers.

X = horizontal source/receiver distance

HJ = thickness of the first layer

HD = thickness of the second layer

HT = thickness of the third layer

GD = anisotropic parameter in the second layer

GT = anisotropic parameter in the third layer

VJ = vertical speed in the first layer

VD = vertical speed in the second layer

VT = vertical speed in the third layer

(Calculation of the "take-off" angle and the ray parameter)

$Q_i = \text{ArcTan}[(X-r)/HJ]$

$x = \text{Sin}[Q_i]/VJ$

(Calculation of phase zd and group sd angle in the second layer)

$z_d = \text{ArcCos}[(1-\text{Sqrt}[1-(2*x*VD)^2*GD])/(2*x*VD*GD)]$

$dz_d = 2*z_d$

$rd = 1/(VD*(1+GD*\text{Cos}[z_d]^2))$

$drd = GD*\text{Sin}[dz_d]/(VD*(1+GD*\text{Cos}[z_d]^2)^2)$

$sd = N[\text{ArcCot}[(drd-rd*\text{Tan}[z_d])/(drd*\text{Tan}[z_d]+rd)]]$

(Calculation of phase zt and group st angle in the third layer)

$z_t = \text{ArcCos}[(1-\text{Sqrt}[1-(2*x*VT)^2*GT])/(2*x*VT*GT)]$

$dz_t = 2*z_t$

$rt = 1/(VT*(1+GT*\text{Cos}[z_t]^2))$

$drt = GT*\text{Sin}[dz_t]/(VT*(1+GT*\text{Cos}[z_t]^2)^2)$

$st = N[\text{ArcCot}[(drt-rt*\text{Tan}[z_t])/(drt*\text{Tan}[z_t]+rt)]]$

(Iterative procedure of finding the appropriate value of r)

$\text{FindRoot}[r+HD*\text{Tan}[sd]+HT*\text{Tan}[st]==0, \{r, \{0.5*X, 0.99*X\}\}]$

CHAPTER V

TRAVELTIMES IN WEAKLY ANISOTROPIC MEDIA

5.0. INTRODUCTION

Dealing with wave phenomena in anisotropic media one must distinguish between group and phase velocities. Field measurements of traveltimes and distance often yield group velocity. Phase velocity is linked intimately with mathematical description of reflection and transmission, e.g., Snell's law. Thus experimental testing of applicability of a mathematical formalism would often require the establishment of a relationship between group and phase velocities.

By definition (e.g., Winterstein, 1990), group velocity is the speed at which wave energy travels in a given direction radially outward from a point source in a homogeneous elastic anisotropic medium. In anisotropic media both group and phase velocities vary with direction, just as they vary with frequency in attenuating media. The quotient of distance between a point source and a point receiver, and elapsed traveltimes, yields the value of group velocity.

By definition (e.g., Crampin, 1989), phase velocity is the velocity in the direction of the phase propagation vector, normal to the surface of constant phase. Phase velocity appears naturally in most analytical and numerical expressions. The quotient of distance between a source generating plane waves and a receiver, and the elapsed traveltimes yields the value of phase velocity. Such measurements can be performed in laboratory setting (e.g., Dellinger and Vernik, 1994; Vestrum, 1994).

In isotropic elastic media, group and phase velocities coincide. In anisotropic media, group and phase velocities can coincide along particular trajectories. For instance, in transversely isotropic media with a vertical symmetry axis (TIV) at vertical and horizontal propagation, group velocity equals phase velocity. This property plays a key rôle in linking theoretical development with experimental verification of results. It allows one to physically measure vertical sound speeds α_o and β_o , for compressional and shear waves, respectively, that are equivalent to phase velocities and appear throughout the entire theoretical development.

5.1. MAGNITUDE OF GROUP VELOCITY

5.1.1. Magnitude of group velocity using the linearized method

Berryman (1979) gives the equation for the scalar magnitude of group velocity in terms of phase velocity and phase angle. Employing the form used by, e.g., Thomsen (1986) and Brown et al. (1991), and measuring phase angle, ξ , from the horizontal for consistency with development in this dissertation, yields:

$$V^2 [\theta(\xi)] = v^2 (\xi) + \left(\frac{dv}{d\xi} \right)^2, \quad (5.1)$$

or

$$V = v \sqrt{1 + \frac{1}{v^2} \left(\frac{dv}{d\xi} \right)^2}, \quad (5.2)$$

where V and v refer to group and phase velocities respectively.

Developing equation (5.2) into a Taylor series one obtains:

$$V = v \left[1 + \frac{1}{2v^2} \left(\frac{dv}{d\xi} \right)^2 - \frac{1}{8v^4} \left(\frac{dv}{d\xi} \right)^4 + \dots \right]. \quad (5.3)$$

Based on equation (5.3), one can say that, correct to the first order:

$$V[\theta(\vartheta)] = v(\vartheta). \quad (5.4)$$

In some applications, within the realm of weak anisotropy, equation (5.4) can yield results of sufficient accuracy.

Equation (5.4) is not to be understood as an equivalence of group and phase velocities. Except for a spherical wavefront, i.e., perfect isotropy, and particular symmetry directions where the normal to the wavefront (direction of phase velocity) is parallel to the radius (direction of group velocity) the two velocities are not equivalent. In this dissertation, equation (5.4) means that in weakly anisotropic media, for a given group angle, θ , the group velocity can be approximated using the form of equations (3.1), (3.20) and (3.30).

In the case of two layers separated by a planar interface, in the anisotropic medium of transmission the group speed of a given ray can be calculated using the group angle, θ , derived from the phase angle, ξ , and the ray parameter x_0 .

Method of Computation: Group Speed for a qP wave, qSV wave or qSH wave Transmitted Across an Isotropic/Anisotropic Interface assuming Full Linearization.

Given a planar, horizontal interface between an isotropic medium with an incident P wave, SV wave or SH wave with speed v at an angle of incidence, θ_i , and an anisotropic medium with the vertical group/phase speed of a compressional wave α_0 , and the vertical group/phase speed of a shear wave, β_0 , anisotropic parameters δ , ε and γ , as well as the angle of transmission, θ_t , calculated using the Snell's law formalism, the group speed, V , can be calculated using the steps below.

Incident P or SV \Rightarrow Transmitted qP

Step 1

Calculate the angle of transmission, θ_t , using Snell's law for isotropic/anisotropic interface

Step 2

Calculate the group speed, $V(\theta_t)$.

$$|V(\theta_t)| = \alpha_0 (1 + \delta \sin^2 \theta_t \cos^2 \theta_t + \varepsilon \sin^4 \theta_t)$$

Incident P or SV \Rightarrow Transmitted SV

Step 1

Calculate the angle of transmission, θ_t , using Snell's law for isotropic/anisotropic interface

Step 2

Calculate the group speed, $V(\theta_t)$.

$$|V(\theta_t)| = \beta_0 \left[1 + \frac{\alpha_0^2}{\beta_0^2} (\varepsilon - \delta) \sin^2 \theta_t \cos^2 \theta_t \right]$$

Incident SH \Rightarrow Transmitted SH

Step 1

Calculate the angle of transmission, θ_t , using Snell's law for isotropic/anisotropic interface

Step 2

Calculate the group speed, $V(\theta_t)$.

$$|V(\theta_t)| = \beta_0 (1 + \gamma \sin^2 \theta_t).$$

Note: The angle, θ , is the transmitted group angle, usually referred to, e.g., Thomsen (1986), Brown et al (1991), as ϕ .

5.1..2. Magnitude of group velocity using the approximate method

More accurate and, above all, physically more interesting results reflecting the distinction between phase and group velocities are obtained using the exact expression provided by Berryman (1979):

$$V^2[\theta(\vartheta)] = v^2(\vartheta) + \left(\frac{dv}{d\vartheta} \right)^2, \quad (5.5)$$

where V and v refer to group and phase velocities respectively. Using the expressions for phase velocities of P, SV, and SH waves, in terms of the phase angle, ϑ , measured with respect to the normal to the interface, shown below (Thomsen, 1986):

$$v_{qP}(\vartheta) = \alpha_0(1 + \delta \sin^2 \vartheta \cos^2 \vartheta + \varepsilon \sin^4 \vartheta), \quad (5.6)$$

$$v_{qSV}(\vartheta) = \beta_0 \left[1 + \frac{\alpha_0^2}{\beta_0^2} (\varepsilon - \delta) \sin^2 \vartheta \cos^2 \vartheta \right], \quad (5.7)$$

and

$$v_{SH}(\vartheta) = \beta_0(1 + \gamma \sin^2 \vartheta), \quad (5.8)$$

one can obtain expressions for group velocities:

$$V_{qP}[\theta(\vartheta)] = \alpha \sqrt{\left[1 + \delta \cos^2 \vartheta \sin^2 \vartheta + \varepsilon \sin^4 \vartheta \right]^2 + \sin^2(2\vartheta) [\varepsilon + (\delta - \varepsilon) \cos(2\vartheta)]^2}, \quad (5.9)$$

$$V_{qSV}[\theta(\vartheta)] = \beta \sqrt{\left[1 + \frac{\alpha^2(\varepsilon - \delta) \sin^2 \vartheta \cos^2 \vartheta}{\beta^2} \right]^2 + \frac{\alpha^4(\varepsilon - \delta)^2 \sin^2(4\vartheta)}{4\beta^2}}, \quad (5.10)$$

and

$$V_{qSH}[\theta(\vartheta)] = \beta \sqrt{[1 + \gamma \sin^2 \vartheta]^2 + [\gamma \sin(2\vartheta)]^2} . \quad (5.11)$$

In order to use equations (5.9), (5.10) and (5.11) one must first express ray angle, θ , as a function of the corresponding phase angle, ϑ . Note that one could also apply equation (5.5) to exact expressions for phase velocities (equations (A2.1), (A2.2), and (A2.3)). However, the resulting expressions for qP and qSV waves become very complicated, and, in the case of weak anisotropy, a very small increase in accuracy is paid for by a very large increase in complexity (see Appendix 6). Nevertheless, should one desire to derive the Snell's law for strong anisotropy there appear to be no fundamental difficulties (see Appendix 7).

Method of Computation: Group Speed for a qP wave, qSV wave or qSH wave Transmitted Across an Isotropic/Anisotropic Interface using weak-anisotropy formulation.

Given a planar, horizontal interface between an isotropic medium with an incident P wave, SV wave or SH wave with speed v at an angle of incidence, θ_i , and an anisotropic medium with the vertical group/phase speed of a compressional wave α_0 , and the vertical group/phase speed of a shear wave, β_0 , anisotropic parameters δ , ε and γ , as well as the angle of transmission, θ_t , calculated using the Snell's law formalism, the group speed, V , can be calculated using the steps below.

Incident P or SV \Rightarrow Transmitted qP

Step 1

Calculate the angle of transmission, θ_t , using Snell's law for isotropic/anisotropic interface, while retaining the corresponding phase-angle colatitude, ϑ , measured with respect to the normal to the interface

Step 2

Calculate the group speed, $V[\theta_t(\vartheta)]$, i.e., the group speed of a ray propagating at a group angle, θ , associated with the phase angle, ϑ .

$$V_{qP}[\theta(\vartheta)] = \alpha \sqrt{\left[1 + \delta \cos^2 \vartheta \sin^2 \vartheta + \varepsilon \sin^4 \vartheta\right]^2 + \sin^2(2\vartheta) \left[\varepsilon + (\delta - \varepsilon) \cos(2\vartheta)\right]^2}$$

Incident P or SV \Rightarrow Transmitted SV**Step 1**

Calculate the angle of transmission, θ_t , using Snell's law for isotropic/anisotropic interface, while retaining the corresponding phase-angle colatitude, ϑ , measured with respect to the normal to the interface

Step 2

Calculate the group speed, $V[\theta_t(\vartheta)]$, i.e., the group speed of a ray propagating at a group angle, θ , associated with the phase angle, ϑ .

$$V_{qSV}[\theta(\vartheta)] = \beta \sqrt{\left[1 + \frac{\alpha^2(\varepsilon - \delta) \sin^2 \vartheta \cos^2 \vartheta}{\beta^2}\right]^2 + \frac{\alpha^4(\varepsilon - \delta)^2 \sin^2(4\vartheta)}{4\beta^2}}$$

Incident SH \Rightarrow Transmitted SH**Step 1**

Calculate the angle of transmission, θ_t , using Snell's law for isotropic/anisotropic interface, while retaining the corresponding phase-angle colatitude, ϑ , measured with respect to the normal to the interface

Step 2

Calculate the group speed, $V[\theta_t(\vartheta)]$, i.e., the group speed of a ray propagating at a group angle, θ , associated with the phase angle, ϑ .

$$V_{qSH}[\theta(\vartheta)] = \beta \sqrt{\left[1 + \gamma \sin^2 \vartheta\right]^2 + \left[\gamma \sin(2\vartheta)\right]^2}.$$

5.2. TRAVELTIME CALCULATIONS

As mentioned above, the measured traveltime is the function of the group velocity. Thus having an expression for group velocity one can compute the time taken by a signal to travel between a given source and receiver. For a medium composed of an isotropic and an anisotropic layer such calculations can be performed with the aid of Snell's law derived in Chapters II and III. The Mathematica® codes to perform traveltime calculations using nonlinearized expressions for group velocity (equations (5.9), (5.10), and (5.11)) are given below.

Computational Method: Traveltime Between a Source and Receiver Across a Two-Layer Isotropic/Anisotropic Medium.

Incident P or SV \Rightarrow Transmitted qP

N.B. The programme below takes, as a starting point, the incident angle, θ_i , and, for given layer thicknesses, h_1 and h_2 , as well as other model parameters, calculates the traveltime and the horizontal source-receiver distance. I.e., it does not search for the take-off angle corresponding to a given source receiver separation.

```

m = angle of incidence (in radians)
ht = thickness of the isotropic layer,  $h_1$ .
hb = thickness of the anisotropic layer,  $h_2$ .
v = wave speed in the isotropic layer,  $v$ .
A = vertical compressional wave speed in the anisotropic layer,  $\alpha_0$ .
d = anisotropic parameter,  $\delta$ .
e = anisotropic parameter,  $\epsilon$ .
x = Sin[m]/v
FindRoot[A*x*(e-d)*C^4+A*x*d*C^2-C+A*x==0,{C,0.5,0,1}]
z = ArcCos[C/.]
dz = 2*z
r = 1/(A*(1+d*Sin[z]^2*Cos[z]^2+e*Cos[z]^4))
dr = (Sin[dz]*Abs[d*Cos[dz]-
2*e*Cos[z]^2))/(A*(1+d*Sin[z]^2*Cos[z]^2+e*Cos[z]^4)^2)
s = ArcCot[Abs[(dr-r*Tan[z])/(dr*Tan[z]+r)]]
phi = Pi/2-z
N[ht/(Cos[m]*v)+
hb/(Cos[s]*
A*Sqrt[(1+d*Sin[phi]^2*Cos[s]^2+e*Sin[phi]^4)^2
+Sin[2*phi]^2*(e+(d-e)*Cos[2*phi]^2)]]

```

$$N[ht*\tan[m]+hb*\tan[s]]$$

Incident P or SV \Rightarrow Transmitted qSV

N.B. The programme below takes, as a starting point, the incident angle, θ_i , and, for given layer thicknesses, h_1 and h_2 , as well as other model parameters, calculates the traveltime and the horizontal source-receiver distance. I.e., it does not search for the take-off angle corresponding to a given source receiver separation.

m = angle of incidence (in radians)

ht = thickness of the isotropic layer, h_1 .

hb = thickness of the anisotropic layer, h_2 .

v = wave speed in the isotropic layer, v .

A = vertical compressional wave speed in the anisotropic layer, α_0 .

B = vertical shear wave speed in the anisotropic layer, β_0 .

d = anisotropic parameter, δ .

e = anisotropic parameter, ϵ .

$x = \sin[m]/v$

FindRoot[($A^2*x*(e-d)/B$)* $C^4-(A^2*x*(e-d)/B)C^2+C-x*B=0$, { $C, 0.5, 0, 1$ }]

$z = \text{ArcCos}[C/.]$

$dz = 2*z$

$r = 1/(B*(1+(A/B)^2*(e-d)*\sin[z]^2*\cos[z]^2))$

$t = \sin[z]/r+(A^2/B)*\cos[z]*(e-d)*\sin[dz]*\cos[dz]$

$b = \text{Sqrt}[1/r^2+((A^2/B)*(e-d)*\sin[dz]*\cos[dz])^2]$

$s = \text{ArcCos}[Abs[t/b]]$

$N[ht/(\cos[m]*v)+$

$hb/(\cos[s]*$

$(B*\text{Sqrt}[(1+(A/B)^2*(e-d)*\sin[\phi]^2*\cos[\phi]^2)^2$
 $+ (A^4*(e-d)^2*\sin[4*\phi]^2)/(4*B^2)]))$

$N[ht*\tan[m]+hb*\tan[s]]$

Incident SH \Rightarrow Transmitted qSH

N.B. The programme below calculates the traveltime given the horizontal source-receiver separation, X , and other model parameters. I.e., it does search for the take-off angle corresponding to a given source-receiver separation.

X = horizontal distance between the source and receiver

ht = thickness of the isotropic layer, h_1 .

hb = thickness of the anisotropic layer, h_2 .

v = shear wave speed in the isotropic medium, v .

B = vertical shear wave speed in the anisotropic medium, β_0 .

g = anisotropic parameter, γ .

```

x = Sin[m]/v
z = ArcCos[(1-Sqrt[1-(2*x*B)^2*g])/(2*x*B*g)]
dz = 2*z
r = 1/(B*(1+g*Cos[z]^2))
t = Sin[z]*(2*B*g*Cos[z]^2-1/r)
b = Sqrt[1/r^2+(B*g*Sin[dz])^2]
s = ArcCos[Abs[t/b]]
Cr = N[ArcCot[Sqrt[((B/v)*(g+1))^2-1]]]
FindRoot[ht*Tan[m]+hb*Tan[s]==X,{m,{0.000001,0.5}}]
mf = m/.%
sf = ArcTan[(X-ht*Tan[mf])/hb]
xf = Sin[mf]/v
zf = ArcCos[(1-Sqrt[1-(2*xf*B)^2*g])/(2*xf*B*g)]
phi = Pi/2-zf
N[ht/(Cos[mf]*v)+hb/
(Cos[sf]*B*Sqrt[(1+g*Sin[phi]^2)^2+(g*Sin[2*phi]^2))]

```

Appendix 6 provides a study, based on SH waves, involving traveltime calculations using exact, approximate, and linearized expressions for velocity. All in all, within the realm of weak anisotropy, the discrepancies between numerical values yielded by the three approaches are relatively small. More importantly, however, certain physical attributes are obscured by the process of linearization. For instance, the distinction between the phase and group angle becomes less clear in the raytracing process. The importance of this distinction, particularly in relation to SV waves, is demonstrated in Chapter VI.

CHAPTER VI

ANISOTROPIC/ANISOTROPIC INTERFACE

6.0. INTRODUCTION

Chapter II provided a rather general formalism for calculating reflection and transmission angles (Snell's law) at an interface between two anisotropic media. The two media were characterized by phase slowness surfaces expressed in terms of Cartesian components x , y , and z . Chapter III used the rather general, but less directly applicable template provided in Chapter II to express the relation between incidence and transmission angles for compressional and shear waves under the assumption and approximations of weak anisotropy. The explicit formulæ were derived for a case of isotropic/anisotropic interface. This scenario allows a more straightforward initiation of the process of raytracing (Chapter IV and Chapter V), and, above all, is perfectly applicable to the prediction and analysis of results of physical modelling (Chapter VII). If the medium of incidence is anisotropic the ray parameter, x_0 , cannot be found directly from the angle of incidence because, in general, the group and phase angles are not equal. In this chapter, the basic formulæ relating incident and transmitted angles for shear and compressional waves are derived, under the assumptions of weak anisotropy for a case of an interface between two anisotropic media.

In the transversely isotropic (TI) medium there are, similarly to the isotropic case, three distinct and independent solutions. They correspond to the quasi-longitudinal, quasi-transverse and transverse waves. The directions of polarization are mutually orthogonal. The purely transverse wave, denoted as SH, has a direction of particle

displacement, i.e., polarization, perpendicular to the direction of propagation. Its slowness curves in the plane of the symmetry axis are always elliptical, even in the case of strong anisotropy (e.g., Helbig 1994). The polarization of the remaining waves is not pure. In the case of compressional (P) wave, the particle displacement is not perfectly aligned with the direction of propagation. In the case of shear (SV) wave, the particle displacement is not perfectly perpendicular to the direction of propagation. For this reason those two waves should be referred to as quasi-longitudinal and quasi-shear. In some cases of extreme anisotropy it is conceivable for the polarization to be so impure that the description of a wave as quasi-compressional or quasi-shear becomes impossible. As remarked by Winterstein (1990), theory allows for phenomena that are not observed from data in real rocks. There seems to be no experimental evidence that such impure polarizations exist in sedimentary rocks (Winterstein, 1990).

Therefore, it appears reasonable and useful to derive refraction formulæ for two principal scenarios. The first one consisting of the incidence and transmission of a perfectly transverse (SH) wave, and the second one of the incidence and transmission of quasi-compressional (qP) and quasi-shear (SV) wave. Those two cases result from the Christoffel equation in the transversely isotropic medium which is separated into two decoupled systems (e.g., Dellinger, 1991). Assuming, without any loss of generality, that the propagation occurs in the xz -plane, the particle displacement of an SH wave is perfectly parallel with the y -axis. In the case of propagation in the TIV-medium, where any azimuth constitutes a symmetry plane, the polarizations of quasi-compressional (qP) and quasi-shear (qSV) waves are contained in the plane of propagation, i.e., xz -plane. Probably, in the case of weak anisotropy, as encountered in sedimentary rocks, the off-plane component of polarization, in any symmetry system, is small. Thus considering the two distinct cases (SH and P, SV) mentioned above should constitute a valid approach. It is important to realize, however, that since the polarization of quasi-compressional and quasi-shear waves, in a general case, contains all three Cartesian components an incident wave of one type will generate all three reflected and transmitted waves.

Since, in the present case, there is no danger of confusion one can refer, particularly under the assumption of weak anisotropy, to the aforementioned waves as P

and SV thus omitting the prefix *quasi*. Such notation is strictly correct with respect to SH waves.

6.1. THE APPROACH

In the generalized formalism dealing with the interface between two anisotropic media, derived in Chapter II, the angles of incidence and refraction are related through the continuity conditions across the boundary, i.e., through the ray parameter, x_0 . Thus, in the general method, one does not necessarily express the angle of transmission as a function of the angle of incidence, but both are expressed as functions of the ray parameter. In many cases it is possible to express the angle of transmission as a function of the angle of incidence, e.g., in the case of the elliptical velocity dependence illustrated in Chapter II. In other cases such an expression can be very complicated or outright impossible. In such a case one needs to resort to some numerical scheme. In Chapter III, the difficulty was overcome by assuming the medium of incidence to be isotropic. This implies that the ray (group) and phase angles coincide and the ray parameter can be very easily related to the angle of incidence, θ_i , and the wave speed in the isotropic medium, v , namely:

$$x_0 = \frac{\sin \theta_i}{v} . \quad (6.1)$$

In an anisotropic medium, i.e., with a nonspherical phase-slowness surface, one first needs to find a point on the phase-slowness surface at which the direction of the normal is the same as that of the desired incident ray¹⁵. The horizontal component of the slowness curve at this point yields the desired ray parameter, x_0 . This requires finding the phase angle, ξ , as a function of a group angle, θ , i.e., the opposite of the procedure illustrated in Chapter III.

A considerable simplification of the process could be provided by considering the linearized expressions for the relationships between phase and group angles (Thomsen,

¹⁵ Note that for a sufficiently complex slowness surface there may be several points exhibiting the same direction of the normal to the surface.

1986). For instance, in the case of P waves the group, θ , and phase, ϑ , angles are expressed as follows:

$$\tan \theta = \tan \vartheta \left[1 + 2\delta + 4(\varepsilon - \delta) \sin^2 \vartheta \right], \quad (6.2)$$

where ε and δ denote the anisotropic parameters. Similar formulæ are given for SV and SH waves (Thomsen, 1986)¹⁶. They all stem from simplifying assumptions which are a further consequence of the notion of weak anisotropy. Using the basic equations of weak anisotropy, which allow for mathematically manageable manipulations without all the entailing simplifications, leads to more accurate results as shown in the Appendix 6. This dissertation, attempts to avoid, wherever possible, the use of approximate formulæ and thus the more complicated route is taken. The repeated use of approximate formulæ, for instance in a multi-layer case, can lead to a significant numerical errors about which a geophysicist should be aware (e.g., Brown, 1988).

6.2. SPECIFIC CASES

In the remainder of this chapter the algorithms for several cases are developed and described. Firstly, a distinct case of a purely polarized shear (SH) wave is treated. Secondly, the most common case in exploration seismology of incident and transmitted compressional waves (P-P) is shown. Thirdly, an interesting case of a converted wave is considered; namely, the incident compressional and reflected shear wave (P-SV). The remaining two cases (SV-P and SV-SV) are not shown explicitly but their treatment is analogous to the ones shown.

¹⁶ The results obtained using the linearized relationship between phase and group angles for SV waves seems to yield incorrect results (see Figures 6.10 and 6.12). For this particular reason, as well as to increase the accuracy of the approach the non-linearized expressions are used.

6.2.1. SH-SH case

The case of the incident SH wave and the transmitted SH wave has several appealing features. Above all it stands on its own as a physical phenomenon occurring in a transversely isotropic medium. Mathematically, the expressions related to SH waves exhibit greater simplicity than either P or SV waves. Also, since it is known (e.g., Helbig, 1994) that the slowness curves of SH waves in any vertical plane of a transversely isotropic (TIV) medium are always elliptical, one can compare the results obtained under the weak-anisotropy assumption with the results obtained using elliptical geometry in the general scheme as described in Chapter II. Such a comparison is equivalent to the comparison between the exact and an approximate solutions (see Appendix 6).

Computation Method: Incidence and transmission Angles at an Anisotropic/Anisotropic Interface

Incident SH \Rightarrow Transmitted SH

Step 1

Solve for the phase angle, ξ , in the medium of incidence, given the incidence angle, θ_i .

$$\theta_i = \text{Arc cot} \left\{ \frac{\frac{dr(\xi)}{d\xi} - r(\xi) \tan \xi}{\frac{dr(\xi)}{d\xi} \tan \xi + r(\xi)} \right\},$$

where

$$r(\xi) = \frac{1}{\beta_0 (1 + \gamma \cos^2 \xi)},$$

and

$$\frac{dr}{d\xi} = \frac{\gamma \sin(2\xi)}{\beta_0 (1 + \gamma \cos^2 \xi)^2}.$$

The equation can be written as a double cubic in $\cos\xi$, and thus, in principle, can be solved analytically.

Step 2

Calculate the ray parameter, x_0 , using the equation below. Choose the value of ξ which corresponds to the quadrant of the incidence angle.

$$x_0 = \frac{\cos\xi}{\beta_0(1 + \gamma \cos^2 \xi)}$$

Note that for a ray incident to the left of the normal, i.e., the second quadrant, $x_0 < 0$.

Step 3

Using the ray parameter, x_0 , constant for all interfaces, calculate the phase angle, ξ , in the medium of transmission

$$\xi = \text{Arc cos} \left\{ \frac{1 - \sqrt{1 - (2x_0\beta_0)^2 \gamma}}{2x_0\beta_0\gamma} \right\}$$

Step 4

Calculate the angle of transmission, θ_t .

$$\theta_t = \text{Arc cos} \left\{ \frac{\sin\xi \left(2\beta_0\gamma \cos^2 \xi - \frac{1}{r(\xi)} \right)}{\sqrt{\frac{1}{[r(\xi)]^2} + [\beta_0\gamma \sin(2\xi)]^2}} \right\}$$

where:

$$r(\xi) = \frac{1}{\beta_0(1 + \gamma \cos^2 \xi)}$$

The Mathematica® code is given below.

Q_i = angle of incidence, θ_i , in radians.

VJ = vertical speed in the medium of incidence

VD = vertical speed in the medium of transmission

GJ = anisotropic parameter, γ , for SH-waves or $\delta = \varepsilon$, for elliptical P-waves, in the medium of incidence.

GD = anisotropic parameter, γ , for SH-waves or $\delta = \varepsilon$, for elliptical P-waves, in the medium of transmission.

```

R = Qi
ri = 1/(VJ*(1+GJ*Cos[zi]^2))
dri = 2*GJ*Sin[zi]*Cos[zi]/(VJ*(1+GJ*Cos[zi]^2)^2)
FindRoot[Cot[Qi]==
(dri-ri*Tan[zi])/(dri*Tan[zi]+ri), {zi,R,-Pi,Pi}]
zif = Abs[zi/.%]
x = N[Abs[Cos[zif]/(VJ*(1+GJ*Cos[zif]^2))]]
zt = ArcCos[(1-Sqrt[1-(2*x*VD)^2*GD])/(2*x*VD*GD)]
dzt= 2*zt
rt = 1/(VD*(1+GD*Cos[zt]^2))
phi = N[Abs[Pi/2 - zif]]
Vpi = VJ*(1+GJ*Cos[zif]^2)
Vgi = N[VJ*Sqrt[(1+GJ*Sin[phi]^2)^2+
(GJ*Sin[2*phi]^2)]
s = N[ArcCos[
Abs[Sin[zt]*(2*VD*GD*Cos[zt]^2-1/rt)/
Sqrt[1/rt^2+(VD*GD*Sin[dzt])^2]]]]
pht = N[Abs[Pi/2 - zt]]
Vpt = VD*(1+GD*Cos[zt]^2)
Vgt = N[VD*Sqrt[(1+GD*Sin[pht]^2)^2+
(GD*Sin[2*pht]^2)]

```

Note that the resulting value of ξ appears in radians.

To completely describe the phenomena occurring at the boundary one needs to provide both phase, ϑ , and group, θ , angles as well as phase, v , and group, V , velocities. The phase velocity is the inverse of already obtained phase slowness, $r(\xi)$. Note that while the symbol, ξ , denotes the phase latitude, i.e., the angle measured from the horizontal, the symbol, ϑ , denotes the phase colatitude, i.e., the angle measured from the vertical. This notation is consistent throughout the entire dissertation.

The group velocity is obtained from a well known relationship (see Chapter V and Appendix 6),

$$V^2[\theta(\vartheta)] = v^2(\vartheta) + \left(\frac{dv(\vartheta)}{d\vartheta} \right)^2, \quad (6.3)$$

and for SH waves, under the assumption of weak anisotropy, is given by:

$$V[\theta(\vartheta)] \cong \beta \sqrt{(1 + \gamma \sin^2 \vartheta)^2 + [\gamma \sin(2\vartheta)]^2}. \quad (6.4)$$

Note that a fully linearized consequence of weak anisotropy implies:

$$V[\theta(\vartheta)] = v(\vartheta) \Rightarrow \beta(1 + \gamma \sin^2 \vartheta), \quad (6.5)$$

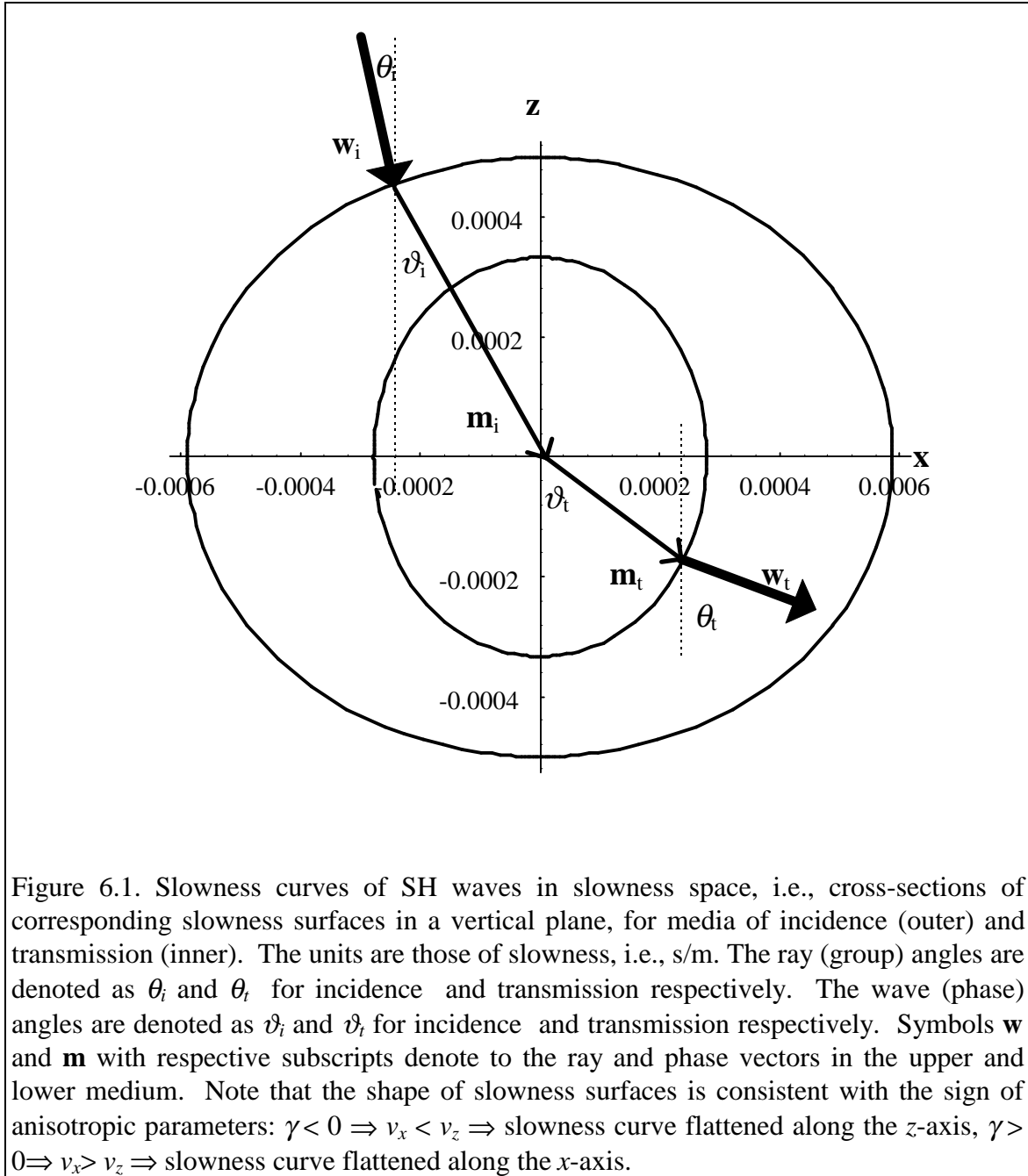
i.e., the second additive term under the square root which exists in equation (6.4) disappears in equation (6.5). The linearization increases the discrepancy between the exact and the approximate solutions and therefore is not used in this development. For a more thorough investigation of various degrees of approximation, the reader is referred to the Appendix 6.

6.2.1.1 Numerical example

Consider a planar horizontal interface between two anisotropic media. The upper medium has the vertical wave speed, $\beta = 2000$ m/s, and the anisotropic parameter $\gamma = -0.15$. The lower medium has the vertical wave speed, $\beta = 3000$ m/s, and the anisotropic parameter, $\gamma = +0.2$. The ray strikes the interface from above at the angle, $\theta_i = 20^\circ$.

Using the graphical illustration one can, to facilitate the construction, superpose two slowness curves (Figure 6.1). Since the phase velocity in the medium of transmission is significantly higher than the phase velocity in the medium of incidence, the entire slowness curve of the lower medium lies inside the slowness curve of the upper medium. Since the anisotropic parameters for either medium are of the opposite signs the major and minor axes of either curve coincide with different coordinate axes. A positive anisotropic parameter, $\gamma > 0$, means that the horizontal speed is greater than the vertical speed, which entails flattening on the equator of the slowness surface. Negative anisotropic parameter, $\gamma < 0$, means that the vertical speed is greater than the horizontal

speed, which entails flattening on the poles of the slowness surface. Using the fact that the ray parameter, in this case measured along the horizontal axis, i.e., parallel to the interface, is equal for both incident and transmitted waves one can construct corresponding angles.



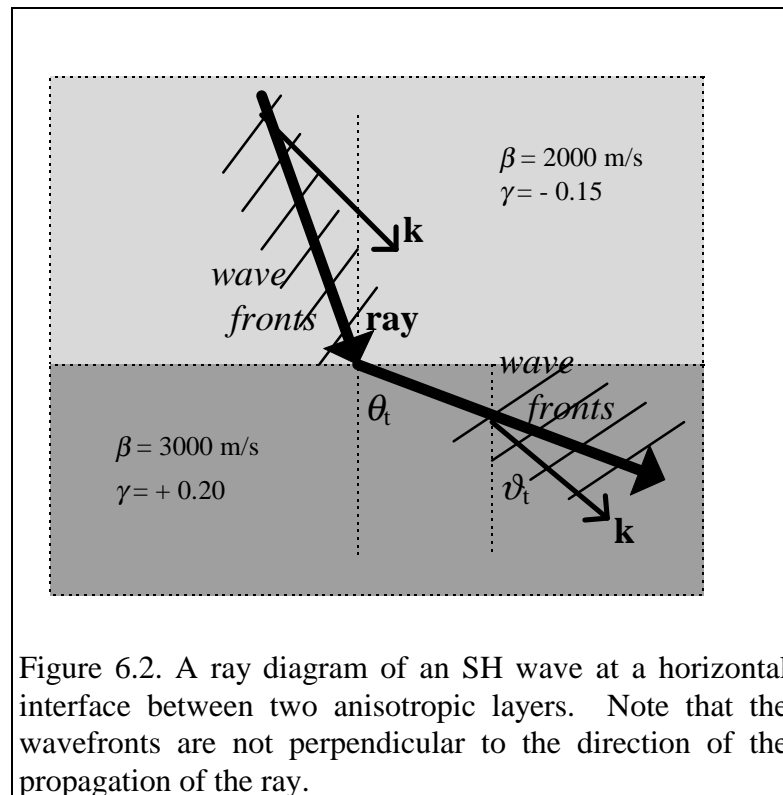
Using the derived algorithm one can calculate all the quantities illustrated above. The examination of results shows a clear distinction between phase and group

phenomena, which form an intrinsic element of wave propagation in anisotropic media. Several important relations between those quantities are described in section 6.3.

	Medium of Incidence, SH wave	Medium of Transmission, SH wave
Group angle, θ , [deg.]	20	62.57915511
Phase angle, ϑ , [deg.]	27.17059411	52.83375609
Group velocity, V , [m/s]	1952.72	3430.02
Phase velocity, v , [m/s]	1937.44	3381.02
Ray parameter, x_0 , [s/m] (horizontal slowness)	0.000235694	0.000235694

Table 6.1. Computational results for an SH-SH case. (N.B. All digits returned by the computer programme were kept in order to compare various approaches and algorithms used within Mathematica®.)

To better visualize the events at the interface the ray diagram at the interface is illustrated by Figure 6.2. The energy propagates in the direction of the ray, while the wavefronts propagate in the direction of the wave vector, \mathbf{k} .



6.2.2. P-P case

In spite of growing interest in shear waves, compressional waves are still the most commonly recorded waves in seismic exploration. Shear waves are difficult to generate and record at the surface due to the unconsolidated surficial material which poorly support shear stresses. In the case explicitly considered in this chapter, namely propagation within a symmetry plane, or equivalently, within any plane of a TIV medium containing the symmetry axis, the incidence of a P wave entails, apart from the generation of transmitted P wave, generation of a transmitted SV wave. Such mode conversion is treated in section 6.2.3, while below only incident and transmitted P waves are considered. One should note that although neglecting the mode conversion in the calculation of the reflection and transmission coefficients leads to erroneous results, the calculation of reflection and transmission angles, on the other hand, can be considered separately for each case.

Computation Method: Incidence and transmission Angles at an Anisotropic/Anisotropic Interface

Incident P \Rightarrow Transmitted P

Step 1

Solve for the phase angle, ξ , in the medium of incidence, given the incident angle, θ_i .

$$\theta_i = \text{Arc cot} \left\{ \frac{\frac{dr(\xi)}{d\xi} - r(\xi) \tan \xi}{\frac{dr(\xi)}{d\xi} \tan \xi + r(\xi)} \right\},$$

where

$$r(\xi) = \frac{1}{\alpha_0(1 + \delta \sin^2 \xi \cos^2 \xi + \varepsilon \cos^4 \xi)},$$

and

$$\frac{dr}{d\xi} = \frac{\sin(2\xi)[\varepsilon - \delta \cos(2\xi) + \varepsilon \cos(2\xi)]}{\alpha_0(1 + \delta \sin^2 \xi \cos^2 \xi + \varepsilon \cos^4 \xi)^2}.$$

Step 2

Calculate the ray parameter, x_0 , using the equation below. Choose the value of ξ which corresponds to the quadrant of the incidence angle.

$$x(\xi) = \frac{\cos \xi}{\alpha_0(1 + \delta \sin^2 \xi \cos^2 \xi + \varepsilon \cos^4 \xi)}.$$

Note that for a ray incident to the left of the normal, i.e., the second quadrant, $x_0 < 0$.

Step 3

Using the ray parameter, x_0 , constant for all interfaces, calculate the phase angle, ξ , in the medium of transmission

$$\alpha_0 x_0 (\varepsilon - \delta) \cos^4 \xi_0 + \alpha_0 x_0 \delta \cos^2 \xi_0 - \cos \xi_0 + \alpha_0 x_0 = 0$$

This is a quartic equation yielding a unique real angle.

Step 4

Calculate the angle of transmission, θ_t .

$$\theta_t = \text{Arc cos} \left\{ \frac{\alpha_0 \cos \xi \sin(2\xi)(\delta \cos(2\xi) - 2\varepsilon \cos^2 \xi) - \frac{\sin \xi}{r(\xi)}}{\sqrt{\frac{1}{[r(\xi)]^2} + [\alpha_0 \sin(2\xi)(\delta \cos(2\xi) - 2\varepsilon \cos^2 \xi)]^2}} \right\}$$

where:

$$r(\xi) = \frac{1}{\alpha_0(1 + \delta \sin^2 \xi \cos^2 \xi + \varepsilon \cos^4 \xi)}$$

The Mathematica® code is given below.


```

Qi      = angle of incidence in radians
VJ      = vertical speed in the medium of incidence
VD      = vertical speed in the medium of transmission
EJ      = anisotropic parameter in the medium of incidence,  $\epsilon$ 
DJ      = anisotropic parameter in the medium of incidence,  $\epsilon$ 
ED      = anisotropic parameter in the medium of transmission,  $\delta$ 
DD      = anisotropic parameter in the medium of transmission,  $\delta$ 
R = Qi
ri = 1/(VJ*(1+DJ*Sin[zi]^2*Cos[zi]^2+EJ*Cos[zi]^4))
dri = Sin[2*zi]*(EJ-DJ*Cos[2*zi]+EJ*Cos[2*zi])/
      (VJ*(1+EJ*Cos[zi]^4+DJ*Cos[zi]^2*Sin[zi]^2)^2)
FindRoot[Cot[Qi]==
      (dri-ri*Tan[zi])/(dri*Tan[zi]+ri), {zi,R,-Pi,Pi}]
zif = Abs[zi/.]
x = N[Abs[Cos[zif]/
      (VJ*(1+DJ*Sin[zif]^2*Cos[zif]^2+EJ*Cos[zif]^4))]
FindRoot[VD*x*(ED-DD)*C^4+VD*x*DD*C^2-C+VD*x==0,{C,0.5,0,1.5}]
z = ArcCos[C/.]
dz = 2*z
r = 1/(VD*(1+DD*Sin[z]^2*Cos[z]^2+ED*Cos[z]^4))
t = VD*Cos[z]*Sin[dz]*(Abs[DD*Cos[dz]-2*ED*Cos[z]^2])-Sin[z]/r
b = Sqrt[1/r^2+(VD*Sin[dz]*(DD*Cos[dz]-2*ED*Cos[z]^2))^2]
m = Qi
phj = N[(Pi/2-zif)]
Vpj = VJ*(1+DJ*Sin[phj]^2*Cos[phj]^2+EJ*Sin[phj]^4)
Vgj = Sqrt[(VJ*(1+DJ*Sin[phj]^2*Cos[phj]^2+EJ*Sin[phj]^4))^2+
      (VJ*Sin[2*phj]*(EJ+DJ*Cos[2*phj]-EJ*Cos[2*phj]))^2]
s = ArcCos[Abs[t/b]]
phd=N[(Pi/2-z)]
Vpd = VD*(1+DD*Sin[phd]^2*Cos[phd]^2+ED*Sin[phd]^4)
Vgd = Sqrt[(VD*(1+DD*Sin[phd]^2*Cos[phd]^2+ED*Sin[phd]^4))^2+
      (VD*Sin[2*phd]*(ED+DD*Cos[2*phd]-ED*Cos[2*phd]))^2]

```

6.2.2.1. Numerical example

Consider a planar horizontal interface between two anisotropic media. In the upper medium, the vertical wave speed, $\alpha_1 = 3000$ m/s, $\epsilon_1 = -0.2$ and $\delta_1 = 0.1$. In the lower medium, the vertical wave speed, $\alpha_2 = 4000$ m/s, and $\epsilon_2 = +0.15$ and $\delta_2 = -0.2$. The ray strikes the interface from above at an incidence angle of $\theta_i = 30^\circ$.

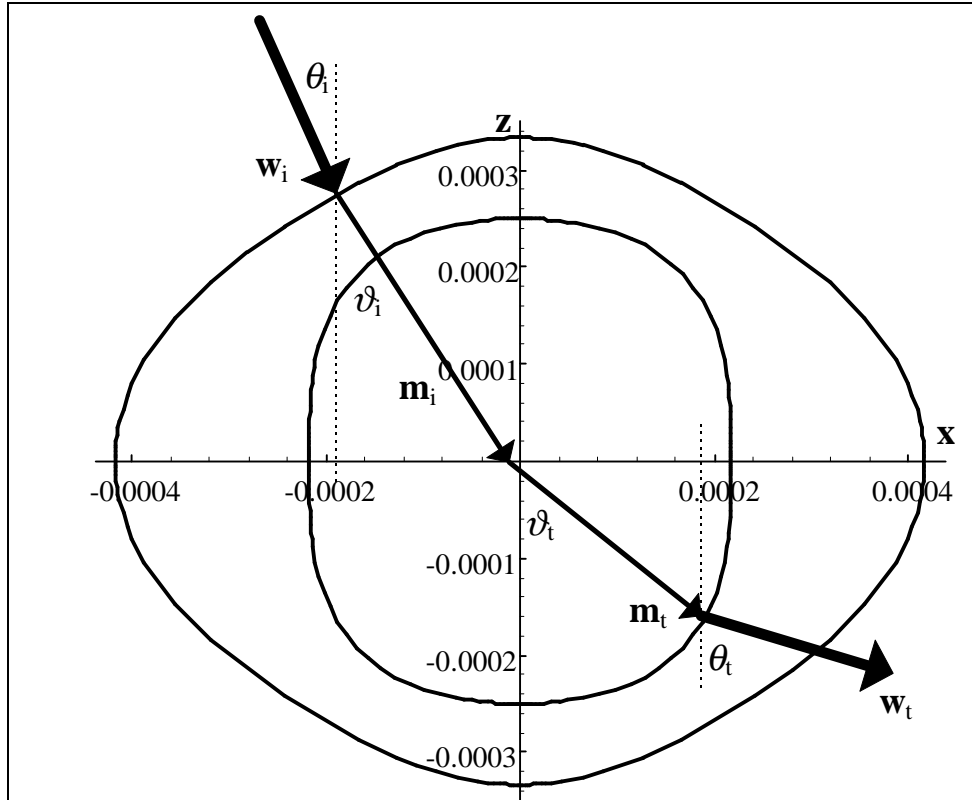


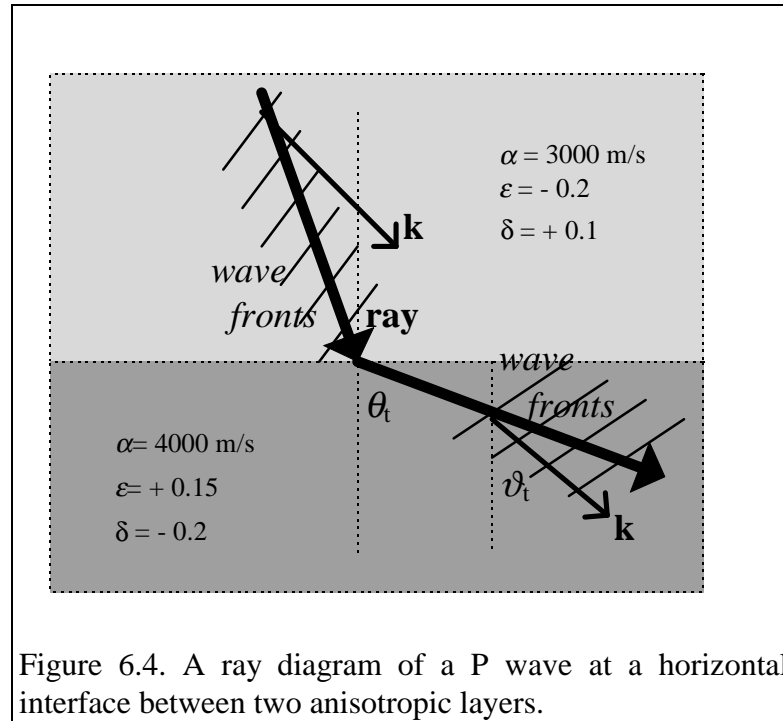
Figure 6.3. Compressional (P) wave slowness curves, i.e., cross-sections of corresponding slowness surfaces in a vertical plane. $\alpha_1 = 3000$ m/s, $\alpha_2 = 4000$ m/s, $\varepsilon_1 = -0.2$, $\varepsilon_2 = 0.15$, $\delta_1 = 0.1$, $\delta_2 = -0.2$. The outer curve corresponds to the “slower” medium of incidence. The inner curve corresponds to the “faster” medium of transmission. The meaning of various symbols is described in Figure 6.1.

	Medium of Incidence, P waves	Medium of Transmission, P wave
Group angle, θ , [deg.]	30	64.00912599
Phase angle, ϑ , [deg.]	35.57282955	51.53445969
Group velocity, V , [m/s]	3012.69	4133.32
Phase velocity, v , [m/s]	2998.45	4035.73
Ray parameter, x_0 , [s/m] (horizontal slowness)	0.000194013	0.000194013

Table 6.2. Computational results for a P-P case.

Using the algorithm presented above for incident and transmitted compressional waves one can calculate all the quantities illustrated above. Several important relations between those quantities are described in section 6.3.

To better visualize the events at the interface the ray diagram at the interface is illustrated by Figure 6.4. The energy propagates in the direction of the ray, while the wavefronts propagate in the direction of the wave vector, \mathbf{k} .



6.2.3. P-SV case

As already mentioned above, P and SV waves are coupled, i.e., an incident P wave generates an SV wave and vice-versa. As an interesting case, a converted P-SV propagation is illustrated. Clearly, one can easily combine several approaches to also obtain refraction laws for SV-SV and SV-P cases.

Computation Method: Incidence and transmission Angles at an Anisotropic/Anisotropic Interface

Incident P \Rightarrow Transmitted SV

Step 1

Solve for the phase angle, ξ , in the medium of incidence, given the incidence angle, θ_i .

$$\theta_i = \text{Arccot} \left\{ \frac{\frac{dr(\xi)}{d\xi} - r(\xi) \tan \xi}{\frac{dr(\xi)}{d\xi} \tan \xi + r(\xi)} \right\},$$

where

$$r(\xi) = \frac{1}{\alpha_0 (1 + \delta \sin^2 \xi \cos^2 \xi + \varepsilon \cos^4 \xi)},$$

and

$$\frac{dr}{d\xi} = \frac{\sin(2\xi) [\varepsilon - \delta \cos(2\xi) + \varepsilon \cos(2\xi)]}{\alpha_0 (1 + \delta \sin^2 \xi \cos^2 \xi + \varepsilon \cos^4 \xi)^2}.$$

Step 2

Calculate the ray parameter, x_0 , using the equation below. Choose the value of ξ which corresponds to the quadrant of the incidence angle.

$$x(\xi) = \frac{\cos \xi}{\alpha_0 (1 + \delta \sin^2 \xi \cos^2 \xi + \varepsilon \cos^4 \xi)}.$$

Note that for a ray incident to the left of the normal, i.e., the second quadrant, $x_0 < 0$.

Step 3

Using the ray parameter, x_0 , constant for all interfaces, calculate the phase angle, ξ , in the medium of transmission

$$\frac{\alpha_0^2 x_0 (\varepsilon - \delta)}{\beta_0} \cos^4 \xi - \frac{\alpha_0^2 x_0 (\varepsilon - \delta)}{\beta_0} \cos^2 \xi + \cos \xi - x_0 \beta_0 = 0$$

This is a quartic equation yielding a unique real angle.

Step 4

Calculate the angle of transmission, θ_t .

$$\theta_t = \text{Arc cos} \left\{ \frac{\frac{\sin \xi}{r(\xi)} + \frac{\alpha_0^2}{\beta_0} \cos \xi (\varepsilon - \delta) \sin(2\xi) \cos(2\xi)}{\sqrt{[r(\xi)]^2 + \left[\frac{\alpha_0^2}{\beta_0} (\varepsilon - \delta) \sin(2\xi) \cos(2\xi) \right]^2}} \right\}$$

where:

$$r(\xi) = \frac{1}{\beta_0 \left(1 + \frac{\alpha_0^2}{\beta_0^2} (\varepsilon - \delta) \sin^2 \xi \cos^2 \xi \right)}$$

The Mathematica® code is given below.

```

Qi      = angle of incidence in radians
VJ      = vertical speed of the compressional wave in the medium of incidence
VPD     = vertical speed of the compressional wave in the medium of transmission
VSD     = vertical speed of the shear wave in the medium of transmission
EJ      = anisotropic parameter in the medium of incidence, ε
DJ      = anisotropic parameter in the medium of incidence, ε
ED      = anisotropic parameter in the medium of transmission, δ
DD      = anisotropic parameter in the medium of transmission, δ
R       = Qi
ri      = 1/(VJ*(1+DJ*Sin[zi]^2*Cos[zi]^2+EJ*Cos[zi]^4))
dri     = Sin[2*zi]*(EJ-DJ*Cos[2*zi]+EJ*Cos[2*zi])/
          (VJ*(1+EJ*Cos[zi]^4+DJ*Cos[zi]^2*Sin[zi]^2)^2)
FindRoot[Cot[Qi]==
          (dri-ri*Tan[zi])/(dri*Tan[zi]+ri), {zi,R,-Pi,Pi}]
zif     = Abs[zi/.%]
x       = N[Abs[Cos[zif]/
          (VJ*(1+DJ*Sin[zif]^2*Cos[zif]^2+EJ*Cos[zif]^4))]
FindRoot[(VPD^2*x*(ED-DD)/VSD)*C^4-
          (VPD^2*x*(ED-DD)/VSD)C^2+C-x*VSD==0,{C,0.5,0,1}]
z       = ArcCos[C/.%]
dz      = 2*z
r       = 1/(VSD*(1+(VPD/VSD)^2*(ED-DD)*Sin[z]^2*Cos[z]^2))
t       = Sin[z]/r+(VPD^2/VSD)*Cos[z]*(ED-DD)*Sin[dz]*Cos[dz]
b       = Sqrt[1/r^2+((VPD^2/VSD)*(ED-DD)*Sin[dz]*Cos[dz])^2]
m       = Qi
phj     = N[(Pi/2-zif)]

```

$$\begin{aligned}
V_{pj} &= VJ*(1+DJ*\sin[\text{phj}]^2*\cos[\text{phj}]^2+EJ*\sin[\text{phj}]^4) \\
V_{gj} &= \text{Sqrt}[(VJ*(1+DJ*\sin[\text{phj}]^2*\cos[\text{phj}]^2+EJ*\sin[\text{phj}]^4))^2+ \\
&\quad (VJ*\sin[2*\text{phj}]*(EJ+DJ*\cos[2*\text{phj}]-EJ*\cos[2*\text{phj}]))^2] \\
s &= \text{ArcCos}[Abs[t/b]] \\
\text{phd} &= N[(\text{Pi}/2-z)] \\
V_p &= \text{VSD}*(1+(\text{VPD}/\text{VSD})^2*(\text{ED}-\text{DD})*\sin[\text{phd}]^2*\cos[\text{phd}]^2) \\
V_g &= \text{Sqrt}[\\
&(\text{VSD}*(1+(\text{VPD}/\text{VSD})^2*(\text{ED}-\text{DD})*\sin[\text{phd}]^2*\cos[\text{phd}]^2))^2+ \\
&((\text{ED}-\text{DD})*\text{VPD}^2*\sin[4*\text{phd}]/(2*\text{VSD}))^2]
\end{aligned}$$

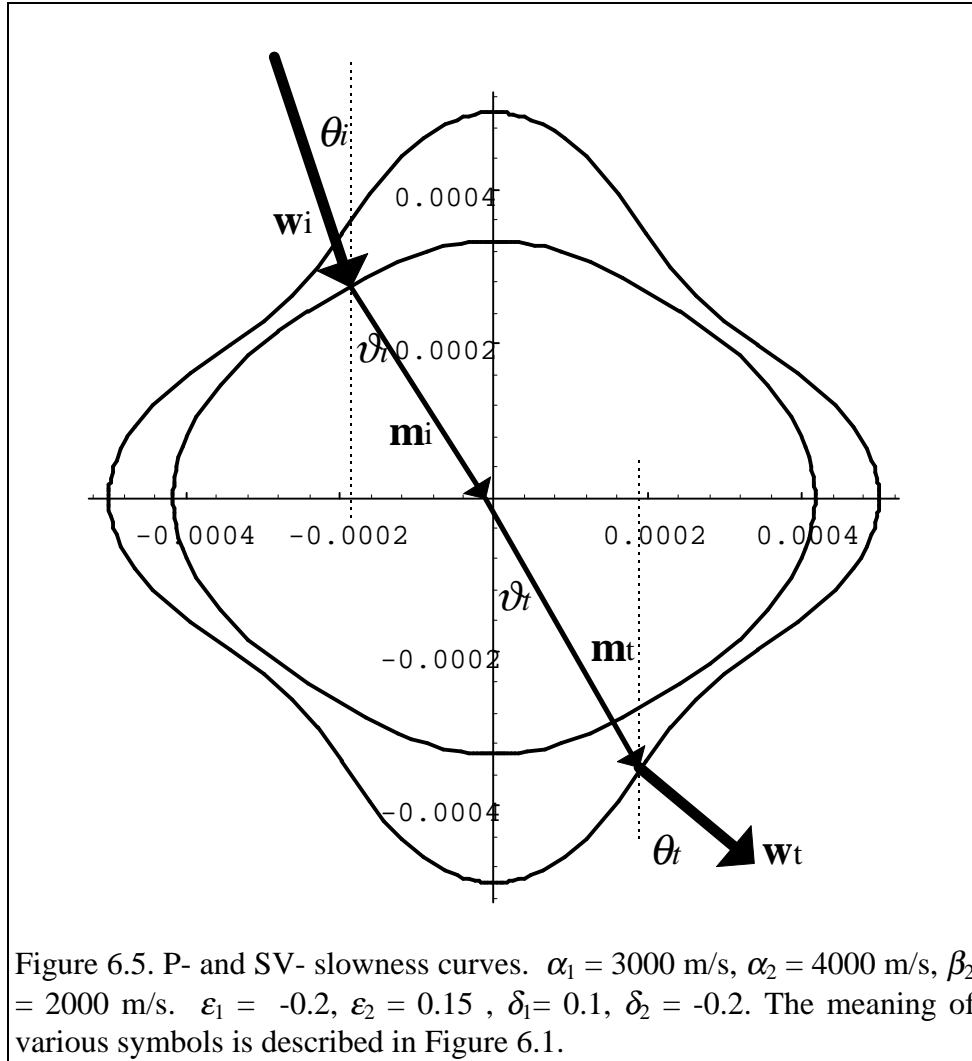
6.2.3.1. Numerical example

Consider a planar horizontal interface between two anisotropic media. In the upper medium, the vertical P-wave speed, $\alpha_1 = 3000$ m/s, and $\varepsilon_1 = -0.2$ and $\delta_1 = 0.1$. In the lower medium, the vertical P-wave speed, $\alpha_2 = 4000$ m/s, the vertical SV-wave speed, $\beta_2 = 2000$ m/s, $\varepsilon_2 = +0.15$ and $\delta_2 = -0.2$. The ray strikes the interface from above at an angle of $\theta_i = 30^\circ$.

Incidentally, one notices that the SV slowness curve of the for the chosen anisotropic parameters δ and ε would be difficult to approximate by an ellipse for the entire range of angles. One could, however, use the elliptical approximation in the neighbourhood of the vertical and horizontal axes, or use the double-elliptical approximation for the entire slowness curve (see Michelena et al., 1993). In this case Thomsen's (1986) equations were used.

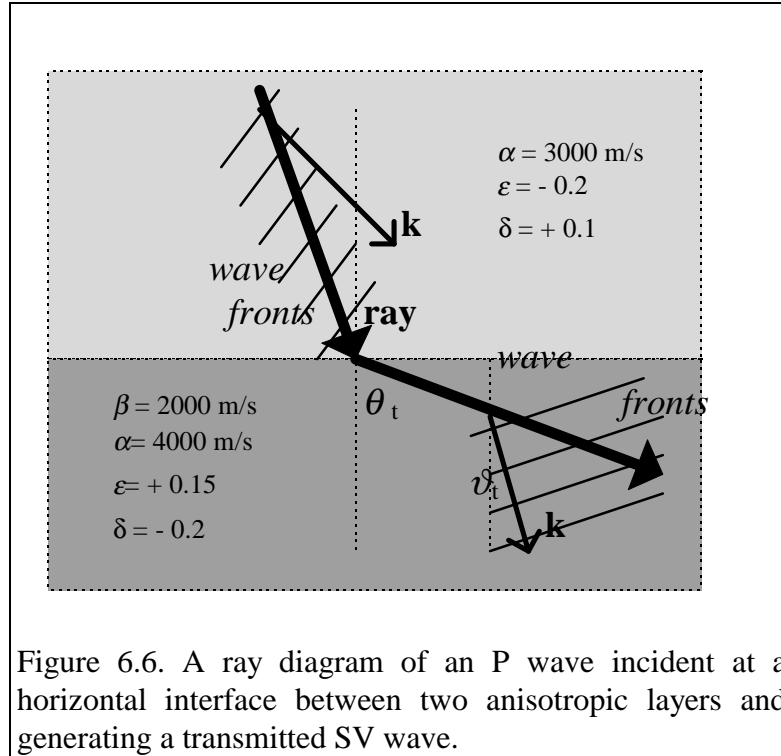
	Medium of Incidence, P wave	Medium of Transmission, SV wave
Group angle, θ , [deg.]	30	55.68662754
Phase angle, ϑ , [deg.]	35.57282955	29.08058748
Group velocity, V , [m/s]	3012.69	2801.9
Phase velocity, v , [m/s]	2998.45	2505.2
Ray parameter, x_0 , [s/m] (horizontal slowness)	0.000194013	0.000194013

Table 6.3. Computational results for a P-SV case.



Using the algorithm presented above for incident compressional wave and transmitted shear wave, one can calculate all the quantities illustrated in Figure 6.5. Several important relations between those quantities are described in section 6.3.1.

To better visualize the events at the interface the ray diagram at the interface is illustrated by Figure 6.6. The energy propagates in the direction of the ray, while the wavefronts propagate in the direction of the wave vector, \mathbf{k} .



6.3. PHYSICAL IMPLICATIONS

6.3.1. Points of verification

There are several ways which allow to confirm the correctness of the solution, i.e., to verify that the results obtained from the proposed algorithm are in agreement with certain fundamental requirements. The fulfillment of those requirements constitutes necessary conditions for the validity of the method.

Firstly, the phase, ϑ , and group, θ , angles, as well as the magnitudes of phase, v , and group, V , velocities must satisfy the following equation in either medium:

$$\cos(\theta - \vartheta) = \frac{|v(\vartheta)|}{|V(\theta)|}. \quad (6.6)$$

Secondly, the phase angles and phase velocities must satisfy the following equation across the interface:

$$\frac{\sin(\vartheta_1)}{v_1(\vartheta_1)} = \frac{\sin(\vartheta_2)}{v_2(\vartheta_2)}, \quad (6.7)$$

where the subscripts 1 and 2 correspond to the upper and lower medium respectively. This, of course, is the most standard form of Snell's law, which is always valid for phase angles and phase velocities.

Thirdly, Fermat's principle of stationary time must be satisfied. This is not obvious from a quick inspection. As a matter of fact, if one observes the P-SV case with "isotropic" intuition, one might suspect a contradictory result. Namely, if the energy of the signal travels at the group velocity, why is the transmitted ray, going from the "faster" to the "slower" medium bent away from the normal? In other words, isotropic intuition would dictate the following relationship:

$$|V_1| > |V_2| \Leftrightarrow \theta_1 > \theta_2, \quad (6.8)$$

where subscripts 1 and 2 correspond to quantities in the medium of incidence and transmission respectively. No such relation can be formulated in anisotropic media, as illustrated, for instance, by comparing the P-P and the P-SV cases. Nevertheless, Fermat's principle of stationary time is satisfied, although in a less intuitive way due to the complexity of the slowness surfaces. By calculating traveltimes for various neighbouring paths one could convince oneself that Fermat's principle implies a stationary traveltime path. An analogous procedure is performed in Chapter VIII. To gain deeper understanding of phenomena related to wave propagation in anisotropic media, it is important to investigate further this "nonintuitive" behaviour in the context presented above.

6.3.2. Refraction angle and Fermat's principle

Considering primary rays in horizontal layers one assumes that Fermat's principle of stationary time is equivalent to the principle of least time. In other words, one expects

the chosen path to be such as to minimize the traveltime with respect to all the neighbouring paths. Since the “unusual” occurrence of a ray bending away from the normal upon the transmission into the slower medium originates in the complicated appearance of the slowness curve in the medium of transmission, one can assume the upper medium to be isotropic and focus one’s investigation on the lower, anisotropic medium.

To demonstrate that the phenomenon of “unusual” ray bending occurs even if the medium of incidence is isotropic one can use the developed algorithm while setting the anisotropic parameters in the upper medium to zero. The results are displayed in Table 6.4.

	Medium of Incidence, P wave	Medium of Transmission, SV wave
Ray (group) angle, θ, [deg.]	30	53.80320067
Phase (wave) angle, ϑ, [deg.]	30	23.24799172
Ray (group) velocity [m/s]	3000	2750.16
Phase (wave) velocity [m/s]	3000	2368.27
Ray parameter, x_0, [s/m] (horizontal slowness)	0.000166667	0.000166667

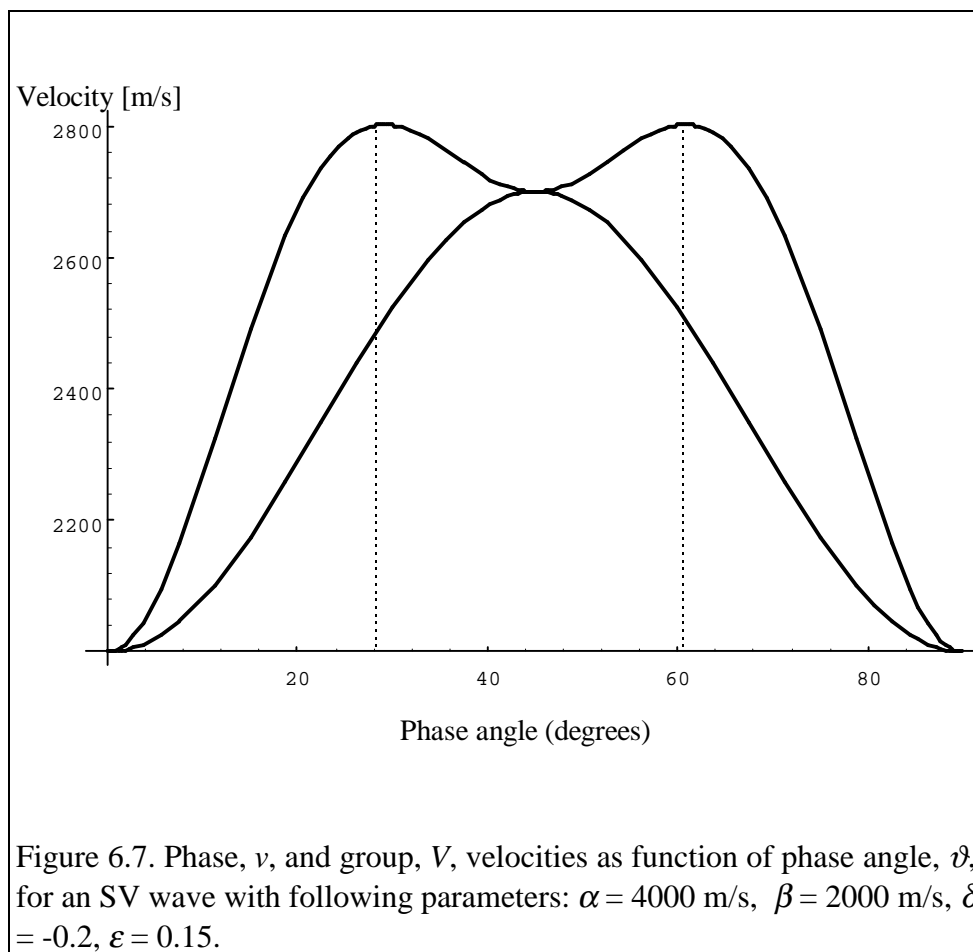
Table 6.4. Computational results for an isotropic/anisotropic model.

Quick verification of results in Table 6.4 shows that the continuity conditions, and the relationship between the magnitudes of phase and group velocities, as described in section 6.3.1, are satisfied. The ray bends away from the normal in spite of the fact that the group velocity decreases across the interface. The purpose of this section is to develop a more intuitive understanding of this phenomenon which is not immediately obvious using intuition derived from the realm of isotropy.

To visualize more clearly the way in which Fermat’s principle of stationary time is satisfied one has to recall that it minimizes the time between two fixed points on the trajectory of the ray. Inspecting the behaviour of relationship between incident and

transmitted angles without a clear understanding of the consequences of this condition can lead one's intuition astray.

Preparatory to considering two fixed points and propagation from one to the other, let us first consider a plot of phase, v , and group, V , velocities as a function of the phase angle, ϑ , (Figure 6.7). Note two local maxima of group velocity, $V = 2801.9$ m/s, at $\vartheta = 29.2^\circ$, and at $\vartheta = 60.8^\circ$. Note that the magnitudes of phase, v , and group, V , velocities are equal to each other at $\vartheta = 0, \pi/4, \pi/2$, i.e., points where phase and group angles are equal to each other, as can be seen from the slowness surface illustrated in Figure 6.5, or the plot of group versus phase angle shown in Figure 6.10. The minimization of traveltime creates an optimal compromise between the distance travelled by the ray and angle at which the group speed is high.



Consider now a suite of angles of incidence and observe the behaviour of the phase and group angles. Examining Figure 6.8 and Table 6.5 one notices that the phase angle in medium 2 is always smaller than the incident phase angle, i.e., the phase vector always bends towards the normal upon the refraction. The ray vector, on the other hand, bends away from the normal for smaller angles of incidence and towards the normal for larger angles of incidence. It is the trajectory of the ray that is directly related to Fermat's principle of stationary time. Note that since the medium of incidence is assumed to be isotropic, both wave and ray vectors coincide in medium 1.

angle of incidence [deg.]	group angle [deg.] transmission	phase angle [deg.] transmission	phase velocity [m/s] transmission	group velocity [m/s] transmission
0	0	0	2000	2000
10	24.1519	6.77613	2038.44	2135.91
20	42.7885	14.2521	2159.42	2458.04
30	53.8032	23.248	2368.27	2750.16
40	54.5711	33.8401	2599.04	2778.97
50	46.5519	43.5496	2698.21	2701.92
60	39.3765	50.5321	2674.22	2725.72
70	35.9959	55.0618	2617.14	2769.04
80	34.8479	57.622	2572.68	2790.21
89	34.6118	58.4451	2556.81	2795.17

Table 6.5. Group and phase angles and velocities of an SV wave in an anisotropic medium of transmission ($\alpha = 4000$ m/s, $\beta = 2000$ m/s, $\delta = -0.2$, $\varepsilon = 0.15$) related to the set of angles of incidence in an isotropic medium ($\alpha = 3000$ m/s). Note that although the phase angle in the medium of transmission grows monotonically with increasing angle of incidence, the behaviour of the group angle is more complicated.

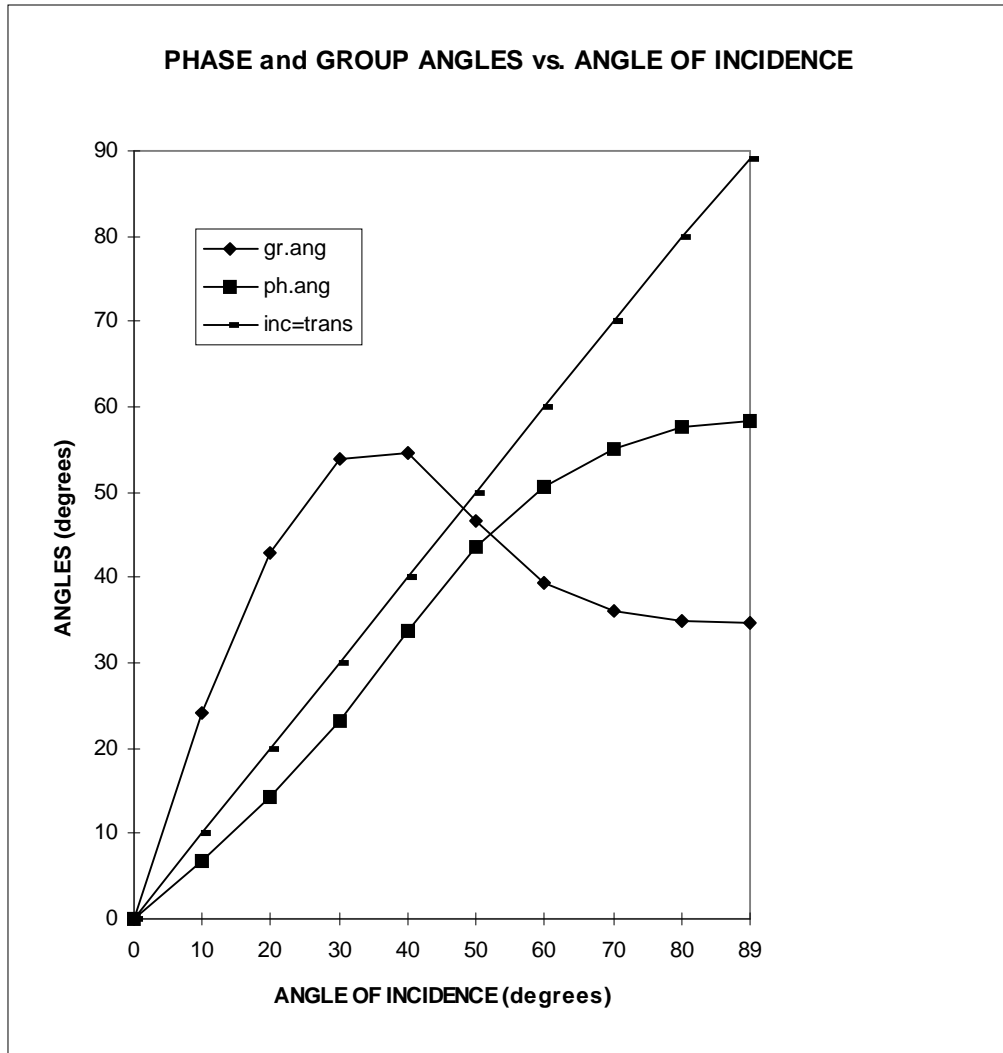


Figure 6.8. Phase and group angles as functions of the incidence angle for SV waves with the following parameters: $\alpha = 4000$ m/s, $\beta = 2000$ m/s, $\delta = -0.2$, $\varepsilon = 0.15$. The velocity in the isotropic medium of incidence is $v = 3000$ m/s. The line with the slope equal to unity, i.e., group and phase angle in medium 1, allows one to see clearly that, although the phase angle in the medium of transmission is always smaller than either phase or group angle in the medium of incidence, the behaviour of the group angle in the medium of incidence is more complicated.

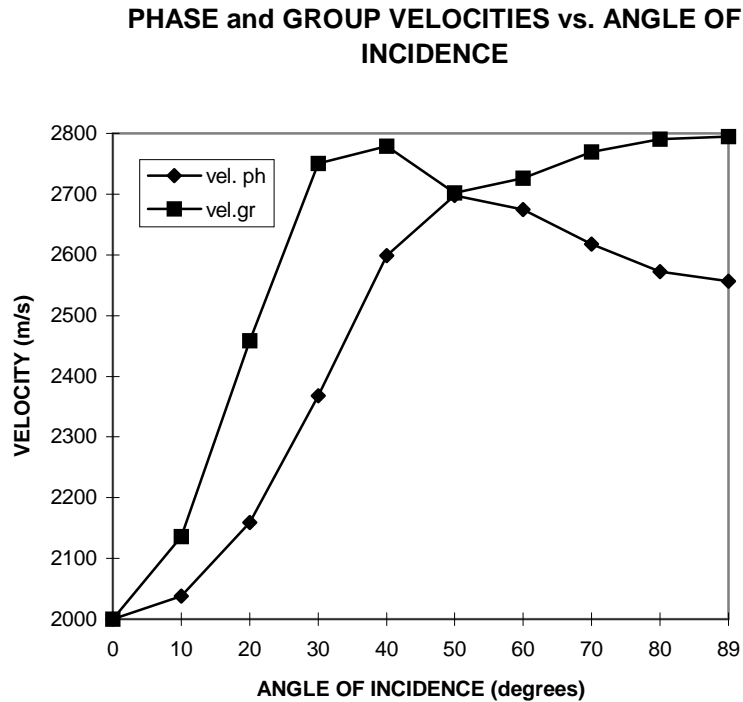


Figure 6.9. Phase and group velocities as a function of the incidence angle for SV waves with following parameters: $\alpha = 4000$ m/s, $\beta = 2000$ m/s, $\delta = -0.2$, $\varepsilon = 0.15$. The velocity in the isotropic medium of incidence $v = 3000$ m/s.

Let us now consider two trajectories of rays between points A-B, and A-C, respectively. Point A is located in the upper, incidence medium, at a vertical distance of 1000 metres from the horizontal, planar interface separating the isotropic and anisotropic layers. Points B and C are located in the lower, transmission medium, at a vertical distance of 1000 metres from the horizontal, planar interface. The horizontal distance (offset) between points A and B is 2163.99 metres, and between points A and C is 6367.54 metres.

OFFSET	ANGLE OF INCIDENCE	PHASE ANGLE	GROUP ANGLE	GROUP VELOCITY
2163.99	35	28.44198746	55.66067255	2801.25
6367.54	85	57.62198311	34.84792335	2790.21

Table 6.6. Computational results for two source-receiver offsets (see also Table 6.7).

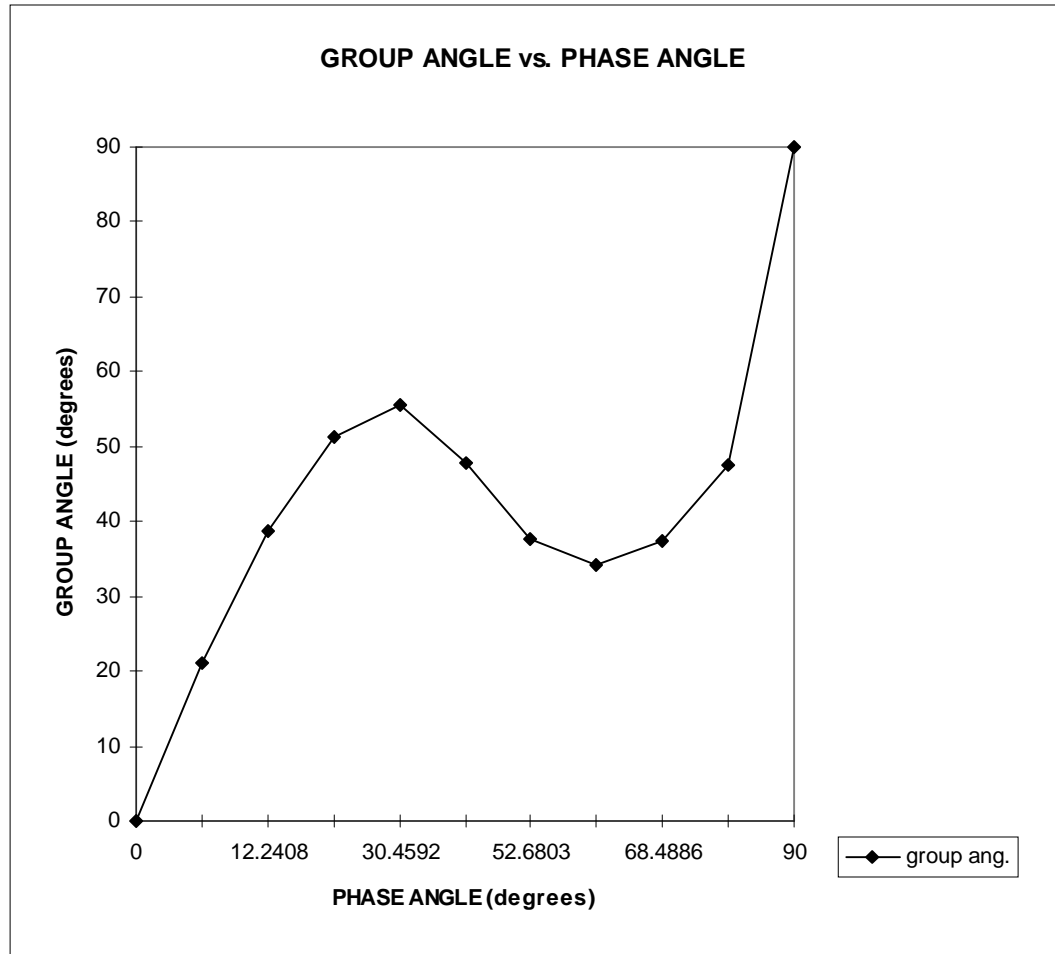
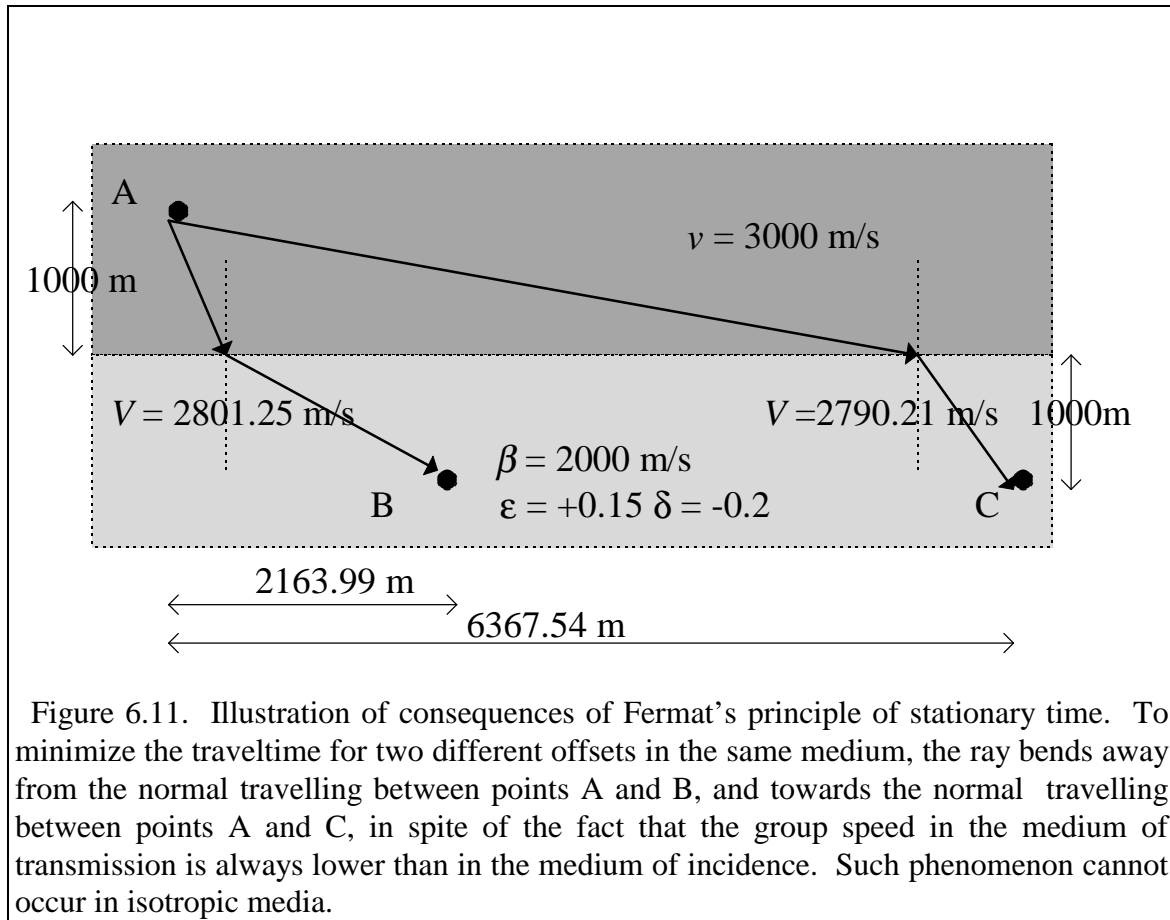


Figure 6.10. Group angle as a function of phase angle for an SV wave with following parameters: $\alpha = 4000$ m/s, $\beta = 2000$ m/s, $\delta = -0.2$, $\varepsilon = 0.15$. Notice the triplication of the group angle, i.e., the same value of the group angle corresponds to three distinct values of phase angle.

In the first case, A - B, the ray bends away from the normal upon transmission into the slower medium. In the second case, A - C, the ray bends towards the normal upon transmission into the slower medium. Notice that the highest speed in the medium of transmission, $V = 2801.9$ m/s, is always smaller than the isotropic speed in the medium of incidence, $V = 3000$ m/s. One observes that in either case the group velocity in medium 2 is close to its maximum. In the first case, the group velocity is close to the local maximum corresponding to the phase angle, $\vartheta = 29.2^\circ$, and in the second case the group velocity is close to the local maximum corresponding to the phase angle, $\vartheta = 60.8^\circ$; see Figure 6.7.



The traveltimes for a signal travelling from point A to B, and from A to C are 1.08681 s and 2.38543 s, respectively. No other trajectory for either pair of points can yield a shorter traveltime. Consider the signal between points A and B. Shortening of the raypath in the slower medium of transmission entails a smaller group angle in this medium. At a smaller group angle, the group velocity, within the range allowed by the two end-points A and B, is lesser than at larger group angles (at smaller values, group angle is monotonically increasing with the phase angle as illustrated by Figure 6.7). Thus the optimization requires a larger propagation angle in medium 2, entailing a longer raypath in the slow, anisotropic medium of transmission in order to approach the relative maximum of propagation speed. The local maximum available within the constraint of two fixed points A and B is the one located at the phase angle, $\vartheta = 29.2^\circ$. For travelling between points A and C, which because of the larger distance separating the two points allows a wider range of incidence and transmission group angles, both local maxima are

available and the maximization of group velocity can be achieved together with shortening the raypath in the slow medium of transmission.

Thus one can conclude that incidence and transmission angles result, just like in the isotropic case, from an optimal compromise between the distance traveled and speed at which the signal travels. In the anisotropic case there is an additional degree of freedom, stemming from the very concept of velocity anisotropy, and provided by the variation of speed with the propagation angle. This introduces an additional complication rendering the intuitive understanding more difficult, yet not impossible. “Anisotropy is not hopeless” (Dellinger, 1991).

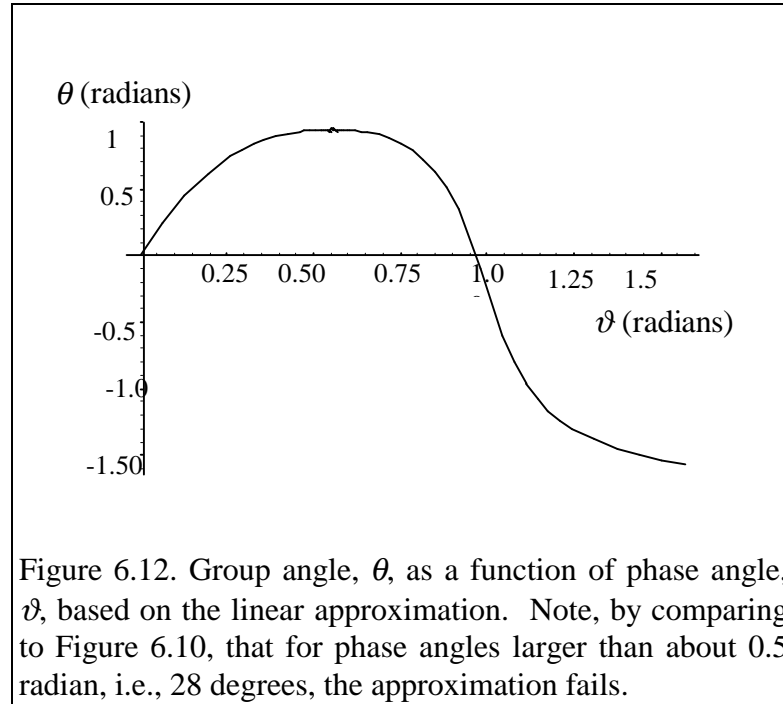
6.4. REMARKS ON THE METHOD

The treatment shown above illustrates another instance of considerations described in detail in Appendix 6. The development of exact expressions for phase velocities for P, SV and SH waves in Taylor series, and subsequent truncation of higher-order terms under the assumption of weak anisotropy (Thomsen, 1986) allows for a very accurate analytical treatment of physical phenomena occurring at the interface between anisotropic media. Distinction between phase and group angles is preserved, and ray bending according to Snell’s law is consistent with Fermat’s principle. One might argue, therefore, that compromise between mathematical simplification and physical consideration is acceptable, i.e., no major physical phenomenon is lost in the process of simplification.

This is not the case under full linearization, i.e., while carrying out the simplification process further in all equations, e.g., the relationship between phase and group velocity or the relationship between the phase and group angles. The linearized expression between the group, θ , and phase, ϑ , angles is given by Thomsen (1986):

$$\tan \theta = \tan \vartheta \left[1 + \frac{1}{\sin \vartheta \cos \vartheta} \frac{1}{v(\vartheta)} \frac{dv}{d\vartheta} \right]. \quad (6.9)$$

The plot using relationship (6.9) yields, in the case of SV waves, the graph of group vs. phase angles displayed in Figure 6.12.



Furthermore, the fully linearized expression for group velocity uses only the first term on the right-hand side of equation (6.3), ignoring the derivative term (Thomsen, 1986). This implies that the group velocity, V , as a function of the group angle, θ , is identical to the phase velocity, v , as a function of phase angle, ϑ , illustrated in Figure 6.7. The two local maxima are lost in the process of linearization. Also, the highest value of group velocity obtained through a linearized scheme is lower than the value obtained based on the assumption of weak anisotropy without full linearization. Considering Fermat's principle of stationary time and minimizing the traveltime using a fully linearized scheme yields results shown in Table 6.7.

The traveltimes are 1.03522 s and 2.3379 s for A-B and A-C cases respectively. One might, at first, be disturbed by the fact that in the fully linearized case the traveltimes are smaller than in the more complete approach. Is Fermat's principle violated in the more complete approach? The answer to this question is negative. The linearized method, by ignoring a physically more realistic description, provides a

mathematical minimum of a traveltime function. The linearized method does not take into account some consequences of angular dispersion.

OFFSET	ANGLE OF INCIDENCE	GROUP ANGLE IN MEDIUM OF TRANSM.	GROUP VELOCITY IN MEDIUM OF TRANSM.
2163.99	49.77104235	44.47564370	2699.77
6367.54	79.07536780	49.87792552	2679.90

Table 6.7. Computational results using linearized scheme (see also Table 6.6).

The interesting concept of bending away or towards the normal in order to optimize the propagation speed is lost in the linearized approach. Nevertheless, the traveltimes obtained by either approach are within a few percent of each other whereas the traveltime calculation ignoring anisotropy altogether leads to a much larger discrepancy (1.20111 s and 2.52532 s for A-B and A-C cases respectively).

It has been observed through many modelling results involving various “anisotropic” approaches that, regardless of the method used, the values of resulting traveltime are relatively close to each other and, most importantly, to experimental results (Chapter VII). It is the values of phase and group angles, rather than traveltimes, which vary much more significantly. Such a state of affairs is not surprising. All approaches attempt to minimize the traveltime within given constraints. Therefore, the final result, i.e., the values of traveltime are rather similar, although the means by which the minimization is achieved, i.e., various degrees of ray-bending, differ significantly. One should not forget that, after all, the concept of a single raypath corresponding to the path of least time constitutes an approximation to the result that one would obtain by the full-wave treatment, rather than the physical entity.

Concluding this chapter one may state that the truncation of the Taylor expansion under the weak-anisotropy assumption provides a considerable mathematical simplification without a loss of physical attributes. The essence of physics of anisotropic wave propagation is preserved in the “weak-anisotropy approximation”, and numerical answers are quite close to the exact approach (see Appendix 2 and Appendix

6 for a more complete discussion). In the case of linearized approach, on the other hand, certain fundamental problems arise (see Figure 6.12), several physical attributes of anisotropic wave propagation are lost, but the traveltimes calculations yield very reasonable results. The confirmation of the latter statement can be found in Chapter VII dealing with physical laboratory measurements of wave propagation in anisotropic media.

It seems appropriate to close this chapter with a quote from Dellinger's doctoral dissertation (1991): "Approximations are useful if you know what you are losing". As demonstrated in Chapter VII both approximate and linearized methods yield results which are much closer to the experimentally measured values than the approach ignoring anisotropy altogether.

CHAPTER VII

PHYSICAL MODELLING

7.0. INTRODUCTION

Physical modelling provides result of controlled experiments, which can be compared with numerically obtained predictions. A reliable comparison requires some consideration of experimental apparatus, most notably, the size of ultrasonic source and receiver transducers (Vestrum, 1994). If the size of transducer is sufficiently large in comparison with the sample size, the generated waves have an appearance of plane waves over some area of wavefront, and the velocity calculated as a ratio of distance and traveltime yields the phase velocity. If, on the other hand, the size of transducers is sufficiently small compared with the sample size, they can be viewed as point sources and point receivers yielding the group velocity as a ratio of distance and traveltime. Obviously, the latter case resembles much more closely the geophysical field acquisition. Denoting the transducer diameter as D and the shortest raypath considered as H , Vestrum (1994) uses a simple Pythagorean formula to determine, e ,

$$e = \sqrt{D^2 + H^2} - H, \quad (7.1)$$

a quantity used to decide whether or not one can consider the experimental results to yield the value of group velocity. When the value of e is very small, a group traveltime will be measured, without serious concerns of transducer effects. The maximum error in raypath length for the experimental geometry used in this study is even smaller than the one considered as negligible in of Vestrum's (1994) investigation, namely, $e \approx 0.0007$ m, since $D = 0.014$ m and $H = 0.1400$ m.

7.1. MATERIALS

The medium through which the signal is transmitted is composed of two layers. Scaled dimensions and parameters of this physical model were also used for numerical calculations in several chapters of this dissertation. The model with its anisotropic parameters in the 31-plane were considered as a standard model.

The top, isotropic layer consists of PVC and the lower, anisotropic layer consists of Phenolic CE. The CE-grade phenolic laminate is composed of layers of a woven canvas fabric saturated and bonded with phenolic resin (e.g., Cheadle et al, 1991). The woven pattern results in anisotropic behaviour. Former studies (e.g., Cheadle et al, 1991, Brown et al, 1991, Vestrum, 1994) show that Phenolic CE can be classified as belonging to the orthorhombic symmetry class. The experiments were conducted in the plane parallel to the Face 3 along the 31-axis and 32-axis.

Principal dimensions¹⁷ and quantities are shown in Tables 7.1, 7.2 and 7.3.

Layer #	Material	Thickness (m)	Symmetry Class
1	PVC	0.0355 m	isotropic
2	Phenolic CE	0.1045 m	orthorhombic

Table 7.1. The principal dimensions and characteristics of the physical model.

¹⁷ A series of measurements performed with high-precision calipers yielded the following thickness values (0.03518, 0.03565, 0.03545, 0.03550, 0.03540, 0.03537) \Rightarrow 0.0355 m for PVC, and (0.1045, 0.1045, 0.1043, 0.1046) \Rightarrow 0.1045 m for Phenolic CE. The manufacturing process of PVC slabs renders their thickness less uniform, E.V. Gallant (pers. comm., 1995).

Since the sagittal planes, i.e., the planes containing sources, receivers and all the rays, coincide with symmetry planes (the 31- and 32-planes) which are perpendicular to each other, the shear-wave vertical speeds for SH-type and SV-type polarizations are reversed for either case. Notice, however, that different anisotropic parameters govern the angular velocity dependence for SH and SV waves. As a result the shapes of slowness curves encompassing all angles of propagation in the 31- and 32-planes, as well as other entailing quantities, cannot be obtained by simple reversal of labels.

Layer # / Symmetry plane	Vertical P wave speed (m/s)	Vertical SV wave speed (m/s)	Vertical SH wave speed (m/s)
1	2250	1030	1030
2 / 31-plane	2925	1609	1516
2 / 32-plane	2925	1516	1609

Table 7.2. Vertical speeds in the physical model.

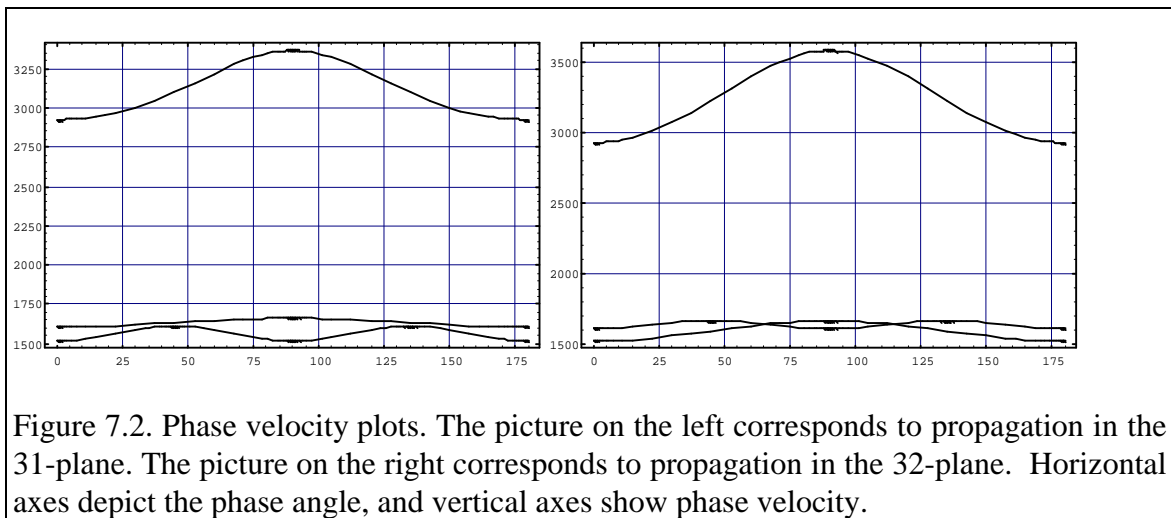
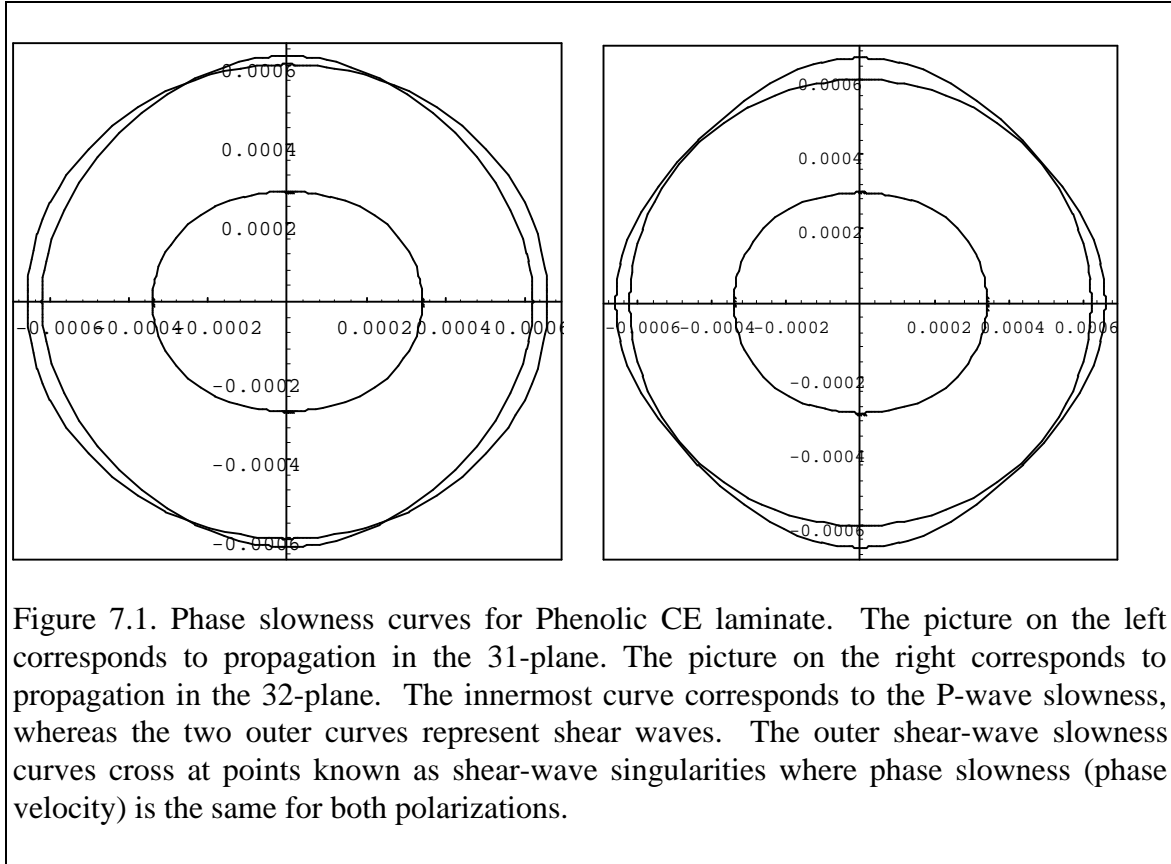
The value of anisotropic parameters results from experimental measurements on the very same material performed in the same laboratory setting and reported by Cheadle et al. (1991). The results were confirmed by subsequent study of Vestrum (1994).

Layer # / Symmetry plane	δ	ϵ	γ
1	0	0	0
2 / 31-plane	0.183	0.224	0.096
2 / 32-plane	0.081	0.150	0.035

Table 7.3. Anisotropic parameters of the physical model.

A useful illustration for familiarization with the anisotropic materials is provided by the phase slowness curves in the 31-plane and in the 32-plane (Figure 7.1). Equivalent information to that contained in the slowness curves which are represented by polar plots,

can be provided by plots of phase velocity versus phase angle in Cartesian coordinates (Figure 7.2).



From Figure 7.2 one observes that while in either symmetry plane the P-wave velocity is significantly different from either SH or SV velocity, both shear wave are relatively close to each other. In the 32-plane the SH and SV velocities actually coincide at points referred to as singularities. At those points one can write:

$$v_{qSH}(\xi) = v_{qSV}(\xi), \quad (7.2)$$

or using equations (3.20) and (3.30), one can express the angle at which the singularity occurs, in terms of the parameters of the medium, that is:

$$\xi_s = \text{Arc cos} \left\{ \frac{\beta}{\alpha} \sqrt{\frac{\gamma}{\varepsilon - \delta}} \right\}. \quad (7.3)$$

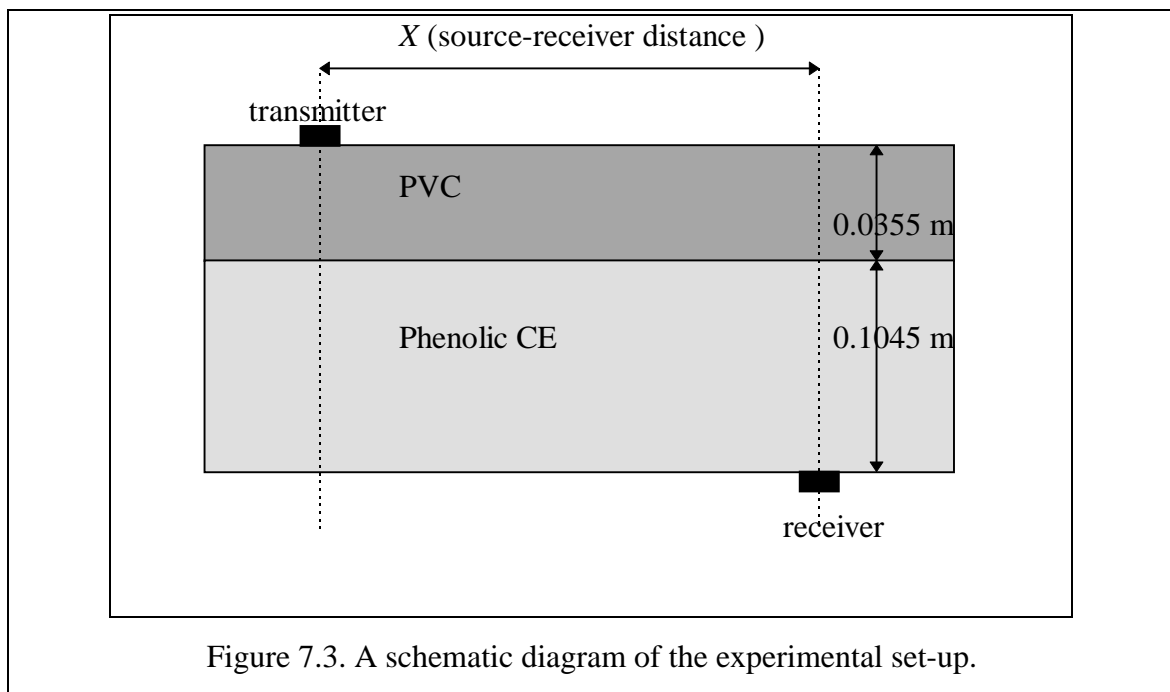
An application of equation (7.3) assumes a single value of speed for vertically propagating shear waves. This occurs for all azimuths in transverse isotropy with a vertical symmetry axis. Since for Phenolic CE the speed of vertical propagation of the SH wave is only slightly different in the 31- or 32-planes, the average value was used in equation (7.3). Thus obtained approximate values are about 35° and 68° , in the first quadrant, for the 31- and 32-planes, respectively, as illustrated in Figure 7.2. Note that although in the 31-plane, velocity values approach one another there is no actual singularity. The use of an average value for vertical speed, β , in the algebraic solution using equation (7.3) yields only a very approximate result.

There is a good agreement between the plots displayed in Figure 7.2 and the results of Vestrum (1994), in particular Figure 4.2. (b) and (c). This confirms the reasonable reliability of the approximation based on the assumption of weak anisotropy. Furthermore, examining plots shown in Appendix 2, it can be inferred that the discrepancy between results of the exact and approximate approaches are very small for the case of the elastic constants measured for Phenolic CE.

7.2. EXPERIMENTAL SET-UP

The data were recorded using two transducers of 1-MHz frequency, one being a transmitter the other a receiver. The transmitter was fixed in one location, while the The readings were taken at every millimetre between horizontal distances of 0 mm and 300 mm. The readings were performed for P-P, P-SV (i.e., transmitted P wave and received SV wave), SV-P, SV-SV, and SH-SH waves for both symmetry planes. Two types of transducers were used: compressional-wave, and shear-wave. The shear-wave transducer was used in two different positions (rotated by 90°) to create SV- or SH-type waves. The sample interval was 10^{-7} s, i.e., the sampling frequency was an order of magnitude higher than the frequency of the signal; thus avoiding aliasing in the range of interest. The time delay between the sending and receiving of the signal for the two transducers placed face-to-face in contact with each other was measured, on the oscilloscope, to be 2×10^{-9} s for the P-P combination and 3×10^{-9} s for S-S. This is viewed as negligible in the present experimental setting as the traveltimes were of the order of 1×10^{-5} s.

The apparatus used in data acquisition was a converted high-precision plotter (Figure 7.3) The entire acquisition process was performed automatically.



7.3. DATA ANALYSIS

Recorded signals were plotted as a standard seismic display. In order to use standard plotting devices, as well as to render the results more immediately applicable to a geophysical context, the distances and traveltimes were scaled by a factor of 10,000. Scaling both distance and time by the same factor preserves original velocity, i.e., the ratio of distance and time remains constant. Selected results are presented in different parts of this dissertation. The data were not processed and all displays illustrate raw records. This implies that no wavelet processing was applied and the traveltime for a given signal corresponds to the initial deflection. Two selected data sets for P-P and SH-SH cases are described below.

7.3.1. P-P case

The case of transmitted and received compressional waves resulting from using vertical-component (“P”) transducers, served as a test for the predictive power of raytracing procedures described in this dissertation. This case was selected as giving the cleanest first arrivals, i.e., “first breaks” because of compressional waves being the first ones to arrive at the receiver. Numerous interesting phenomena can be observed from the seismic records (Figure 7.4 and Figure 7.5). The traveltime at zero offset, and hence the vertical velocity is the same in both symmetry planes considered. This observation is consistent with the theoretical predictions since the particle displacement remains within the symmetry axis for both cases. Progressing down the seismic record one notices a “peg-leg” multiple crossing a 1.0 s time line at about trace # 80. Further down a shear wave (SV) appears, exhibiting higher amplitude for traces in the neighbourhood of # 60; compare the arrival traveltime in Figure 7.4 and Figure 7.5 for 31-plane and 32-planes respectively and notice a slight difference in traveltime, even for zero-offset traces (faintly visible). The existence of the shear wave is explained by the fact that a normally-polarized transducer, used as a P-wave source, generates some shear-wave energy, while the normally-polarized transducer, used as a P-wave receiver, is sensitive to the normal component thereof. For a limited set of offsets (# 50 - # 75) one can also observe the

aforementioned higher amplitude zone due, most likely, to a converted P-SV wave. The event exhibiting a reasonably high amplitude (below 1.5 s) at the bottom of the seismic record is a compressional-wave multiple travelling in a waveguide created by two free surfaces at the top and the bottom of the model. The traveltimes of this event is thrice the traveltime of direct transmission. Considering all events observed on the P-P seismic records, however, it is clear that the main event, i.e., P-P transmission exhibits the highest amplitude, as expected.

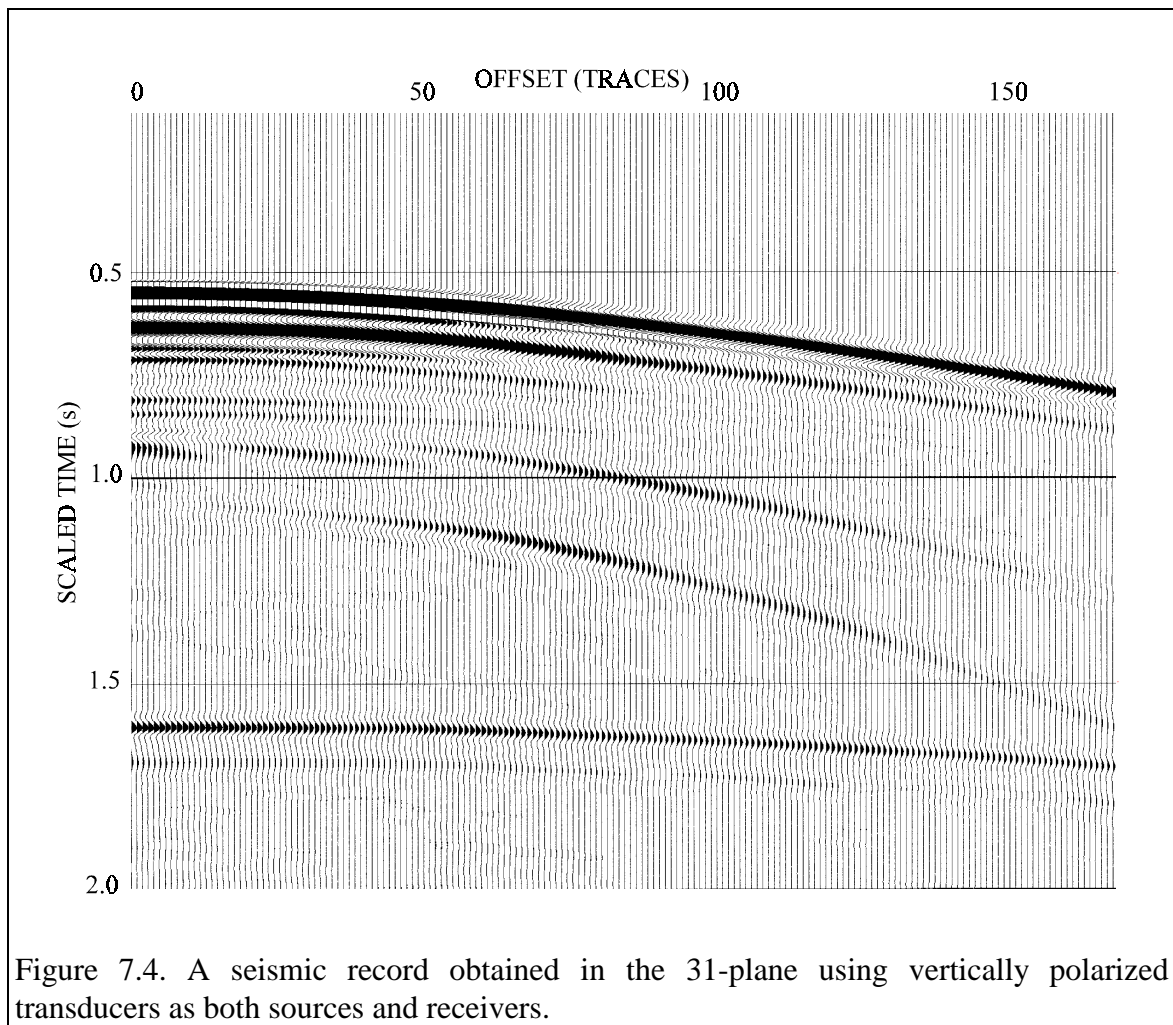


Figure 7.4. A seismic record obtained in the 31-plane using vertically polarized transducers as both sources and receivers.

The results show, as expected, that the raytracing incorporating the anisotropic effects predicts better the experimental results than an equivalent procedure which

ignores the anisotropic effects, i.e., “isotropic approach” which assumes that the vertical P-wave velocity applies in all directions. (see Tables 7.4 and 7.5). The calculation based on the anisotropic approach using the values of anisotropic parameters published for the block of Phenolic CE, by Cheadle et al. (1991) approximates the measured times (see Table 7.4) much more closely than the calculation based on the isotropic approach (see Table 7.5). This indicates strongly that the anisotropic approach reflects better the reality of the experiment (see Figure 7.6). In the context of exploration geophysics, it implies that in certain areas one might consider the analysis of the data which takes anisotropy into account.

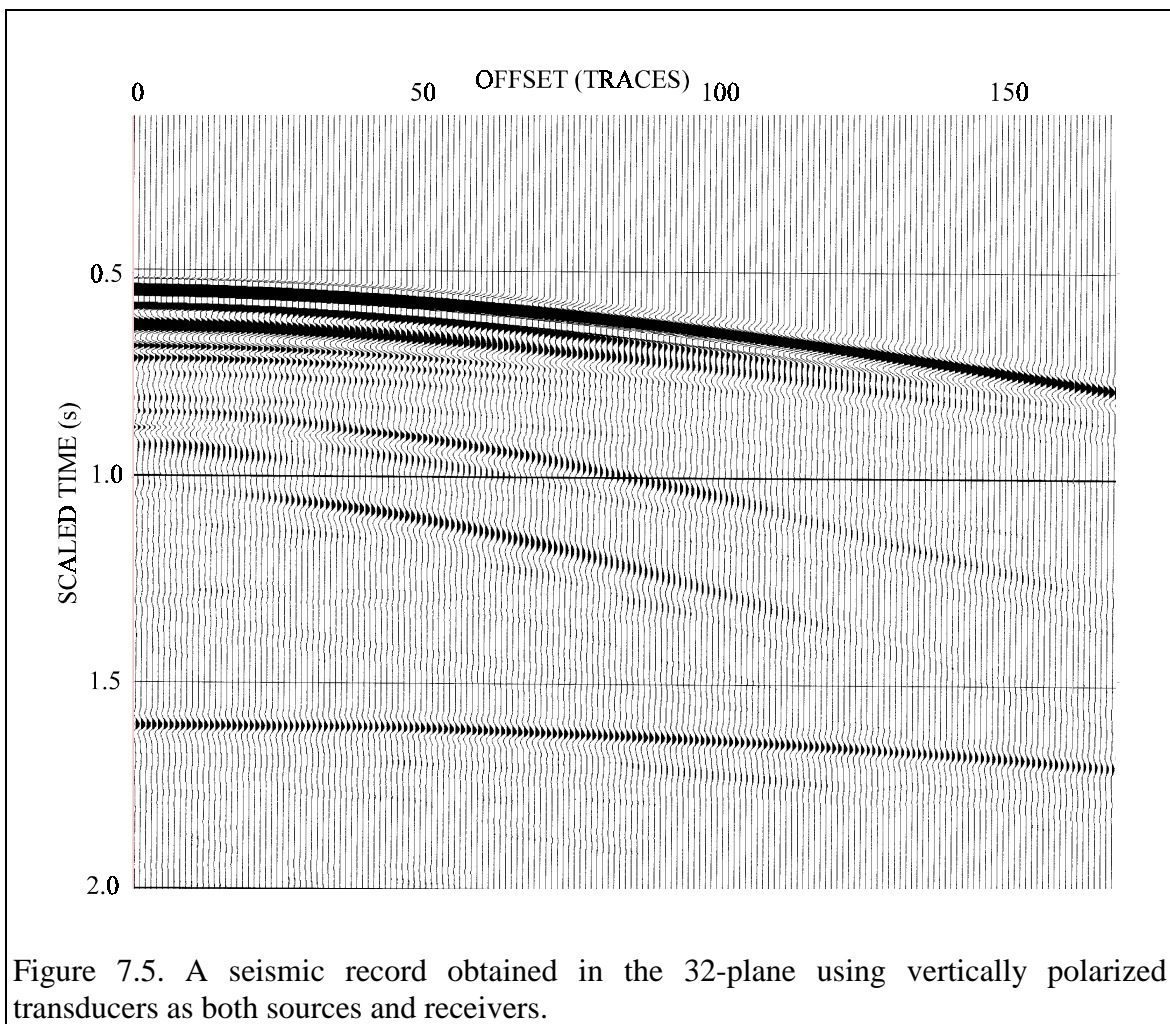


Figure 7.5. A seismic record obtained in the 32-plane using vertically polarized transducers as both sources and receivers.

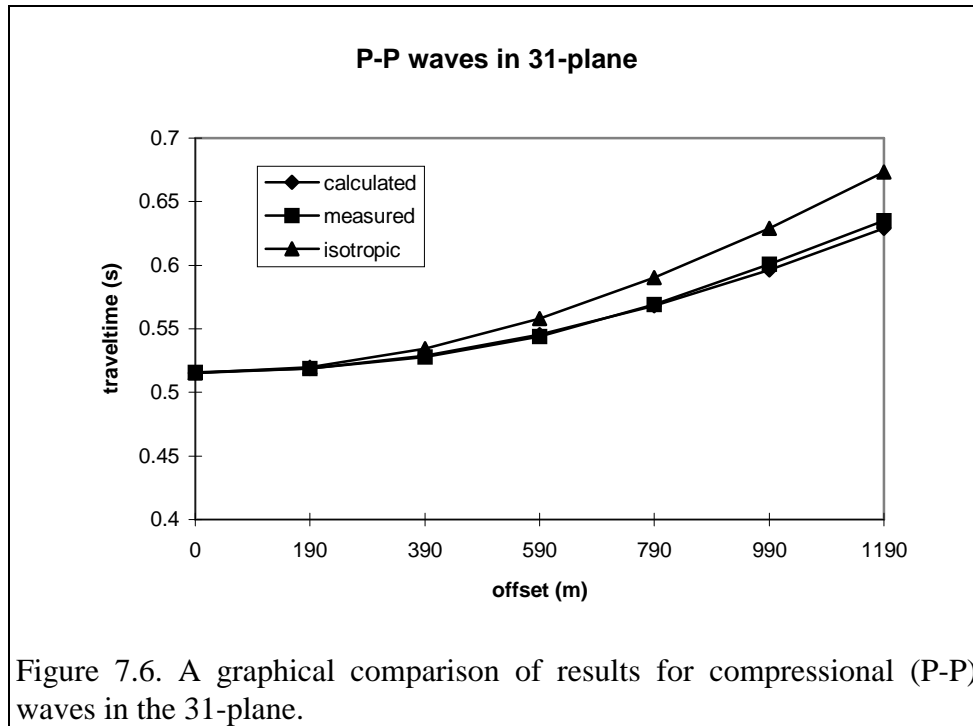
In the presented case, for the propagation along the 31-plane, the match is very good. For the propagation along the 32-plane, the match is slightly less good. The possible reasons for this difference are discussed in Section 7.4.

Scaled offset (m)	Traveltime in 31-plane (s)		Traveltime in 32-plane (s)	
	calculated (anisotropic) $\alpha_0 = 2925$ m/s $\delta = 0.183$ $\epsilon = 0.224$	measured	calculated (anisotropic) $\alpha_0 = 2925$ m/s $\delta = 0.081$ $\epsilon = 0.150$	measured
0	0.515(385)	0.516	0.515(385)	0.516
190	0.518(585)	0.519	0.519(414)	0.518
390	0.528(745)	0.528	0.532(018)	0.527
590	0.545(512)	0.544	0.552(287)	0.543
790	0.568(328)	0.569	0.579(075)	0.565
990	0.596(497)	0.601	0.611(289)	0.592
1190	0.629(263)	0.635	0.647(990)	0.624

Table 7.4. Comparison of measured and calculated traveltimes for P waves; the calculations are based on anisotropic approach using values of anisotropic parameters published by Cheadle et al, 1991. In the present comparison, the values of vertical wave speed are taken to be exact since, for P waves, they were repeatable to 0.5% (Cheadle et al, 1991). The same assumption is made for anisotropic parameters. A large number of decimal points is provided for various comparisons of performance of the algorithm.

Scaled offset (m)	Traveltime (s) calculated (isotropic) $\alpha = 2925$ m/s
0	0.5150(43)
190	0.5197(02)
390	0.5343(88)
590	0.5582(83)
790	0.5902(14)
990	0.6288(89)
1190	0.6730(73)

Table 7.5. Traveltimes for P waves calculated based on isotropic approach.



7.3.2. SH-SH case

The comparison of results of SH-SH waves is analyzed in the same manner as the P-P waves. Numerous interesting phenomena can be observed from the seismic records (Figure 7.7 and Figure 7.8).

Firstly one notices, that the traveltime at zero offset, and hence the vertical velocities, are different for propagation in the 31- and 32-planes. This observation is consistent with theoretical prediction, the particle displacements for the two case being perpendicular to each other. In a TI medium the zero-offset SH traveltimes, and hence the vertical SH velocities are the same for all azimuths. In the present case, however, propagation occurs in symmetry planes of an orthorhombic medium.

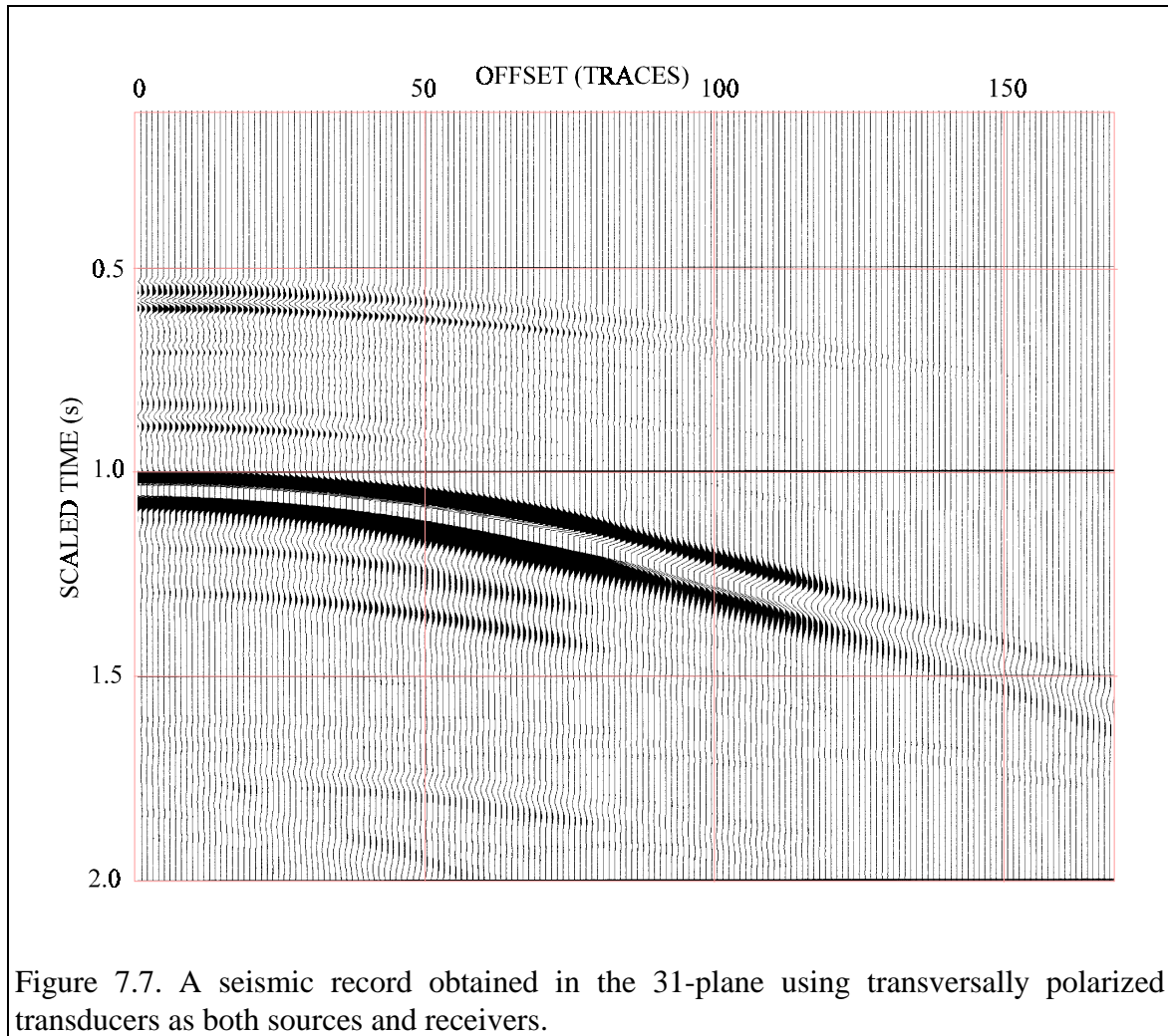


Figure 7.7. A seismic record obtained in the 31-plane using transversally polarized transducers as both sources and receivers.

The first energy arrival that one notices is the transmitted P-P wave (compare the traveltime in Figure 7.4 and 7.5). The appearance of the compressional wave is explained by the fact that the SH-wave-source transducer generates some compressional energy, while the SH-wave-receiver transducer is sensitive to it. The three-leg shear-wave multiple was not recorded since it occurs at multiples of thrice the traveltime of the direct wave. Considering all events observed on the SH-SH seismic records, however, it is clear that the main event, i.e., SH-SH transmission exhibits the highest amplitude, as expected Tables 7.6, 7.7, and Figure 7.9 summarize the results for SH waves. One notices that a better match between experimental and computational data is obtained using the proposed anisotropic raytracing than using an isotropic approach.

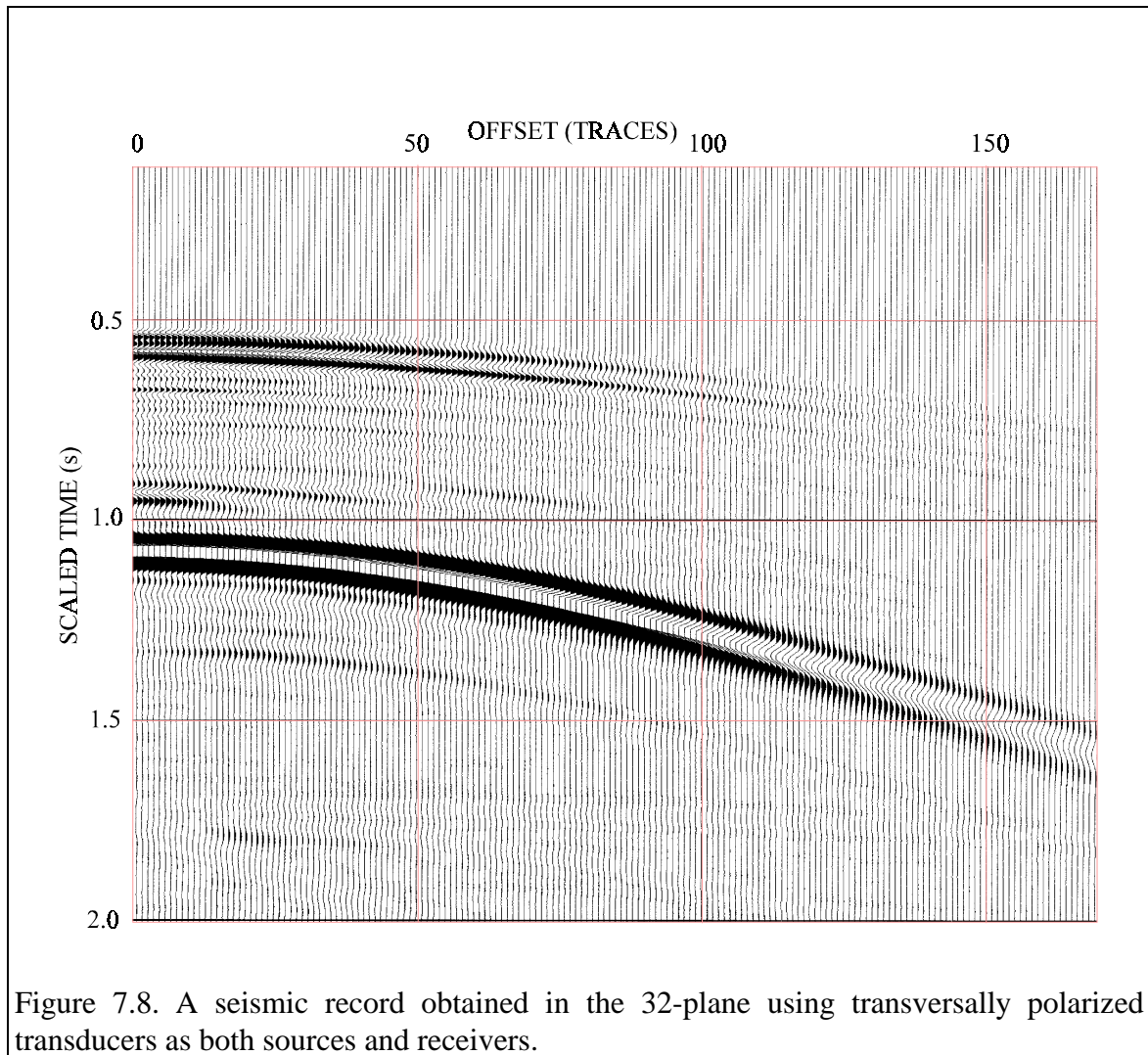


Figure 7.8. A seismic record obtained in the 32-plane using transversally polarized transducers as both sources and receivers.

SH waves, due to their being characterized by only one anisotropic parameter, γ , were selected as corresponding to the analytical algorithm for inversion. They are described in more detail in Chapter VIII.

Scaled offset (m)	Traveltime in 31-plane (s)		Traveltime in 32-plane (s)	
	calculated (anisotropic) $\beta_0 = 1609$ m/s $\gamma = 0.096$	measured	calculated (anisotropic) $\beta_0 = 1516$ m/s $\gamma = 0.035$	measured
0	0.994(132) 0.994(132) 0.994(132)	0.994	1.033(97) 1.033(97) 1.033(97)	1.034
190	1.001(67) 1.001(71) 1.001(48)	1.001	1.042(68) 1.042(69) 1.042(66)	1.040
390	1.025(44) 1.025(63) 1.024(75)	1.024	1.070(14) 1.070(17) 1.070(04)	1.064
590	1.064(20) 1.064(59) 1.062(86)	1.052	1.114(83) 1.114(89) 1.114(63)	1.102
790	1.116(14) 1.116(73) 1.114(19)	1.108	1.174(56) 1.174(65) 1.174(27)	1.156
990	1.179(22) 1.179(98) 1.176(78)	1.182	1.246(92) 1.247(04) 1.246(55)	1.223

Table 7.6. Comparison of measured and calculated traveltimes for SH waves; the calculated values are based on anisotropic approach using values anisotropic values published by Cheadle et al, 1991. The three values for the calculated traveltime, correspond to the method using the exact, approximate and linearized schemes, respectively (see Appendix 6, for a fuller treatment). Note that any of the “anisotropic” approaches yields a significantly better match with the observed data than the approach ignoring the effects of anisotropy (see Table 7.7). In the present comparison, the values of vertical wave speed are taken to be exact since, for S waves, they were repeatable to 0.25% (Cheadle et al, 1991). The same assumption is made for the anisotropic parameter. A large number of decimal points is provided for various comparisons of performance of the algorithm.

Scaled offset (m)	Traveltime in 31-plane (s) calculated (isotropic) $\beta = 1609$ m/s	Traveltime in 32-plane (s) calculated (isotropic) $\beta = 1516$ m/s
0	0.994(132)	1.033(97)
190	1.002(91)	1.043(18)
390	1.030(53)	1.072(19)
590	1.075(40)	1.119(34)
790	1.135(20)	1.182(24)
990	1.207(42)	1.258(27)

Table 7.7. Traveltimes for SH waves calculated based on isotropic approach. Note that the vertical SH speed, or so-called, isotropic SH velocity, having polarization vector perpendicular to the symmetry plane of propagation yields, for Phenolic CE, different traveltimes for 31- and 32-planes.

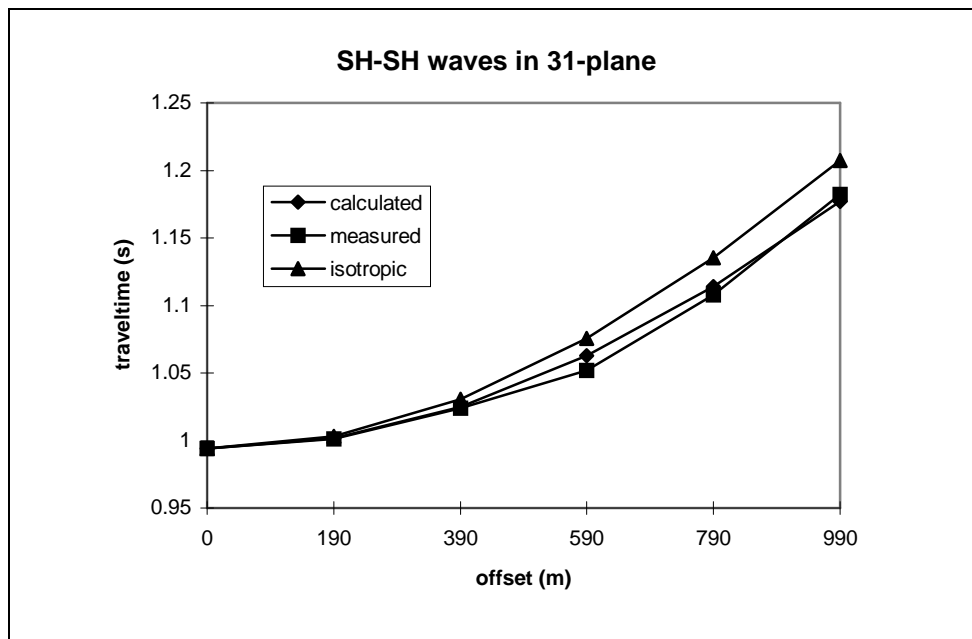


Figure 7.9. A graphical comparison of results for SH-SH waves in 31-plane

7.4. EXPERIMENTAL ERRORS

of error which can account for discrepancy between traveltimes calculated using the anisotropic approach and the measured values. The qualitative description of those sources is presented below.

7.4.1. Measurement errors

Firstly, the dimensions of the PVC and Phenolic CE blocks are subject both to measurement errors and inconsistencies of actual thickness of the material within one slab. Those errors, however, compared to other measurements, can be considered very small (see Footnote 17).

Secondly, the measurements of spacing between the source and receiver transducers are subject to error. All the measurements, however, were performed with automatic moving of the receiver transducer by an arm of a device converted specially for this purpose from a high-quality plotter. Thus, the precision and accuracy can be considered very high.

Thirdly, the uncertainties due to the finite dimensions of transducers causing raypath problems and a mixture of phase and group velocity measurements, has to be considered. In view of Vestrum's (1994) criterion, discussed above, and considering the weak anisotropy of the material, the errors originating from the size of the transducers are negligible.

7.4.2. Computational errors

Two main sources of possible computational errors have to be considered in this category. It is assumed that errors due to computer precision are negligible (Appendix 3).

Firstly, the values of anisotropic parameters, δ , ε , and as well as the values of vertical speed, α and β , are subject to various errors (see Brown et al, 1991, Vestrum, 1994). Especially, the anisotropic parameters calculated from inversion of traveltimes on the phenolic CE block can be burdened with a significant error.

Secondly, there is some imperfection due to the raytracing being done with simplified equations, under the assumption of weak anisotropy. Considering, however, that the assumptions seem to be fully honoured, as well as considering the fact that the angle of propagation for all cases is not very large, thus rendering the approximate equations even more accurate than if the entire range of propagation angles were involved, one can confidently rely on results obtained through those equations.

7.4.3. Interpretation errors

The results obtained through numerical and physical modelling are compared based on traveltimes values. In the case of physical modelling of compressional waves, the traveltimes were obtained from the raw record, as the first deflection of the trace corresponding to the arrival of the P wave. The data are very clean and the first arrivals are very well defined. For SH or SV waves, appearing later in the record, the initial arrival is slightly less obvious. The process of establishing the time of arrival for all traces and wave types was performed using the Pro-Max® processing software allowing a display of traces in great magnification, so as to time the selected point with considerable precision.

The difficulty, however, is of an interpretive nature, namely, where to select the point which corresponds to the onset of energy, i.e., to the first arrival time, with a high enough accuracy. It is this interpretive nature of picking the arrival time that appears to be responsible for most of the discrepancy. The degree of difficulty is also offset-dependent. At larger offsets, the effect of anisotropic propagation becomes more pronounced, thus easier to detect, but the wavelet becomes more stretched due to frequency dispersion, and the picking of first arrivals becomes less reliable.

If the method is to be used repeatedly, a calibration scheme or a criterion can be developed for a process of automatic picking. Furthermore, one can deconvolve the data in an attempt to collapse the wavelet and phase-shift to a zero-phase wavelet in order to facilitate the picking.

CHAPTER **VIII**

INVERSION FOR ANISOTROPIC PARAMETER IN LAYERED MEDIA

8.0. INTRODUCTION

In previous chapters various solutions of forward problems were developed and verified. They allow, given all parameters of the medium, to calculate expected physical consequences. In many physical sciences, notably in geophysics, one would like to infer the characteristics of the medium from the observation of consequences. This is the inverse problem. This chapter presents the solution of such an inverse problem in an anisotropic medium.

Numerous inversion methods for multilayer anisotropic media have been proposed by various researchers. Stewart (1988) proposed a modification of an algebraic reconstruction technique (ART). It attempts to estimate anisotropic velocity using only straight rays in a discretized weakly anisotropic medium. Michelena, Muir and Harris (1993) propose an inversion which is a simple extension of an isotropic scheme for traveltimes tomography. Their approach does not consider ray-bending at interfaces, an omission that can introduce errors into the estimation of velocity anisotropy if the velocity contrasts are large. Recently, an interesting inversion scheme using genetic algorithms (originally developed for biological sciences) was suggested by Horne and

MacBeth (1994). It can be viewed as a variation of the Monte Carlo method. Kebaili and Schmitt (1986) presented an inversion technique operating in the intercept time-ray parameter (τ - p) domain.

The method described in this chapter allows one to obtain, based on the measurements made at the surface, a unique value for the SH-wave anisotropic parameter, γ , in an anisotropic layer at depth, i.e., separated from the surface by another layer. In other words, one inverts the travelttime information to obtain crucial information about anisotropic characteristics of a layer at depth. The innovative aspect of the method consists of the analytical approach for obtaining the solution, particularly since it applies in the context of more than one layer, incorporating the concept of an anisotropic generalization of Snell's law discussed in Chapter III and Chapter IV. Thus the method incorporates the effects of ray-bending at an interface under anisotropic conditions. The analytical aspect, illustrated by geometrical representation of solution spaces retains an immediacy of physical significance and provides an insight so often difficult to maintain in numerical approaches. Furthermore, the method is free of wanderings of solutions and criteria for various search patterns which are of great concern in various numerical methods.

The treatment is described explicitly in terms of SH waves in a TI (transversely isotropic) medium. It can, however, be applied without any modification to any waves exhibiting elliptical velocity dependence, and in any symmetry class, as long as the sagittal plane coincides with a symmetry plane. The consequences of the method provide stepping stones to more complicated cases.

8.1. FORMULATION OF THE PROBLEM

Consider a layered medium consisting of an isotropic layer of thickness H_1 superposed on an anisotropic layer of thickness, H_2 . The SH-wave speed, V , in the upper, isotropic medium and vertical SH-wave speed, β , in the lower anisotropic medium, are assumed to be known. The SH-wave anisotropic parameter, γ , in the lower medium is to be determined, based on the measurements performed on the surface of the isotropic layer.

In the subsequent development, the upper-case letters correspond to known, or measured quantities, whereas lower-case letters are the unknown quantities, or variables in the equations.

8.2. GENERAL MATHEMATICAL FORMULATION

Consider propagation through the medium between the source and receiver separated by a horizontal distance, X , see Figure 8.1. (In the present case, since the method is based on traveltimes measurements, there is no loss of generality in such recording geometry (transmission study), as compared to both source and receiver situated on the surface (reflection study). In the latter case one must make a couple of straightforward substitutions, namely: $T \Rightarrow 2T$ and $X \Rightarrow 2X$.) The ray undergoes refraction at the interface separating the isotropic and the anisotropic layers. For a given source-receiver configuration, a set of three independent equations in three unknowns has to be satisfied.

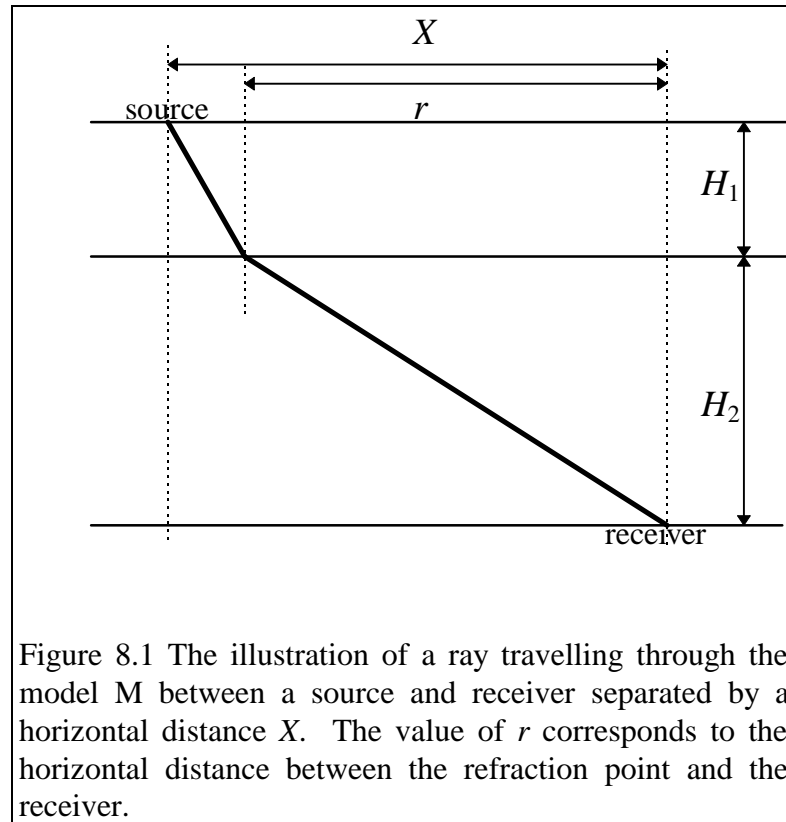
The unknowns in the system of equations are the incidence angle (take-off) angle, θ_1 , in the upper medium and the transmission angle, θ_2 , and the anisotropic parameter, γ , in the lower medium. The angles of incidence and transmission are related by the phase angle, ξ , here given explicitly for SH waves, and involving the value of the ray parameter, x_0 . The first equation in (8.1) describes the measured traveltimes, T . The second equation in (8.1) describes the known lateral, source-receiver separation, X , which must be solved by a numerical method, as we cannot solve for the take-off angle explicitly. The third, fourth and fifth equations in (8.1) embody the expression of a generalized Snell's law at the isotropic/anisotropic interface. The angle of transmission, θ_2 , is a function of both θ_1 and γ .

The conditions stated above would require a rather special algorithm. A direct input of system of equations (8.1) into Mathematica®, fails to yield satisfactory results because of the non-algebraic form of equations.

$$\left\{ \begin{array}{l}
 \frac{H_1}{\cos \theta_1} + \frac{H_2}{\beta(1 + \gamma \sin^2[\theta_2(\gamma, \xi; \theta_1)])} = T \\
 H_1 \tan \theta_1 + (H_2) \tan[\theta_2(\gamma, \xi; \theta_1)] = X \\
 \frac{\sin \theta_1}{V} - \frac{\cos \xi}{\beta(1 + \gamma \sin^2 \xi)} = 0 \\
 \left\{ \xi = \text{Arc cos} \left\{ \frac{1 - \sqrt{1 - (2x_0(\theta_1)\beta)^2 \gamma}}{2x_0(\theta_1)\beta\gamma} \right\} \right. \\
 \left. r(\xi) = \frac{1}{\beta(1 + \gamma \cos^2 \xi)} \right.
 \end{array} \right. \quad (8.1)$$

8.3. FORMULATION IN TERMS OF PARAMETERIZED FERMAT'S PRINCIPLE

Fermat's principle of stationary time plays an important rôle in raytracing theory. It states that the path of the ray between two points is such that the first-order traveltime variation with respect to all infinitesimally perturbed neighbouring paths is zero. In other words, it is the path of least or greatest time. One of general expressions of Fermat's principle in anisotropic media requires a functional derivative involving both phase and group slownesses; see equation (2.31).



If, however, the physical problem is parameterized by a specific case as illustrated in Figure 8.1, the solution is reduced to minimization of the traveltime in terms of choice of trajectory. Under the linearizing assumption (first-order theory) following the weak-anisotropy concept, one makes use of the fact that the expressions for both phase and group speeds are identical to first order for a given phase or group angle.

Referring to the lateral distance between the refraction point and receiver as r , and expressing the trigonometric function as ratios of appropriate segments, one parameterizes the entire choice of trajectory as a function of r . This leads to a system of two equations with two unknowns, r and γ . The two equations are the traveltime equation and the mathematical statement of Fermat's principle of stationary time:

$$\left\{ \begin{array}{l} \frac{\sqrt{(X-r)^2 + H_1^2}}{V} + \frac{\sqrt{r^2 + H_2^2}}{\beta \left(1 + \gamma \frac{r^2}{r^2 + H_2^2} \right)} = t(r; \gamma) \\ \frac{dt(r)}{dr} = 0 \end{array} \right. \quad (8.2)$$

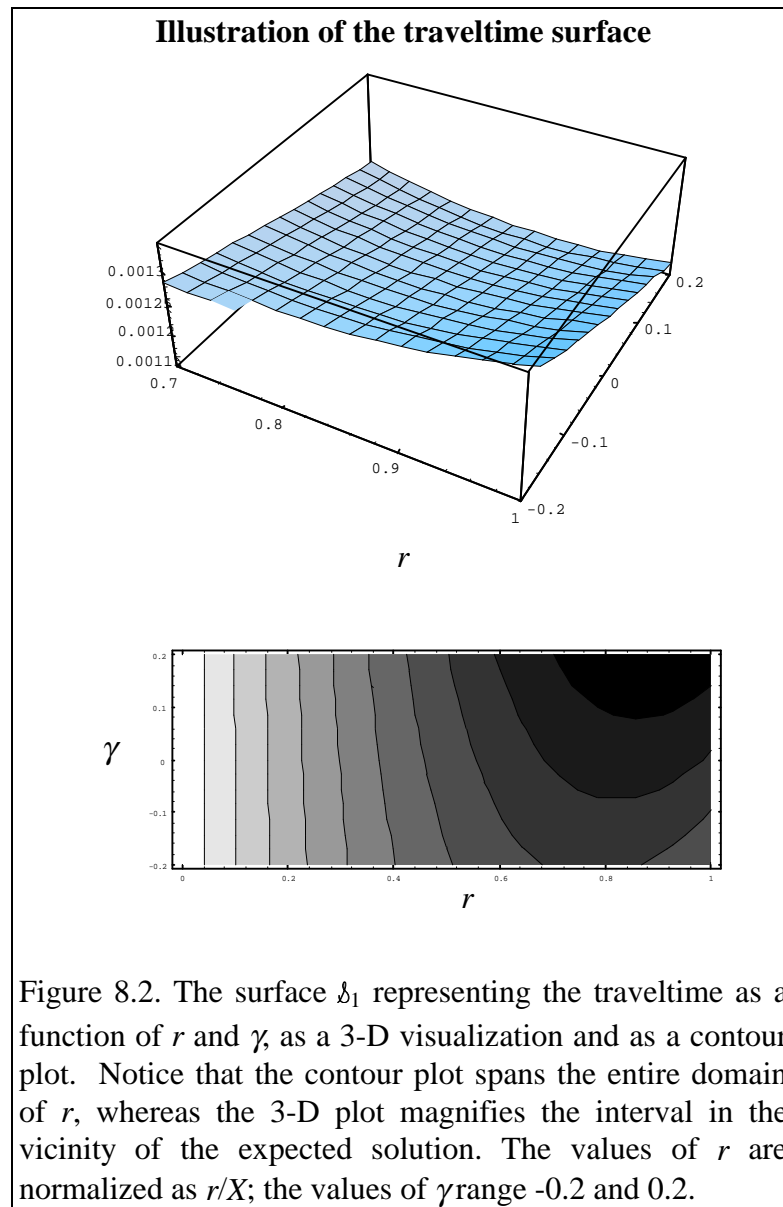
In spite of the apparent simplicity, these equations are highly nonlinear and their general solution is not a trivial matter. They can, however, be simplified further with an insight gained through geometrical visualization of solution spaces.

8.4. VISUALIZATION OF SOLUTION SPACES

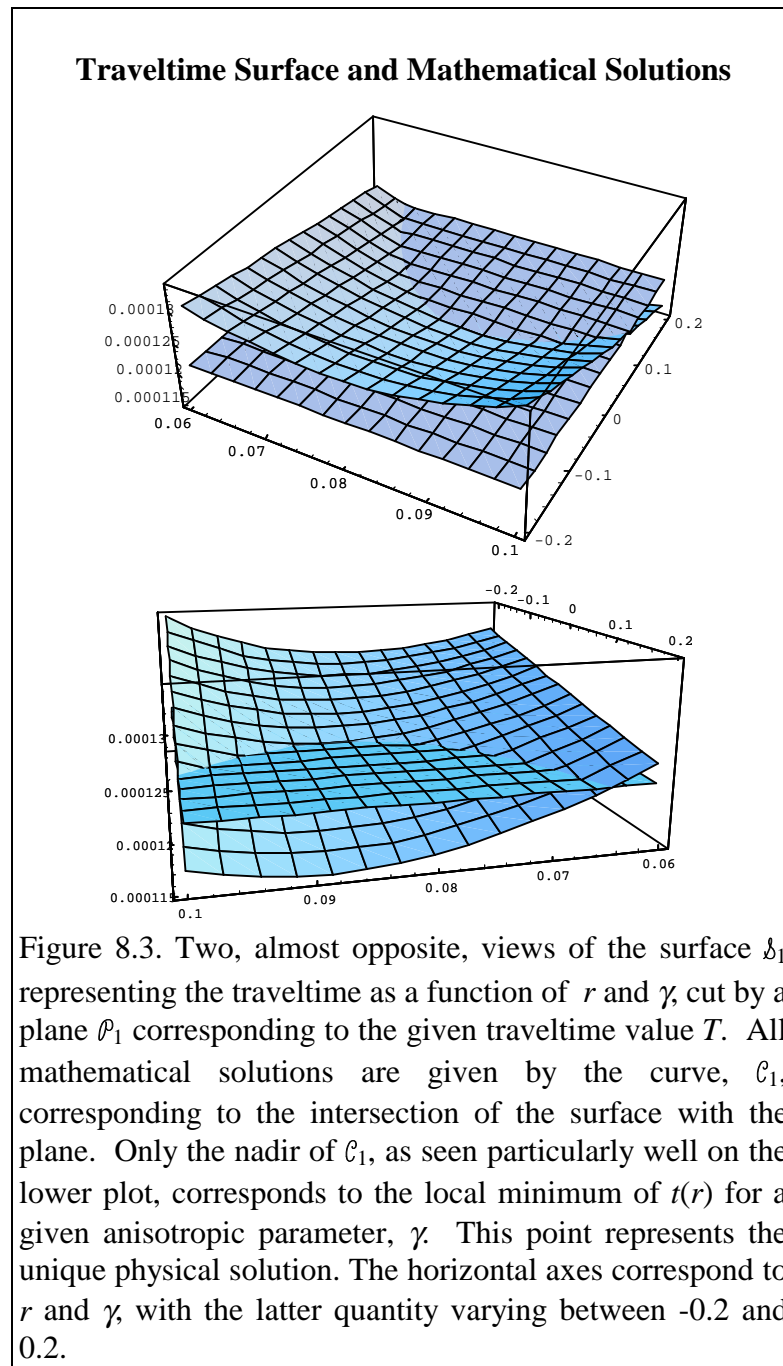
For given X, H_1, H_2, V and β , one can construct a surface $\delta_1 = t(r; \gamma)$, i.e., a three-dimensional representation of the first equation in (8.2) with r and γ as horizontal axes and $t(r; \gamma)$ as the vertical one. The surface is smooth, and the curve corresponding to the vertical cross-section through the surface for a given value of γ , has a single extremum; see Figures 8.2 and 8.4. This extremum is always a minimum yielding the shortest traveltime corresponding to some r for a given value of γ .

Having a measurement of traveltime $t = T$, one can consider the horizontal plane, $\rho_1 = T$, in the space (t, r, γ) . The intersection of the surface δ_1 and plane ρ_1 forms a curve, \mathcal{C}_1 , e.g., any one of the contours in Figure 8.2. This curve is a set of mathematical solutions to the equation:

$$t(r; \gamma) = T. \quad (8.3)$$



In other words, it is a set of combinations of r and γ , for which $t(r, \gamma) = T$. There is however, only one physical solution. To find it one must not forget that γ is an unknown constant parameter and not a variable. It is through r , not γ , that one minimizes the traveltime; γ is an unknown but it is a constant. For all combinations of r and γ , it is only the nadir of the intersection curve which satisfies Fermat's principle, i.e., minimizes t with respect to r . This becomes obvious by imagining several vertical cross-sections of the diagram in Figure 8.3, for different values of γ , i.e., along the r -axis.



The consequences of Fermat's principle lead to a convenient method of solution. In the plane ρ_1 , the curve of mathematical solutions, \mathcal{C}_1 , can be viewed as an expression of γ in terms of r at a constant value of $t = T$, i.e., $\mathcal{C}_1: \gamma = \gamma(r; T)$. The physical solution

corresponds to the extremum of $\gamma(r;T)$. It can, therefore, be easily found as a solution to the condition below:

$$\frac{d[\gamma(r)]}{dr} = 0, \quad (8.4)$$

where $\gamma(r)$ is obtained by solving the traveltime equation, i.e., the first equation in (8.2) with $t(r, \gamma) = T$. Thus,

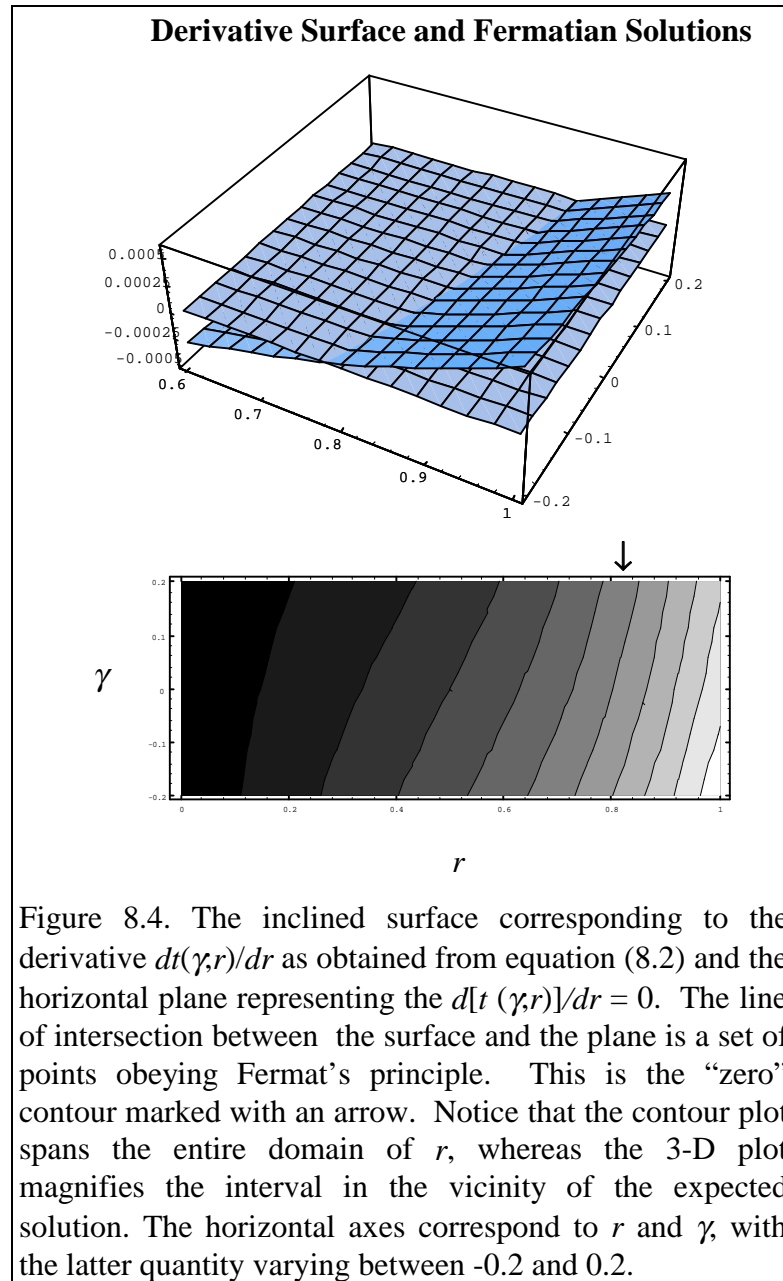
$$\gamma(r) = \frac{V(r^2 + H_2^2)^{\frac{3}{2}}}{\beta r^2 \left[TV - \sqrt{(X-r)^2 + H_1^2} \right]} - \frac{r^2 + H_2^2}{r^2}, \quad (8.5)$$

and its derivative with respect to r can be set to zero:

$$\begin{aligned} \frac{d\gamma}{dr} = & -\frac{2}{r} + \frac{2(H_2^2 + r^2)}{r^3} - \frac{V(H_2^2 + r^2)^{\frac{3}{2}}(X-r)}{\beta r^2 \sqrt{H_1^2 + (X-r)^2} \left(TV - \sqrt{H_1^2 + (X-r)^2} \right)^2} + \\ & + \frac{3V\sqrt{H_2^2 + r^2}}{\beta r \left(TV - \sqrt{H_1^2 + (X-r)^2} \right)} - \frac{2V(H_2^2 + r^2)^{\frac{3}{2}}}{\beta r^3 \left(TV - \sqrt{H_1^2 + (X-r)^2} \right)} = 0 \end{aligned} \quad (8.6)$$

The resulting real value of r corresponds to the minimum of $\gamma(r;T)$. This is guaranteed by the fact that the plot of is always concave-up within the physically meaningful domain of $r \in (0, X)$; see Figure 8.5. It can be visualized as a consequence of the traveltime surface, δ_1 , sloping down towards higher values of γ . The sloping results

from the denominator in the traveltime equation (8.2), increasing monotonically¹⁸ with increasing γ .

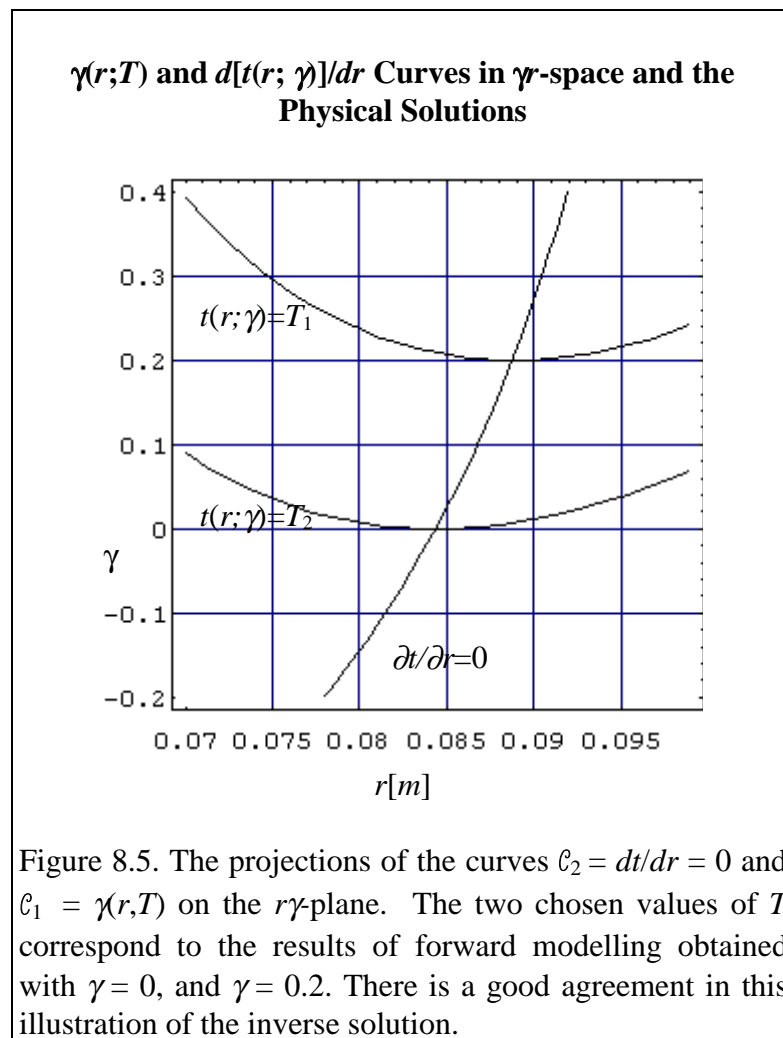


The resulting real value of r is unique. This can be visualized by plotting, for given X , H_1 , H_2 , V and β , the derivative surface of the traveltime equation, i.e., $\delta_2 =$

¹⁸ Note that $\frac{d}{d\gamma} \left[\beta \left(1 + \gamma \frac{r}{r^2 + H_2^2} \right) \right] > 0$, for physically meaningful values of r , and β .

$d[t(r, \gamma)]/dr$. The curve, \mathcal{C}_2 , formed by intersection of the surface \mathcal{S}_2 and the plane $\mathcal{P}_2 = d[t(r, \gamma)]/dr = 0$ is a set of solutions satisfying Fermat's principle of stationary time for various combinations of r and γ . The only physical solution of the entire problem corresponds to the intersection point of the projection of the two curves, \mathcal{C}_1 and \mathcal{C}_2 , on the $r\gamma$ -plane (see Figure 8.5). There is only one such a point and it always occurs at the minimum of the curve $\mathcal{C}_1 = \gamma(r; T)$; i.e., at the point where γ is minimum. The mathematical proof of this appears in Appendix 4.

Having thus calculated the value of r , using equation (8.6), one can easily obtain the corresponding γ , by substituting it into equation (8.5). Thus the traveltime equation, i.e., the first equation in (8.2) is the only one necessary for computational purposes.



One can calculate the $dt/dr = 0$ contour, i.e., the steeply rising curve in Figure 8.5 for an experiment knowing the horizontal source-receiver separation, X , the vertical speeds, V and β , and layer thicknesses, H_1 and H_2 . The position of the other curve, i.e., $t(r;\gamma)=T$, on the other hand, depends on the result of the experiment, namely, the measured travelttime, T . Thus with all model and recording parameters fixed, the travelttime is a function of the anisotropic parameter, γ , whose value corresponds to the intersection of these two curves.

Method of Computation: Anisotropic parameter, γ , from travelttime measurements in the isotropic/anisotropic case

Step 1

Express γ as a function of r , and known parameters:

$$\gamma = \gamma(r; T, X, V, \beta, H_1, H_2) = \frac{V(r^2 + H_2^2)^{\frac{3}{2}}}{\beta r^2 \left[TV - \sqrt{(X-r)^2 + H_1^2} \right]} - \frac{r^2 + H_2^2}{r^2}$$

Step 2

Calculate the local extremum of γ , by setting the derivative of γ w.r.t. r to zero, and solving for r . The process, although analytic, is very laborious and the use of some mathematical software is recommended in order to ease the task. In searching the solution one may use the fact that, the solution of interest is situated between $r = 0$ and $r = X$.

$$\begin{aligned} \frac{d\gamma}{dr} = & -\frac{2}{r} + \frac{2(H_2^2 + r^2)}{r^3} - \frac{V(H_2^2 + r^2)^{\frac{3}{2}}(X-r)}{\beta r^2 \sqrt{H_1^2 + (X-r)^2} \left(TV - \sqrt{H_1^2 + (X-r)^2} \right)^2} + \\ & + \frac{3V\sqrt{H_2^2 + r^2}}{\beta r \left(TV - \sqrt{H_1^2 + (X-r)^2} \right)} - \frac{2V(H_2^2 + r^2)^{\frac{3}{2}}}{\beta r^3 \left(TV - \sqrt{H_1^2 + (X-r)^2} \right)} = 0 \end{aligned}$$

Step 3

Insert the value of r , calculated in Step 2, into the expression for γ , in Step 1.

A Mathematica® code for the entire calculation is given below.

X = *horizontal distance between the source and receiver*
 HJ = *thickness of the upper, isotropic layer*
 HD = *thickness of the lower anisotropic layer*
 V = *wave speed in the upper, isotropic layer*
 B = *vertical wave speed in the lower, anisotropic layer*
 TT = *traveltime between the source and receiver (one way)*
 $D[$
 $V*(r^2+HD^2)*Sqrt[r^2+HD^2]/(B*r^2*(TT*V-Sqrt[(X-r)^2+HJ^2]))$
 $-(r^2+HD^2)/r^2,r]$
 $FindRoot[\% == 0, \{r, 0.01*X, X/2, 0.99*X\}]$
 $N[$
 $V*((r/.%)^2+HD^2)*Sqrt[(r/.%)^2+HD^2]$
 $/(B*(r/.%)^2*(TT*V-Sqrt[(X-(r/.%))^2+HJ^2]))$
 $-((r/.%)^2+HD^2)/(r/.%)^2]$

8.5. EXAMPLE OF INVERSION APPLICATION

8.5.1. Numerical modelling

Consider a model composed of two layers. The upper, isotropic layer has an SH-wave velocity of 1030 m/s and a thickness of 355 m. In the lower, anisotropic (TI) layer, the SH-wave velocity for vertical propagation is 1609 m/s and the thickness is 1045 m. The anisotropic parameter in the TI layer is $\gamma = 0.096$. The results of forward modelling and inversion are summarized in Table 8.1.

8.5.2. Physical modelling

The elastic modelling method described in more detail in Chapter V was used to test the usefulness of the inversion algorithm. A traveltime for an SH wave was recorded through an isotropic PVC, and anisotropic Phenolic CE, at a range of offset, between 0 mm and 300 mm at 1 mm increments. Because of the significant decrease of amplitude for offsets greater than about 120 mm, due to variation of transmission coefficients with offset, i.e., the angle of incidence (see Daley and Hron, 1979), the offsets selected for

inversion lie between 0 mm and 120 mm. The speed of vertical propagation of SH waves in the 31-plane, calculated at the zero offset, using independent knowledge of speed in the isotropic layer and thicknesses of both layers, is 1609 m/s. This result agrees closely with direct laboratory measurements on the Phenolic CE by Cheadle et al. (1991), where the range of SH velocity for measurements in the 31-plane is 1602 m/s - 1610 m/s. The expected value of the anisotropic parameter is $\gamma = 0.096$. The inversion results are shown in Table 8.2.

Offset (m)	Traveltime (s)	Inverted γ (perfect information¹⁹)	Inverted γ (1% error in vertical speed) (1626 m/s)	Inverted γ (up to 1% random error in traveltime)
0	1.25	N/A	N/A	N/A
90	1.25104	0.0959772	*	-0.734978
190	1.27558	0.0961738	-0.437334	-0.232223
290	1.3484	0.0958288	-0.116718	-0.0170171
390	1.02475	0.0959165	-0.0227692	0.0755439
490	1.04204	0.0959752	0.0178276	0.117534
590	1.06286	0.0959918	0.0390921	0.110076
690	1.08699	0.0959842	0.051623	0.0843938
790	1.11419	0.0959669	0.0596263	0.0830911
890	1.1442	0.0959865	0.065086	0.0816758
990	1.17678	0.0959947	0.068952	0.117695

Table 8.1. The results of forward numerical modelling and inversion.

8.5.3. Discussion of inversion applications

The numerical example, on noise-free data, shows that the inversion works very well in ideal circumstances. Both numerical and physical modelling examples indicate, however, that the method is very sensitive to errors in the input information. Geometrically, the sensitivity of inversion can be visualized by observing the gentle slope of the traveltime function in Figure 8.2. This implies that a slight variation in the

¹⁹ As mentioned in Section 8.4, the inversion relies on the linearized, i.e., first-order approximation of expression for group velocity. Thus, “perfect information” implies that the traveltime is also computed using the same approach. If a higher-order approximation for group velocity is used in forward modelling, a slight discrepancy between actual and inverted values of γ results. For instance, for offsets of 490 and 990 metres, a higher-order approximation of group velocity yields traveltimes of 1.04305 and 1.7922 seconds, respectively, which, in turn, gives corresponding values of 0.0852466 and 0.0882306 for γ .

vertical position of the plane depicting the measured traveltime will result in a considerable lateral shift of the curve \mathcal{C}_1 , and hence the value of the anisotropic parameter, γ . In principle, however, using modern measuring devices, it is possible, to measure the traveltime with high enough precision to obtain good inversion results.

Scaled offset (m)	Scaled time (s)	Inverted γ
0	0.994	N/A
90	0.997	-0.304444
190	1.001	0.127213
290	1.010	0.129247
390	1.024	0.108049
490	1.036	0.159402
590	1.052	0.177814
690	1.076	0.159333
790	1.108	0.124404
890	1.145	0.0929694
990	1.182	0.0794125

Table 8.2. Measured traveltimes and inverted anisotropic parameter, γ for SH waves in 31-plane.

8.6. ANISOTROPIC/ANISOTROPIC CASE

The logic described above can be extended to cases where both layers are anisotropic. The anisotropic parameter, $\gamma_1 \equiv \Gamma$, as well as the vertical wave speed, β_1 , of the first or surface layer, are assumed to be known. In such a case, the set of equations has a slightly more complicated appearance but no additional unknowns. The only difference is the substitution of an angle-dependent formula for the velocity in the upper medium, that is:

$$\left\{ \begin{array}{l} \frac{\sqrt{(X-r)^2 + H_1^2}}{\beta_1 \left(1 + \Gamma \frac{(X-r)^2}{(X-r)^2 + H_1^2} \right)} + \frac{\sqrt{r^2 + H_2^2}}{\beta_2 \left(1 + \gamma \frac{r^2}{r^2 + H_2^2} \right)} = t(r) \\ \frac{dt(r)}{dr} = 0 \end{array} \right. \quad (8.7)$$

Method of Computation: Anisotropic parameter, γ , from travelttime measurements
in the anisotropic/anisotropic case

Step 1

Express γ as a function of r , and known parameters:

$$\gamma = \gamma(r; T, X, \beta_1, \beta_2, \Gamma, H_1, H_2) =$$

$$= \frac{\beta_1 \left(1 + \Gamma \frac{(X-r)^2}{(X-r)^2 + H_1^2} \right) (r^2 + H_2^2)^{\frac{3}{2}}}{\beta_1 r^2 \left[TV - \sqrt{(X-r)^2 + H_1^2} \right]} - \frac{r^2 + H_2^2}{r^2}$$

Step 2

Calculate the local extremum of γ , by setting the derivative of γ w.r.t. r to zero, and solving for r . The process is very laborious and it might be recommended to use a mathematical software. In searching for a solution one may use the fact that the solution of interest is situated between $r = 0$ and $r = X$.

$$\frac{d\gamma}{dr} = -\frac{2}{r} + \frac{2(H_2^2 + r^2)}{r^3} -$$

$$\frac{\beta_1 \left(1 + \Gamma \frac{(X-r)^2}{(X-r)^2 + H_1^2} \right) (H_2^2 + r^2)^{\frac{3}{2}} (X-r)}{\beta_2 r^2 \sqrt{H_1^2 + (X-r)^2} \left(T\beta_1 \left(1 + \Gamma \frac{(X-r)^2}{(X-r)^2 + H_1^2} \right) - \sqrt{H_1^2 + (X-r)^2} \right)^2} +$$

$$+ \frac{3\beta_1 \left(1 + \Gamma \frac{(X-r)^2}{(X-r)^2 + H_1^2} \right) \sqrt{H_2^2 + r^2}}{\beta_2 r \left(T\beta_1 \left(1 + \Gamma \frac{(X-r)^2}{(X-r)^2 + H_1^2} \right) - \sqrt{H_1^2 + (X-r)^2} \right)} -$$

$$\frac{2\beta_1 \left(1 + \Gamma \frac{(X-r)^2}{(X-r)^2 + H_1^2} \right) (H_2^2 + r^2)^{\frac{3}{2}}}{\beta_2 r^3 \left(T\beta_1 \left(1 + \Gamma \frac{(X-r)^2}{(X-r)^2 + H_1^2} \right) - \sqrt{H_1^2 + (X-r)^2} \right)} = 0$$

Step 3

Insert the value of r , calculated in Step 2, to the expression for γ in Step 1.

A Mathematica® programme for the entire calculation is given below.

X = horizontal distance between the source and receiver
 HJ = thickness of the upper anisotropic layer
 HD = thickness of the lower anisotropic layer
 V = vertical wave speed in the upper, anisotropic layer
 B = vertical wave speed in the lower, anisotropic layer
 G = anisotropic layer in the upper medium, i.e., medium of incidence
 TT = travelt ime between the source and receiver (one way)

```
D[
(V*(1+G*(X-r)^2/((X-r)^2+HJ^2)))*(r^2+HD^2)
*sqrt[r^2+HD^2]/(B*r^2*(TT*(V*(1+G*(X-r)^2/((X-r)^2+HJ^2)))
-Sqrt[(X-r)^2+HJ^2])
-(r^2+HD^2)/r^2,r]
FindRoot[%==0,{r,0.5*X,0.001*X,0.99*X}]
N[
(V*(1+G*(X-r/.%)^2/((X-r/.%)^2+HJ^2)))*((r/.%)^2+HD^2)*
sqrt[(r/.%)^2+HD^2]
/(B*(r/.%)^2*(TT*(V*(1+G*(X-r/.%)^2/((X-r/.%)^2+HJ^2)))
-Sqrt[(X-(r/.%))^2+HJ^2])
-((r/.%)^2+HD^2)/(r/.%)^2]
```

8.7. MULTI-LAYER CASE

In this section the usefulness of the inversion scheme is enhanced by deriving an algorithm applicable to propagation of SH waves in multiple layers. In exploration geophysics the proposed scheme appears to be particularly applicable in vertical seismic profiling (VSP).

It is assumed that the surface layer is isotropic. The assumption of an isotropic surface layer, besides facilitating the mathematics of inversion, is not unreasonable in the geophysical context. One might argue that the unconsolidated material composing the near-surface layer consists, in general, of a rather random arrangement of particles and does not exhibit any directionality and hence is quite isotropic, even if strongly inhomogeneous. Also, the velocity of wave propagation in the surface layer is, in

general, significantly smaller than that in the deeper layers. This entails, particularly in the multilayer case, a near-vertical direction of propagation of the ray in the surface layer. Therefore, even if the surface layer exhibits some anisotropy, the velocity of propagation would be very well approximated by the vertical wave speed. Thus, the above assumption does not limit considerably the practical application of the method.

It is further assumed that all interval vertical speeds are known. Particularly if one considers vertical seismic profiling, this information is provided by the velocity survey from the *zero-offset* VSP, and thus the above assumption does not constitute any significant practical limitation of the method.

Moreover, it is assumed that anisotropic parameters for all layers above the layer in question are known. Considering, however, that, in the case of VSP recording, one could have the traveltimes information from receivers in the entire well-bore, one can perform the inversion for each layer starting at the first subsurface layer and repeating it sequentially for all subsequent layers. In this manner, the anisotropic parameters of the overlying layers are always known, and this assumption does not, therefore, constitute any major practical limitation of the method.

The extension of the inversion scheme results from combining the inversion scheme proposed above, for a two-layer medium, with the anisotropic formulation of Snell's law derived in Chapters II and III. The Snell's-law formalism allows for the parameterization of the travelpath in terms of a single value, r , denoting the distance between the refraction point at the first interface and the receiver. One considers a model containing N horizontal layers. The surface layer ($j = 1$) is assumed to be isotropic entailing the equivalence of phase and group velocities. Thus to initialize the raytracing process, the ray parameter, x_0 , can be calculated directly from the value of r , from the expression:

$$x_0 \equiv \frac{\sin \theta_1}{\beta_1} = \frac{\frac{X - r}{\sqrt{(X - r)^2 + H_1^2}}}{\beta_1}. \quad (8.8)$$

The traveltime in the first layer is given in terms of X , r , and the vertical SH wave speed, β_1 , in the first layer as:

$$t_1(r) = \frac{X - r}{\beta_1}. \quad (8.9)$$

Then, the raytracing follows through a series of horizontal layers, $j = 2$ through $j = N - 1$, with known anisotropic parameters obeying the conditions imposed by the anisotropic form of Snell's law, until the N th layer with the unknown anisotropic parameter is reached. The total horizontal distance, d , travelled through the stack of $N - 2$ horizontal, anisotropic layers is calculated based on the knowledge of layer thicknesses, H_j , and propagation angles, θ_j , from Snell's law:

$$d = \sum_{j=2}^{j=N-1} H_j \tan \theta_j. \quad (8.10)$$

The traveltime in the $N - 2$ layers, i.e., all layers without the surface and the deepest layer in question, is calculated as a sum of traveltimes in each layer. The traveltime in terms of the propagation angle, θ_j , the vertical speed, β_j , and the known anisotropic parameter, Γ_j , is given as:

$$t_{j=2 \rightarrow N-1}(r) = \sum_{j=2}^{j=N-1} \frac{H_j}{\cos \theta_j [V_j]} = \sum_{j=2}^{j=N-1} \frac{H_j}{\cos \theta_j [\beta_j (1 + \Gamma_j \sin^2 \theta_j)]}. \quad (8.11)$$

The expression in square brackets in equation (8.11) represents the group velocity in the j th layer, V_j .

The total horizontal distance, D , travelled prior to reaching the N th layer, for which the anisotropic parameter is to be found, is the distance travelled in the first layer, i.e., $X - r$, and the distance travelled through a stack of horizontal anisotropic layers, d . Thus:

$$D = (X - r) + \sum_{j=2}^{j=N-1} H_j \tan \theta_j. \quad (8.12)$$

The angle of incidence in the N th layer with the unknown anisotropic parameter is chosen in such a way that the ray arrives at the receiver, i.e., the horizontal distance, Δ , travelled in this layer is given by:

$$\Delta = |X - D| = |r - d|. \quad (8.13)$$

The absolute value is important if the initialization of raypath by r is such that horizontal distance travelled in the first $N - 1$ layers is greater than the horizontal source-receiver offset. The travelttime of the ray in the N th layer is given in terms of the horizontal distance, r , between the refraction point at the first interface and the receiver, the horizontal distance, d , travelled by the ray through the stack of anisotropic layers with known anisotropic parameters, Γ_j , the thickness of the N th layer H_N , and the group velocity, V_N , is given by:

$$t_N(r) = \frac{\sqrt{\Delta^2 + H_N^2}}{V_N} = \frac{\sqrt{(r-d)^2 + H_N^2}}{\beta_N \left[1 + \gamma \frac{(r-d)^2}{(r-d)^2 + H_N^2} \right]}. \quad (8.14)$$

The group velocity, V_N , is given in terms of the vertical wave speed, β_N , and the unknown anisotropic parameter, γ . Only one value of r , i.e., the value minimizing the travelttime, is physically acceptable. In general, the refraction point on the first interface must be located quite close to the source, i.e., the first raypath must be close to the vertical. Otherwise, if the angle of incidence is large the horizontal distance traveled by the ray through a stack of layers in which Snell's law is followed, overshoots the receiver, making the last segment go backwards (see raypath B in Figure 8.6). This is clearly an

aphysical situation, and one that yields a value of traveltime very much greater than the minimum value. Furthermore, a certain sufficiently small value of r leads to a large take-off angle, resulting in a critical angle at one of the interfaces.

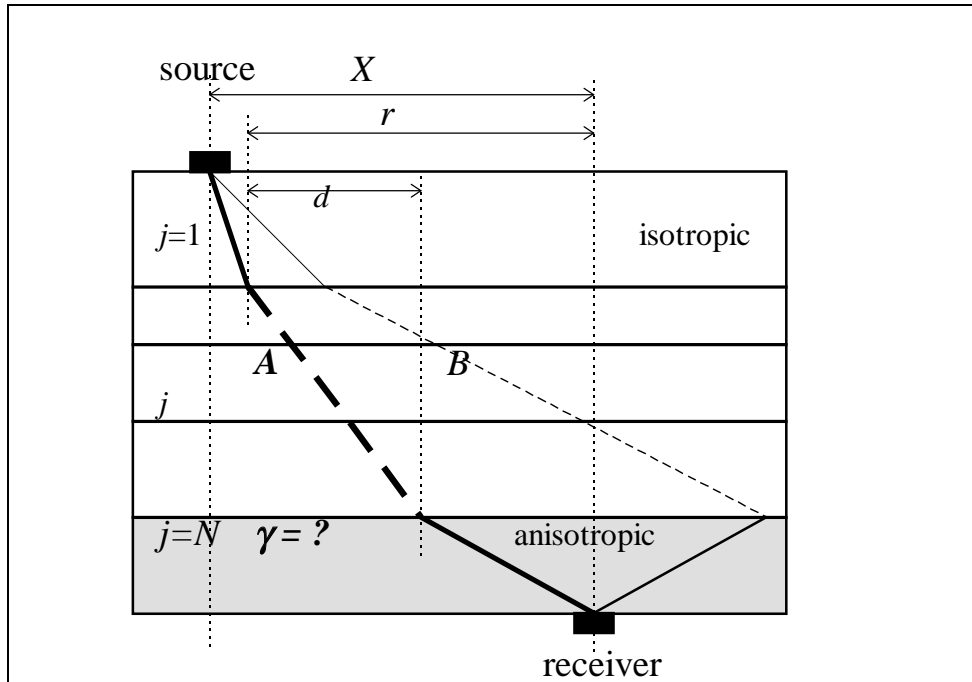


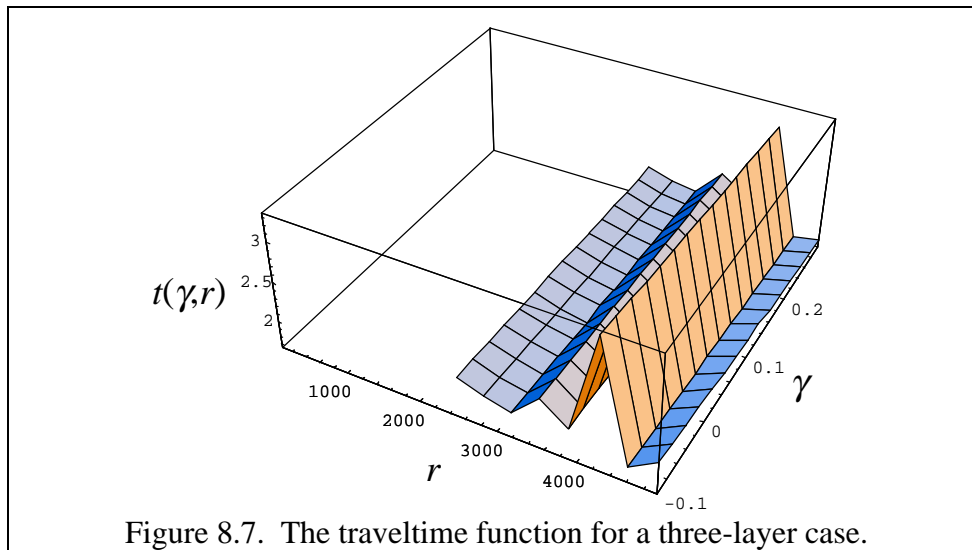
Figure 8.6. The multilayer model used to explain the inversion algorithm. The surface layer is assumed to be isotropic, while the anisotropic parameters of layers $j = 2$ through $j = N-1$ are assumed to be known. The travelpath, and hence the traveltime are parametrized in terms of the horizontal distance, r , between the refraction point at the first interface and the receiver. The raytracing through a stack of horizontal anisotropic layers with known anisotropic coefficient obeys Snell's law initialized by the choice of r . The raypath in the lowest layer with unknown anisotropic coefficient is always such as to arrive at the receiver. The physically acceptable solution corresponds to the value of r which minimizes the traveltime.

The complicated traveltime surface is illustrated in Figure 8.7, in which r is allowed to span the entire range from 0 to X . The largest value of traveltime corresponds to the point where the lateral location of the receiver is reached on the last interface, i.e.,

the raypath in the last layer is vertical. Eventually, a complex value of traveltime is reached and no real surface can be plotted.

Figure 8.8 is an illustration of the traveltime surface with the values of r limited to the neighbourhood of a Fermatian solution. The general appearance of the surface resembles the two-layer case illustrated in Figures 8.2 and 8.3. Again, when cutting the traveltime surface with a horizontal plane corresponding to the actual traveltime, one obtains the physical solution corresponding to the nadir of the intersection curve.

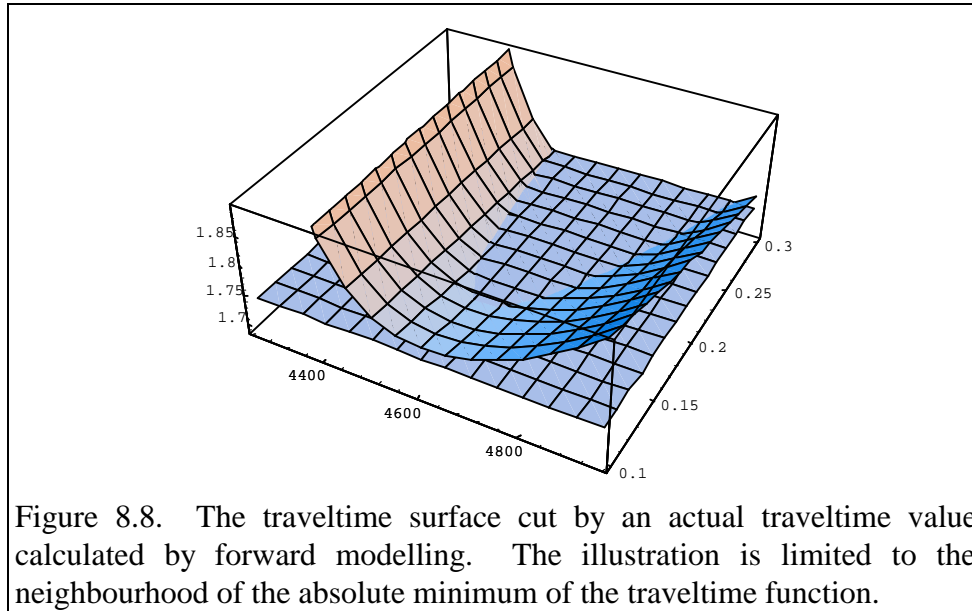
In practice, one can first generate a plot of the entire range of r , and then limit it to the neighbourhood of the absolute minimum. It is important to establish visually, from the three-dimensional plot, the range of values within which the absolute minimum is to be found. Otherwise, the inversion algorithm might return a local minimum that does not correspond to the absolute minimum.



The traveltime function illustrated in Figures 8.7 and 8.8 derives from a three layer model whose parameters are shown in Table 8.3. The traveltime obtained by forward modelling with a lateral source-receiver separation of 5000 metres and an assumed anisotropic parameter in the third layer of $\gamma = 0.15$, is 1.74208 seconds.

Layer #	Layer Thickness (m)	Vertical Wave Speed (m/s)	Anisotropic Parameter, γ
1	1000	3000	0
2	2000	4000	0.2
3	3000	5000	unknown (0.15)

Table 8.3. The parameters of the model used in numerical calculation of a multilayer case.



The value of γ can be obtained, as in the two-layer case, by setting $d\gamma/dr$ to zero, i.e., in our case, by finding the minimum of the intersection curve of two surfaces illustrated in Figure 8.8. In the multilayer case, one has to be careful to select the proper local minimum. Graphical output is very helpful in visualizing the solution. Figure 8.9.a. shows that the function $\gamma(r)$, given by equation (8.16) is discontinuous and has several extrema. One must choose an extremum (minimum) corresponding to the Fermatian solution visualized by examining Figure 8.7. Figure 8.9.b. shows a smooth continuous segment in the neighbourhood of the solution. Note that the minimum of is around 0.15, as expected from parameters of the forward model (Table 8.3).

The solution, as in the two-layer case, can be obtained by finding the minimum of $\gamma(r)$, based on the total traveltime function with the known value of a particular

traveltime, T , corresponding to the given source-receiver configuration. The total traveltime function is trivially given by:

$$t_{TOT}(r) = t_1(r) + t_{j=2 \rightarrow N-1}(r) + t_N(r). \quad (8.15)$$

Equation (8.15) can be solved explicitly for γ , which appears only in the third term on the right-hand side. Hence, for a measured traveltime, T , the expression for γ can be written as:

$$\gamma(r) = \left[\left(\frac{H_N}{r-d} \right)^2 + 1 \right] \left\{ \frac{\sqrt{(r-d)^2 + H_N^2}}{\beta_N [T - (t_1(r) + t_{j=2 \rightarrow N-1}(r))]} \right\}. \quad (8.16)$$

The plot of equation (8.16) is shown in Figure (8.9. a, b). Equation (8.15) represents a complicated entity. The traveltime functions $t_i(r)$ are quite complicated, particularly, the traveltime expression for the stack of horizontal layers which involves the use of the anisotropic formalism of Snell's law. For this reason, mathematical software becomes extremely helpful.

It is important to realize that in the proposed procedure one does not minimize the traveltime explicitly. Due to the fact that a minimum of $\gamma(r)$ corresponds to a stationary time, Fermat's principle is guaranteed by the implicit function theorem (see Appendix 4). Therein lies the power of the proposed method of inversion.

The inversion process can be performed using the Mathematica® software. In the algorithm given below the *FindMinimum* command is used since an algebraic expression for the derivative of γ with respect to r could not be found. For concerns of numerical precision and accuracy see Appendix 3.

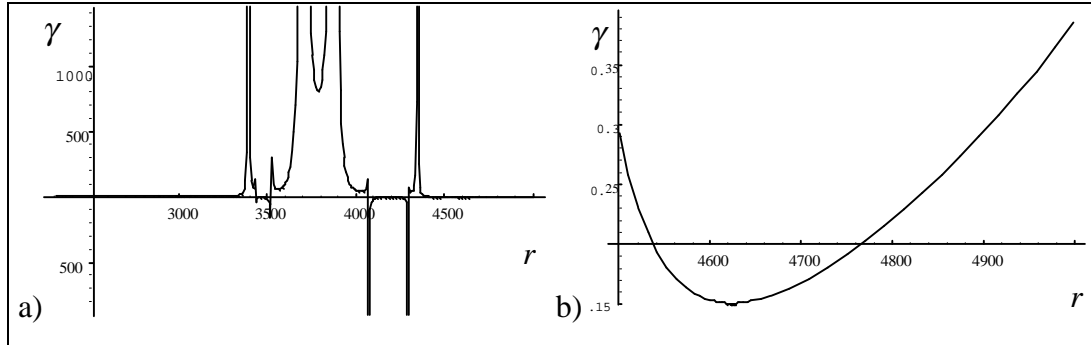


Figure 8.9. a & b. The graph of γ as a function of r for a given value of the traveltime T . Picture a) illustrates the behaviour of the function for the entire range of r . Picture b) illustrates the behaviour of the function in the neighbourhood of the Fermatian solution, as visualized in Figure 8.7. The solution corresponds to the minimum clearly illustrated in b). Note that the scales of the axes are different.

Method of Computation: Anisotropic parameter, γ from traveltime measurements for a three-layer case.

Step 1

Express the unknown γ in the bottom layer as a function of r , measured traveltime, T , and known parameters of the upper layers.

$$\gamma = \frac{(r - H_2 \tan \theta_t)^2 + H_3^2}{(r - H_2 \tan \theta_t)^2} \left\{ \frac{\sqrt{(r - H_2 \tan \theta_t)^2 + H_3^2}}{\beta_3 \left[T - \left(\frac{\sqrt{(X - r)^2 + H_1^2}}{\beta_1} + \frac{H_2}{\cos \theta_t (\beta_2 (1 + \gamma_2 \sin^2 \theta_t))} \right) \right]} - 1 \right\}$$

where

$$\theta_t = \text{Arc cos} \left\{ \frac{\sin \xi \left(2\beta_0 \gamma \cos^2 \xi - \frac{1}{r(\xi)} \right)}{\sqrt{\frac{1}{[r(\xi)]^2} + [\beta_0 \gamma \sin(2\xi)]^2}} \right\},$$

$$r(\xi) = \frac{1}{\beta_0(1 + \gamma \cos^2 \xi)}$$

and

$$\xi = \text{Arc cos} \left\{ \frac{1 - \sqrt{1 - (2x_0\beta_0)^2 \gamma}}{2x_0\beta_0\gamma} \right\}$$

with the ray parameter obtained by expressing $\sin\theta_1$ in terms of r :

$$x_0 = \frac{\frac{X-r}{\sqrt{(X-r)^2 + H_1^2}}}{\beta_1}$$

Step 2

Find the local and absolute minimum of γ corresponding to the Fermatian solution.

A Mathematica® programme for the entire calculation is given below :

- T = *measured traveltime*
 X = *horizontal source-receiver offset*
 HJ = *thickness of the first (isotropic) layer*
 HD = *thickness of the second (anisotropic) layer*
 HB = *thickness of the bottom (anisotropic) layer*
 VJ = *wave speed in the first (isotropic) layer*
 VD = *vertical wave speed in the second (anisotropic) layer*
 VB = *vertical wave speed in the bottom (anisotropic) layer*
 GD = *anisotropic parameter in the second layer*

$$TJ = \text{Sqrt}[(X-r)^2 + HJ^2] / VJ$$

$$x = ((X-r) / \text{Sqrt}[(X-r)^2 + HJ^2]) / VJ$$

raypath and traveltime calculation in the second layer; analogous modules for subsequent layers can be added

$$ZD = \text{ArcCos}[(1 - \text{Sqrt}[1 - GD*(2*x*VD)^2]) / (2*x*VD*GD)]$$

$$RD = 1 / (VD*(1 + GD*\text{Cos}[ZD]^2))$$

$$nd = \text{Sin}[ZD]*(2*VD*GD*\text{Cos}[ZD]^2 - 1/RD)$$

$$dd = \text{Sqrt}[1/RD^2 + (VD*GD*\text{Sin}[(2*ZD)])^2]$$

$$sd = \text{ArcCos}[Abs[nd/dd]]$$

calculation of the traveltime in the second layer:

$$TD = HD / (\text{Cos}[sd]*VD*(1 + GD*\text{Sin}[sd]^2))$$

calculation of the horizontal distance traveled through the stack of the anisotropic layers; by adding terms it can be easily extended to accommodate more layers:

$$DD = HD * \tan[\text{sd}] + \dots$$

calculation of the minimum of $\chi(r)$ with given initial search parameters (Value1 and Value 2), to be chosen in the neighbourhood of the Fermatian solution:

```
FindMinimum[
  (((r-DD)^2+HB^2)/(r-DD)^2)*
  (Sqrt[(r-DD)^2+HB^2]/(VB*(T-(TJ+TD+....)))-1),
  {r,{Value1,Value2}}
```


CHAPTER IX

CONCLUSIONS

9.1. GENERAL REMARKS

An analytical scheme relating incidence, reflection and transmission angles in anisotropic media has been derived. In Chapter II a rather general method based on vector calculus was suggested. It works well in cases in which a phase-slowness surface can be described by Cartesian coordinates in phase-slowness space, e.g., an ellipsoid. Direct application of this method can be rather cumbersome as it might be exceedingly difficult to express a complicated slowness surface in Cartesian coordinates.

The weak-anisotropy approximation allows a useful implementation of the aforementioned analytical scheme relating incidence, reflection and transmission angles. A simplification of the phase-velocity formulæ under the assumption of weak anisotropy allows one to express clearly the relationship among angles (Chapter III). This yields a straightforward method for calculating both phase and group angles, as well as phase and group velocities. A raytracing scheme is developed based on this approach. It allows for raytracing in multilayer anisotropic media with planar, but not necessarily horizontal, interfaces.

The weak-anisotropy approximation works well within its realm of applicability.

The results of a physical experiment involving wave propagation across the boundary between isotropic and anisotropic media indicated that the traveltimes calculated using the raytracing method agreed reasonably well with the measured values (Chapter VII). Furthermore, the traveltimes calculated using the weak-anisotropy approach were significantly closer to the measured values than traveltimes calculated based on an isotropic approach.

Results pertaining to SV waves are more affected by the weak-anisotropy approximation than those relating to P and SH waves. SV waves exhibit, in general, more complicated shapes of slowness curves than either P or SH waves, as illustrated in Appendix 2. Therefore, in the case of SV waves, the loss of higher-order terms results in a larger discrepancy between results obtained using exact and approximate approaches than in the case of either P or SH waves.

An analytic traveltime inversion for SH waves has been developed. A method which uses the traveltime through a stack of anisotropic layers to obtain the single anisotropic parameter, γ , has been proposed. The method works well with perfect information, but is very sensitive to input errors. Therefore, it can be used for data acquired in the laboratory with very precise apparatus and in noise-free conditions. However, in its present form, the method cannot be confidently used in geophysical field measurements.

In principle, there seems to be no obstacle to the implementation of exact equations in the proposed scheme (Appendix 7). Any extension of the development presented in this dissertation to the realm of strong anisotropy would necessitate use of exact equations, or at least higher-order approximations. One would certainly gain some accuracy of results at the expense of clarity. If, however, the development proposed in

this dissertation were to be used in geophysical practice, such a course of action is strongly recommended.

9.2. SOME PRACTICAL APPLICATIONS

9.2.1. Modelling

A reliable method allowing one to generate experimental results synthetically can play a very important rôle. Such a technique incorporated into the planning of a seismic experiment allows one to anticipate the results and thus to correctly deploy sources, receivers, and other experimental apparatus. Furthermore, it allows the interpreter (while keeping in mind the intrinsic non-uniqueness) to verify the results of interpretation by comparing synthetic data, generated based on a given interpretation, with experimental results.

The raytracing method presented here allows one to generate synthetically results of wave propagation in weakly anisotropic layered media. The raytracing method presented can provide the basis of decision as to whether or not an "anisotropic" approach should be followed. The degree of anisotropy can be varied by modifying anisotropic parameters and the discrepancy between isotropic and anisotropic approaches can thus be investigated. As indicated by physical experiments, the anisotropic-modelling approach reflects very closely the experimental results; one should, however, keep in mind that the algorithm is designed for weakly anisotropic media, and the accuracy of results relies on this assumption. As a reasonable rule, one can regard a degree of anisotropy of about 20% as being the limit of applicability.

9.2.2. Near-surface static corrections

The calculation of static corrections, dealing with shallow reflections and refractions, employs obliquely travelling rays. For such rays, the effects of anisotropy are, in general, more pronounced than for deep reflections, for which all rays are nearly vertical. Furthermore, large differences in velocities among near-surface layers

emphasize the raybending at interfaces, calling for an accurate description of this phenomenon.

The anisotropic raytracing presented in this dissertation allows one to calculate static corrections including the effects of anisotropy. For instance, it is important to realize that the value of the critical angle is not the same for isotropic and anisotropic cases, thus directly affecting results of refraction statics.

9.2.3. Vertical seismic profiling (VSP)

The recording geometry of an offset VSP, with receivers deployed throughout a long section of the wellbore and the source located on the surface at a considerable lateral distance from the well, can be particularly affected by anisotropic effects. The data set contains information derived from propagation directions ranging from nearly vertical to nearly horizontal, thus creating the opportunity for any angular dependence to manifest itself.

The VSP geometry is ideally suited for employing the method presented in this dissertation assuming that the anisotropy of the rock mass can be characterized as a TI system, i.e., transverse isotropy, with a symmetry axis perpendicular to the planar geological layering. As a matter of general practice, in addition to the offset source, one usually records with a near-offset source as well. For the latter case, the rays are nearly vertical and, since the distance travelled is measured by the geophone cable, the traveltime reliably yields the vertical speed, which is required by the formalism. Subsequently, by modifying anisotropic parameters, one can fit modelled and observational data.

Furthermore, VSP geometry provides an excellent experimental setup for traveltime inversion, which can yield the anisotropic parameters. As already mentioned, this geometry gives reliable information on the vertical speed from the zero-offset record and on the angle-dependent traveltime measurements from the far-offset record. Moreover, the presence of the wellbore provides information about thicknesses of the sedimentary layers.

9.2.4. Intuitive understanding

I believe that an important aspect of the presented method is the educational one. The method allows a rather straightforward manipulation of various quantities characteristic of wave propagation in anisotropic media. Concepts of phase and group angles and velocities can be investigated, allowing a geophysicist to become more familiar with notions extending beyond an isotropic approach.

Particularly with the aid of “user-friendly” mathematical software, some of the ideas included in this dissertation can be used as starting points for hours of geophysical enjoyment. Have fun!

REFERENCES

- Auld, B.A., 1973, Acoustic fields and waves in solids, Volume I and II: John Wiley and Sons.
- Brown, R.J., 1988, Computational errors in closed-form expressions with an electromagnetic example: the conducting-sphere response: *Geophysics*, **53**, 1122-1125.
- Brown, R.J., Lawton, D.C., and Cheadle, S.P., 1991, Scaled physical modelling of anisotropic wave propagation: multioffset profiles over an orthorhombic medium: *Geophys. J. Int.* **107**, 693-702.
- Byun, B.S., 1982, Seismic parameters for media with elliptical velocity dependencies: *Geophysics*, **47**, 1621-1626.
- Byun, B.S., 1984, Seismic parameters for transversely isotropic media: *Geophysics*, **49**, 1908-1914.
- Carcione, J.M., 1992, Wavefronts in dissipative anisotropic media: Expanded Abstracts of 62nd SEG Meeting, 1363-1365.
- Cheadle, S.P., Brown, R.J., and Lawton, D.C., 1991, Orthorhombic anisotropy: a physical seismic modelling study: *Geophysics*, **56**, 1603-1613.
- Crampin, S., and Kirkwood, S.C., 1981, Velocity variations in systems of anisotropic symmetry: *J. Geophys.* **49**, 35-42.
- Crampin, S., and Yedlin, M., 1981, Shear-wave singularities of wave propagation in anisotropic media: *J. Geophys.*, **49**, 43-46.
- Daley, P.F., and Hron, F., 1977, Reflection and transmission coefficients for transversely isotropic media: *Bull., Seis. Soc. Am.*, **67**, 661-675.
- Daley, P.F., and Hron, F., 1979, Reflection and transmission coefficient for seismic waves in ellipsoidally anisotropic media: *Geophysics*, **44**, 27-38.
- Dellinger, J., 1991, Anisotropic seismic wave propagation: Ph.D. dissertation, Univ. of Stanford.

- Dellinger, J., and Vernik, L., 1994, Do traveltimes in pulse-transmission experiments yield anisotropic group or phase velocities?: *Geophysics*, **59**, 1774-1779.
- Dellinger, J., and Muir, F., 1988, Imaging reflections in elliptically anisotropic media: *Geophysics*, **53**, 1616-1618.
- Dunoyer de Segonzac, Ph., and Laherrere, J., 1959, Applications of the continuous velocity log to anisotropic measurements in northern Sahara; results and consequences: *Geophys. Prosp.*, **7**, 202-217.
- Epstein, M., and Sniatycki, J., 1992, Fermat's principle in elastodynamics: *Journal of Elasticity*, **27**, 45-56.
- Helbig, K., 1983, Elliptical anisotropy-its significance and meaning: *Geophysics*, **48**, 825- 832.
- Helbig, K., 1994, *Foundations of anisotropy for exploration seismics*: Pergamon.
- Horne, S., and MacBeth, C., 1994, Inversion for seismic anisotropy using genetic algorithms: *Geophys. Prosp.*, **42**, 953-974.
- Keith, C. M., and Crampin, S., 1976, Seismic body waves in anisotropic media: reflection and refraction at a plane interface: *Geophys. J. R. astr. Soc.*, **49**, 181-208.
- Kebaili A., and Schmitt, D.R., 1996, Velocity anisotropy observed in wellbore seismic arrivals: Combined effects of intrinsic properties and layering: *Geophysics*, **61**, 12-20.
- Krebes, E.S., and Le, L.H.T., 1994, Inhomogeneous plane waves and cylindrical waves in anisotropic anelastic media, *J. Geophys. Res.*, **99**, 23,899-23,919.
- Levin, K.L., 1979, Seismic velocities in transversely isotropic media: *Geophysics*, **44**, 918- 936.
- Love, A.E.H., 1927, *A treatise on the mathematical theory of elasticity*: Dover Publications, Inc., N.Y.
- Marsden, J.E., and Tromba, A.J., 1981, *Vector calculus*, 2nd ed: W.H. Freeman and Company, San Francisco.
- Michelena, R.J., Muir, F., and Harris, J.M., 1993, Anisotropic travelttime tomography: *Geophys. Prosp.*, **41**, 381-412.
- Olmsted, J.M.H., 1961, *Advanced Calculus*, Prentice-Hall, Inc.

- Postma, G.W., 1955, Wave propagation in a stratified medium: *Geophysics*, **20**, 294-392.
- Rokhlin, S. I., Bolland, T.K., and Adler, L., 1986, Reflection and refraction of elastic waves on a plane interface between two generally anisotropic media: *J. Acoust. Soc. Am.* **79**, 906-918.
- Schoenberg, M., 1994, Transversely isotropic media equivalent to thin isotropic layers: *Geophys. Prosp.*, **42**, 885-915.
- Sheriff, R.E., 1973, *Encyclopedic dictionary of exploration geophysics*: Society of Exploration Geophysics.
- Slawinski, M.A., 1995, The characteristic biquadratic: An illustration of transmission in anisotropic media: *CREWES Research Report*, **7**, 8.1-8.5.
- Slawinski, M.A., and Slawinski, R.A., 1994, Energy partition at the boundary between anisotropic media; Part one: Generalized Snell's law: *CREWES Research Report*, **6**, 9.1-9.12.
- Slawinski, M.A., Slawinski, R..A., and Brown, R.J., 1995, Energy partition at the boundary between anisotropic media; Part two: Raytracing in layered, anisotropic media - comparison of traveltimes for synthetic and experimental results: *CREWES Research Report*, **7**, 9.1-9.13.
- Stewart, R.R., 1988, An algebraic reconstruction technique for weakly anisotropic velocity: *Geophysics*, **53**, 1613-1615.
- Thomsen, L., 1986, Weak elastic anisotropy: *Geophysics*, **51**, 1954-1966.
- Vestrum, R.W., 1994, Group- and phase-velocity inversion for the general anisotropic stiffness tensor: M. Sc. thesis, Univ. of Calgary.
- Winterstein, D.F., 1990, Velocity anisotropy terminology for geophysicists: *Geophysics*, **55**, 1070-1088.
- Winterstein, D.F., and Paulsson, B.N.P., 1990, Velocity anisotropy in shale determined from crosshole seismic and vertical seismic profile data: *Geophysics*, **55**, 470-479.
- Wolfram, S., 1991, *Mathematica*, a system for doing mathematics by computer, 2nd edition: Addison-Wesley Publishing Company, Inc.,

APPENDIX 1

THE CHARACTERISTIC BIQUADRATIC²⁰

A1.1. PHASE VELOCITY AND RAY PARAMETER IN WEAKLY ANISOTROPIC MEDIA

The very appearance of equations involving phenomena of wave propagation through anisotropic media is often intimidating. It is of great benefit to gain an intuitive insight into some of these formulæ. This can be achieved, at times, with the help of graphical illustrations. Graphical illustrations can often allow one to observe the effects of a smooth transition between isotropic and anisotropic cases, i.e., from a well known scenario to a less intuitive one. There exist various approximations rendering some of these equations more manageable. Notably, Thomsen (1986), under the assumption of weak anisotropy, provided a set of formulæ which achieve the required simplicity of form, while retaining their validity in the context of most situations encountered in exploration geophysics. A weakly anisotropic medium, as far as compressional waves are concerned, can be characterized by a vertical speed and a pair of anisotropic parameters.

Consequently, the phase velocity, v , of a compressional wave is given in terms of the vertical speed, α_0 , anisotropic parameters, δ and ε , and the phase angle, ϑ , measured with respect to the normal to the interface, so that:

²⁰ This appendix was published by Slawinski, M.A., in the CREWES Research Report (1995).

$$v(\vartheta) = \alpha_0 \left(1 + \delta \sin^2 \vartheta \cos^2 \vartheta + \varepsilon \sin^4 \vartheta \right). \quad (\text{A1.1})$$

The reciprocal of the phase velocity, v , i.e., the phase slowness, plays an important rôle in various studies of anisotropic phenomena, notably in raytracing methods for layered media. The horizontal component of phase slowness (for horizontal interfaces) is equal across all boundaries. It is referred to as the ray parameter, x_0 .

Using the expression for this horizontal slowness component in terms of polar coordinates, one can write the equation for the ray parameter, x_0 , in weakly anisotropic media:

$$x_0 = \frac{\sin \vartheta}{\alpha_0 (1 + \delta \sin^2 \vartheta \cos^2 \vartheta + \varepsilon \sin^4 \vartheta)}. \quad (\text{A1.2})$$

A1.2. QUARTIC EQUATION AND THE CHARACTERISTIC BIQUADRATIC

Expressing all trigonometric functions in terms of $\sin \vartheta$, and rearranging, one can write equation (A1.2) as a fourth-order polynomial:

$$x_0 \alpha_0 (\varepsilon - \delta) \sin^4 \vartheta + x_0 \alpha_0 \delta \sin^2 \vartheta - \sin \vartheta + x_0 \alpha_0 = 0. \quad (\text{A1.3})$$

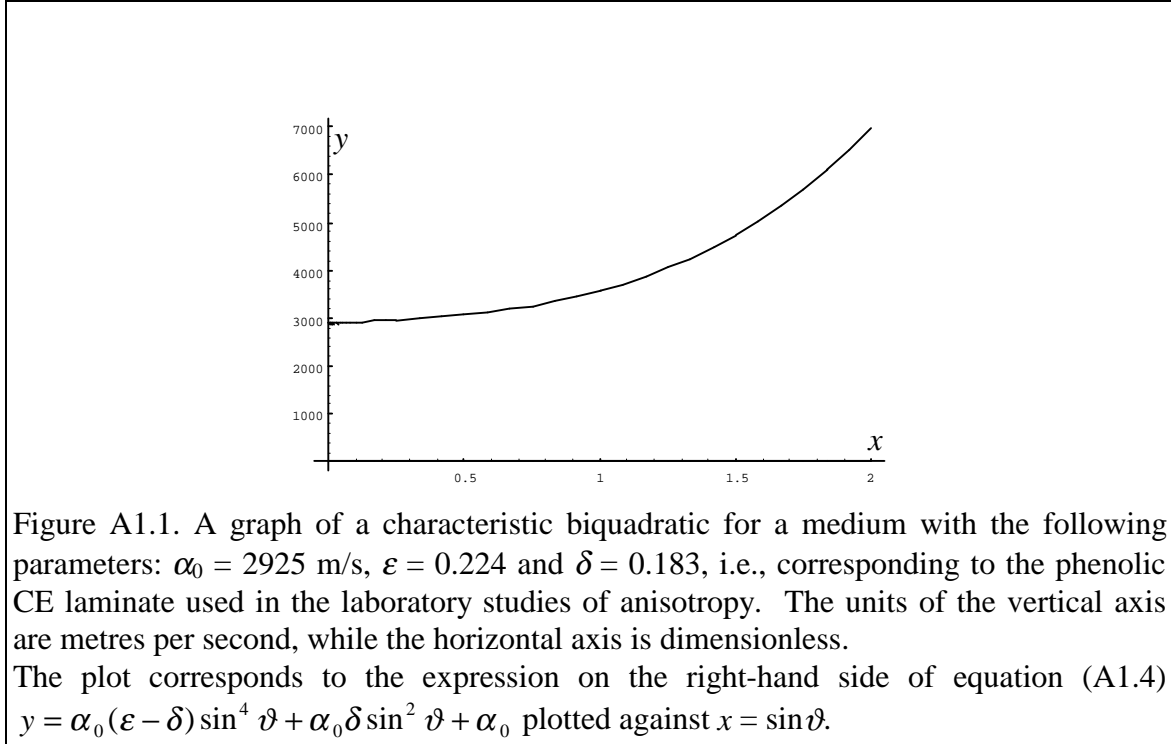
A general solution of a fourth-order polynomial is a very laborious task. But, a rather trivial manipulation gives an insight into the character of the solution of equation (A1.3).

One can write:

$$\alpha_0 (\varepsilon - \delta) \sin^4 \vartheta + \alpha_0 \delta \sin^2 \vartheta + \alpha_0 = \frac{1}{x_0} \sin \vartheta. \quad (\text{A1.4})$$

The left-hand side of equation (A1.4) is a biquadratic expression with coefficients dependent only upon the vertical speed, α_0 , and anisotropic parameters of the medium, ε

and δ (see Figure A1.1) . The coefficients are independent of the ray direction, and are characteristic of a given medium (as long as one is considering compressional waves only).



The coefficient on the right-hand side of equation (A1.4) depends only on the ray parameter, x_0 , which is a function of the angle of incidence. Letting both sides of equation (A1.4) equal y , and setting $\sin \vartheta \equiv x$, and plotting both sides of equation (A4.1) separately versus x , one notices that the left-hand side is a curve whose y -intercept $y(0) = \alpha_0$. The right-hand side is a straight line passing through the origin, with a slope equal to the inverse of the ray parameter, x_0 ; see Figure A1.2.

Such innocent transformation leads immediately to several interesting conclusions. The original quartic (equation (A1.3)) has at most two real solutions. They correspond to the points of intersection of the straight line and the curve corresponding to the right-hand side, which often resembles a parabola. These two real roots can degenerate to just one real root when the straight line is tangent to the graph. Finally, the original equation may have no real solutions if the straight line and the graph never touch.

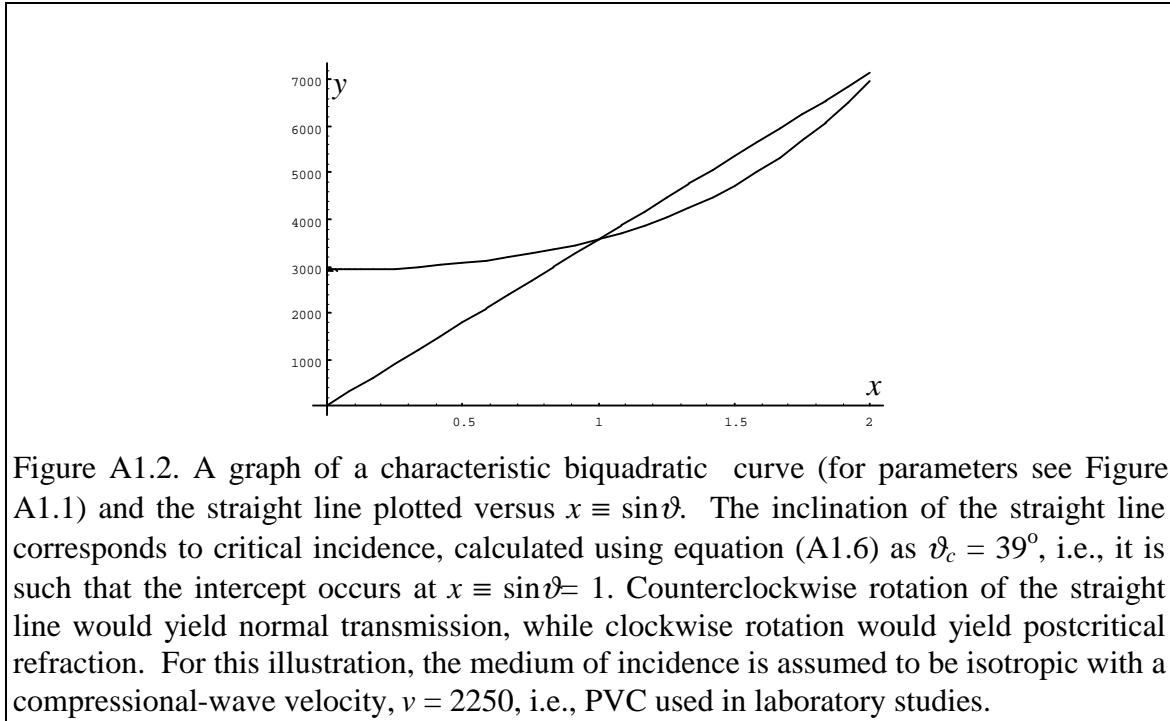


Figure A1.2. A graph of a characteristic biquadratic curve (for parameters see Figure A1.1) and the straight line plotted versus $x \equiv \sin \vartheta$. The inclination of the straight line corresponds to critical incidence, calculated using equation (A1.6) as $\vartheta_c = 39^\circ$, i.e., it is such that the intercept occurs at $x \equiv \sin \vartheta = 1$. Counterclockwise rotation of the straight line would yield normal transmission, while clockwise rotation would yield postcritical refraction. For this illustration, the medium of incidence is assumed to be isotropic with a compressional-wave velocity, $v = 2250$, i.e., PVC used in laboratory studies.

For a given medium, the quantity which determines which case is applicable is the slope of the straight line. The biquadratic remains constant for all angles of incidence as long as one is considering compressional waves. Hence, it is referred to as a *characteristic biquadratic*.

A1.3. THE CRITICAL ANGLE

For a physically meaningful solution, i.e., real ϑ , it is required that $\sin \vartheta$ not be greater than unity. This leads to the formulation of the critical-angle expression. The critical angle corresponds to the point where $\vartheta = \pi/2$ in equation (A1.2). This gives a value of the ray parameter, x_0 , that corresponds to the critical angle for compressional waves at the boundary between weakly anisotropic media:

$$x_0 = \frac{1}{\alpha_0(\varepsilon + 1)}. \quad (\text{A1.5})$$

Recalling the definition of the ray parameter in isotropic media, i.e., $x_0 \equiv \sin\theta_i/v$, one obtains the critical incidence angle for compressional waves at the isotropic/anisotropic interface:

$$\vartheta_c = \text{Arc sin} \left\{ \frac{v}{\alpha_0(\varepsilon + 1)} \right\}. \quad (\text{A1.6})$$

Setting the anisotropic parameter, ε , to zero reduces equation (A1.6) to the case of an isotropic/isotropic interface. One can easily rewrite equation (A1.6) as:

$$\vartheta_c = \text{Arc sin} \left\{ \frac{v_1}{v_2} \right\}, \quad (\text{A1.7})$$

where $v \equiv v_1$ is the velocity in the medium of incidence and $\alpha_0 \equiv v_2$ is the velocity in the medium of transmission. Equation (A1.7) is the well known formula for critical incidence angle, ϑ_c , at the boundary between two isotropic media.

A1.4. REDUCTION TO THE PURELY ISOTROPIC CASE

To complete the concept, one notices that in the limiting case, $\varepsilon = \delta = 0$, i.e., isotropy, equation (A1.4) reduces to the standard form of Snell's law. Thus, similar graphs can be obtained for isotropic media. As the values, δ and ε , approach zero, tending towards isotropy, the curve opens up. For a perfectly isotropic case, the curve of the left-hand side of equation (A1.4) becomes a horizontal straight line, $y(x) = \alpha_0$. Also, in the context of isotropy, just as in the anisotropic case, transmission occurs for values of $\sin\vartheta < 1$, the critical angle at $\sin\vartheta = 1$, and postcritical incidence for $\sin\vartheta > 1$, as illustrated in Figure A1.3.

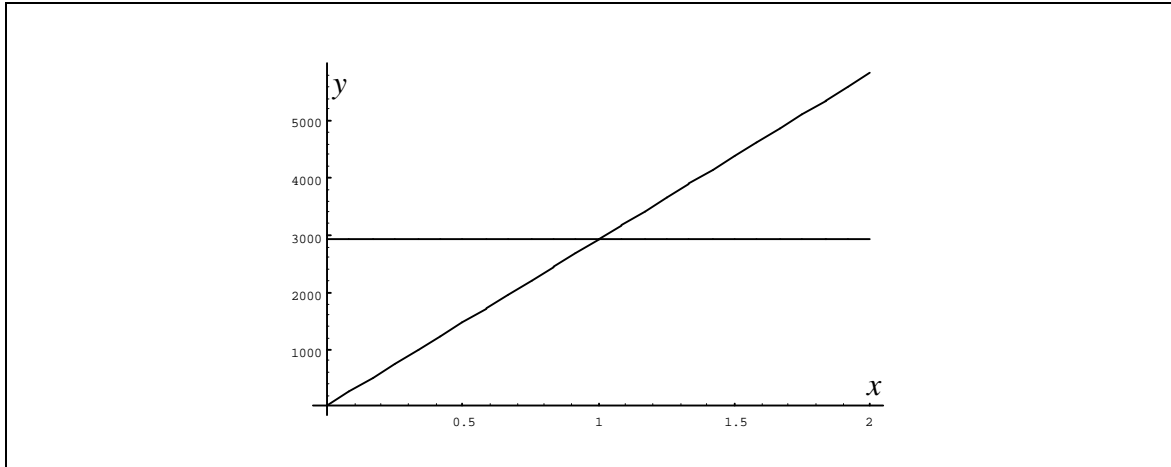


Figure A1.3. Degenerate biquadratic, the graph of a fourth-order polynomial becomes a horizontal straight line. A sloping line corresponds to critical incidence at the interface between two isotropic media with velocities of 2250 m/s and 2925 m/s, i.e., it is such that the intercept occurs at $x \equiv \sin \vartheta = 1$. Counterclockwise rotation of the straight line would yield a normal transmission, while clockwise rotation would yield postcritical refraction.

A1.5. CONCLUSIONS

A graphical illustration corresponding to the fourth-order polynomial governing the transmission/refraction of compressional waves at the boundary between weakly anisotropic media has been presented. The concept of a characteristic biquadratic, a curve whose shape depends only on anisotropic parameters of a given medium, has been introduced. It is believed that the presented graphical approach allows one to gain a more intuitive understanding of the phenomenon in question than offered by equations alone. An analogous illustration can be elaborated for SV waves (see equation (3.29)).

APPENDIX 2

IMPLICATIONS OF WEAK-ANISOTROPY APPROXIMATION ON PHASE-SLOWNESS CURVES

A considerable part of this dissertation uses the weak-anisotropy approximation, which transforms exact equations of phase velocity into approximate equations (Thomsen, 1986). Exact formulæ for P, SV, and SH waves were given by Daley and Hron (1977). Using anisotropic parameters ε , δ , and γ defined by Thomsen, the exact expressions for P, SV, and SH waves can be written as follows:

$$v_p = \alpha \sqrt{1 + \varepsilon \sin^2 \vartheta + \frac{1}{2} \left(1 - \frac{\beta^2}{\alpha^2}\right)} \left\{ \sqrt{1 + \frac{4(2\delta - \varepsilon) \sin^2 \vartheta \cos^2 \vartheta}{1 - \frac{\beta^2}{\alpha^2}} + \frac{4\varepsilon \left(1 - \frac{\beta^2}{\alpha^2} + \varepsilon\right) \sin^4 \vartheta}{\left(1 - \frac{\beta^2}{\alpha^2}\right)^2} - 1} \right\} \quad (\text{A2.1})$$

$$v_{sv} = \beta \sqrt{1 + \frac{\alpha^2}{\beta^2} \left[\varepsilon \sin^2 \vartheta - \frac{1}{2} \left(1 - \frac{\beta^2}{\alpha^2}\right) \right]} \left\{ \sqrt{1 + \frac{4(2\delta - \varepsilon) \sin^2 \vartheta \cos^2 \vartheta}{1 - \frac{\beta^2}{\alpha^2}} + \frac{4\varepsilon \left(1 - \frac{\beta^2}{\alpha^2} + \varepsilon\right) \sin^4 \vartheta}{\left(1 - \frac{\beta^2}{\alpha^2}\right)^2} - 1} \right\} \quad (\text{A2.2})$$

$$v_{SH} = \beta \sqrt{1 + 2\gamma \sin^2 \vartheta}, \quad (\text{A2.3})$$

where α and β are vertical compressional and shear wave speed respectively, δ , ε , and γ are anisotropic parameters, while ϑ denotes the phase angle. Developing the above equations into a Taylor series and neglecting higher-order terms assuming anisotropic parameters to be smaller than unity yields (Thomsen, 1986):

$$v_p \cong \alpha \left(1 + \delta \sin^2 \vartheta \cos^2 \vartheta + \varepsilon \sin^4 \vartheta \right), \quad (\text{A2.4})$$

$$v_{SV} \cong \beta \left[1 + \frac{\alpha^2}{\beta^2} (\varepsilon - \delta) \sin^2 \vartheta \cos^2 \vartheta \right], \quad (\text{A2.5})$$

and

$$v_{SH} \cong \beta \left(1 + \gamma \sin^2 \vartheta \right). \quad (\text{A2.6})$$

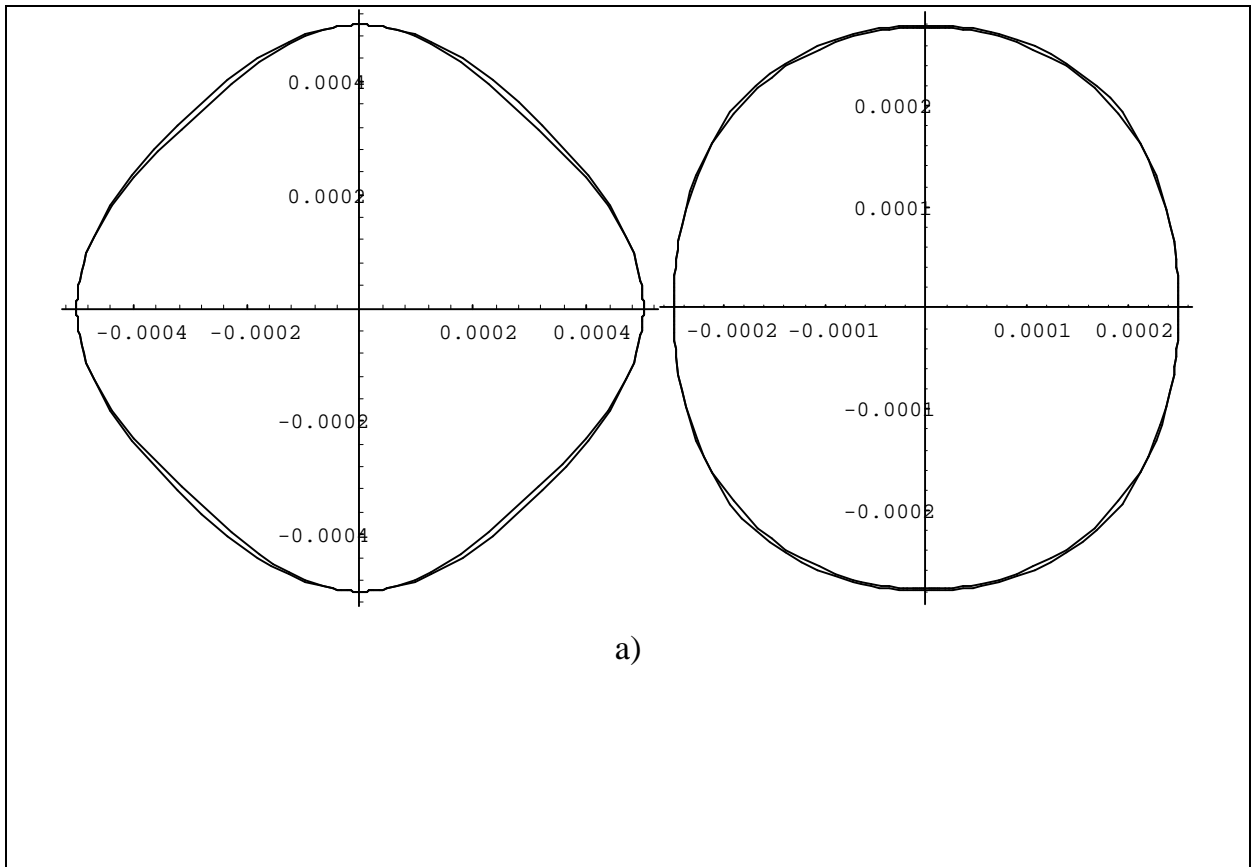
The considerable algebraic simplification facilitates mathematical operations and enables one to easily express slowness curves as level curves in polar coordinates (equations (3.7), (3.22), and (3.33)), in a form adaptable to the anisotropic formalism of Snell's law. Thomsen (1986) provides numerous further simplifications/linearization which are avoided in this dissertation since they lead to a loss of several physical attributes characteristic of wave propagation in anisotropic media, e.g., triplication of group angle as a function of phase angle (see section 6.3 and Appendix 6). No physical attributes are lost by application of equations (A.2.4), (A.2.5), and (A.2.6); the question arises, however, whether significant accuracy is sacrificed in this elegant process of simplification.

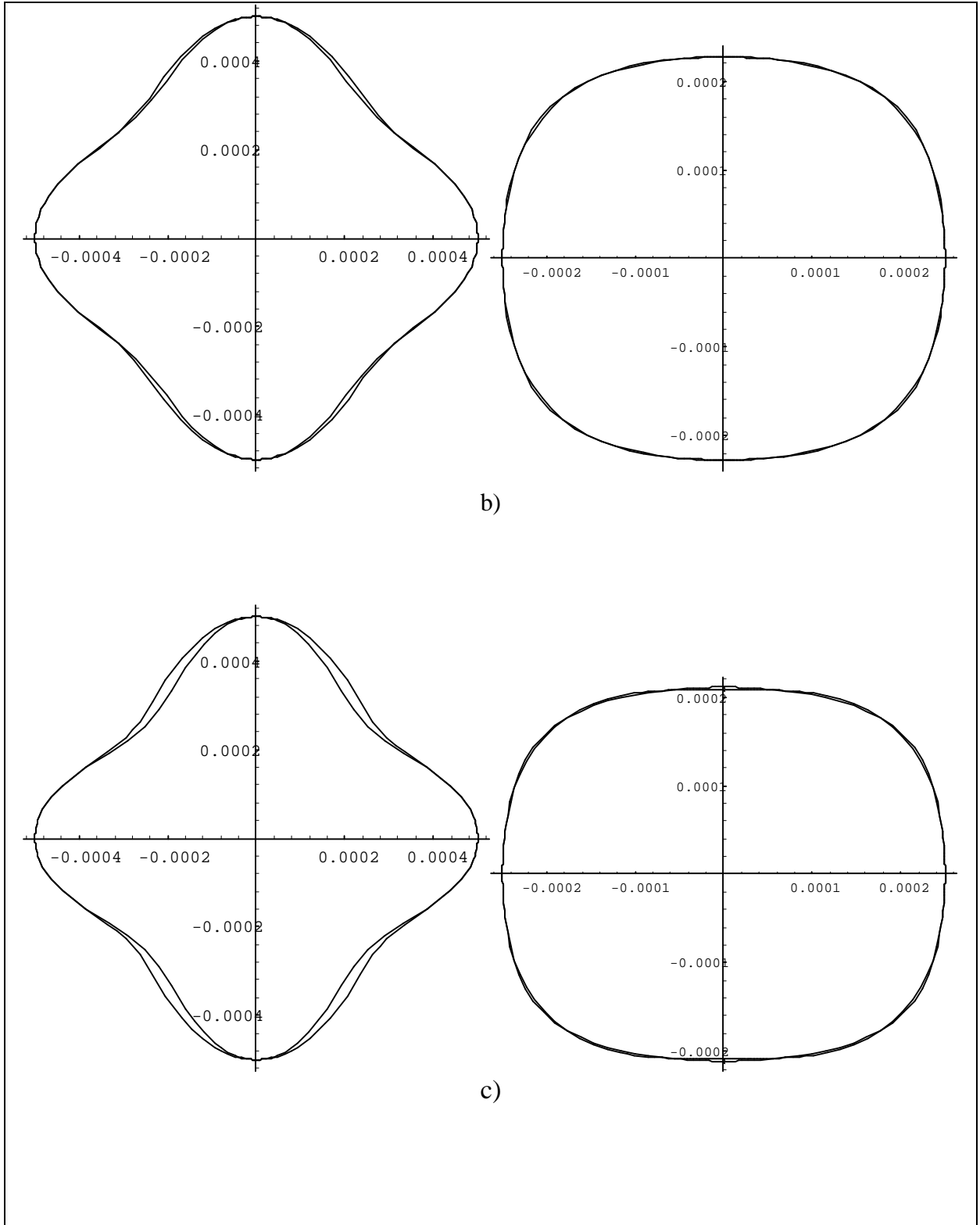
To gain an understanding of the consequences of approximation, several plots are generated using exact formulæ ((A2.1), (A2.2), (A2.3)) and their approximate

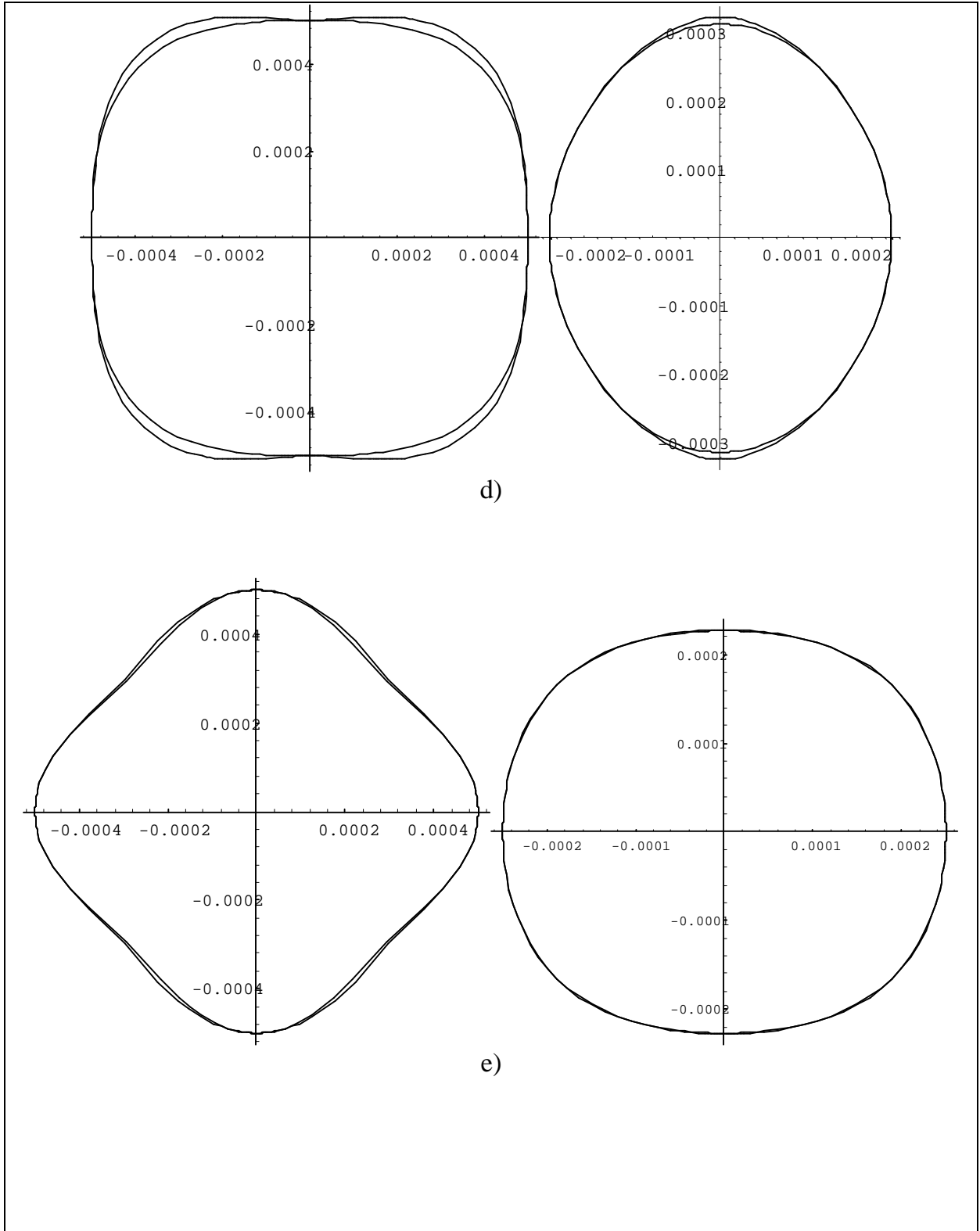
counterparts ((A2.4), (A2.5), (A2.6)). The plots represent phase-slowness curves. The values chosen for δ and ε , together with corresponding plot letter are given in Table A2.1. for P and SV waves. The cases where $\varepsilon = \delta$ are not illustrated. Such a fortuitous combination of anisotropic parameters leads to spherical wavefronts of SV waves.

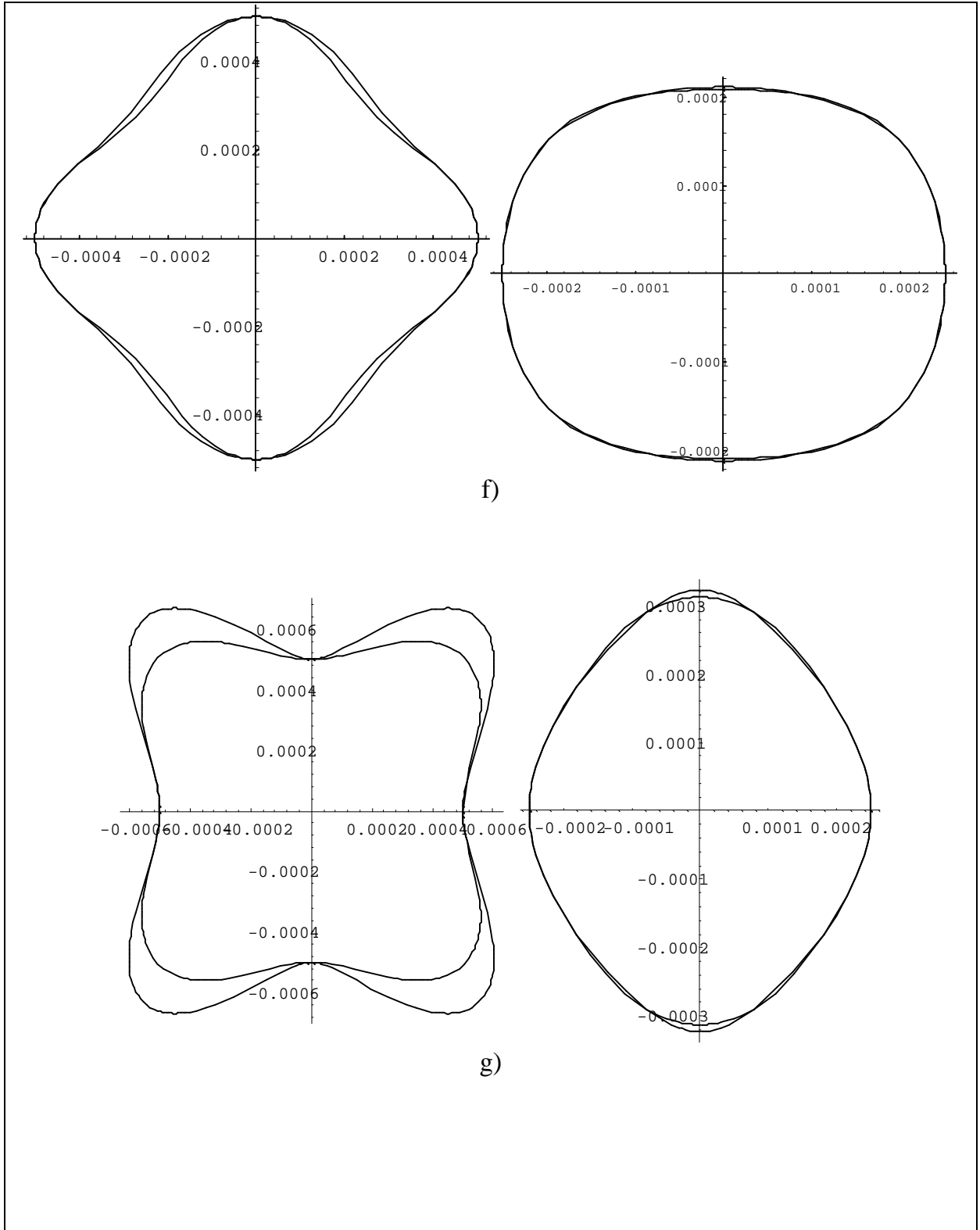
$\delta \setminus \varepsilon$	-0.2	-0.1	0.1	0.2
-0.2	X	a	b	c
-0.1	d	X	e	f
0.1	g	h	X	I
0.2	j	k	l	X

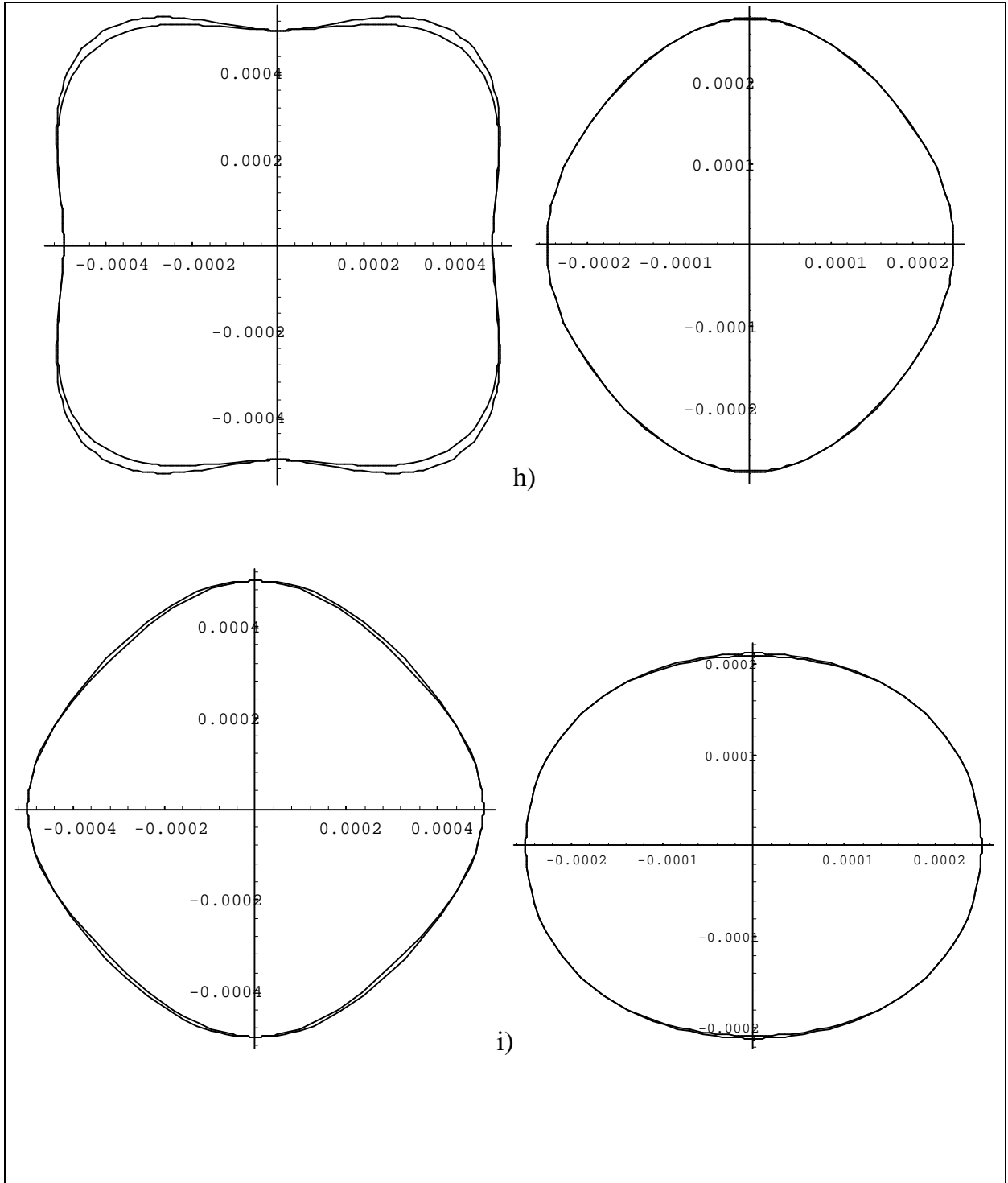
Table A2.1. A selection of anisotropic parameters ε and δ with letters corresponding to plots shown in Figure A2.1.

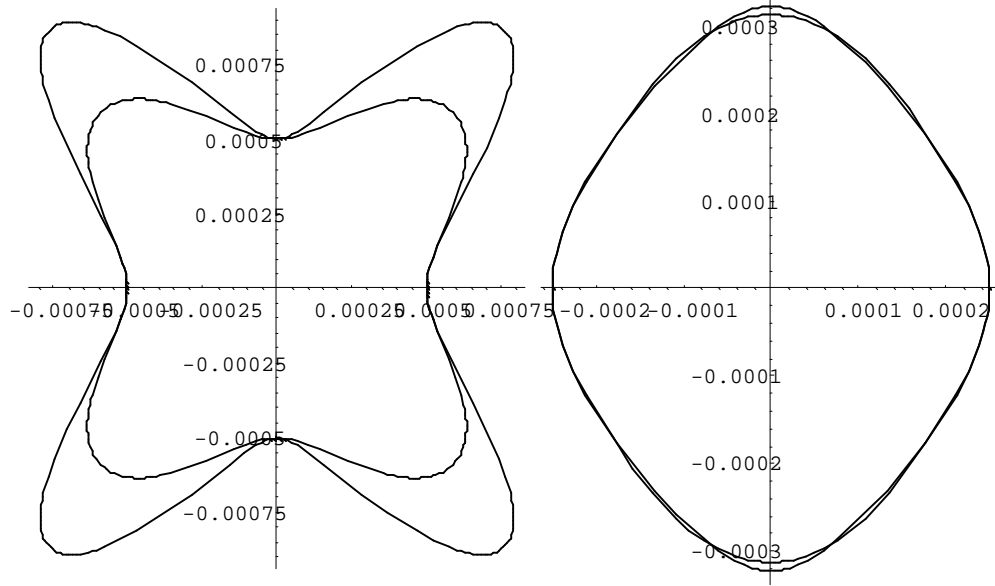




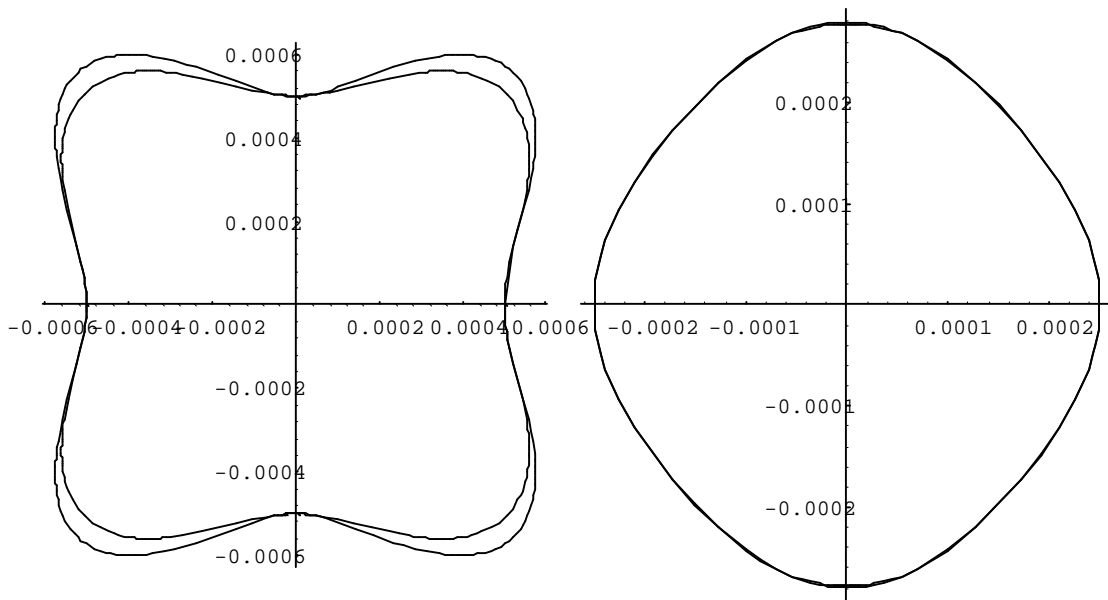




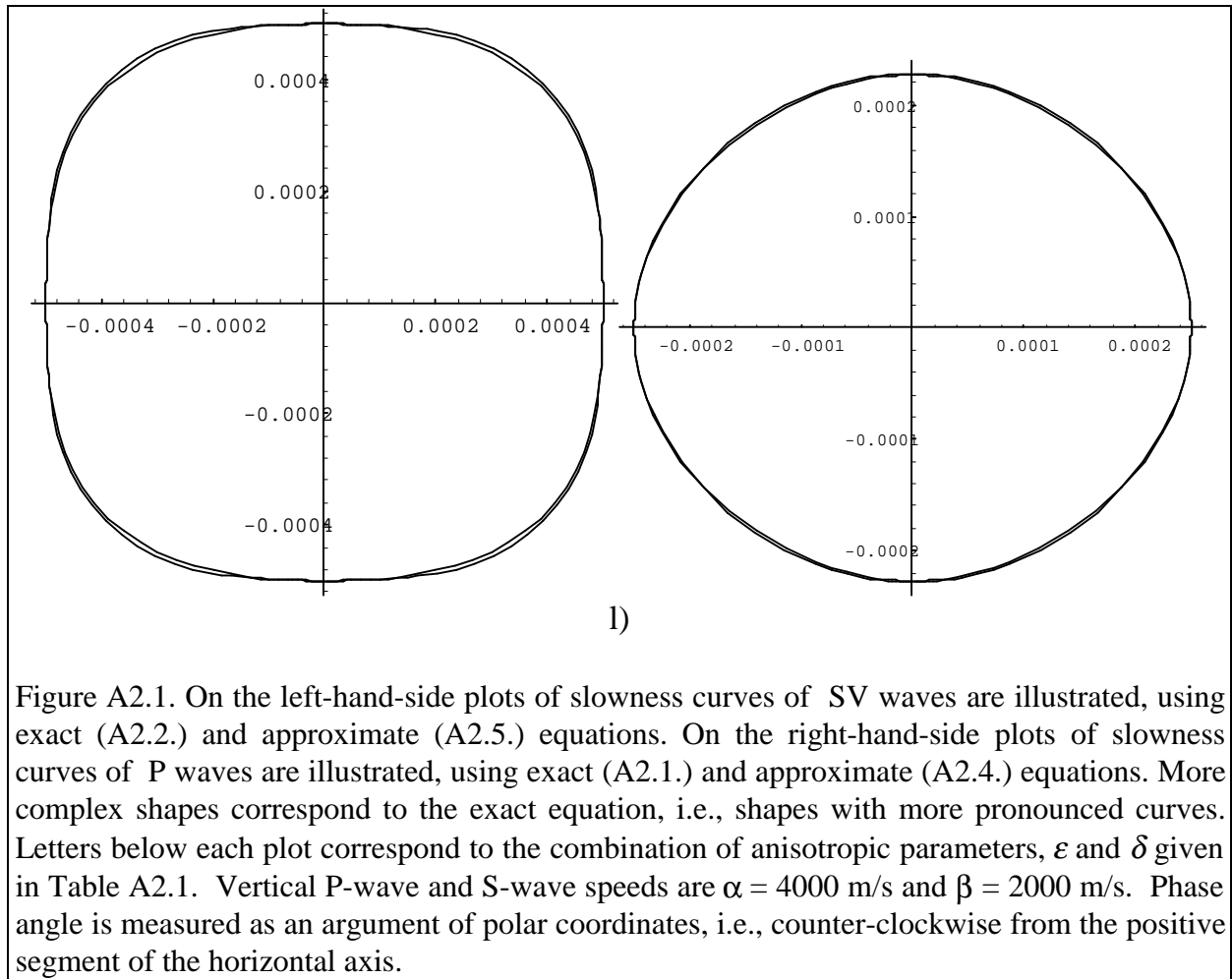




j)



k)



The SV wave exhibits the most complex slowness curve, which, as a result, is the most difficult to approximate. In most cases, however, the fit is quite good and the appearance of the graph is well preserved, i.e., the approximate solution exhibits all principal characteristics of the exact equation. In the case of P and SH waves the correlation between the exact and the approximate equations is very good.

Remaining within the realm of weak anisotropy, containing most observations of geophysical interest, the sacrifice of accuracy is relatively small, particularly in the case of P and SH waves. Using slowness surfaces or curves, derived using the weak-anisotropy equations, while employing exact equations in subsequent steps (e.g., calculation of group velocities or group angles) yields results that are adequate for many purposes (see also Appendix 6). Also, crucial physical attributes

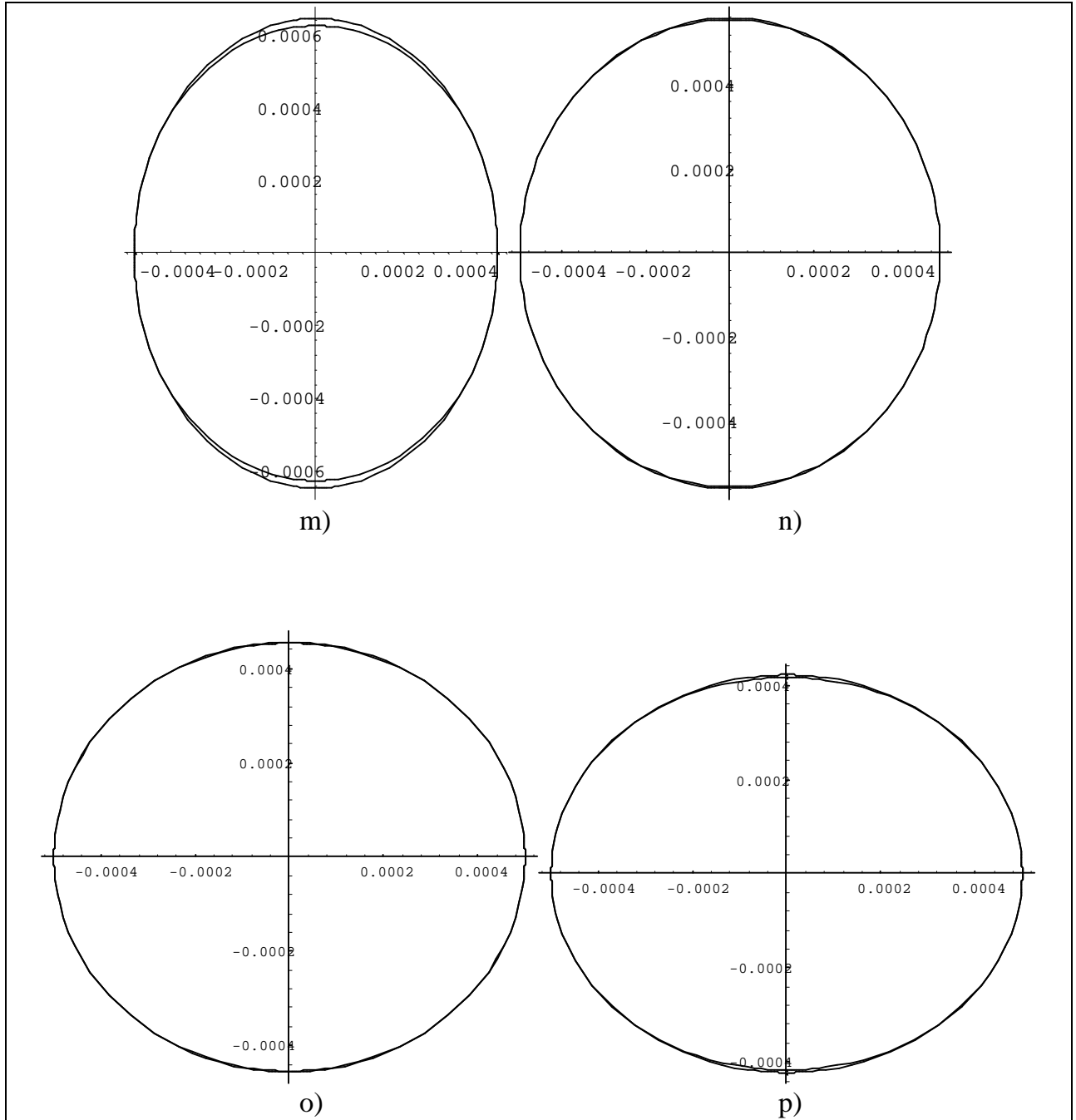


Figure A2.2. Slowness curves of SH waves using exact (A2.3) and approximate (A2.6) equations. Letters below each plot correspond to the given value of the anisotropic parameter, γ : m, -0.2; n, -0.1; o, 0.1; p, 0.2. Vertical SH wave speed is $\beta = 2000$ m/s. Phase angle is measured as an argument of polar coordinates, i.e., counter-clockwise from the positive segment of the horizontal axis.

characteristic of wave propagation in anisotropic media are preserved, thus the educational benefits are considerable, while comparison of slowness surfaces generated

using exact and approximate approaches, as well as the physical laboratory measurements (Chapter VII) suggest that in many instances the approximate method constitutes an adequate practical approach.

It could, perhaps, be argued that initial loss due to the weak-anisotropy approximation, is somewhat compensated by operating, for the most part, on simple analytical expressions, thus avoiding many pitfalls of numerical calculations. This might be particularly true since many calculations involve values differing by many orders of magnitude, e.g., ray parameter (10^{-4}), velocity (10^3) and their powers. Using the symbolic mathematical software Mathematica®, one benefits, in most cases from infinite precision (Wolfram, 1991).

Slowness curves were generated using a plotting routine within the Mathematica® software. The programme is given below.

Mathematica® code for generating exact and approximate (weak anisotropy) slowness curves for P, SV, and SH waves.

```
<<Graphics`Graphics`
A      =      vertical speed of a compressional wave,  $\alpha$ .
B      =      vertical speed of a shear wave,  $\beta$ .
e      =      anisotropic parameter,  $\epsilon$ .
d      =      anisotropic parameter,  $\delta$ .
g      =      anisotropic parameter,  $\gamma$ .

                                Calculation of SV curves
svexact=PolarPlot[1/(
  B*Sqrt[
    1+((A/B)^2)*(e*Sin[p]^2-
      0.5*(1-(B/A)^2)*
      (Sqrt[1+4*(2*d-e)*Sin[p]^2*Cos[p]^2/(1-(B/A)^2)+
        4*(1-(B/A)^2+e)*e*Sin[p]^4/(1-(B/A)^2)^2
        -1)]),
    {p,0,2*Pi}]
svapprox=PolarPlot[1/(B*(1+(A/B)^2*(e-d)*Sin[p]^2*Cos[p]^2)),
  {p,0,2*Pi}]
Show[svexact,svapprox]
```

Calculation of P curves

```

pexact=PolarPlot[1/(
  A*Sqrt[1+e*Sin[p]^2+0.5*(1-(B/A)^2)*
    (Sqrt[1+4*(2*d-e)*Sin[p]^2*Cos[p]^2/(1-(B/A)^2)+
      4*(1-(B/A)^2+e)*e*Sin[p]^4/(1-(B/A)^2)^2]
    -1)),
  {p,0,2*Pi}]
papprox=PolarPlot[1/(
  A*(1+d*Sin[p]^2*Cos[p]^2+e*Sin[p]^4)),
  {p,0,2*Pi}]
Show[pexact,papprox]

```

Calculation of SH curves

```

shexact=PolarPlot[1/(
  B*Sqrt[1+2*g*Sin[p]^2]),
  {p,0,2*Pi}]
shapprox=PolarPlot[1/(
  B*(1+g*Sin[p]^2)),
  {p,0,2*Pi}]
Show[shexact,shapprox]

```

APPENDIX 3

CONCERNS OF NUMERICAL PRECISION

A3.1. INTRODUCTION

It is the intention of this dissertation to achieve analytically as many results as possible. At times, however, it is neither practical nor possible. For instance, the calculation of the take-off angle for raytracing requires an iterative method of solution, for it is impossible to express the take-off angle explicitly in terms of other parameters. All numerical (and most analytical) operations were performed using Mathematica®, a software package allowing both numerical and symbolic calculations. Since as many operations as possible are performed symbolically, it allows one to retain, for those operations, infinite precision (Wolfram, 1991). In general, one expects some errors in cases of truncated series, finite-element solutions, etc. However, it has been demonstrated, that even some closed-form expressions arising in geophysics are not free from the perils of computational errors (Brown, 1988). Thus a geophysicist should be on the alert for such computational problems. Often I have used different approaches, utilizing several algorithms to obtain the same physical quantity. At times the numerical results vary slightly. What follows is an example of applying different approaches in the investigation of a particular case exhibiting numerical errors.

A3.2. OBSERVATION

An SH wave is transmitted across the two-layer medium. The thicknesses are $h_1 = 0.0356$ m and $h_2 = 0.1046$ m, for the upper and lower layers respectively. The upper

layer is isotropic, with an SH-wave speed $v = 1030$ m/s. The lower layer is anisotropic with a vertical speed $\beta = 1606$ m/s, and the anisotropic parameter $\gamma = 0.096$.

Three methods are used to calculate the traveltimes, t , and the take-off angle, θ_i , for a horizontal distance between the source and receiver, $X = 0.1$ m. The first method uses the anisotropic formalism of Snell's law developed in Chapter II and in Chapter III. The second and third methods use the approach based on Fermat's principle of stationary time described in Chapter IV.

The first method, utilizing the anisotropic formalism of Snell's law, is based on calculating the ray parameter corresponding to the desired source-receiver configuration. The traveltimes are computed using expressions for group velocities in weakly anisotropic media. The results obtained are $t = 0.000118309$ s, and $\theta_i = 20.70067866^\circ$.

Both the second and third methods, utilize Fermat's principle of stationary time. The methods seek to minimize the traveltimes between source and receiver. The travel path and trigonometric functions are expressed in terms of a distance, r , between the refraction point and the receiver. In the second case, the derivative dt/dr is set to zero, the value of r is found, and hence propagation angles and then traveltimes, t , are calculated. The results obtained are $t = 0.000118309$ s, and $\theta_i = 20.52767868^\circ$.

The third method finds directly the minimum of the traveltimes function using the Mathematica® command "FindMinimum". The results obtained are $t = 0.000118314$ s, and $\theta_i = 19.67525212^\circ$.

A3.3. FURTHER INVESTIGATION

The discrepancies illustrated above prompted further investigation. For this purpose three analogous methods were used to calculate the take-off angle and traveltimes in a purely isotropic medium. The assumption of perfect isotropy facilitates various comparisons. All parameters of the medium are the same as the ones shown above, except the anisotropic parameter, γ , is identically zero.

A3.3.1. Calculation using ray parameter, p .

$$X = \sum_{j=1}^n \frac{h_j v_j p}{\sqrt{1 - p^2 v_j^2}} \Rightarrow \frac{36.668p}{\sqrt{1 - 1,060,900p^2}} + \frac{167.9876p}{\sqrt{1 - 2,579,236p^2}} = 0.1$$

The Mathematica® code and result are given below:

```
FindRoot[36.668*p/Sqrt[1-1060900*p^2]+
167.9876*p/Sqrt[1-2579236*p^2]==0.1,
{p,{0.0005,0.001}}]
{p -> 0.000390847 + 1.3171 10-10 I}
```

Ignoring a very small imaginary part yields a take-off angle of 23.73909105° , and transmission angle of 38.88065658° . Of course, the same transmission angle is obtained using Snell's law. Knowing layer thicknesses one can calculate the resulting offset, $X = 0.099999555$ m, giving an error of about 0.000445%. One can also calculate the traveltime to be $t = 0.000121425$ s.

A3.3.2. Calculation using the traveltime function, t

$$t(r) = \frac{\sqrt{(X-r)^2 + h_1^2}}{v} + \frac{\sqrt{r^2 + h_2^2}}{\beta} = \frac{\sqrt{(0.1-r)^2 + 0.00126736}}{1030} + \frac{\sqrt{r^2 + 0.01094116}}{1606}$$

Method A

This method consists of setting $dt/dr = 0$, and solving for r . The Mathematica® code and result are given below:

```
D[Sqrt[(0.1-r)^2+0.00126737]/1030+
Sqrt[r^2+0.01094116]/1606,r]
FindRoot[%,{r,{0.01,0.099}}]
{r -> 0.0843436}
```

Using the value of r , one obtains a take-off angle equal to 23.73924596° and a transmission angle of 38.88076608° . Using the given velocities, the take-off angle and Snell's law, one obtains the transmission angle of 38.88094059° , which leads to $X = 0.100000526$ m, i.e., an error of about 0.000525700%. One can also calculate the traveltime as $t = 0.000121425$ s; t is the same, within the number of digits displayed, regardless of the method used for obtaining the angle of transmission.

Method B

This method consists of finding directly the value of r , for which the traveltime, $t(r)$, is minimum. The Mathematica® code and result are given below:

```
FindMinimum[Sqrt[(0.1-r)^2+0.00126737]/1030+
  Sqrt[r^2+0.01094116]/1606,
  {r,{0.01,0.099}}]
{0.000121425, {r -> 0.0842846}}
```

Using the value of r , one obtains a take-off angle equal to 23.81876456° . and a transmission angle of 38.86117634° . Calculating the path in each layer and adding yields a traveltimes value computed by the programme to be $t = 0.000121425$ s. This result, however, is not entirely consistent with Snell's law. Using the given velocities and the take-off angle one obtains a transmission angle of 39.02684347° , which leads to $X = 0.100499982$ m, i.e., within an error of about 0.4999821%, a couple of orders of magnitude larger than for the other two methods.

A3.4. CONCLUSIONS

For an isotropic case, all three algorithms yield the same value of traveltime, $t = 0.000121425$, within the number of digits displayed by the output. Similarly, in the anisotropic case, the values of traveltime were very close to each other, $t = \{0.000118309$ s, 0.000118309 s, 0.000118314 s}. As a matter of fact, the only discrepancy results from the third method, i.e., the algorithm of Mathematica® which calculates directly the minimum of a traveltime function. If the only purpose of the computational study is the traveltime calculation, for instance, a comparison between isotropic and anisotropic

calculation of traveltimes, any of the three approaches could be used in either case. Particularly for comparison with experimental results, they all yield adequate theoretical prediction.

For an isotropic case the values of the take-off angle are $\theta_i = \{23.73909105^\circ, 23.73924596^\circ, 23.81876456^\circ\}$, again, the largest discrepancy appearing when using the third method. Similarly, in the anisotropic case, the values of the take-off angles are $\theta_i = \{20.70067866^\circ, 20.52767868^\circ, 19.67525212^\circ\}$, the largest discrepancy appearing when using the third method. Thus, if one desires to calculate the raypath, it is preferable to avoid the “FindMinimum” command, which leads to the largest discrepancies, both within itself when considering Snell’s law, and with respect to the other two methods. In the dissertation, this command, although very convenient, was avoided altogether.

A3.5. FINAL REMARKS

Throughout the entire study, whenever possible, numerical errors were investigated. For example, if both forward and inverse algorithms were available, a careful comparison of results was performed. The high accuracy of inversion of synthetic results for the values of anisotropic parameter (see Chapter VIII), indicates that the use of numerical algorithms has been successful.

APPENDIX 4

PROOF THAT $d\gamma/dr = 0$ FOR THE ACTUAL γ ²¹

Suppose there exists a function of three variables, T , r , and γ :

$$F(T, r, \gamma) = t(r, \gamma) - T, \quad (\text{A4.1})$$

for which all first derivatives exist in an open set D , $D \subset \mathfrak{R}^3$ (this is expected to hold true in all cases of physical interest); suppose further that there exists a point $P(T_0, r_0, \gamma_0)$, $P \in D$, such that $F(P) = 0$, i.e., $t(r_0, \gamma_0) = T_0$, and that $\partial t / \partial \gamma \neq 0$ at P . Then by the implicit function theorem (e.g., Olmsted, 1961), there exists a function $g(T, r)$ possessing all first derivatives, that satisfies the equation:

$$F(T, r, g(T, r)) = t(r, g(T, r)) - T = 0, \quad (\text{A4.2})$$

in an open neighbourhood $N \subset \mathfrak{R}^2$ of $(T_0, r_0) \in \mathfrak{R}^2$, such that $g(T_0, r_0) = \gamma_0$.

Geometrically, note that $F(T, r, \gamma) = 0$ implicitly defines a 2-D surface in \mathfrak{R}^3 . Now, consider a curve on this surface defined by its intersection with the surface $T = T_0$. The implicit form of the equation of this curve, with r as the parameter, is:

$$F(T_0, r, g(T_0, r)) = t(r, g(T_0, r)) - T_0 = 0 \quad (\text{A4.3})$$

²¹ Raphaël A. Slawinski (pers. comm., 1995)

Differentiating equation (A4.3) with respect to r gives:

$$\frac{dF}{dr} = \frac{d[t(r, g(T_0, r)) - T_0]}{dr} = \frac{\partial t}{\partial r} + \frac{\partial t}{\partial g} \frac{d[g(T_0, r)]}{dr}. \quad (\text{A4.4})$$

Equation (A4.4) is satisfied everywhere along the curve.

Now consider the point defined by the intersection of the above curve with the surface implicitly defined by the equation $\partial t(r, \gamma)/\partial r = 0$. Then, at this point, the following equation holds:

$$\frac{\partial t}{\partial g} \frac{dg(T_0, r)}{dr} = 0. \quad (\text{A4.5})$$

Assume $\partial t/\partial g = \partial t/\partial \gamma \neq 0$; then:

$$\frac{dg(T_0, r)}{dr} = 0. \quad (\text{A4.6})$$

Hence, at the point defined by the intersection of the surfaces:

$$\begin{cases} t(r, \gamma) = T \\ \frac{\partial t}{\partial r} = 0 \\ t(r, \gamma) = T_0 \end{cases} \quad (\text{A4.7})$$

corresponding to ray traveltime for specific r and γ , Fermat's principle of stationary time, and a particular (measured) time, respectively, the following equation holds:

$$\frac{dg(T_0, r)}{dr} = 0, \tag{A4.8}$$

where the function $g(T, r)$ is obtained by solving $F(T, r, \gamma) = 0$ for γ .

APPENDIX **5****AN APPROXIMATE METHOD FOR CALCULATING
ANISOTROPIC PARAMETERS FROM P-WAVE
TRAVELTIMES****A5.1. INTRODUCTION**

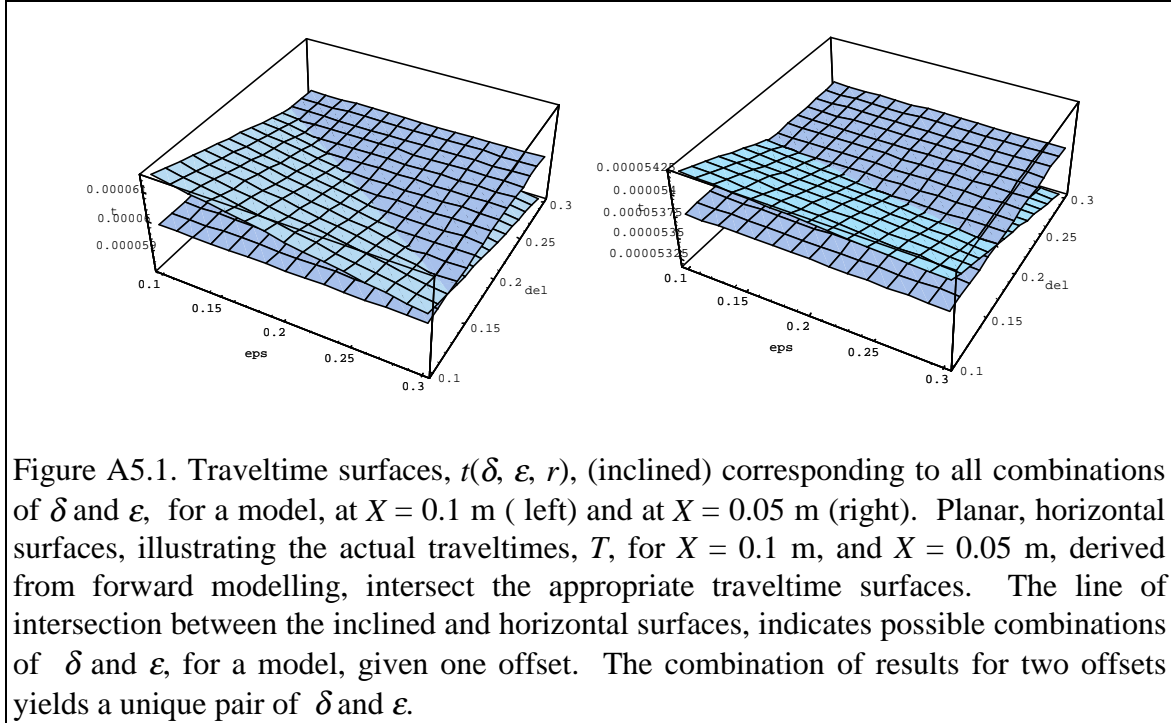
The group speed, and hence the traveltime, of a P wave in an anisotropic medium depend on the direction of propagation. To determine the speed, for a given propagation direction, one requires, the value of anisotropic parameters, δ and ε . The method below provides a method for obtaining approximate values of δ and ε of a buried layer by performing the traveltime measurements on the surface. The method requires the traveltime information acquired with two different recording geometries. The method is analogous to the inversion presented in Chapter VIII and as such possesses all its characteristics, including extreme sensitivity to errors in input parameters. Consequently, the applicability of an approximate method for calculating anisotropic parameters from P wave (or SV wave) traveltimes is limited to numerical examples. It is included here for educational interest.

A5.2. OBSERVATION ON THE FORWARD MODEL

The travelttime of a P wave travelling in a model depicted in Figure (4.1), can be written in terms of the dimensions of the model, group speeds dependent on anisotropic parameters δ , ε and a variable, r , denoting the distance between the receiver and the refraction point, chosen in such a way as to satisfy Fermat's principle of stationary time, i.e.:

$$\left\{ \begin{array}{l} \frac{\sqrt{(X-r)^2 + H_1^2}}{V} + \frac{\sqrt{r^2 + H_2^2}}{\alpha \left(1 + \delta \frac{r^2 H_2^2}{r^2 + H_2^2} + \varepsilon \frac{r^4}{(r^2 + H_2^2)^2} \right)} = t(r; \delta, \varepsilon) \\ \frac{dt(r; \delta, \varepsilon)}{dr} = 0 \end{array} \right. \quad (\text{A5.1})$$

By forward modelling, i.e., raytracing through the model, between the given source and receiver, assuming knowledge of all parameters, one can calculate both travelttime t , and the distance, r , intimately related to the take-off angle. A 3-D surface representing travelttime on the vertical axis, spanning δ and ε , as the horizontal axes, can be generated. The value of r used to generate the surface, is the value satisfying Fermat's principle of stationary time, obtained from forward modelling. The surface, describing all possible travelttime values for δ and ε combinations displayed on horizontal axes, can be intersected by the plane at $t(\delta, \varepsilon; r) = T$, i.e., the travelttime calculated from the forward model.



The δ - and ε -coordinates of the curve, corresponding to the intersection between the surface and the plane, are the possible pairs of anisotropic parameters satisfying the solution of the traveltime equation at $t(\delta, \varepsilon; r) = T$. It is impossible, from measurement at a single source-receiver configuration to obtain a unique (δ, ε) pair. Another measurement, however, at a different offset, provides analogous illustration with a different intersection curve. It is the intersection of two curves which yields a unique pair of values of δ and ε .

A5.3. STRATEGY FOR AN INVERSE CALCULATION

In the inverse case, one does not know the values of anisotropic parameters or the value of r . An approximate solution, however, can be obtained.

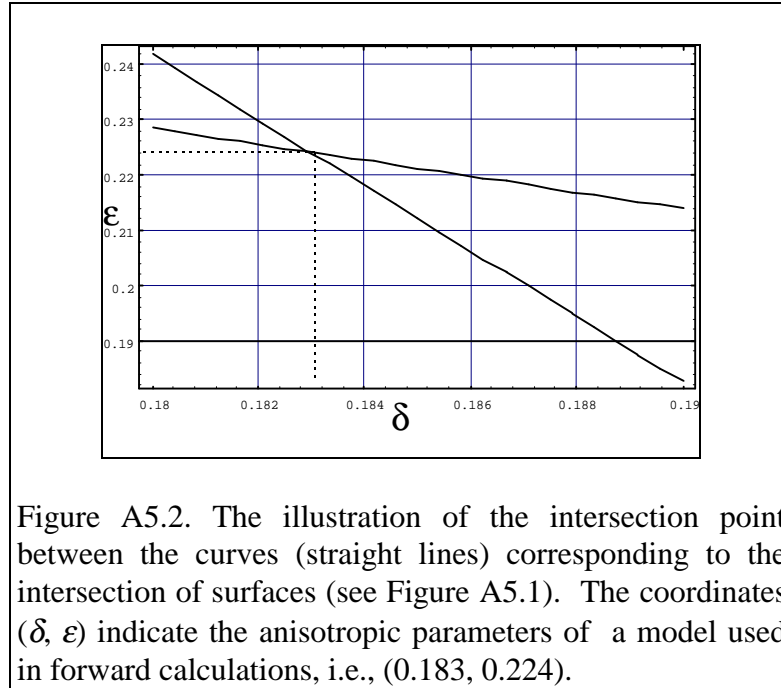


Figure A5.2. The illustration of the intersection point between the curves (straight lines) corresponding to the intersection of surfaces (see Figure A5.1). The coordinates (δ, ϵ) indicate the anisotropic parameters of a model used in forward calculations, i.e., (0.183, 0.224).

The initial guess consists of estimating the value of r . In weak anisotropy the raypath of a ray calculated using the anisotropic approach is not radically different from the raypath of a ray calculated using the isotropic approach, in which one assumes the isotropic speed to be equal to the vertical speed. The position of refraction point, r , moves along the interface to satisfy Fermat's principle of stationary time. If, as in the case in the considered model, the upper layer is isotropic, the point r moves towards the receiver, from its isotropic equivalent, if the anisotropic speed in the medium of transmission decreases with angle of propagation. The point r moves away from the receiver, from its isotropic equivalent, if the anisotropic speed in the medium of transmission increases with angle of propagation .

A5.4. ALGEBRAIC FORMULATION

For a set value of T corresponding to a value of r , satisfying Fermat's principle, the expressions for δ and ϵ are linear. Considering two measurement points, A and B , of traveltime of compressional waves, the expressions for δ and ϵ can be written a set of

two linearly independent equations in which all values except for the isotropic parameters are assumed to be known or estimated:

$$\begin{bmatrix} \frac{r_A^2 H_2^2}{r_A^2 + H_2^2} & \frac{r_A^4}{(r_A^2 + H_2^2)^2} \\ \frac{r_B^2 H_2^2}{r_B^2 + H_2^2} & \frac{r_B^4}{(r_B^2 + H_2^2)^2} \end{bmatrix} \begin{bmatrix} \delta \\ \varepsilon \end{bmatrix} = \begin{bmatrix} \frac{V \sqrt{r_A^2 + H_2^2}}{\alpha \left(T_A V - \sqrt{(X_A - r_A)^2 + H_1^2} \right)} \\ \frac{V \sqrt{r_B^2 + H_2^2}}{\alpha \left(T_B V - \sqrt{(X_B - r_B)^2 + H_1^2} \right)} \end{bmatrix} \quad (\text{A5.2})$$

Note that the group speed of an SV wave depends on the same anisotropic parameters as the group speed of P waves. Thus, an analogous process performed using SV waves provides an independent verification. Furthermore, if only a single source-receiver configuration is available, the traveltimes of P and SV waves provide the two necessary independent equations, which yield a unique pair of values (δ, ε) .

APPENDIX 6

DEGREES OF APPROXIMATION**A6.1. INTRODUCTION**

This appendix discusses the results of raytracing through an anisotropic medium obtained with several different methods. The discussed methods use different degrees of approximation.

The first (*exact*) method starts with an exact formulation for phase velocity (Thomsen, 1986). Also, all subsequent relations (e.g., group angle, group velocity) are derived using exact formulæ.

The second (*approximate*) method uses an approximate formulation for phase velocity based on the weak-anisotropy assumption (Thomsen, 1986). However, all subsequent relations are derived using exact formulæ.

The third (*linearized*) method uses an approximate formulation for phase velocity based on the weak-anisotropy assumption (Thomsen, 1986). Moreover, many subsequent relations are derived using simplified formulæ.

All results correspond explicitly to the SH-wave case, but the concepts and principle conclusions can be, with due care, extended to SV- and P-wave cases. In particular, this appendix concentrates on the travelttime and the ray trajectory obtained using three aforementioned methods. All results are compared to the method that ignores anisotropic phenomena.

A6.2. EXACT METHOD

The group velocity, V , is obtained from the exact formula relating group and phase velocity, v , as a function of the phase angle, ϑ :

$$V^2[\theta(\vartheta)] = v^2(\vartheta) + \left(\frac{dv(\vartheta)}{d\vartheta} \right)^2, \quad (\text{A6.1})$$

where ϑ is a phase angle measure with respect to the vertical.

The exact equation for phase velocity is given by Thomsen (1986), and it represents an equation of an ellipse in polar coordinates expressed as a function of the phase angle, ϑ , vertical wave speed, β , and the anisotropic parameter, $\tilde{\gamma}$. The tilde placed above the symbol denotes the anisotropic parameter in the exact equation (A6.2) as opposed to the anisotropic parameter used in the weak-anisotropy approximation (equation (3.30)). Specific reasons for this distinction are discussed in section A6.3. Thus,

$$v^2(\vartheta) = \beta^2 [1 + 2\tilde{\gamma} \sin^2 \vartheta]. \quad (\text{A6.2})$$

The derivative, with respect to the phase angle is given by:

$$\frac{dv}{d\vartheta} = \beta \frac{\tilde{\gamma} \sin(2\vartheta)}{\sqrt{1 + 2\tilde{\gamma} \sin^2 \vartheta}}. \quad (\text{A6.3})$$

Thus, the group velocity in terms of phase velocity may be expressed as:

$$V[\theta(\vartheta)] = \beta \sqrt{1 + 2\tilde{\gamma} \sin^2 \vartheta + \frac{[\tilde{\gamma} \sin(2\vartheta)]^2}{1 + 2\tilde{\gamma} \sin^2 \vartheta}}. \quad (\text{A6.4})$$

Note that the value of group velocity, V , could also be determined directly from the elliptical geometry using the method presented in Chapter II. Here, however, the above method was used.

To determine the phase angle, ϑ , one can start with an expression for the radius, r , of the phase-slowness surface:

$$r(\xi) = \frac{1}{\beta\sqrt{1+2\tilde{\gamma}\cos^2\xi}}, \quad (\text{A6.5})$$

where ξ is a phase angle measured from the horizontal, i.e.,

$$\vartheta = \frac{\pi}{2} - \xi. \quad (\text{A6.6})$$

The horizontal component of the slowness surface, x_0 , equivalent to the ray parameter is:

$$x_0 = r \cos \xi = \frac{\cos \xi}{\beta\sqrt{1+2\tilde{\gamma}\cos^2\xi}}. \quad (\text{A6.7})$$

Equation (A6.7) can be solved uniquely for ξ to give:

$$\xi = \text{Arc cos} \frac{x_0\beta}{\sqrt{1-2x_0^2\beta^2\tilde{\gamma}}}. \quad (\text{A6.8})$$

Note that in contrast to the derivation in the case of weak anisotropy (equations (3.38) - (3.41)), in the above derivation, there is only one mathematical solution corresponding to the physical case. Also, in the case of perfect isotropy, $\tilde{\gamma} = 0$, equation (A6.8) reduces immediately to the familiar isotropic expression without requiring the application of limits (recall that de l'Hôpital's rule had to be used in equation (3.43)).

A6.3. ANISOTROPIC PARAMETER AS γ AND $\tilde{\gamma}$

Note that one can set $\xi = 0$, in equation (3.30) and by solving for γ arrive at equation (3.31). Equivalently, if one sets $\vartheta = \pi/2$ in equation A6.2. one obtains:

$$\tilde{\gamma} = \frac{1}{2} \left[\frac{v^2 \left(\frac{\pi}{2} \right) - \beta^2}{\beta^2} \right]. \quad (\text{A6.9})$$

By comparing expressions for $\tilde{\gamma}$ and γ , given by equations (A6.9) and (3.31) one can see that:

$$\tilde{\gamma} = \gamma + \frac{\gamma^2}{2}. \quad (\text{A6.10})$$

Considering the elliptical case described by Cartesian coordinates (Chapter II), one can use, without loss of generality or accuracy, the definition of γ used throughout the thesis, since it only serves to define the major and minor axes. Furthermore, the relationship between $\tilde{\gamma}$ and γ falls-out naturally from following the elliptical geometry²². Following the form of equation (2.16), yields:

$$[\beta(\gamma + 1)x]^2 + [\beta z]^2 = 1. \quad (\text{A6.11})$$

For a given $x = x_0$, one can express the corresponding $z = z_0$, and hence calculate the phase angle, ξ , as an inverse trigonometric function:

²² One can view the anisotropic parameter as a fixed quantity regardless of the approach taken. In this appendix the definition was adjusted so as to yield a perfect equivalence, i.e., equation of an ellipse, through both Cartesian and polar coordinates.

$$\xi = \text{Arc cos} \left\{ \frac{x_0}{r} \right\} = \text{Arc cos} \left\{ \frac{x_0}{\sqrt{x_0^2 + z_0^2}} \right\} = \text{Arc cos} \left\{ \frac{x_0 \beta}{\sqrt{1 - 2x_0^2 \beta^2 \left(\gamma + \frac{\gamma^2}{2} \right)}} \right\}.$$

(A6.12)

Note that equation (A6.8) and equation (A6.12) differ by the term $\tilde{\gamma}^2/2$, as expected from equation (A6.10). This is a natural consequence of the difference in definitions $\tilde{\gamma}$ and γ , described above.

A6.4. APPROXIMATE METHOD (WEAK ANISOTROPY)

The approximate method uses Thomsen's (1986) equation for phase velocity resulting from developing expression (A6.2) into a Taylor series, and truncating higher-order terms under the assumption of weak anisotropy, i.e., small γ . Thus:

$$v(\vartheta) \cong \beta [1 + \gamma \sin^2 \vartheta + \dots]. \quad (\text{A6.13})$$

Equation (A6.13) is used in deriving Snell's law, i.e., it serves as the basis for constructing the slowness curve, to which the ray is normal at a point corresponding to the ray parameter (Chapters II and III). The derivative with respect to the phase angle is given as:

$$\frac{dv}{d\vartheta} \cong \beta \gamma \sin(2\vartheta). \quad (\text{A6.14})$$

Thus the group velocity in terms of phase velocity is given as:

$$V[\theta(\vartheta)] \cong \beta \sqrt{(1 + \gamma \sin^2 \vartheta)^2 + [\gamma \sin(2\vartheta)]^2}. \quad (\text{A6.15})$$

The value of the phase angle, ϑ , (measured from the vertical, i.e., phase colatitude) is found from:

$$\vartheta = \frac{\pi}{2} - \xi, \quad (\text{A6.16})$$

where the phase angle, ξ , (measured from the horizontal, i.e., phase latitude) is given by:

$$\xi \equiv \text{Arc cos} \left\{ \frac{1 - \sqrt{1 - (2x_0\beta_0)^2 \gamma}}{2x_0\beta_0\gamma} \right\}. \quad (\text{A6.17})$$

The method of calculating the phase angle, ξ , is demonstrated in Chapter III (equations (3.38) - (3.41)).

A6.5. LINEARIZED METHOD (WEAK ANISOTROPY WITH FURTHER SIMPLIFICATION)

Thomsen (1986) derives, based on the weak-anisotropy formulæ, further simplified expressions. For instance, the expressions for phase and group velocity are the same. One can write:

$$V(\theta) \approx v(\vartheta). \quad (\text{A6.18})$$

Other simplifications imply, for instance, that the relationship between the phase and group angles (ϑ and θ , respectively), rather than being expressed through the vector-

calculus formalism as described in Chapters II and III, can be expressed for SH waves as²³:

$$\tan \theta \approx (1 + 2\gamma) \tan \vartheta . \quad (\text{A6.19})$$

The linearized method, as already stated, goes beyond the simplification resulting directly from the assumption of weak anisotropy (approximate method). Consequently, as demonstrated below, results obtained by the linearized approach depart more from the exact results than the results obtained through the approximate method.

A6.6. NUMERICAL EXAMPLE

Consider a horizontal two-layer model with layer thickness of 1000 metres each. The upper layer is isotropic with wave speed $V_1 = 3000$ m/s, and the vertical speed in the lower, anisotropic layer is $\beta = 4000$ m/s. Assume the anisotropic parameter to be $\gamma = 0.1$. The several traveltimes values are displayed in Table A6.1.

OFFSET (m)	TIME (s) EXACT	TIME (s) APPROX.	TIME (s) LINEARIZED	TIME (s) ISOTROPIC
0	0.583333	0.583333	0.583333	0.583333
250	0.587304	0.587324	0.587228	0.587779
500	0.599034	0.599109	0.598758	0.600903
1000	0.643508	0.643744	0.642716	0.650531
2000	0.793277	0.793717	0.792035	0.816813
3000	0.985823	0.986253	0.984727	1.02992

Table A6.1. Traveltimes values for $\gamma = 0.1$ using the exact, approximate, linearized and isotropic methods.

Now, keeping other parameters of the model constant let $\gamma = 0.2$.

²³ The linearized relationship between phase and group angles for SV waves in Thomsen's (1986) development, yields completely erroneous results for a choice of anisotropic parameters consistent with the weak-anisotropy assumption (see Figure 6.12). The exact relationship from the aforementioned publication leads to correct results.

OFFSET (m)	TIME (s) EXACT	TIME (s) APPROX.	TIME (s) LINEARIZED	TIME (s) ISOTROPIC
0	0.583333	0.583333	0.583333	0.583333
250	0.586888	0.586953	0.586587	0.587779
500	0.597396	0.597642	0.596318	0.600903
1000	0.637332	0.638128	0.634374	0.650531
2000	0.772539	0.774154	0.768223	0.816813
3000	0.947246	0.948926	0.943529	1.02992

Table A6.2. Traveltime values for $\gamma = 0.2$ using the exact, approximate, linearized and isotropic methods.

The values of Table A6.2 are plotted in Figure A.6.1. One can see that all the curves corresponding to the different anisotropic methods are positioned very close to each other. The curve corresponding to the isotropic approach is clearly more removed. To visualize the differences between the anisotropic approaches the values of Table A6.2. were replotted as a difference between the given value and the value obtained from exact calculation, normalized to the value of exact calculation (Figure A6.2). It shows that the approximate method based on the weak anisotropy assumption yields more accurate results than the fully linearized method. Again, it is clearly shown that the isotropic approach leads to the least accurate results.

It seems that in the context of geophysics, both approximate and linearized methods provide a reasonable accuracy for traveltime calculations, while offering a considerable facility of mathematical manipulation. The superiority of the approximate method over the linearized method appears twofold. Firstly, the computational results are slightly more accurate (e.g., see Figure A6.2). Secondly, and perhaps more importantly, the approximate method yields distinct phase and group velocities and angles, i.e., it clearly illustrates one of the fundamental concepts in anisotropic wave propagation (see Figure A6.3 and Table A.6.4). In the process of linearization this physical distinction is lost.

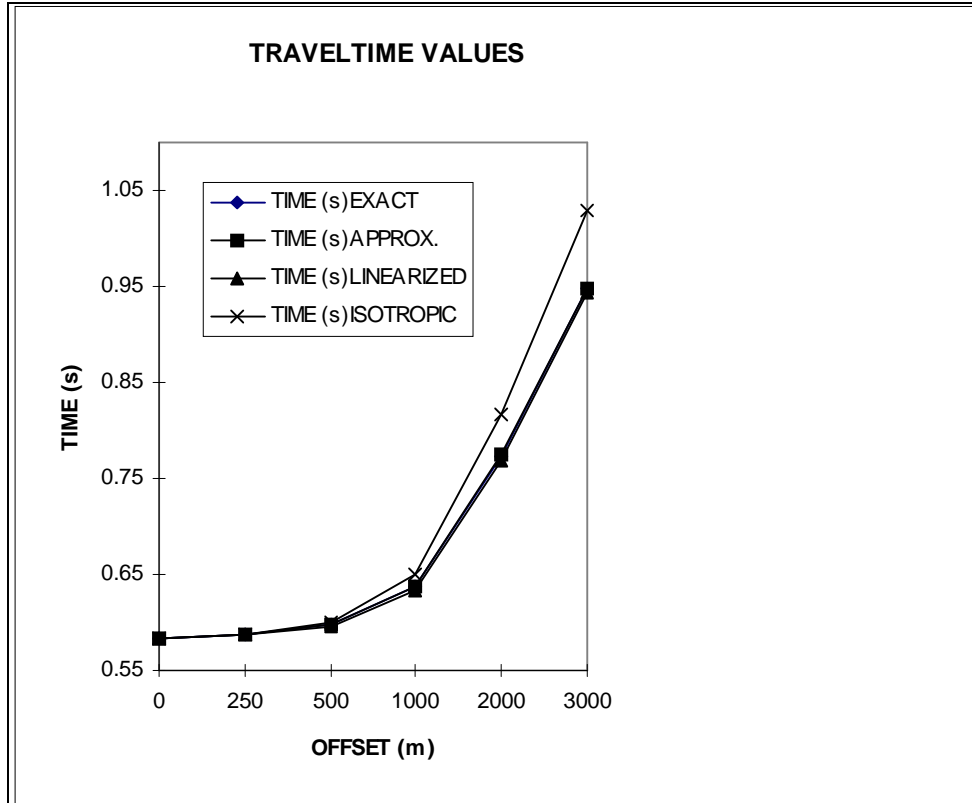
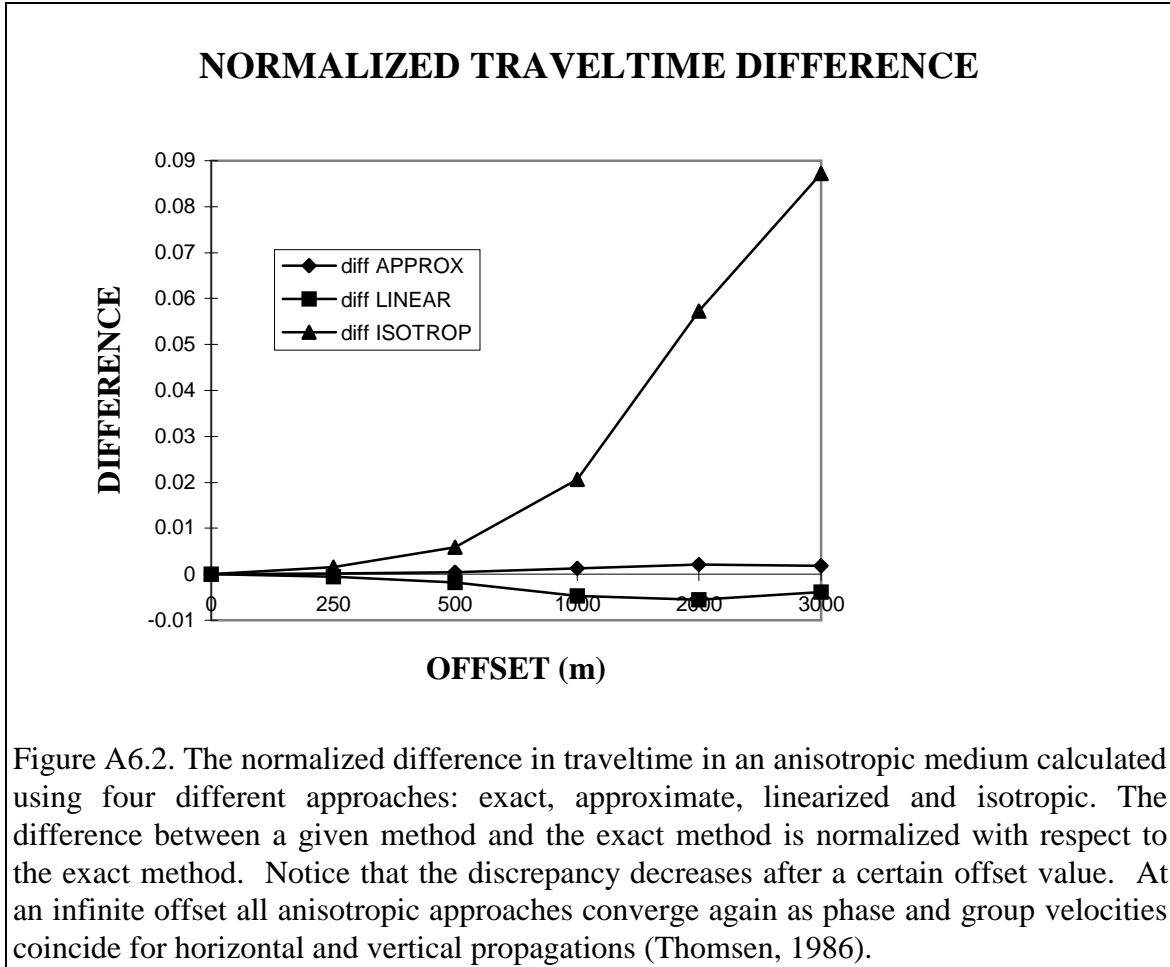


Figure A6.1. The traveltime of SH waves between the source and receivers calculated using four different approaches: exact, approximate, linearized and isotropic. The value of anisotropic parameter is $\gamma = 0.2$.

Now, keeping other parameters of the model constant let $\gamma = 0.3$.

OFFSET (m)	TIME (s) EXACT	TIME (s) APPROX.	TIME (s) LINEARIZED	TIME (s) ISOTROPIC
0	0.583333	0.583333	0.583333	0.583333
250	0.586524	0.586645	0.585861	0.587779
500	0.595964	0.596423	0.593624	0.600903
1000	0.631922	0.633442	0.625765	0.650531
2000	0.754373	0.757675	0.745875	0.816813
3000	0.913615	0.917287	0.906406	1.02992

Table A6.3. Traveltime values for $\gamma = 0.3$ using the exact, approximate, linearized and isotropic methods.



Note that the case of $\gamma = 0.3$ may be viewed as being outside the accepted domain of applicability under the weak anisotropy assumption. In spite of that fact, all methods behave very well, and certainly any method including the anisotropic phenomena yields a more accurate result than the isotropic approach.

A6.7. GEOMETRICAL EXPLANATION

A further insight is gained by the investigation of ray and phase angle. For the purpose of illustration a case of $\gamma = 0.3$, and offset of 3000 metres is used. The ray vector, \mathbf{w} , and lines of constant phase with phase vector, \mathbf{v} , are illustrated in Figure A6.3

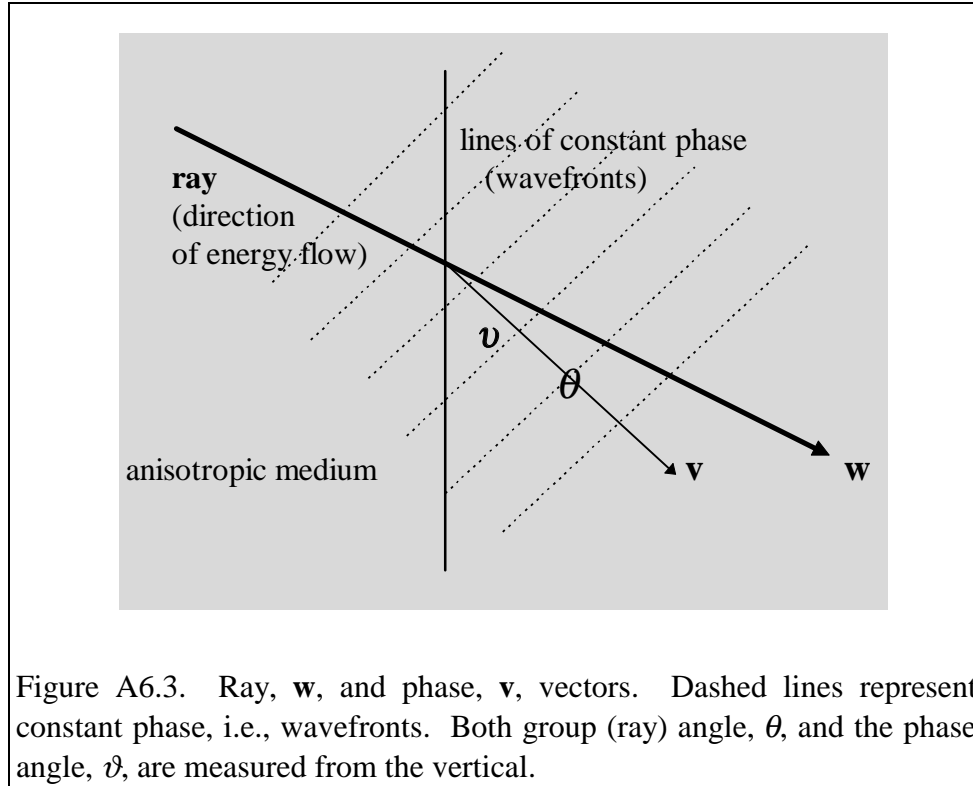


Figure A6.3. Ray, \mathbf{w} , and phase, \mathbf{v} , vectors. Dashed lines represent constant phase, i.e., wavefronts. Both group (ray) angle, θ , and the phase angle, ϑ , are measured from the vertical.

Table A6.4. gives the values of phase, ϑ , and group angles, θ , as well as the phase, $|\mathbf{v}|$ and group (ray, energy), $|\mathbf{w}|$, speeds, calculated with appropriate formulae. The magnitude of phase velocity, $|\mathbf{v}|$, is obtained, for each case, from the appropriate equation for phase velocity given the corresponding phase angle. Note that for the linearized scheme phase, ϑ , and group, θ , angles are equal for all angles of propagation, a physically unsatisfactory description, but computationally yielding good results. Also, phase, $|\mathbf{v}|$, and group, $|\mathbf{w}|$, speeds are equal. Recall that for body waves in anisotropic media, the phase speed, $|\mathbf{v}|$, is always smaller than the group speed, $|\mathbf{w}|$ as seen from (e.g., Auld, 1972):

$$|\mathbf{v}| = |\mathbf{w}| \cos(\theta - \vartheta). \quad (\text{A6.20})$$

Results of exact and approximate methods shown in Table A6.4. are consistent with equation (A6.20).

	EXACT	APPROX.	LINEARIZED	ISOTROPIC
θ ; [deg]	67.4692181	67.4732288	67.3520912	64.3492525
ϑ ; [deg]	54.9664383	54.0742285	67.3520912	64.3492525
$ w $; [m/s]	4955.06	4920.83	5022.07	4000
$ v $; [m/s]	4837.55	4786.89	5022.07	4000

Table A6.4. Group and phase angles and speeds at the offset of 3000 metres for the model using $\gamma = 0.2$.

A6.8. ANGLE OF PROPAGATION AND PHASE AND GROUP CONCEPTS

The results of Table A6.5 and Figures A6.4 and A6.5 explain the appearance of plots in Figure A6.2. Unlike the case of the isotropic approach, which diverges monotonically from the exact approach with increasing angle of propagation, all the anisotropic approaches coincide with each other at zero offset and at infinite offset, regardless of the method used to describe the distinction between phase and group velocities or angles. As a matter of fact, their coincidence at vertical and horizontal propagations might be used as a check on an algorithm.

Large discrepancies among the anisotropic approaches occur when the propagation in the anisotropic medium is about 45° . This illustration is applicable to all symmetry systems with the vertical symmetry axes. In an arbitrary symmetry system, oriented in an arbitrary fashion, the consequences of this illustration need not hold.

Note that Table A6.5 and Figures A6.4 and A6.5 illustrate well the dependence of the magnitude of the group velocity upon that of the phase velocity (equation A6.1). Namely, the dependence is limited to the derivative and thus, for instance, at $\vartheta = 40^\circ$, the difference between phase and group angles is over 20%, while the difference between phase and group velocities is less than 2%. The limited sensitivity of phase and group velocities justifies, in many cases, approximate solutions under various simplifying assumptions.

phase angle ϑ [deg]	group angle θ [deg]	phase velocity $ v $ [m/s]	group velocity $ w $ [m/s]	angle difference $(\theta - \vartheta)$ [deg]	speed difference $(w - v)$ [m/s]
0	0	3000	3000	0	0
10	13.8898	3018.09	3025.06	3.8898	6.97
20	27.1599	3070.19	3094.32	7.1599	24.13
30	39.367	3150.00	3192.57	9.367	42.57
40	50.3109	3247.91	3301.22	10.3109	53.31
50	59.997	3352.09	3403.77	9.997	51.68
60	68.5651	3450.00	3488.91	8.5651	38.91
70	76.2355	3529.81	3550.82	6.2355	21.01
80	83.279	3581.91	3587.78	3.279	5.87
90	90	3600	3600	0	0

Table A6.5. Group angle as function of phase angle (equation (A6.1)); magnitudes of phase (equation (A6.2)) and group (equation (A6.4)) velocities; and their respective differences for SH waves in an anisotropic medium with $\gamma = 0.2$. Significant difference between phase and group angles and speeds occurs at the oblique propagation while the respective values coincide at vertical and horizontal propagations.

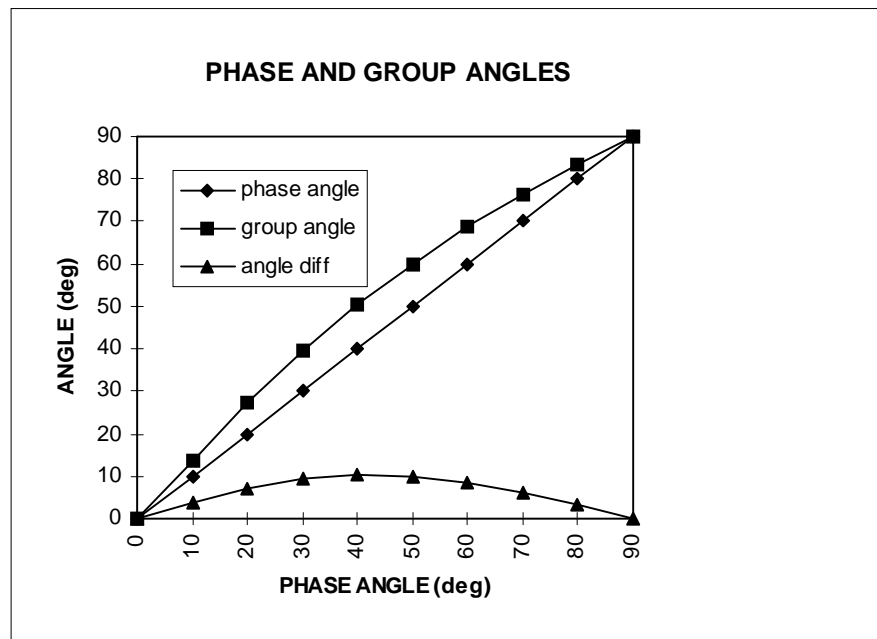


Figure A6.4. Phase and group angles. Note that although at oblique angles of propagation phase and group angles diverge, they are equal to each other at vertical (0) and horizontal (90) directions of propagation. This implies that phase and group velocities are also equal at this angles (both in magnitude and direction).

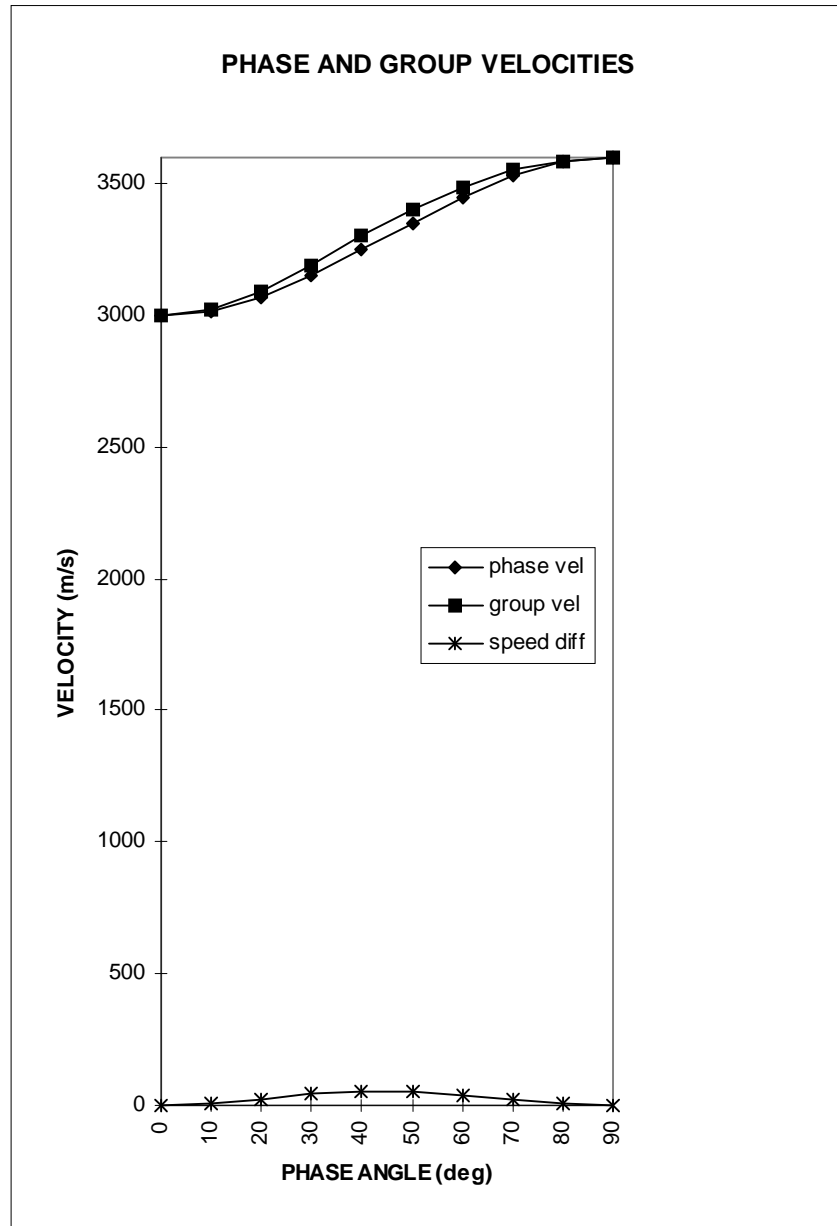


Figure A6.5. Magnitudes of phase (equation (A6.2)) and group (equation (A6.4)) velocities. Note that although at oblique angles of propagation phase and group velocities diverge, they are equal to each other at vertical (0) and horizontal (90) directions of propagation.

APPENDIX 7

THE APPROACH INVOLVING EXACT FORMULÆ

In principle, it seems to be possible to carry out all the derivations described in this dissertation using exact equations (A2.1), (A2.2), and (A2.3). One can express slowness surfaces (curves) for P, SV, and SH waves as level curves in polar coordinates of functions $F(r, \xi)$, $G(r, \xi)$ and $H(r, \xi)$, respectively (equations (A7.1), (A7.2), and (A7.3)). The symbol ξ denotes the phase angle measured from the horizontal, i.e., phase latitude. Notice that equivalent slowness curves, under the weak-anisotropy assumption, constitute a starting point for development in Chapter III, i.e., equations (3.7), (3.22), and (3.33).

$$F(r, \xi) = \frac{1}{r} - \alpha \sqrt{1 + \varepsilon \cos^2 \xi + D(\xi)} = 0 \quad (\text{A7.1})$$

$$G(r, \xi) = \frac{1}{r} + \beta \sqrt{1 + \frac{\alpha^2}{\beta^2} [\varepsilon \cos^2 \xi - D(\xi)]} = 0 \quad (\text{A7.2})$$

$$H(r, \xi) = \frac{1}{r} - \beta \sqrt{1 + 2\gamma \cos^2 \xi} = 0 \quad (\text{A7.3})$$

The symbol $D(\xi)$ denotes the following expression:

$$D(\xi) \equiv \frac{1}{2} \left(1 - \frac{\beta^2}{\alpha^2} \right) \left\{ \sqrt{1 + \frac{4(2\delta - \varepsilon) \sin^2 \xi \cos^2 \xi}{1 - \frac{\beta^2}{\alpha^2}} + \frac{4\varepsilon \left(1 - \frac{\beta^2}{\alpha^2} + \varepsilon \right) \cos^4 \xi}{\left(1 - \frac{\beta^2}{\alpha^2} \right)^2}} - 1 \right\} \quad (\text{A7.4})$$

Equations (A7.1) and (A7.2) can be subjected to the procedure illustrated in Chapter III involving vector calculus (gradient) and linear algebra (normalizing, dot product). The above mentioned manipulations on such complicated expressions constitute a tedious yet not impossible task, particularly with the help of mathematical software. In this dissertation, for the sake of clarity and with a rather negligible loss of accuracy, the simplified version of the above expressions obtained by Thomsen (1986) was used. Such an approach allows one to gain some insight by inspecting equations at certain stages of development - a benefit which could be hindered by a more complicated appearance of equations.

Equation (A7.3) exhibits already, even in its exact form, a simplicity which allows one to use it conveniently in various calculations used in the derivation of Snell's law or in subsequent calculations of the magnitude of group velocity, e.g., Appendix 6. It is particularly useful for various comparisons between exact and approximate approaches. In most cases, however, the approximate equation (3.3) is used for consistency with P and SV waves.

Equations (A7.1), (A7.2) and (A7.3) are both exact and analytic. Those attributes deserve attention in developing code. With the aid of mathematical software involving symbolic operations, one can derive exact equivalents of all the formulæ in Chapter III, and benefit from infinite precision. Although the complexity of equation would prevent an immediate intuitive understanding, which given by the use of the approximate formulæ in this dissertation, the final result would be exact and obtainable without employing any numerical methods.